Defining Novel Mechanisms in Cardiovascular Development

Alice Rebecca Plein

Thesis submitted in fulfilment for the degree of Doctor of Philosophy

University College London (UCL)

Institute of Ophthalmology

Supervisor: Prof Christiana Ruhrberg

Secondary Supervisor: Prof John Greenwood

DECLARATION

I, Alice Rebecca Plein, confirm that the work presented in this thesis is my own. Where information has been derived from other sources, I confirm that this has been indicated in the thesis.

ACKNOWLEDGEMENTS

I have really enjoyed the time spent studying for my PhD and in a large part this is due to the fantastic people I have had the pleasure of working with. First and foremost, I thank my supervisor Christiana Ruhrberg for being such an excellent supervisor and pouring so much of her enthusiasm and effort into my PhD. I would also like to thank everyone in the Ruhrberg group, in particular Alex Fantin for his help and advice, Laura Denti and Andy Joyce for being such a great help with all kinds of lab and animal work, Mat Tata for help with dissections, and everyone else for being such amazing colleagues as well as friends.

I am also thankful to members from other groups such as Natasha Jeffs, David Kallenberg, Maz Ehteramyan, Bridget-Ann Kenny, Carolina Estevao, Fran Mackenzie and Ding Luo for being such great help and making work so much fun.

I would also like to thank other staff at the Institute of Ophthalmology, in particular the Biological Resources Unit for their support with mouse husbandry, Peter Munro for his assistance with the confocal microscope and the porters for always providing a helping hand, when needed. I am also grateful to Ayad Eddaoudi for his help with FACS analysis, as well as the British Heart Foundation for supporting and funding my research.

I would finally like to thank my family Jos, Rudi, Lotti and Hanna, and my grandmother Brenda, for always being there for me and helping me along the way! I am also grateful to Spike and Millie for always being so understanding, patient and supportive, and cheering me up when things were not working.

ABSTRACT

The cardiovasculature is one of the earliest organ systems to develop in the mammalian embryo and its formation relies on the transmembrane receptor neuropilin (NRP) 1. Thus, the cardiovasculature in NRP1 knockout mice develops abnormally. In addition, the cardiac outflow tract (OFT), a transient, embryonic vessel located at the arterial pole of the heart, fails to septate in these mutants.

NRP1 has traditionally been thought to regulate these processes by binding to the vascular endothelial growth factor (VEGF) A in the vascular endothelium. Nevertheless, NRP1 is also expressed by non-endothelial cells and binds alternative ligands of the class 3 semaphorin (SEMA3) family. During my PhD, I contributed to two studies examining NRP1's role in organ vascularisation, which revealed that non-endothelial NRP1 is dispensable for vascular development, and that NRP1 does not exclusively function as a VEGF-A receptor during this process. I also demonstrated that NRP1, instead of being required as a VEGF-A receptor during OFT remodelling, acts as a SEMA3C receptor to induce an endothelial-to-mesenchymal transition that enables OFT remodelling.

In a complementary project, I investigated the role of vascular precursors marked by a novel lineage trace. Vascular progenitors contribute to the formation of the earliest embryonic vessels, but their involvement in later developmental and pathological vessel growth is less well understood. Using a *Csf1r-Cre* transgene, originally thought to be specific for the monocyte/macrophage lineage, I found that this transgene also labels a subpopulation of endothelial cells in brain and retinal vessels. This labelling was not caused by endothelial CSF1R or unspecific *Csf1r-Cre* or $Rosa^{Yfp}$ expression. Furthermore, by analysing embryos from myeloid/macrophage-deficient mice, I demonstrated that *Csf1r-Cre*-labelled endothelial cells were not derived from the myeloid/macrophage lineage. In adults, the analysis of bone marrow and blood from these mice as well as tamoxifen-inducible *Csf1r-Cre* mice suggested that *Csf1r-Cre* labels a bone marrow-derived population of cells that contributes to tissue-resident and circulating vascular precursors.

In conclusion my results have helped further characterise the mechanism by which NRP1 regulates cardiovascular development and provided evidence for the contribution of vascular progenitors to developmental and pathological blood vessel growth.

TABLE OF CONTENTS

LIST OF TABLES

LIST OF FIGURES

ABBREVIATIONS

AP	alkaline phosphatase
AGM	aorta-gonad-mesonephros
ANG	angiopoietin
AMD	age-related macular degeneration
Ao	aorta
bp	base pair
BCIP	5-bromo-4-chloro-3’-indolyphosphate p-toluidine salt, 50 mg/ml in 100% DMF
BMP	bone morphogenetic protein
BSA	bovine serum albumin
CAT	common arterial trunk
cDNA	complementary DNA
CSF1	colony stimulating factor 1
DA	dorsal aorta
DABCO	1,4-diazabicyclo-[2.2.2]octane
DAPI	4’-6-diamidino-2-phenylindole
DIG	digoxigenin
DLL4	delta like ligand 4
dNTP	deoxynucleoside triphosphate
DMEM	Dulbecco’s modified eagle medium
DMF	dimethylformamide
DNA	deoxyribonucleic acid
DNAse	deoxyribonuclease
DTT	dithiothreitol
E	embryonic day
EC	endothelial cell

ECM	extracellular matrix
EDTA	ethyldiaminotetraacetic acid, disodium salt
EMP	erythromyeloid progenitor
EPC	endothelial progenitor cell
FBS	fetal bovine serum
FGF	fibroblast growth factor
FHF	first heart field
FITC	fluorescein isothiocyanate
G	gauge
GFP	green fluorescent protein
GIPC	RGS-GAIP-interacting protein
GTC	giant trophoblast cell
h	hour
HCl	hydrochloric acid
HEC	hemogenic endothelial cell
HRP	horseradish peroxidase
HSC	haematopoietic stem cell
HSPG	heparin sulphate proteoglycan
IB4	isolectin b4 (*bandeirea simplicifolia*)
IL	interleukin
JLS	jugular lymph sac
kb	kilobase
KDR	kinase insert domain-containing receptor
l	litre
LA	left atrium
LB	Luria-Bertani
LCA	left common carotid artery

LSA	left subclavian artery
M	molar
MHC	myosin heavy chain
MLC2a	myosin light chain-2a
µ	micro
m	milli
MESP 1	mesoderm posterior 1
min	minute
MMP	metalloproteinase
mRNA	messenger RNA
MW	molecular weight
N	nano
NBT	nitro-blue tetrazolium chloride, 75 mg/ml in 70% DMF
NCCs	neural crest cells
NGS	normal goat serum
NRP1	neuropilin 1
NRP2	neuropilin 2
NRS	normal rabbit serum
NSS	normal sheep serum
OFT	outflow tract
OIR	oxygen-induced retinopathy
P	postnatal day
PA	pulmonary artery
PAA	pharyngeal arch artery
PBS	phosphate buffered saline
PBT	1X PBS+ Triton X-100
PCR	polymerase chain reaction

PECAM-1	platelet endothelial cell adhesion molecule
PFA	paraformaldehyde
RA	right atrium
RALDH2	retinaldehyde dehydrogenase 2
RCA	right common carotid artery
RNA	ribonucleic acid
RNAse	ribonuclease
RNAseq	RNA sequencing
rpm	rotations per minute
RSA	right subclavian artery
RT	room temperature
qRT-PCR	quantitative real-time PCR
s	seconds
SD	standard deviation
SDS	sodium dodecyl sulfate
SEMA3	class III semaphorin
SHF	second heart field
siRNA	small interfering RNA
SMA	smooth muscle actin
SMC	smooth muscle cell
SSC	saline sodium citrate buffer
SVP	subventricular plexus
TAE	tris acetate EDTA
TE	tris EDTA buffer
TGFβ	transforming growth factor β
TNF	tumour necrosis factor
Tris	tris (hydroxymethyl) aminomethane

tRNA	transferRNA
VEC	vascular endothelial cadherin
VEGF	vascular endothelial growth factor
(v/v)	volume to volume ratio
(w/v)	weight to volume ratio
Xgal	5-bromo-4-chloro-3-indoyl-β-D-galactopyranoside
YFP	yellow fluorescent protein

Chapter 1 INTRODUCTION

1.1 The Formation of the Cardiovascular System

A circulatory system is crucial for large multicellular organisms, because it enables the transport of oxygen and nutrients when diffusion is no longer adequate to reach all cells. Moreover, the circulatory system facilitates the effective removal of waste products. Thus, animals as well as plants have evolved vascular transportation systems: animals the blood vessels, and plants the xylem and phloem.

The cardiovasculature, consisting of blood vessels and the heart, is the first functional organ system to form in the vertebrate embryo. The embryonic processes, which result in the generation of the cardiovascular system, have mostly been studied in mouse, as they are firstly very similar between murine and human embryos. Secondly, due to the thorough knowledge of the murine genome, mouse embryos are easily manipulated genetically, allowing the investigation of specific gene functions during cardiovascular development (Rossant, 1996). I shall therefore outline the developmental processes by focusing on the mouse embryo (Krishnan et al., 2014).

1.1.1 Heart development

The heart is the first functional organ to form during mammalian development. Initially, it mainly consists of myocardial cells with an endothelial lining and simply functions as a pumping tube; nevertheless, throughout development the heart gradually remodels into a complex, four-chambered structure comprised of cardiomyocytes as well as multiple non-muscular cell lineages such as cells of the connective tissue and conductive system.

To date, three temporally and spatially distinct cardiac progenitor populations have been identified: the cardiogenic mesoderm, the pro-epicardium and the cardiac neural crest cells (NCCs). The cardiogenic mesoderm consists of the earliest cardiac progenitors, which ultimately give rise to the ventricular, atrial and outflow tract (OFT) myocardium. It is generated shortly after gastrulation from a common cardiac precursor population, which is characterised by the expression of mesoderm posterior 1 (MESP 1) (Bondue and Blanpain, 2010, Bondue et al., 2008, Saga et al., 2000).

Following their specification, the cardiogenic progenitors initially migrate to an anterior lateral position, where they condense into a structure referred to as the cardiac crescent. At this stage the progenitors can be divided into two subpopulations termed the first (or primary) heart field (FHF) and the second heart field (SHF) (reviewed in Harvey, 2002), where the FHF is situated in a more anterior and lateral position compared to the SHF (**Figure 1.1**).

Due to their position relative to the SHF, the cells of the FHF are exposed to higher levels of cytokines of the bone morphogenetic protein (BMP) (Schultheiss et al., 1997) and fibroblast growth factor (FGF) family (Reifers et al., 2000). This induces the expression of key regulators of the cardiac lineage such as *Nkx2.5* (Lints et al., 1993), *Gata-4* (Arceci et al., 1993, Heikinheimo et al., 1994), *Tbx5* (Hiroi et al., 2001, Horb and Thomsen, 1999) and *Baf60c* (Li et al., 2015). Subsequently, the FHF cells differentiate into cardiomyocytes, which is marked by their expression of contractile proteins such as sarcomeric myosin heavy chain (MHC) and myosin light chain-2a (MCL2a). In contrast, the cells within the SHF remain undifferentiated and continue proliferating until they are recruited to the heart at a later stage (reviewed in Kelly, 2012). Upon differentiation, the cells of the FHF progenitors migrate ventrally to the midline, where they merge to form a linear heart tube by E8.0 which starts beating as soon as it forms (Ji et al., 2003) (**Figure 1.1**). Even before heart tube formation is completed at its caudal end, the tube starts undergoing a complex right-ward looping process, which results in the first signs of asymmetry within the embryo. In addition, the linear heart tube lengthens due to the proliferation of the cardiomyocytes, as well as the recruitment of additional cells from the SHF, which are added to both the arterial as well as the venous pole of the heart tube (**Figure 1.1**) (van den Berg et al., 2009, Soufan et al., 2006).

Whilst there are no specific markers unique to the FHF progenitors, the SHF cells can be identified at E8.5 by the expression of certain markers such as *Isl-1*, which is required for their survival as well as proliferation (Cai et al., 2003). Thus, the *Isl-1-Cre* transgene has been utilised to visualise the derivates of the SHF, which mainly constitute of the right ventricle as well as the inflow region (atria) of the heart (Meilhac et al., 2004). Nevertheless, recent findings have demonstrated that cardiac

NCCs are also labelled by *Isl-1-Cre* (Engleka et al., 2012) and thus studies, which have used this *Cre* to specifically target genes in the SHF, need to be re-examined.

Upon migration, *Isl-1* expression is reduced and SHF cells differentiate into cardiomyocytes as well as endothelial and smooth muscle cells (SMCs) in response to cytokines of the BMP, Notch and non-canonical Wnt pathway (reviewed in Vincent and Buckingham, 2010). By E14.5, the looping and addition of SHF-derived cells has transformed the linear heart tube into a four-chambered structure, where the FHF-derived cells contribute to the formation of both ventricles and atria, and the SHF-derived cells mainly form the right ventricle as well as the myocardium of the OFT (Meilhac et al., 2004) (see **1.4.3**) (**Figure 1.1**).

Further remodelling through the addition of cardiac NCCs (see **1.4.3**) and epicardium-derived cells (reviewed in Brade et al., 2013), as well as the proliferation and regression of cardiomyocytes ultimately results in the adult version of the heart.

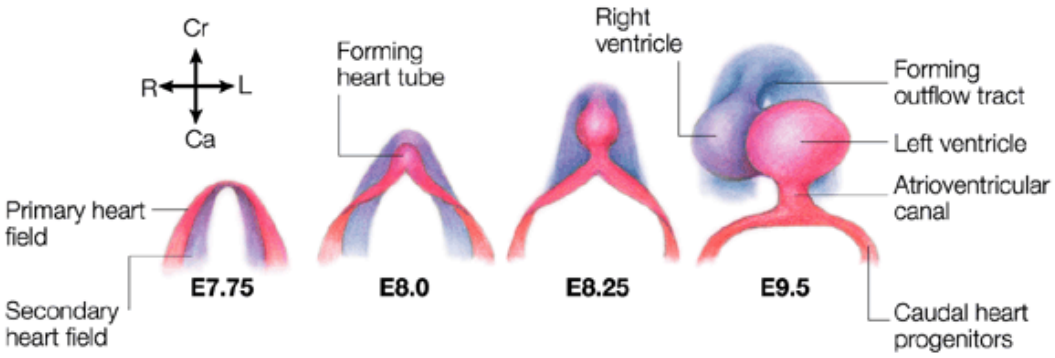

Figure 1.1. Formation of the heart in the murine embryo.

Schematic representation of the first and secondary heart field and their relative contributions to the mammalian heart. Processes are matched to the indicated stages of murine embryonic development. Ca: caudal, Cr: cranial, L: left, R: right. Adapted from "Patterning the vertebrate heart" (Harvey, 2002).

1.1.2 Blood vessel development

1.1.2.1 Vasculogenesis

The first blood vessels are formed by a process called vasculogenesis, in which endothelial precursors termed angioblasts coalesce into cords and differentiate into lumen-forming ECs (Risau and Flamme, 1995). These angioblasts are derived from the intraembryonic mesoderm, and endoderm-derived factors such as Indian hedgehog (IHH) are thought to play a role in their specification (Belaoussoff et al., 1998, Dyer et al., 2001). The angioblasts then migrate to the yolk sac, an extra-embryonic membrane that is an important site for the maternal-fetal exchange of amino acids and ions (King, 1993, Beckman et al., 1996, Lloyd et al., 1996), from E7.25 onwards, where they coalesce to form the first blood vessels of the murine embryo. The other site, where *de novo* extra-embryonic vessel formation occurs, is the allantois, a transient embryonic structure important for the induction of placentation and formation of the umbilical vessels located at the rostral end of the embryo (Downs and Harmann, 1997).

Following this first wave of extra-embryonic vasculogenesis between E7.0 and E7.5, angioblasts also give rise to vessels within the embryo proper. The endocardium and the great vessels such as the dorsal aortae are the first intraembryonic endothelial structures. Thus, angioblasts derived from the aortic primordial, the mesoderm just lateral to the midline, coalesce and form the dorsal aortae by E8.0 (Dzierzak, 2003). These vessels fuse at later stages of development and thereby give rise to the adult aorta (Drake and Fleming, 2000).

Vasculogenesis is thought to only contribute to the earliest embryonic vessels, whereas most other vasculature is believed to be formed by angiogenesis (see **1.1.2.2**). Nevertheless, recent studies have postulated that angioblasts also referred to as endothelial progenitor cells (EPCs) might also contribute to the development of later embryonic and even adult vessels (reviewed in Drake, 2003) (see **1.1.2.4**).

1.1.2.2 Angiogenesis

Angiogenesis defines the formation of new vessels from pre-existing ones. This process can occur when new vessels sprout from previously formed ones, which is termed sprouting angiogenesis. In addition, new vessels can be formed when tissue folds are inserted into the lumen of a pre-existing vessel. This is referred to as intussusceptive angiogenesis.

Sprouting angiogenesis arises when a subset of ECs acquire tip cell properties, which allow them to invade the surrounding tissue in response to pro-angiogenic growth factors such as vascular endothelial growth factor (VEGF-A) (Gerhardt et al., 2003) (see **1.2**). The tip cells are followed by stalk cells, which form the trunk of new vessels and maintain connectivity with parental vessels (Blanco and Gerhardt, 2013). The specification of tip versus stalk cells is thought to be a dynamic process, where cells are constantly competing for the tip cell position (Jakobsson et al., 2010, Fantin et al., 2013a). The tip and its trailing stalks cells together form a new vessel sprout.

In contrast to vasculogenesis, angiogenesis also occurs postnatally. Thus, vessels continue sprouting after birth and into young adulthood to support the growth of tissues. However, once tissue growth is completed, most blood vessels become quiescent. The reactivation of angiogenesis in adults only occurs under specific circumstances; for example, in the cycling uterus and ovary, in the placenta during pregnancy, and during exercise-induced muscle growth (reviewed in Hoeben et al., 2004). ECs are also stimulated to divide rapidly in response to hypoxia; for instance in the ischemic myocardium after myocardial infarction to promote the vascularisation of the hypoxic tissue (Tian et al., 2010). However, hypoxia can also induce detrimental neoangiogenesis. For instance, both tumours and atherosclerotic plaques create a hypoxic microenvironment. In both cases, neoangiogenesis promotes disease progression, because blood vessel growth promotes tumour expansion and plaque rupture (Virmani et al., 2005). Hypoxia-induced neoangiogenesis is also associated with ocular pathologies, such as diabetic retinopathy or the ‘wet’ form of age-related macular degeneration (AMD). In such diseases, neo-angiogenesis typically leads to the formation of abnormal vessel beds,

which prevent effective re-oxygenation of ischemic tissues, and is accompanied by excessive vascular permeability that causes tissue oedema.

In addition to hypoxia, several other signals can induce adult neoangiogenesis. For instance, metabolic stress signals such as reactive oxygen species (Okuno et al., 2012) and inflammatory molecules, which are released during wound healing or exercise-induced muscle growth, can activate adult vessel growth. Nevertheless, these molecules are also synthesised by certain tumours or during chronic inflammation e.g. during rheumatoid arthritis (Noort et al., 2014), where blood vessel growth is detrimental (see above).

1.1.2.3 Vessel specification

Following the formation of a primitive vascular network, the homogenous vascular plexus is remodelled to generate a hierarchical system composed of arteries, veins and capillaries (reviewed in Kume, 2010). Vessel remodelling relies on several distinct mechanisms such as intussusceptive angiogenesis, vascular regression, the increase in luminal calibre as well as arteriovenous specification.

During intussusceptive angiogenesis, vessels give rise to smaller vessels through insertion of tissue folds and columns of interstitial tissue into its lumen (reviewed in Burri and Djonov, 2002). This process is important for the rapid formation of capillary plexi, for example in the lung, where the capillary network has to dramatically increase in complexity to accommodate the developing alveoli (Caduff et al., 1986). Other mechanisms of vascular remodelling include induced apoptosis to remove excess vessel segments or unwanted vessel beds. For example, in the retina the hyaloid vasculature, which supplies the eye throughout embryonic development, regresses in humans during the last weeks of gestation to attain a transparent visual axis. In the mouse, this process also occurs, albeit postnatally (Ito and Yoshioka, 1999, Mitchell et al., 1998) (see **1.5.2.1**). In addition during embryonic development, vessels acquire specific properties depending on their later function in the adult. Thus, blood vessels, which will ultimately be part of the arterial, high-pressure system, develop thick muscular layers, whereas the venous vasculature develops valves, which aid blood flow back to the heart.

Arteriovenous specification was initially believed to occur only in response to varying hemodynamic forces in different vessel beds following the formation of the primary vascular plexus. Whilst hemodynamic forces are important for this process (le Noble et al., 2004), several studies since have demonstrated that arteriovenous specification occurs much earlier in development. Thus, vessels already become specified before the onset of circulation due to the expression of distinct genes. For example, already within the primary plexus the receptor ephrin B2 (EFNB2) is only expressed by arterial vessels, whereas its ligand (EPHB4) is found exclusively on venous cells (Wang et al., 1998). This signalling pathway is critical for vessel identity, as mice lacking *Efnb2* or *Ephb4* display defective remodelling of the primary plexus and lack clear boundaries between arterial and venous vessels (Gerety et al., 1999, Adams et al., 1999). Nevertheless, arteriovenous specification is not completely abolished in these mutant mice, demonstrating that additional pathways are also involved. *Efnb2* and *Ephb4* expression are regulated by multiple signals; zebrafish studies, for instance, have revealed that sonic hedgehog (SHH) is secreted by the notochord, which induces arterial specification in angioblasts by up-regulating ephrin B2 expression. Accordingly, SHH-deficient zebrafish embryos lack arteries; instead, their dorsal aorta adopts a venous morphology (Lawson et al., 2002).

Another important step during blood vessel development is mural cell recruitment, which is essential for vascular stability. For example, the recruitment of smooth muscle cells (SMCs) plays an important role in arterio-venous specification. Thus, in particular larger arteries are covered in a thick muscular coat with vasomotor properties, which is essential for the formation of a regulated high pressure arterial network. Moreover, pericytes, together with astroglial cells, are critical for the formation of the blood-brain barrier.

Finally, ECs within specific vessel adopt features depending on their physiological requirements. Thus, the ECs in endocrine glands become discontinuous and fenestrated to allow the passage of peptide hormones, whereas the endothelium of the central nervous system (CNS) becomes highly impermeable by forming tight junctions (Kniesel and Wolburg, 2000).

1.1.2.4 Endothelial progenitors

Apart from the earliest vessels of the yolk sac and embryo, the remaining vessels are thought to arise exclusively through sprouting angiogenesis. Nevertheless, in recent years a growing amount of literature has suggested that angioblasts, also referred to EPCs, might continue to contribute to blood vessel growth throughout embryonic as well as adult life (reviewed in Yoder, 2012).

EPCs were first described in the adult human peripheral blood by Asahara *et al.* (Asahara et al., 1997). They found that by sorting blood cells positive for the cell surface markers cluster of differentiation (CD) 34 or VEGF receptor 2 (VEGFR2), they could isolate circulating cells with the ability to differentiate into ECs *in vitro* and incorporate into sites of active angiogenesis *in vivo*. VEGFR2 and CD34 were chosen as markers, as it was believed that ECs and haematopoietic cells emerge from the same precursor. Thus, CD34 and VEGFR2 are both expressed by the embryonic mesoderm during angioblast specification (see **1.1.2.1**) (Cortes et al., 1999), and by the earliest hematopoietic progenitors (Matthews et al., 1991, Millauer et al., 1993, Krause et al., 1994), but are down-regulated once the cell becomes committed. Since then, however, evidence suggests that haematopoietic and ECs arise from separate precursors, with the exception of the earliest erythrocytes which share a lineage with the earliest ECs of the yolk sac during primitive haematopoiesis (see **1.3.1**). Thus, EC are usually derived from angioblasts or pre-existing ECs, whereas haematopoietic stem cells (HSCs) are generated from the hemogenic endothelium (see **1.3.2**) (Zovein et al., 2008, Chen et al., 2009b). Furthermore, both CD34 and VEGFR2 are expressed by multiple cell types. For instance, CD34 is expressed by some mesenchymal, epithelial and even cancer stem cell populations (Hirschi et al., 2008), and VEGFR2 is also expressed by multiple cell types such as blood, endothelial and cardiac cells and thus fails to be a helpful discriminator. As a result, the cells isolated by Asahara *et al.* will have contained a heterogeneous group of progenitors including mesenchymal stem cells and differentiated ECs aside from the putative EPCs.

Since Asahara *et al.*'s initial description of EPCs, other studies have tried to include additional markers to make the isolation procedure more specific to EPCs. For instance, Peichev *et al.* (2000) included the marker CD133, also referred to as

prominin 1, which is a glycoprotein expressed by hematopoietic, as well as epithelial, and cancer stem cells (Peichev et al., 2000). They argued that hematopoietic cells expressing all of these progenitor markers (CD34, VEGFR2 and CD133) were more immature than the cells expressing either marker on their own. By analysing circulating cells for these markers, they found that many $CD34^{+}VEGFR2^{+}$ cells also expressed CD133. Furthermore, after plating $CD34^{+}$ cells from the liver on collagen they found that the cells stopped expressing CD133 and differentiated into cells with an endothelial morphology, suggesting that CD133 is required to maintain EPC identity in the blood. In addition, they found that $CD34^{+}CD133^{+}VEGFR2^{+}$ cells transplanted into human patients colonised the surface of engrafted left ventricular assistance devices (Peichev et al., 2000). However, with respect to the definition of these cells as EPCs, this study had possible caveats. Thus, all three antigens used to isolate EPCs, i.e. CD34, CD133 and VEGFR2, are also expressed by subpopulations of haematopoietic progenitor cells. Furthermore, this study did not address whether the putative EPCs properly differentiated into ECs *in vitro* and engrafted into the endothelium *in vivo*. It is therefore not clear if the cells studied by Peichev *et al*. (2000) were EPCs or pro-angiogenic accessory cells.

Nevertheless, numerous subsequent studies demonstrated that the number of the putative $CD34^{+}CD133^{+}VEGFR2^{+}$ EPCs is reduced in patients at increased risk for cardiovascular disease, but enhanced in response to acute vascular injury. Thus, smoking, old age and diseases such as acromegaly are all associated with a reduction of this cell fraction (Fadini et al., 2014, Vasa et al., 2001, Kondo et al., 2004). Conversely, other studies have shown that the number of these cells is enhanced in patients with endothelial damage for example following burn injuries or myocardial infarction (Gill et al., 2001, Massa et al., 2005). Nevertheless, another study that investigated the potential of the $CD34^{+}CD133^{+}VEGFR2^{+}$ cells to differentiate into ECs *in vitro* demonstrated that these cells only gave rise to haematopoietic progenitors and did not form any ECs (Case et al., 2007). This study further revealed that the majority of $CD34^{+}CD133^{+}VEGFR2^{+}$ cells expressed the hematopoietic lineage-specific antigen CD45 and thus constituted immature haematopoietic progenitors (Case et al., 2007). In contrast, analysis of $CD34^{+}CD45^{-}$ cells demonstrated that these cells only gave rise to endothelial, and not haematopoietic

cells, suggesting that this is the cell population that contains EPCs. Accordingly, the correlation between $CD34^{+}CD133^{+}VEGFR2^{+}$ cell number and disease identified by Peichev *et al.* (2000) and others needs to be re-evaluated, as it may have identified important contributions of hematopoietic lineage cells in addition to or instead of EPCs.

Regarding the origin of adult EPCs, Asahara *et al.* (1999) suggested that EPCs are derived from the bone marrow, as the transplantation of bone marrow into irradiated mice gave rise to donor-derived ECs within neo-angiogenic vessels of the host animal (Asahara et al., 1999). In agreement with this idea, the administration of agents such as colony stimulating factor 1 (CSF1) or the small molecule Me6TREN, which induce the mobilisation of EPCs (defined as $VEGFR2^{+}$ $SCA1^{+}$ in this study) from the bone marrow, promote vascular repair in patients with ischemic disease (Chen et al., 2014, Takahashi et al., 1999).

Other studies have suggested the existence of tissue-resident angioblasts that may act as EPCs. Thus, a recent study using a *P0-Cre* transgene for lineage tracing identified stellate cells within the retina that were able to differentiate into ECs *in vitro* and contribute to vessel growth *in vivo* (Kubota et al., 2011). Thus, whilst retinal ECs did not express *P0*, the stellate cells expressed this gene albeit only at mRNA level. In addition, these cells were negative for pericyte, astrocyte or haematopoietic markers such as PDGFRβ, PDGFRα and CD45, respectively. Instead, the vascular precursors were $VEGFR2^{+}$, and importantly the deletion of *Vegfr2* in these cells resulted in defective retinal vascularisation.

Several studies have also demonstrated that subsets of ECs within the aorta or the lung microvasculature are highly proliferative *in vitro* (Nishimura et al., 2014). These cells, referred to as endothelial colony forming cells (ECFCs), are also thought to release ECs into the circulation, which contribute to endothelial repair (reviewed in Yoder, 2010).

In support of non-bone marrow-derived EPC populations a study used parabiosis to demonstrate that more EPCs (defined as $KIT^{+}CD45^{-}$ in this study)

derived from the liver or intestine incorporated into new vessels formed following hindlimb ischemia than from the bone marrow (Aicher et al., 2007).

In summary, it is likely that EPCs comprise a heterogeneous population of cells with multiple origins, including the bone marrow as well as other tissues, and that these cells are released into the blood as circulating progenitors of varying degrees of commitment along a hematopoietic or endothelial lineage. Furthermore, it is conceivable that these progenitors migrate into the tissue parenchyma of several organs, where they reside until activated.

EPCs are of great therapeutic interest, as they could potentially be used to stimulate vascular repair in adult patients, in whom vessels are mostly quiescent or neoangiogenesis typically gives rise to dysfunctional, leaky vessels (see **1.1.2.2**). For example, it has been shown that the administration of bone marrow-derived $CD34^+$ cells can promote vessel growth following myocardial infarction, thus preventing cardiomyocyte apoptosis and improving cardiac function (Kocher et al., 2001, Strauer et al., 2002). In addition, EPCs are thought to contribute to pathological vessel growth; for example, in patients with pancreatic cancer the number of $CD34^+CD133^+$ cells is increased, and the transplantation of murine $CD34^+CD133^+$ cells into littermates promotes tumour angiogenesis (Li et al., 2011). Conversely, reducing the mobilisation of EPCs from the bone marrow by the administration of agents such as dopamine treatment or the deletion of the C-X-C chemokine receptor type 2 (CXCR2) impairs tumour angiogenesis (Chakroborty et al., 2008, Li et al., 2011). EPCs are also of interest in the context of retinal disease. For example, vascular degeneration in diabetic retinopathy is thought to be exacerbated by the inability of EPCs to promote vascular repair. Thus, $CD34^+$ cells isolated from diabetic patients demonstrated an impaired ability to re-endothelialise damaged retinal vessels compared to $CD34^+$ cells collected from healthy patients (Caballero et al., 2007). EPCs are also thought to contribute to the formation of abnormal retinal vessels in sight-threatening diseases such as AMD and retinopathy of prematurity (see **1.1.2.2**). For instance, transplantation studies demonstrated that donor-derived bone marrow cells gave rise to ECs within newly formed vessels in models of retinal or choroidal neovascularisation (CNV) (Grant et al., 2002, Espinosa-Heidmann et al., 2003a).

Despite the large amount of literature supporting the idea that EPCs or EPC-like cells exist in the adult and contribute to vessel growth by vasculogenesis, multiple studies have suggested that EPCs are in fact pro-angiogenic cells, which express endothelial markers, but do not differentiate into ECs (reviewed in Timmermans et al., 2009). Thus, platelet microparticles, which are positive for multiple endothelial markers such as CD31, may contaminate blood cell cultures resulting in the false endothelial classification of haematopoietic cells (Prokopi et al., 2009). Moreover, several studies have postulated that most EPC types studied to date actually constitute pro-angiogenic macrophages or their monocyte-precursors (Rehman et al., 2003). Firstly, as mentioned above, cell populations isolated for CD34, VEGFR2 and CD133 expression include haematopoietic progenitors, which give rise to cells of the myeloid lineage. Secondly, macrophages are known to acquire EC-like properties *in vitro* when cultured with endothelial growth factors; for instance, cultured macrophages over-expressing VEGF-A adopt an endothelial morphology and express EC markers such as CD31, VEGFR2 and vascular endothelial-cadherin (VEC) (Yan et al., 2011). In addition, macrophages and monocytes are known to promote vessel growth by releasing pro-angiogenic molecules such as VEGF-A (see **1.3.3.2**), tumour necrosis factor α (TNFα), and interleukin-8 (IL-8) (Berse et al., 1992, Leibovich et al., 1987, Koch et al., 1992). Furthermore, macrophages secrete proteases such as matrix metalloproteinase-2 (MMP-2), MMP-9 and cyclooxygenase-2 (COX2), which break down the extracellular matrix (ECM), releasing membrane-bound growth factors and allowing angiogenic sprouts to infiltrate the surrounding tissue (Giraudo et al., 2004, Klimp et al., 2001). Unsurprisingly, therefore, an increased number of macrophages is associated with enhanced tumour angiogenesis (Salvesen and Akslen, 1999), and the depletion of macrophages by synthetic compounds or irradiation reduces tumour vascularisation (Ehling et al., 2014, Evans, 1977a, Evans, 1977b). Some studies that have observed beneficial effects of EPCs on vessel growth may therefore have described pro-angiogenic roles of macrophages/monocytes. Future studies that unequivocally discriminate between the two cell types are therefore needed before the contribution of EPCs in adult and embryonic vessel growth can be fully understood.

1.2 Molecular control of vascular development

The formation of a vascular network, which is able to deliver sufficient nutrients and oxygen to the entire body consisting of tissues with varying metabolic rates, is a complex process that relies on the interaction of multiple signalling molecules. Out of these, the most potent and well-characterised molecule regulating vascular development is VEGF-A, which I shall describe in the following passages.

1.2.1 VEGF-A: An essential regulator of angiogenesis that is expressed in several isoforms

VEGF-A belongs to the cysteine-knot superfamily of secreted glycoproteins that is characterised by its eight conserved cysteine residues and includes VEGF-B, VEGF-C, VEGF-D and placental growth factor (PlGF, also known as PGF), as well as the viral VEGF-E (reviewed in Olsson et al., 2006). These proteins form an anti-parallel dimer that allows receptor binding at both poles to bridge two receptor molecules (Muller et al., 1997). Whilst homodimerisation is typical, VEGF-A and PlGF can also form heterodimers with each other (De Falco et al., 2002), which are less angiogenic than the VEGF-A homodimers. Accordingly, overexpression of PlGF, which results in the increased formation of VEGF-A/PlGF heterodimers at the expense of the pro-angiogenic VEGF-A homodimers, reduces tumour angiogenesis and thus growth. Nevertheless, the physiological role of these heterodimers still remains to be established (reviewed in Dewerchin and Carmeliet, 2012).

VEGF-A is an essential paracrine factor for all stages of vascular development (Ruhrberg, 2003). It is critical for EC differentiation, proliferation and migration and is thus integral to both vasculogenesis and angiogenesis (Ruhrberg, 2003). Accordingly, loss of even one allele of the VEGF-A gene (*Vegfa*) abolishes blood vessel formation in the embryo, demonstrating that *Vegfa* is a critical and haploinsufficient gene (Carmeliet et al., 1996).

VEGF-A is synthesised as a collection of several isoforms that are produced by alternative mRNA splicing (**Figure 1.2A**). During development splicing is regulated to generate various tissue- and stage-specific ratios of these VEGF-A

isoforms, which contain abundant information necessary for the multiple processes involved in vascular growth (reviewed in Ruhrberg, 2003).

Molecularly, the VEGF-A isoforms differ in their amino acid length depending on the presence or absence of domains encoded by exons 6 and 7 (**Figure 1.2A**). Thus, out of the most widely studied human VEGF-A isoforms, the shortest is generated from mRNA lacking both exon 6 and 7. This isoform is 121 amino acids long and thus referred to as VEGF121. In contrast, the longest isoform, VEGF189, is generated from mRNA containing both exon 6 and 7. The intermediate isoforms, VEGF145 and VEGF165 contain exon 6 or 7, respectively. In mice, the corresponding mouse isoforms are all shorter by one amino acid and therefore referred to as VEGF120, VEGF144, VEGF164 and VEGF188 (Ruhrberg, 2003, Fantin et al., 2009) (**Figure 1.2A**).

As exon 6 and 7 both encode heparin-binding domains, the VEGF-A isoforms differ in their affinity for heparin *in vitro*, which is thought to reflect their ability to bind heparan sulfate proteoglycans (HSPGs), which are present in the ECM of cultured cells and *in vivo*. Thus, VEGF189, which contains both exon 6 and 7, has the highest ECM affinity and is therefore retained in the matrix unless it is released by proteases (Park et al., 1993). In contrast, VEGF121 is highly soluble, whereas VEGF145 and VEGF165 are partly diffusible (Poltorak et al., 1997). In this fashion, the isoforms cooperate to form chemotactic VEGF-A gradients that guide vessel sprouts to sites, where VEGF-A is upregulated (Ruhrberg et al., 2002, Gerhardt et al., 2003). The importance of these gradients is demonstrated by the great reduction of blood vessel branching and therefore vascular complexity, for example in the brain and retina, in mice in which the VEGF-A gradients are disrupted (Ruhrberg et al., 2002, Gerhardt et al., 2003, Stalmans et al., 2002).

In addition to their differential affinity for ECM components, the isoforms also differ in their affinity for three distinct vascular VEGF-A receptors, which are all required for normal angiogenesis (see **1.2.2**, **1.2.3**) and described in the following sections.

1.2.2 Tyrosine-kinase VEGF-A receptors in angiogenesis

VEGF-A binds to its two tyrosine kinase receptors with high affinity (Gille et al., 2001). They are termed VEGFR2, also known as kinase insert domain-containing receptor (KDR) or foetal liver kinase 1 (FLK1), and VEGFR1, also referred to as fms-like tyrosine kinase 1 (FLT1). Both receptors are transmembrane glycoproteins, which upon ligand-binding undergo autophosphorylation that in turn activates the kinase activity of these proteins (Olsson et al., 2006).

VEGFR2 is critical for EC differentiation and accordingly mice lacking this receptor (*Flk*$^{-/-}$) do not form any blood vessels, resulting in embryonic lethality by E9.5 (Shalaby et al., 1995). Nevertheless, tissue culture models have been used to demonstrate that VEGFR2 also promotes EC proliferation, migration and survival (Koch et al., 2011). In addition, VEGFR2 has been implicated as a regulator of EC junction stability and therefore vascular permeability (Gavard and Gutkind, 2006), as well as a promoter of arteriogenesis (Lanahan et al., 2010). This receptor is thus essential for all aspects of vascular development and this versatility is reflected in its ability to activate a multitude of downstream signalling pathways after VEGF-A binding (Koch et al., 2011).

In comparison to VEGFR2, VEGFR1 is essential for vascular development. Accordingly, VEGFR1-deficient mice (*Flt1*$^{-/-}$) display endothelial overgrowth preventing network assembly, leading to embryonic death before E10.5 (Fong et al., 1995). Nevertheless, in contrast to VEGFR2, which exerts essential kinase activity, the main function of VEGFR1 is to sequester excess VEGF-A with its extracellular domain. Thus, mice only expressing a tyrosine kinase-deficient form of VEGFR1 (*Flt1*$^{TK-/-}$) do not display any defects in blood vessel formation, branching or remodelling (Hiratsuka et al., 1998). The phenotype observed in *Flt1*$^{-/-}$ mice has thus been interpreted as a failure of cell fate decision based on the increased availability of VEGF-A to signal through VEGFR2 (Fong et al., 1999). Despite not having a role in developmental angiogenesis, studies have suggested that the kinase activity of VEGFR1 might be involved in pathological angiogenesis. For example, *Flt1*$^{TK-/-}$ mice display reduced tumour vascularisation (Autiero et al., 2003a, Hiratsuka et al., 2001). In addition, antibodies against VEGFR1 reduce neovascularisation in tumour

models, as well as ischemic retinopathy (Luttun et al., 2002, Wu et al., 2006). Nevertheless, VEGFR1 is also expressed by macrophages and *Flt1*$^{TK-/-}$ mice demonstrate impaired macrophage migration in response to VEGF-A (Hiratsuka et al., 1998). Thus, these observations suggest an indirect, rather than direct role of VEGFR1's kinase activity in pathological angiogenesis.

1.2.3 Non-tyrosine kinase VEGF-A receptor, NRP1

In addition to VEGFR1 and VEGFR2, VEGF-A also binds to the non-tyrosine kinase receptor, neuropilin (NRP) 1; however, whilst VEGFR1 and VEGFR2 have a high affinity for all VEGF-A isoforms, NRP1 mainly binds to VEGF165 and VEGF189 (Gitay-Goren et al., 1996, Soker et al., 1996, Soker et al., 1998, Tillo et al., 2015). NRP1 is a single-pass transmembrane glycoprotein of 130 kDa (Fujisawa et al., 1995). Before being identified as a receptor for VEGF165 (Gitay-Goren et al., 1996, Soker et al., 1996), NRP1 was originally discovered as an axonal adhesion protein in the developing xenopus optic tectum (Takagi et al., 1995), where it was named after its expression within the neuropils of specific regions within the CNS. It was also independently discovered as a receptor for secreted axon guidance cues of the class 3 semaphorin (SEMA3) family (He and Tessier-Lavigne, 1997, Kolodkin et al., 1997).

Besides NRP1, the neuropilin family also includes NRP2 (Chen et al., 1997), which binds both VEGF165 and VEGF145 (Soker et al., 1998, Gluzman-Poltorak et al., 2000). Despite sharing only 44% sequence homology on the amino acid level, NRP1 and NRP2 possess an identical domain structure (Chen et al., 1997). Thus, both receptors consist of a short secretion signal followed by a large extracellular domain of 840 amino acids, a ~24 amino acid-short transmembrane domain and a small cytoplasmic tail consisting of ~40 amino acids. NRP1 mostly exerts its biological functions as a homodimer; nevertheless, NRP1 heterodimers with NRP2 have also been described (Herzog et al., 2011).

1.2.3.1 NRP1 domain organisation

The multiple functions of NRPs are reflected in the complex organisation of their large extracellular domain, which contain 5 domains termed a1, a2, b1, b2 and c

(**Figure 1.2B**). These domains mediate distinct NRP functions, whereby the a and b domains bind ligands, whilst the c domain promotes oligomerisation (Fujisawa, 2002, Schwarz and Ruhrberg, 2010) (**Figure 1.2B**). Thus, the extracellular NRP domain contains two complement-binding homology (CUB) domains, called a1 and a2, which mediate binding to SEMA3s (Gu et al., 2003). Whilst the a1 and a2 domain within the extracellular domain of NRP1 mediate binding to SEMA3A, the corresponding domains of NRP2 mediate binding to SEMA3F (Chen et al., 1997). Furthermore, both receptors bind to SEMA3C (also known as SEMAE) (Chen et al., 1997, Kolodkin et al., 1997). These domains are followed by two coagulation factor V/VIII homology domains, termed b1 and b2 that mediate binding of heparan sulfate and promote adhesion to other cell types. These domains also bind to VEGF-A via distinct VEGF-A binding sites (Mamluk et al., 2002, Gu et al., 2002, Shimizu et al., 2000, Lee et al., 2003). Following the b1 and b2 domain, the extracellular domain also contains the meprin (MAM) or c domain, which promotes dimerisation and interaction with other receptors within the plasma membrane (Lee et al., 2003). The short intracellular/cytoplasmic domain of NRP1 is thought to lack catalytic activity, however, it contains a C-terminal SEA motif that recruits the PSD-95/Dig/ZO1 (PDZ) domain-containing protein synectin, also known as GIPC or NRP interacting protein NIP (Cai and Reed, 1999, De Vries et al., 1998, Gao et al., 2000).

In addition to the full length versions of NRPs, several isoforms of these receptors are synthesised by alternative splicing (reviewed in Geretti et al., 2008). Thus, soluble forms of NRP1 and NRP2 lacking the c, tm or cytoplasmic domains exist. To date four soluble isoforms of NRP1 (s12NRP1, s11NRP1, sIIINRP,1 and sIVNRP1) and one soluble variant of NRP2 (s9NRP2) have been identified (Gagnon et al., 2000, Gluzman-Poltorak et al., 2000). In contrast to NRP1, alternate transmembrane isoforms of NRP2 are also synthesised and termed NRP2a, including NRP2a(17) and NRP2a(22), and NRP2b, including NRP2b(0) and NRP2b(5). The expression profiles of these isoforms are tissue-specific. For example, NRP2a is highly expressed within the placenta, but only found at low levels within the lung or skeletal muscle, whereas NRP2b displays the opposite expression profile (Rossignol et al., 2000). However, the biological significance of alternative NRP splicing remains to be established.

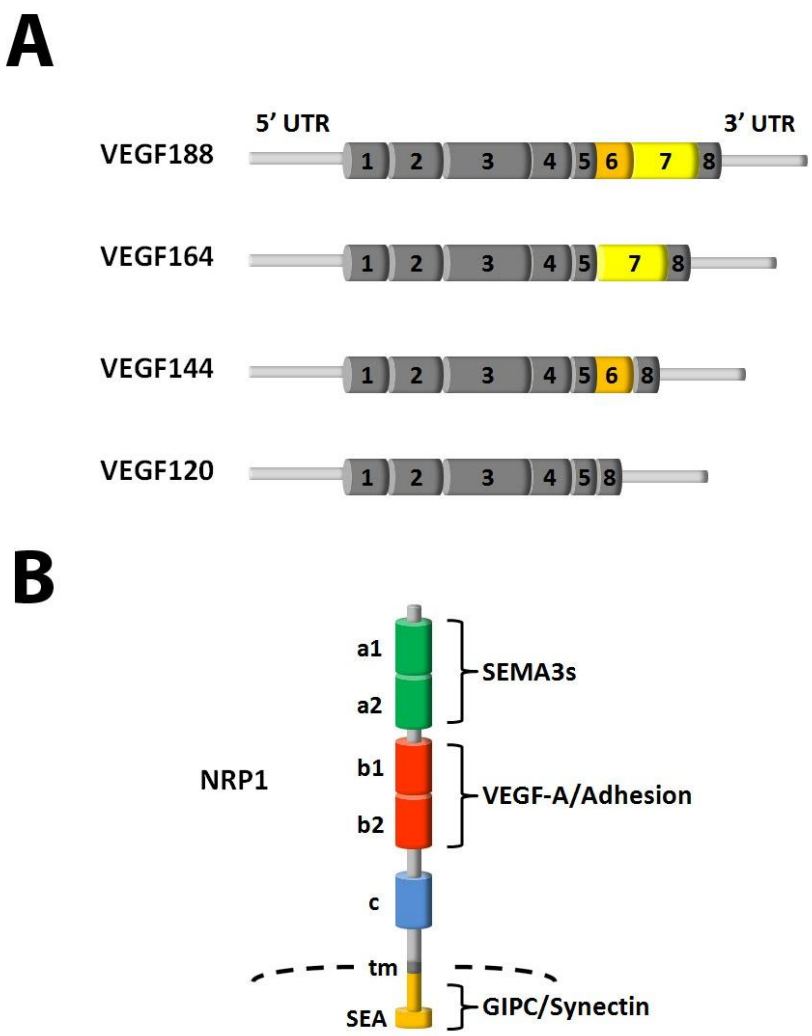

Figure 1.2. Schematic representation of VEGF-A and NRP1 domain structure.

(A) VEGF-A isoforms: VEGF isoforms are generated by alternative splicing. The VEGF isoforms differ by the presence of two heparin-binding domains encoded by exons 6 and 7 (highlighted in yellow). Thus, the VEGF188 mRNA contains both exon 6 and 7, VEGF164 and VEGF144 only exon 7 and 6, respectively, and VEGF120 contains neither exon 6 nor 7. **(B)** NRP1 organisation and ligand binding. The extracellular part of NRP1 contains two domains termed a1 and a2 (green), which bind SEMA3s, two domains called b1 and b2 (red), which bind VEGF164 and VEGF188 and play a role in cell adhesion, one oligomerisation domain (c), and a transmembrane domain (tm). The relatively short cytoplasmic tail (yellow) contains an SEA motif, which binds to GIPC/synectin. This domain is dispensable for developmental angiogenesis, but involved in arteriogenesis.

1.2.3.2 NRP1 in angiogenesis

In contrast to VEGFR1 and VEGFR2, NRP1 is not required for vasculogenesis; instead, it is particularly important for organs vascularised by angiogenesis, such as the brain and retina (Kawasaki et al., 1999, Gerhardt et al., 2004, Raimondi et al., 2014), and for intersomitic vessel sprouting in the zebrafish (Lee et al., 2002). The cardiovascular deficiencies caused by the loss of NRP1 result in embryonic lethality between E10.5 and E14.5 in mouse depending on the genetic background (Jones et al., 2008, Schwarz et al., 2004). Conversely, NRP1 overexpression is also embryonic lethal, as it promotes excessive vessel growth; however, the vessels are leaky and haemorrhagic (Kitsukawa et al., 1995). In contrast to NRP1, NRP2-deficient mice survive postnatally with lymphatic, but not blood vessel defects (Yuan et al., 2002). So far, the physiological significance of VEGF-A isoform binding to NRP2 has not been established; however, double NRP1/NRP2 knockouts display more severe vascular defects than single NRP1 knockouts (Takashima et al., 2002), raising the possibility that NRP2 can partially compensate for NRP1 function in some aspects of vascular development.

NRP1 expression is prominent on developing blood vessels (Fantin et al., 2010, Kawasaki et al., 1999). Furthermore, endothelial deletion of NRP1 results in severe vascular defects (Gu et al., 2003). Thus, NRP1 is thought to exert most of its functions necessary for embryonic angiogenesis within the endothelium. However, NRP1 is also expressed on many other embryonic cell types, for example neurons and their axonal processes (Tillo et al., 2015, Erskine et al., 2011) as well as tissue macrophages (Fantin et al., 2013a), which raises the possibility that non-endothelial NRP1 might also be involved in angiogenesis. A study investigating the role of non-endothelial NRP1 during developmental angiogenesis (Fantin et al., 2013a), which I contributed to, is described in **Chapter 3**.

The essential role of NRP1 in vascular development is commonly attributed to its ability to act as a VEGF165 receptor in ECs (Soker et al., 1998). For example, the reduced neural tube vascularisation of mice lacking NRP1 specifically in the endothelium has been interpreted as evidence that VEGF165 signals through NRP1 to promote angiogenesis (Gu et al., 2003). Furthermore, *Vegfa*$^{120/120}$ mice, which

express VEGF120 at the expense of the NRP1-binding VEGF-A isoforms, display defects in angiogenesis, which were attributed to a lack of VEGFA signalling through NRP1 (Stalmans, 2005). However, the vascular defects caused by loss of NRP1 are different to those in *Vegfa*$^{120/120}$ mice. For example, perisomitic vessels branch poorly in E10.5 *Vegfa*$^{120/120}$, but normally in *Nrp1*-null mutants (Ruhrberg et al., 2002). The hindbrain vascular defects in both types of mutants are also qualitatively different: *Vegfa*$^{120/120}$ mice have less vessel branching in the hindbrain, however the vascular diameter is increased due to the perturbation of VEGF-A gradients (Ruhrberg et al., 2002, Fantin et al., 2010). By contrast, hindbrain vessels in *Nrp1*-null mutants terminate in blind-ended bulbous vessel structures that are rare in *Vegfa*$^{120/120}$ mutants (Gerhardt et al., 2004). A recent study by our group in collaboration with Prof Ian Zachary (Rayne Institute, UCL) investigated the role of VEGF-A signalling through NRP1 during vascular development using a mouse mutant that lacks VEGF-A binding to NRP1 (*Nrp1*$^{Vegfa/Vegfa}$). This study and my findings that contributed to this publication are outlined in **Chapter 3**.

In addition to VEGF165, NRP1 also binds to SEMA3s via distinct domains (Appleton et al., 2007). SEMA3s are secreted glycoproteins, which have mostly been investigated in the context of axonal guidance or neuronal migration (reviewed in Pasterkamp, 2012). Despite initial reports that SEMA3A binding to NRP1 modulates EC migration *in vitro* (Miao et al., 1999, Serini et al., 2003), studies since have demonstrated that SEMA3 signalling through both neuropilins is dispensable for embryonic angiogenesis in mouse (Gu et al., 2003, Vieira et al., 2007). In zebrafish, however, decreasing the levels of the two SEMA3A orthologs impairs vascular development (Shoji et al., 2003, Torres-Vazquez et al., 2004). To date it is not known, why SEMA3A is required vascular development in fish, but not mouse embryos.

Whilst SEMA3s are dispensable during developmental angiogenesis, mouse knockout studies have demonstrated that SEMA3 signalling through NRP is required for cardiac development. Thus, SEMA3A-deficient mice display enlarged atria (Behar et al., 1996) and *Sema3c*-knockout mice have unseptated OFTs, which normally remodel to form the base of the aorta and pulmonary artery (see **1.4.3**). Furthermore, studies have demonstrated that SEMA3A has a role in pathological

angiogenesis. Thus, exogenous delivery of SEMA3A impairs tumour angiogenesis and growth in mice (Maione et al., 2009, Casazza et al., 2013) by eliciting EC apoptosis and normalising pericyte coverage of tumour vessels (Maione et al., 2009). In addition, SEMA3A secreted by ischemic neurons also prevents vascular regeneration in a mouse model of oxygen-induced retinopathy (OIR) that models retinopathy of prematurity (Joyal et al., 2011) (**Figure 1.5C**).

In addition to binding SEMA3s and VEGF-A, NRP1 also exerts important vascular functions by regulating the adhesive properties of ECs (Murga et al., 2005). Thus, in agreement with its initial discovery as an adhesion molecule (Takagi et al., 1995), NRP1 can bind to components of the ECM via its adhesion domains (Raimondi et al., 2014, Murga et al., 2005), which reside in the b1 and b2 region of the extracellular part of the receptor (Shimizu et al., 2000) (**Figure 1.2B**). Furthermore, NRP1 can modulate cell adhesion by directly interacting with integrins (Fukasawa et al., 2007, Valdembri et al., 2009). A recent publication by our group has further demonstrated that NRP1 is stimulated by the integrin ligand fibronectin, which plays a role in EC migration *in vitro* and angiogenesis *in vivo* (Raimondi et al., 2014).

1.2.3.3 Mechanism of NRP1 signal transduction in the vasculature

In the nervous system, NRP1 recruits type A and D plexins to transduce semaphorin signals; accordingly, NRP1's cytoplasmic tail is dispensable for this process (Nakamura et al., 1998). In analogy, it was proposed that NRP1 transduces VEGF165 signals in the vasculature by recruiting co-receptors such as the VEGF-A receptor tyrosine kinases (see **1.2.2**) (Gluzman-Poltorak et al., 2001, Soker et al., 1998). Thus, NRP1 can interact with VEGFR1 and VEGFR2, and the most common model of NRP1 function in angiogenesis suggested that complex formation between VEGF165, NRP1 and VEGFR2 promotes VEGFR2 signalling in angiogenesis (e.g. Prahst et al., 2008, Soker et al., 2002, Whitaker et al., 2001, Becker et al., 2005, Soker et al., 1998). In support of this idea, a recent study by our group analysing mice lacking the cytoplasmic domain of NRP1 ($Nrp1^{Cyto/Cyto}$) demonstrated that these mice did not have any defects in angiogenesis; instead, they were viable demonstrating only mild defects in arteriovenous patterning (Fantin et al., 2011).

Nevertheless, there is also evidence suggesting that NRP1 might function independently of VEGFR2. For instance, fusion of the extracellular domain of the epidermal growth factor (EGF) receptor to the transmembrane and cytoplasmic domains of NRP1 creates a chimeric receptor that promotes EC migration in response to EGF (Wang et al., 2003). Furthermore, the NRP1 cytoplasmic domain promotes VEGF-induced EC migration via p130CAS (CRK-associated substrate) without affecting VEGFR2 phosphorylation (Evans et al., 2011). Nevertheless, because this NRP1 domain is dispensable for developmental angiogenesis (Fantin et al., 2011), these tissue culture studies may have identified signalling pathways that are selectively important for EC migration under pathological circumstances or in non-endothelial migratory cells. For example, NRP1 also promotes the VEGF-dependent migration of neurons (Schwarz et al., 2004) and cancer cells (Jia et al., 2010).

In addition, a recent publication from our lab has demonstrated that NRP1 can induce EC migration independently of VEGF-A/VEGFR2 by forming a complex with the tyrosine kinase, ABL1 (Raimondi et al., 2014). In this context, fibronectin, a component of the ECM, stimulates the NRP1-dependent activation of ABL, which then phosphorylates the focal adhesion component paxillin (PXN) and promotes actin remodelling, which is critical for EC migration *in vitro* and angiogenesis *in vivo*.

In summary, it is clear that NRP1 plays an essential role in angiogenesis, but the conflicting data obtained in tissue culture, zebrafish and mouse models need to be resolved to fully understand the signalling mechanisms of NRP1 during angiogenesis *in vivo*. Furthermore, future studies may wish to elucidate the mechanism by which NRP1 regulates angiogenesis by investigating effects on the cytoskeleton, EC proliferation etc.

1.2.3.4 Role for NRP1 in arteriovenous patterning

NRP2 is enriched in the venous and NRP1 in the arterial parts of vascular networks in chick, mouse and zebrafish (e.g. Herzog et al., 2001, Jones et al., 2008, Fantin et al., 2011). Whilst *Nrp2*-null mice develop to term without obvious arteriovenous or indeed any other type of blood vascular defects (Yuan et al., 2002),

arterial differentiation is compromised by loss of NRP1. Thus, specific arterial markers are missing from arterioles and arteries in full and endothelial-specific *Nrp1* knockouts (Jones et al., 2008, Mukouyama et al., 2005).

Both zebrafish and mouse knockdown studies have suggested that NRP1/Synectin signalling is involved in arterial development. Thus, morpholino-induced *Synectin* knockdown results in zebrafish embryos with severe defects in arteriogenesis including impaired formation of the dorsal aorta causing lethality by 3 days post fertilisation (Chittenden et al., 2006). Nevertheless, these embryos also display defective angiogenesis such as reduced intersomitic vessel branching (Chittenden et al., 2006), which agrees with previous zebrafish studies that demonstrated that the cytoplasmic domain of NRP1 is also required for developmental angiogenesis (Wang et al., 2006b). Thus, the arterial phenotype in *Synectin*-deficient zebrafish embryos is presumably exacerbated by defective angiogenesis. In mice, deletion of either *Synectin* or the cytoplasmic domain of NRP1 does not impair developmental angiogenesis and thus these mice are viable; however, these mutants demonstrate defects in arteriogenesis. Thus, *Synectin*-deficient mice display impaired mural cell recruitment to retinal blood vessels (Paye et al., 2009) and reduced arterial branching in development and disease (Chittenden et al., 2006). Whilst $Nrp1^{Cyto/Cyto}$ mice do not recapitulate the reduction in mural cell recruitment observed in *Synectin*-deficient mice, these mutants also display reduced developmental arteriolar branching as well as in response to injury (Lanahan et al., 2013).

NRP1 is thought to regulate arteriogenesis by tethering a VEGF-A-bound NRP1/VEGFR2/Synectin complex to an intracellular trafficking machinery that ensures the enrichment of activated VEGFR2 in signalling endosomes (Lanahan et al., 2013). Accordingly, VEGF-A/VEGFR2 signalling is reduced in *Synectin*-nulls and $Nrp1^{Cyto/Cyto}$ mice (Lanahan et al., 2013, Lanahan et al., 2010). Furthermore, mice that express a mutated version of NRP1 unable to bind VEGF-A ($Nrp1^{Vegfa/Vegfa}$, see **Chapter 3**) demonstrate defective arteriogenesis (Fantin et al., 2014).

1.3 Haematopoiesis

The cardiovascular system acts as a conduit for cells of the haematopoietic system, which are critical for oxygen delivery as well as protecting the body against pathogens. The generation of these blood cells, which is termed haematopoiesis, occurs from E7.0 onwards in the mouse and E17 in humans, and it continues throughout adult life to replenish ageing blood cells and to support the immune system. In the vertebrate embryo, haematopoiesis occurs in two waves, which are referred to as the primitive and the definitive wave of haematopoiesis (reviewed in Jagannathan-Bogdan and Zon, 2013). These distinct stages of haematopoiesis differ both in the site as well as the type of blood cell generation, as outlined in the following sections.

1.3.1 Primitive haematopoiesis

Primitive haematopoiesis occurs within the mammalian and avian yolk sac (Dzierzak and Speck, 2008) (**Figure 1.3**). Its primary purpose is to generate primitive red blood cells from erythroid progenitors, which together with the emerging blood vessels enable tissue oxygenation when diffusion is no longer adequate. Thus, primitive haematopoiesis is initiated concomitantly with the generation of the first blood vessels.

The first haematopoietic cells, the erythroid precursors, arise within the blood islands of the yolk sac (reviewed in Ferkowicz and Yoder, 2005). These structures were already described by Florence Sabin at the beginning of the 20th century, when she noted that clusters of haematopoietic cells emerge within the earliest vessels of the yolk sac. The close spatial and temporal association of primitive erythrocytes and ECs led to the postulation of a common mesodermal precursor for these two lineages called the “haemangioblast”, which was thought to migrate into the yolk sac and then form the blood islands. Nevertheless, this idea still remains contentious. Thus, experiments have to date failed to demonstrate that a mesodermal progenitor that is selective to only blood and ECs migrates to the yolk sac to generate the blood islands. Thus, whilst studies demonstrated that a population of embryonic stem cells, which expresses both the endothelial marker VEGFR2 and the mesodermal marker brachyury, gave rise to both endothelial and blood cells in culture; these cells also

generated vascular SMCs (Huber et al., 2004). As SMCs are the only other mesodermal cell population found in the yolk sac at this embryonic stage, this cell population most likely constitutes a general mesodermal progenitor.

Instead, lineage-trace studies have suggested that blood and haematopoietic progenitors are independently fated during gastrulation. Thus, experiments using lacZ-labelled mesodermal progenitors showed that when these cells were transplanted into E7.75 mouse embryos, they either gave rise to ECs or haematopoietic cells within the blood islands (Kinder et al., 1999). Likewise, a study analysing blood island formation in embryos generated from fluorescently-labelled tetrachimeras found that the blood islands were never derived from only one progenitor population contradicting the haemangioblast theory (Ueno and Weissman, 2006). Similar results were achieved in zebrafish experiments, where cells were labelled by laser-activated caged fluorescein dextran at gastrulation and their progeny assessed. This revealed that most cells either gave rise to blood or ECs (Vogeli et al., 2006) within the blood islands. A small subpopulation of fluorescein-labelled progenitors, however, also gave rise to both haematopoietic and ECs. Nevertheless, as the labelled progeny was not analysed over time, it is currently not known whether these cells derived from a true haemangioblast or whether the blood cells were in fact derived from labelled ECs at a later stage. Thus, further experiments are required to establish the origins of the earliest blood and ECs within the yolk sac. Be that as it may, once the progenitors have migrated into the yolk sac the cells with a haematopoietic fate form a circumferential band (Ferkowicz et al., 2003) and differentiate into primitive erythrocytes. Subsequently, these cells are ensheathed by ECs giving rise to the first blood cell-filled vessels.

The primitive erythrocytes differ from the mature red blood cells in that they contain a nucleus and express embryonic forms of globin (Brotherton et al., 1979). This results in haemoglobin with a stronger affinity for oxygen, which greatly facilitates the uptake of oxygen from the maternal erythrocytes at the placental interface (reviewed in Carter, 2012).

In addition to the primitive erythrocytes, the yolk sac also gives rise to a subset of macrophages termed the tissue-resident macrophages. These cells stem

from erythromyeloid precursors (EMP), which arise from E8.5 onwards and also give rise to erythrocytes expressing the adult globin (**Figure 1.3**) (Bertrand et al., 2007, Yoder et al., 1997a, Chen et al., 2011b). These cells are thought to arise from a subset of ECs within the yolk sac (Chen et al., 2011b). In contrast to the macrophages produced during definitive haematopoiesis, these cells bypass the monocytic stage (Ginhoux et al., 2010). They colonise the embryo through the blood as soon as the circulation is established between E8.5 and E10, and play important roles during development (see **1.3.3.2**) (Ginhoux et al., 2010).

The progenitors generated during the primitive wave of haematopoiesis differ from the HSCs formed during definitive haematopoiesis, as they do not have the ability to self-renew or give rise to cells of all haematopoietic lineages (**Figure 1.3**). Accordingly, transplantation studies have demonstrated that these cells, in contrast to HSCs, cannot repopulate the bone marrow of irradiated mouse pups (Yoder et al., 1997b).

1.3.2 Definitive haematopoiesis

Definitive haematopoiesis entails the formation of HSCs, which are able to generate all cells of the haematopoietic lineage including lymphocytes (B, T and natural killer cells), erythrocytes, megakaryocytes, granulocytes, and mononuclear phagocytes (monocytes and macrophages) (**Figure 1.3**). In addition, HSCs are able to self-renew, allowing them to continuously replenish blood cells with limited half-lives such as monocytes throughout adult life.

HSCs are generated from a specialised endothelium, referred to as hemogenic endothelium, within certain tissues depending on the stage of embryonic development (reviewed in Hirschi, 2012). Thus, the site of HSC generation changes throughout mammalian embryonic development. It first takes place in the extra-embryonic tissues such as the yolk sac at E8.25 (Palis et al., 1999), and vitelline artery, umbilical vein (de Bruijn et al., 2000) and placenta by E9.5 (Robin et al., 2009, Gekas et al., 2005). Within the embryo proper definitive haematopoiesis begins at E10.0, where the major site of HSC generation is found in the aorto-gonad-mesonephros (AGM) region (Medvinsky and Dzierzak, 1996). Nevertheless, recent

studies have also shown HSC generation in other intra-embryonic tissues such as the endocardium (Nakano et al., 2013) and cephalic arteries (Li et al., 2012).

The AGM-derived HSCs differ in their multi-lineage properties compared to the earlier yolk sac- or placenta-derived progenitors. Thus, they are able to reconstitute bone-marrow irradiated adult mice (Muller et al., 1994, Medvinsky and Dzierzak, 1996), whereas the earlier yolk sac-derived progenitors are only able to reconstitute irradiated neonates (Yoder et al., 1997b). It has been proposed that this reflects the immature nature of the yolk sac-derived progenitors, which are thought to require further maturation signals from the embryonic or neonatal liver (see below) in order to function as "true" HSCs. As the liver does not provide adequate signals in the adult, the yolk sac progenitors fail to develop into proper HSCs when they are transplanted into adult mice (Yoder et al., 1997b).

HSCs are generated from specialised ECs referred to as hemogenic endothelial cells (HECs). The endothelial origin of HSCs was uncovered through endothelial lineage tracing as well as genetic knockout studies. Thus, a study using an inducible VEC *Cre* line demonstrated that HSCs were labelled despite not expressing VEC (Zovein et al., 2008). In addition, the endothelial deletion of *Runx1*, which is critical for the generation of HSCs, abolished HSC formation (Chen et al., 2009b).

The specification of HECs occurs from E8.25 onwards, when the primitive vascular plexus remodels into a hierarchical network of blood vessels (Goldie et al., 2008, Nadin et al., 2003, Silver and Palis, 1997). The earliest HECs, which arise in the yolk sac, can be identified by the co-expression of VEGFR2 and haematopoietic stem cells marker KIT, and the lack of the expression of the haematopoietic marker CD45 (Goldie et al., 2008, Nadin et al., 2003). In addition HECs are characterised by their Hoechst dye-efflux properties, a phenotype that is also common to adult HSCs (Goodell et al., 1996, Kubota et al., 2003). The mechanism underlying HEC specification is still not completely understood; however, it is thought to rely on retinoic acid (RA) signalling. Thus, studies revealed that >90% of yolk sac and AGM HECs exhibit active RA signalling. Furthermore, embryos lacking retinaldehyde dehydrogenase 2 (RALDH2), an enzyme responsible for RA generation, lack HECs

(Goldie et al., 2008). RA is required to regulate the proliferation of ECs and thus it has been proposed that RA is involved in HEC specification by promoting cell cycle exit and subsequent differentiation. A recent study has provided evidence for this by showing that RA regulates KIT expression, which in turn promotes the expression of p27, a cyclin-dependent kinase inhibitor (Marcelo et al., 2013). Thus, KIT expression is reduced in *Raldh2*-deficient embryos; however, re-expression of KIT in *Raldh2*$^{-/-}$ mutants increases p27 expression and thus inhibits cell cycle progression rescuing HEC generation.

Following the initial generation of HSCs from the AGM and extra-embryonic tissues, these cells enter the circulation and colonise first the liver and then the bone marrow (Houssaint, 1981). The liver is unable to generate *de novo* HSCs; instead, it serves as the main organ for HSC expansion and differentiation until late gestation. Thus, in contrast to the adult HSCs found in the bone marrow, the fetal HSCs undergo rapid, symmetrical self-renewing divisions (Morrison et al., 1995, Harrison et al., 1997, Rebel et al., 1996).

The skeletal system develops during the third week of murine development and is vascularised from E15.5 onwards. Nevertheless, HSCs are only found in the bone marrow from approximately E17.5 onwards, when molecules such as stromal derived factor 1 (SDF1) are secreted to attract HSCs (Ara et al., 2003). Within the bone marrow, HSCs are located in specialised niches, which are important to regulate the appropriate balance between self-renewal and differentiation (Arai et al., 2004). For instance, molecules secreted by osteoblasts such as angiopoietin-1 (ANG1) affect proliferation and survival rates of HSCs (Arai et al., 2004). Furthermore, HSCs are commonly found closely associated with the bone microvasculature. This is firstly thought to facilitate the entry of blood cells into the circulation; secondly, ECs are thought to play an important role in blood cell differentiation. Thus, the interaction of haematopoietic progenitors with endothelial molecules such as vascular cell adhesion molecule 1 (VCAM1) during trans-endothelial migration is important for megakaryocyte maturation (Rafii et al., 1997, Rafii et al., 1995).

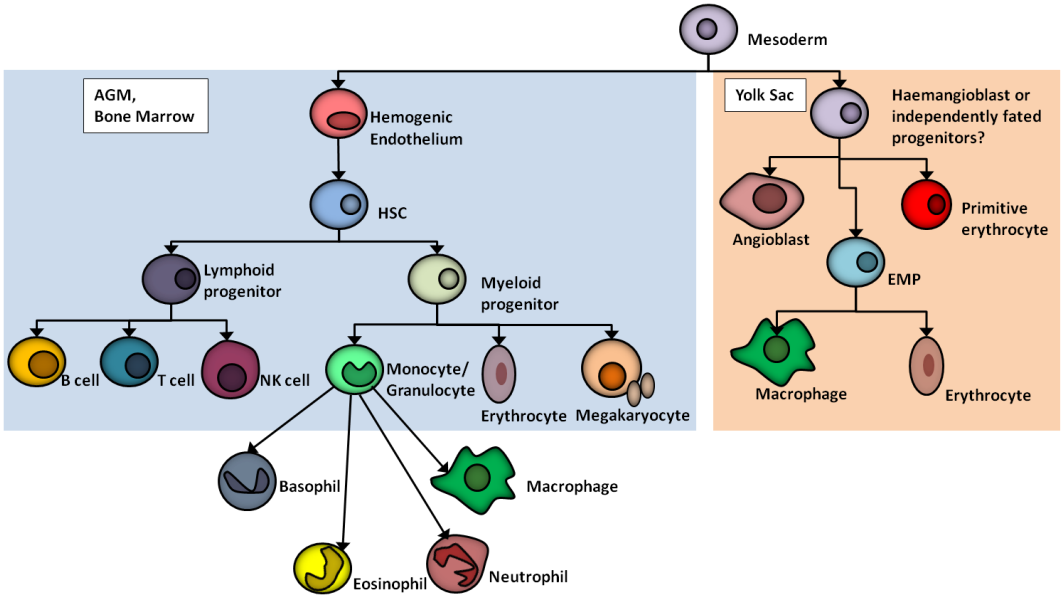

Figure 1.3. The formation of the haematopoietic system.

Schematic representation of primitive haematopoiesis in the yolk sac and definitive haematopoiesis in the AGM and bone marrow. Arrows indicate lineage relatedness. AGM: aorta-gonad-mesonephros, HSC: haematopoietic stem cell, NK: natural killer, EMP: erythromyeloid progenitor.

1.3.3 Monocytes and macrophages

Monocytes and macrophages are mononuclear phagocytes that constitute an essential part of the innate immune system. Both cell types play crucial parts during inflammation by phagocytosing pathogens, releasing cytokines and organising an immune response. In addition, macrophages are essential for development and tissue homeostasis.

Monocytes are a conserved population of mononuclear leukocytes with bean-shaped nuclei that are present in all vertebrates (**Figure 1.3**). In mice and humans they constitute 4% and 10%, respectively, of the nucleated cells in the blood, with considerable reserves in the spleen and lungs that can be mobilised in response to inflammatory signals (van Furth and Sluiter, 1986, Swirski et al., 2009). In humans, monocytes can be identified through the expression of specific markers such as CD11b, CD11c and CD14, whereas in mice they are recognised by the expression of CD11b and F4/80. Within the blood, monocytes can be separated into several distinct subpopulations, which differ in their function and expression of specific markers (reviewed in Ginhoux and Jung, 2014). In humans, monocytes can broadly be split into two main populations, the "classical" population, which is $CD14^{+}CD16^{-}$, and the "non-classical" population, which is $CD14^{-}CD16^{+}$. These populations correspond to the two main monocyte populations found in the mouse, in which the classical population is defined as $LY6C^{hi}CCR2^{+}CD62L^{+}CX_3CR1^{mid}$, whereas the non-classical population is $LY6C^{low}CD43^{+}CX_3CR1^{hi}$.

In both mice and humans, the classical monocytes comprise the majority of monocytes in the blood. These cells only have a half life of 20 h and function as the "inflammatory subset" of monocytes (Geissmann et al., 2003). They circulate within the blood, from where they are recruited to sites of inflammation by CCR2 and release cytokines and/or differentiate into macrophages to activate an immune response (**Figure 1.3**).

In contrast, the non-classical monocytes only comprise 15% of total monocytes in healthy mice and humans. These cells have a longer half life of 5 days and play an important role in patrolling the lumen of blood vessels and surveying the

endothelium for damage. They are often referred to as “resident monocytes”, because they are also found in non-inflamed tissue (Geissmann et al., 2003). In response to tissue injury, these cells can extravasate and coordinate an immune response by differentiating into macrophages and secreting cytokines (Auffray et al., 2007).

Accumulating evidence suggests that, in the steady state, the blood monocyte subsets represent stages in a developmental sequence with the classical LY6C^{hi} monocytes eventually differentiating into LY6C^{low} cells (Yona et al., 2013, Varol et al., 2007). In support of this idea, recent studies have also discovered monocyte populations that display intermediate LY6C expression levels.

Macrophages are large, phagocytic cells, which are characterised by the expression of surface markers such as F4/80, CSF1R, CD11b and CD68 (also known as MAC1). In contrast to their monocytic precursors, these cells have a long life span, which can range from several months to years. These cells are found in multiple tissues, where they play a critical role in tissue development and homeostasis. Depending on the tissue, macrophages can also become specialised to their environment and are referred to as Kupffer cells (liver), Langerhans cells (skin), osteoclasts (bone) and microglia (CNS) (reviewed in Gordon and Taylor, 2005).

Macrophages also comprise an essential part of the innate immune system and can be activated to launch distinct immune responses, sometimes referred to as M1 and M2- a terminology that is based on different *in vitro* responses to distinct cytokines (reviewed in Martinez and Gordon, 2014). This nomenclature mimics the names used to describe the polarisation of T helper cells in response to environmental stimuli. Thus, T helper cells can either launch a TH1 (cell-mediated) or TH2 (antibody-mediated) immune response.

In vitro, macrophages can adapt a pro-inflammatory phenotype, which is termed M1, in response to pathogenic stimuli such as lipopolysaccharides (LPS) or inflammatory cytokines such as interferon-γ or TNF-β. M1 activation results in the release of multiple, pro-inflammatory cytokines e.g. IL-12, TNF, IL-6, and IL-1β and chemokines e.g. C-C motif ligand 2 (CCL2), and the upregulation of antigen presenting molecules. In addition, macrophages increase their production of toxic

intermediates such as nitric oxide (Herbst et al., 2011, Thomas et al., 1997, Piedrafita et al., 2001). Altogether these factors activate additional immune cells and contribute to the destruction of invading pathogens and malignant tumour cells.

In contrast, the anti-inflammatory macrophage phenotype termed M2 results in macrophages promoting tissue remodelling and repair. This response is triggered by various stimuli such as IL-4, a product of the TH2 response, IL-10 and glucocorticoids (Varin et al., 2010, Mantovani et al., 2004, Deng et al., 2012). These factors result in the enhanced expression of scavenger and mannose receptors and the reduced secretion of pro-inflammatory cytokines. The M2 macrophages, thus, promote repair by taking up debris, promoting vascularisation and tissue remodelling.

1.3.3.1 Monocyte and macrophage development

Monocytes were originally thought to constitute the exclusive precursor of macrophages; nevertheless, recent studies have revealed that a subset of tissue resident-macrophages stems from a separate yolk sac-derived precursor termed the EMP (**Figure 1.3**). The EMPs are generated in the yolk sac during primitive haematopoiesis and give rise to macrophages directly without first generating the monocyte stage. These yolk sac-derived macrophages spread through the circulation and into the embryonic tissues when circulation starts between E8 and E12. Within their target tissues they proliferate and ultimately give rise to tissue-resident macrophages, which are critical during development, as they promote and regulate tissue vascularisation (DeFalco et al., 2014, Fantin et al., 2010, Okuno et al., 2011).

The first monocytes are generated from HSC-derived myeloid precursors in the liver and then bone marrow during definitive haematopoiesis (see **1.3.2**). Their generation is dependent on the transcription factor MYB, which is required for HSC formation (Gomez Perdiguero and Geissmann, 2013, Schulz et al., 2012). In contrast, yolk sac-derived macrophages develop in a MYB-independent fashion. As a result, *Myb*-null mice display normal tissue macrophage populations, whilst all other blood cells are lacking (Schulz et al., 2012).

Following monocyte generation, a subset of these cells also extravasates and differentiates into macrophages. Monocytes thus also provide a source of tissue-resident macrophages. Nevertheless, this process is highly tissue-specific (reviewed in Ginhoux and Jung, 2014); thus, monocytes are the predominant source of Langerhans cells, the tissue-resident macrophages in the skin (Hoeffel et al., 2012). In addition, they give rise to the alveolar macrophages of the lung (Guilliams et al., 2013). They do not, however, contribute to the generation of microglia, the tissue-resident macrophages of the CNS (Ginhoux et al., 2010). The varying contribution of monocytes to tissue-macrophage populations of distinct tissues is thought to be an adaption to the relative exposure of certain tissues to pathogens. Thus, the skin and lung are readily exposed to multiple pathogens and macrophages will be depleted more quickly than within the CNS, which is mostly sterile. In addition, monocyte-derived macrophages are also thought to predominantly contribute to tissues with a continuous cyclic recruitment of macrophages such as the uterus or ovary (reviewed in Italiani and Boraschi, 2014).

The differentiation of monocytes and macrophages depends on the E26-transformation-specific (ETS) family transcription factor PU.1. Thus, mice deficient in *Pu.1* (also known as *Spi1* Jego et al., 2014, Batliner et al., 2012) completely lack mature myeloid cells (McKercher et al., 1996). This protein is also required for B cell and neutrophil differentiation (McKercher et al., 1996) and it is thought that PU.1 levels regulate haematopoietic cells towards their lymphoid or myeloid fate. Accordingly, PU.1 is expressed at intermediate levels in progenitors and is down-regulated during B- and T-cell development, but is expressed at higher levels in cells that develop into macrophages (DeKoter and Singh, 2000, Anderson et al., 2002, Spooner et al., 2009, Carotta et al., 2010). PU.1 regulates the expression of another gene that is critical for myeloid differentiation, *Csf1r* (Krysinska et al., 2007).

CSF1R is a type III tyrosine kinase receptor for the ligand CSF1, a growth factor that plays an important part in both monocyte generation, as well as macrophage differentiation and function (Byrne et al., 1981, Guilbert and Stanley, 1980, Tanaka et al., 1993, Dai et al., 2002). Accordingly, mice homozygous for the naturally occurring, inactivating *osteopetrotic* mutation in the coding region of the *Csf1* gene ($Csf1^{Op/Op}$) (Marks and Lane, 1976, Yoshida et al., 1990) lack tissue

macrophages and thus display multiple defects such as osteopetrotic bones due to the lack of osteoclasts. Interestingly, microglia only show a 30% reduction (Ginhoux et al., 2010). Mice lacking the CSF1R receptor (*Csf1r*$^{-/-}$) recapitulate all defects displayed by the *Csf1*$^{Op/Op}$ mouse (Wiktor-Jedrzejczak et al., 1990). In addition, they exhibit a complete absence of all tissue macrophages including the microglia in the CNS (Dai et al., 2002). This discrepancy can be explained by the other CSF1R ligand, IL-34, which presumably plays a role in microglia development or survival (Lin et al., 2008).

1.3.3.2 Role of macrophages in vascular development

Tissue-resident macrophages play an integral part during development (reviewed in Pollard, 2009). For instance, they contribute to tissue remodelling by removing redundant tissues such as the hyaloid vasculature in the eye (see **1.5.2.1**) (Diez-Roux et al., 1999). Furthermore, they are required in developing organs that are formed when epithelial sprouts invade underlying mesenchyme, for instance in the mammary gland or pancreatic islets. In these tissues, macrophages enable lumen formation and ductal branching. Accordingly, *Csf1*$^{Op/Op}$ mice display atrophic mammary glands and abnormal postnatal islet morphogenesis (Geutskens et al., 2005, Gouon-Evans et al., 2000).

In addition, tissue-resident macrophages are essential for tissue vascularisation by promoting the anastomosis of sprouting vessels (Fantin et al., 2010, Okuno et al., 2011). Thus, mice deficient in macrophages display less complex vascular beds. The mechanism underlying this process is currently not well understood; however, it is thought to be independent of VEGF-A signalling. Instead, VEGF-C has been implicated in this process. Thus, microglia located near vessel branch points secrete VEGF-C, whereas vascular sprouts express the VEGFC receptor VEGFR3 (Benedito et al., 2012). Furthermore, retinas of *Vegfc*$^{+/-}$ mice have reduced vessel branching, whilst sprouting is increased (Tammela et al., 2011). Nevertheless, it remains to be shown in what way this signalling pathway contributes to vessel anastomosis. In addition, it is currently not clear whether macrophages are attracted by tip cells or vice-versa.

1.3.3.3 Role of macrophages in pathological angiogenesis

During inflammation, a large number of immune cells including monocytes and macrophages are recruited to the site of injury. There, depending on the inflammatory milieu, macrophages usually either elicit a M1-like pro-inflammatory or M2-like anti-inflammatory/pro-angiogenic response (see **1.3.3**). For example, the presence of pathogens usually triggers an M1-like response in which the macrophages recruit other immune cells and up-regulate their phagocytic activity. Other factors such as hypoxia will instead promote macrophages to adopt an M2-like phenotype, in which they mostly contribute to wound healing by scavenging debris and promoting angiogenesis. This behaviour is mostly beneficial. For example, following hindlimb ischemia, macrophages elicit an M2-like response clearing necrotic tissue and promoting revascularisation (Arras et al., 1998, Patel et al., 2013). However, in situations such as cancer or atherosclerosis, macrophages may wrongly adopt an M2-like response, resulting in pathological angiogenesis and thus disease progression rather than resolution. In cancer for example, tumour cells actively recruit macrophages and monocytes into their microenvironment by expressing attractants such as VEGF-A and CSF1 (Zhou et al., 2015, Leek et al., 2000, Sullivan and Pixley, 2014, Ueno et al., 2000). As a result, tumour-associated macrophages (TAMs) are usually found in close association with tumour cells. In addition, tumour cells secrete cytokines such as periostin, which polarise the TAMs towards the anti-inflammatory M2-like program (see **1.3.3.1**).

M2-like macrophages promote tumour progression in several ways. Firstly, they release immunosuppressive cytokines e.g. IL-10 (Wu et al., 2010). Secondly, they promote tumour angiogenesis by releasing multiple pro-angiogenic cytokines such as TNF-α and VEGF-A (Lewis et al., 2000, Leibovich et al., 1987), as well as metalloproteinases such as MMP-9. Accordingly, a higher number of TAMs often correlates with an increased tumour vascularisation (Bolat et al., 2006, Dirkx et al., 2006, Mantovani et al., 2006). Furthermore, tumour growth and metastasis are reduced in macrophage-deficient mice despite tumour initiation not being affected (Lin et al., 2001).

Macrophages are also at the centre of proliferative neovascular eye diseases. For instance, they are thought to promote pathological angiogenesis from the choriocapillaris into the sub-retinal space and retina in certain cases of AMD (Lim et al., 2012). Accordingly, an increased number of macrophages is found in patients with CNV (Jager et al., 2008, Hageman et al., 2001). Macrophages also promote neoangiogenesis in a laser-induced mouse model of CNV. Thus, macrophage depletion results in decreased lesion size and severity (Espinosa-Heidmann et al., 2003b). In comparison to tumour angiogenesis, macrophages are thought to elicit an inappropriate "wound-healing" or M2 response, which results in the secretion of pro-angiogenic molecule such as VEGF-A (Liu et al., 2013). Accordingly, VEGF-A expression levels correlate with the peak of macrophage recruitment (Sakurai et al., 2003), and macrophage depletion severely reduced VEGF-A levels in laser-treated retinas (Itaya et al., 2007). The macrophages are thought to be polarised towards an M2 response by the ingestion of debris of the damaged retinal pigment epithelium; nevertheless, the exact mechanism remains to be established (Liu et al., 2013).

1.4 Neural crest-mediated remodelling of the cardiovascular system

After the primitive cardiovasculature consisting of a heart and vascular tree has formed, the great vessels around the heart undergo remodelling to lay the foundation for transit from life *in utero* to postnatal life. Specifically, the embryonic circulation of all mammals bypasses the lungs and instead relies on the placenta for oxygenation; however, a switch to the pulmonary circulation at birth is essential to allow oxygen uptake through the lungs. To achieve this switch, vessel remodelling of two types is required: the pharyngeal arch arteries (PAAs) remodel to form the aortic arch, carotid arteries and smaller vessels, and the OFT septates into the base of the aorta and the pulmonary artery (**Figure 1.4C,D**). Both of these remodelling processes depend on a population of cells called the cardiac NCCs.

1.4.1 Neural crest

Cardiac NCCs, like other NCC populations, are a vertebrate-specific cell population that is derived from the dorsal part of the embryonic neural tube through epithelial-to-mesenchymal transition. Even though NCCs were already described in 1868 by Wilhelm His as the "*Zwischenstrang*" (intermediate cord) and were

subsequently renamed "neural crest" by Arthur Marshall in 1879, NCCs with specific functions in heart development were not discovered until the 1980s through transplantation and lineage tracing experiments in avian embryos by Margaret Kirby and colleagues (Kirby et al., 1983, Kirby, 1987, Creazzo et al., 1998). Thus, Kirby and colleagues described how NCCs delaminating from the neural tube between the otic placode and the 3rd somite colonise the embryonic pharyngeal arches and OFT of the heart. They further demonstrated that ablation of this NCC subset causes developmental defects that resemble common congenital heart defects in human patients, such as a common arterial trunk (CAT; also known as persistent truncus arteriosus, PTA). This groundbreaking research initiated an intense era of research to identify the molecular and cellular mechanisms that govern NCC-induced cardiovascular development and the role of NCCs in congenital heart disease (reviewed in Keyte and Hutson, 2012).

1.4.2 Cardiac NCCs enable PAA remodelling into the aortic arch

After cardiac NCCs have delaminated from the neural tube, they migrate ventrally into the circumpharyngeal ridge (**Figure 1.4A,B**). Here, they pause whilst the PAAs form by vasculogenesis (see **1.1.2.1**) to generate a bilateral series of artery pairs, which in the mouse occurs between E8.5 and E9.5. As the 1st and 2nd artery pairs remodel into the mandibular and hyoid arteries, respectively, the cardiac NCCs invade the pharyngeal arches in 3 streams to sequentially associate with the 3rd, the 4th and 6th PAA pairs, reflecting the order of artery formation along the rostrocaudal axis (Hiruma et al., 2002). Notably, current PAA nomenclature refers to the six artery pairs that exist in fish, as the existence of a 5th PAA pair in mammals has been contentious. Nevertheless, certain congenital malformations can only be explained by the persistence of a 5th PAA. Furthermore, a recent study demonstrated that in a small subset of human embryos a structure resembling a 5th PAA was detectable (Bamforth et al., 2013).

Having colonised the PAAs, which initially consist only of a sheath of ECs, the cardiac NCCs differentiate into SMCs (Bergwerff et al., 1998). This process, which occurs between E10.5 and E13.5 in the mouse, is thought to be important for subsequent PAA remodelling (**Figure 1.4C**).

The 3rd PAAs extend to form the right common carotid and basal part of the left internal carotid in both birds and mammals. In mammals, the right 4th artery regresses and becomes part of the right subclavian artery, whereas the left 4th artery persists and forms the segment of the aortic arch that connects the aortic sac to the descending aorta. Moreover, the proximal right 6th PAA contributes to the base of the pulmonary artery, whereas the distal segment regresses (Schneider and Moore, 2006). The left 6th PAA gives rise to the ductus arteriosus, an embryonic structure that connects the pulmonary artery with the descending aorta; this shunt allows blood from the right ventricle to bypass the lungs, because the fetal blood is oxygenated through the placenta. At birth, the ductus arteriosus collapses due to a rise in oxygen levels, and de-oxygenated blood is now able to enter the pulmonary circulation (Leonhardt et al., 2003). The non-functional vestige of the ductus arteriosus persists throughout life and is called *ligamentum arteriosus*.

Ultimately, the asymmetric remodelling of the PAAs in mammals gives rise to a vascular tree in which the aortic sac connects via the left 4th PAA to the descending aorta to form the left-looping aortic arch. In birds, remodelling of the 4th and 6th PAAs occurs in the reverse configuration (Wang et al., 2009): the right 4th artery remodels into the definitive aortic arch, the left 6th PAA forms the proximal segment of the pulmonary artery and the right 6th PAA forms the ductus arteriosus, which collapses at hatching. In contrast to mammals, the right 4th PAA persists and the aortic arch therefore curves to the right.

In both birds and mammals, formation of an asymmetric aortic arch and pulmonary artery is a pre-requisite for blood from the ventricles to enter two distinct circulations. Whilst the aortic arch directs the oxygenated blood into the systemic circulation, the pulmonary artery directs the de-oxygenated blood into the pulmonary circulation. Accordingly, defects in the remodelling process are often lethal or severely impair cardiovascular performance. When cardiac NCCs are ablated in chick or mouse embryos, the PAAs form normally, but regress or persist inappropriately (Kirby et al., 1983, Waldo et al., 1996, Porras and Brown, 2008). For example, a common defect in mouse mutants with abnormal cardiac NCC behaviour is the regression of the left 4th PAA. This defect results in an interrupted aortic arch (IAA) and is referred to as a type b interruption. Despite a multitude of mouse

models with defective cardiac NCC behaviour, only a limited number of the signalling pathways involved have been discovered, and the exact cellular interactions by which cardiac NCCs orchestrate PAA remodelling and survival remain incompletely understood

1.4.3 OFT remodelling into the base of the aorta and pulmonary artery

Congenital heart defects are a leading cause of perinatal mortality and morbidity, affecting 1% of all live births in the Western world (Hoffman and Kaplan, 2002). A CAT is a rare defect caused by faulty remodelling of the heart OFT during embryogenesis. The OFT is a transient embryonic structure at the arterial pole of the heart that initially functions as a conduit for blood flowing from the right ventricle into the aortic sac (**Figure 1.4B,D**). Subsequently, the OFT wall rotates and septates to generate the base of the ascending aorta and pulmonary trunk, which enables the separation of the arterial and venous circulation (**Figure 1.4D**). A failure of OFT septation during embryogenesis, therefore, results in inappropriate mixing of oxygenated and de-oxygenated blood at birth and has an unfavourable clinical prognosis, because surgical correction is difficult (Williams et al., 1999).

Initially, the OFT comprises a solitary tube, which extends from the arterial pole of the heart to the pericardial wall, where it becomes continuous with the aortic sac. At this stage, the OFT possesses a dog-leg bend, which allows the OFT to be separated into a proximal and distal part (reviewed in Anderson et al., 2003). The proximal part describes the section closest to the heart, which will eventually generate the ventricular outflow regions including the segment where the arterial valves are formed. The distal OFT, instead, refers to the part of the vessel, which will ultimately form the intrapericardial parts of the aorta and pulmonary artery.

During early development, when the OFT is first identifiable, it is simply lined by ECs and surrounded by a myocardial layer. The space in between the two layers is filled with an acellular "cardiac jelly" consisting of ECM components. Subsequently, this space is infiltrated by cells from several distinct sources, pushing the endothelium on either side of the tube towards to lumen. These swellings are termed the principal endocardial cushions and they extend the entire length of the OFT spiralling around each other due to the rotation of the OFT itself.

The endocardial cushions are critical for the subsequent septation (Markwald et al., 1981, Eisenberg and Markwald, 1995) and their formation and fusion relies on the interaction of three distinct cell types: cardiac NCCs, SHF-derived (**Figure 1.1**) cells and ECs. Thus, cardiac NCCs migrate from the PAAs into the distal endocardial cushions of the OFT in two streams. Due to their densely stained appearance in the centre of both endocardial cushions, they have historically also been referred to as "prongs" or "rods" (reviewed in Anderson et al., 2003). The colonisation of the OFT by cardiac NCCs also correlates with an endothelial-to-mesenchymal transition (endoMT) of the OFT endothelium, which provides additional mesenchymal cells for the endocardial cushions (Sugishita et al., 2004). Whilst the endocardial cushions expand due to the recruitment of the aforementioned cell populations, the aortic sac at the most distal part of the OFT also remodels. This generates a small transverse protrusion in the posterior wall between the fourth and sixth PAA, which is referred to as the aortico-pulmonary septum. When the endocardial cushions have swollen to a sufficient size, the ECs on opposing cushions abut enabling the fusion of the OFT endothelium in the centre of the OFT. This fusion begins in the distal OFT and progresses to the proximal part of the tract. Whilst it is currently not known what initiates the fusion of the ECs, it is interesting to note that the cardiac NCC "prongs" take on a "whorl"-like appearance at the site of ongoing OFT septation. The fusion of the endocardial cushions within the distal segment of the OFT and the connection of their distal surface to the aortic-pulmonary septum generates the intra-pericardial parts of the aorta and pulmonary artery by E11. In addition, the distal vessel walls remodel to adopt an arterial phenotype and eventually become completely septated. In contrast, the proximal OFT remains encased by a myocardial wall and the fused endocardial cushions are still distinguishable at this stage.

By E12.5 the proximal OFT can be divided into two parts, the medial and the proximal OFT, where the proximal part refers to the vessel segment closest to the heart. The two parts can be distinguished by the fact that two extra cushions, called the intercalated cushions, have formed in the opposite quadrants of the medial OFT, whereas the proximal OFT only contains the two principal cushions. Within the medial OFT, the fused principal cushions along with the intercalated cushions remodel to form the three arterial valve leaflets and sinuses in each vessel, whereas in the proximal OFT, the two principal endocardial cushions are still unfused at this

stage. Nevertheless, by E13.0 the proximal parts of the OFT have also fused, which relies on the recruitment of mesenchymal cells through the process of endoMT (Bai et al., 2013). In addition, whilst the medial OFT wall gradually loses its myocardial cuff and becomes arterialised, myocardial tissue is gradually added to the proximal OFT through a process called “myocardialisation” (van den Hoff et al., 1999). These myocardial cells also migrate into the septal bridge, which transforms it into a muscular septum. Eventually, the leading edge of the muscular septum becomes attached to the roof of the right ventricle. This attachment gradually remodels to finally connect the septal bridge to the interventricular septum, fusing the base of the aorta to the left ventricle and the base of the pulmonary artery to the right ventricle. Thus, blood leaving the left and right ventricle enters distinct circulations.

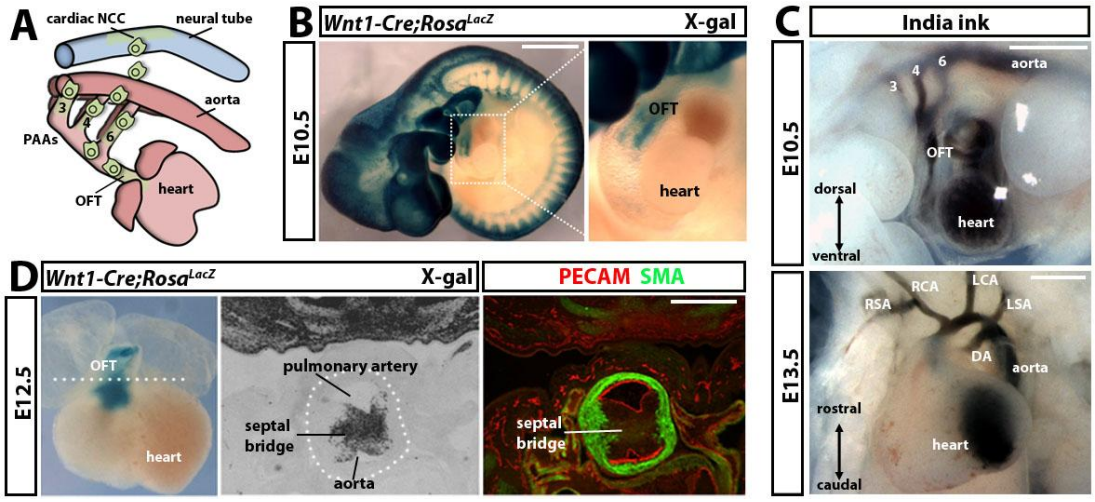

Figure 1.4. Cardiac NCC contribution to murine OFT and PAA development.

Schematic representation of cardiac NCC migration **(A)**. Visualisation of NCCs and their derivatives in an E10.5 *Wnt1-Cre;Rosa*^{LacZ} mouse embryo **(B)**. The higher magnification image shows two prongs of cardiac NCCs in the OFT. PAA remodeling into the aortic arch **(C)**. Ink injections into embryonic hearts at E10.5 and E13.5 show the 3rd, 4th, and 6th PAAs and their remodelled derivatives. Cardiac NCC colonisation of the E12.5 OFT **(D)**. Xgal staining of an E12.5 *Wnt1-Cre;Rosa*^{LacZ} heart shows accumulation of cells from the cardiac NCC lineage in the OFT; the dotted line indicates the level at which a section was taken to illustrate the position of the cardiac NCCs within the OFT in the adjacent panel. Double staining with the endothelial marker PECAM and the myocyte marker SMA illustrates OFT anatomy at E12.5. Scale bars: 1 mm **(B)**, 500 μm **(C,D)**.

1.4.4 Signalling pathways in cardiac NCC-mediated vascular remodelling

A number of genes involved in cardiac NCC-induced PAA remodelling and OFT septation have been uncovered through the analysis of mouse mutants with congenital heart defects (reviewed in Gruber and Epstein, 2004). Several key genetic pathways activated by members of the TGFβ, fibroblast growth factor (FGF), VEGF-A and SEMA3 families of secreted signalling molecules regulate cardiac NCC induction or their migration, survival and differentiation.

The TGFβ superfamily comprises a large group of secreted polypeptides that includes the bona fide TGFβs and the bone morphogenetic proteins (BMPs), with both types of proteins shown to play a role in cardiac NCC-regulated vascular remodelling (reviewed in Keyte and Hutson, 2012). BMP2 and BMP4 are generally required for NCC induction, migration, differentiation and survival, and knockout studies of their receptors have shed light into the role of BMP signalling in regulating cardiac NCC behaviour. For instance, the BMP receptor ALK2 is required by cardiac NCCs for their migration into the PAAs and the OFT, and, accordingly, the NCC-specific ALK2 deletion results in CAT and IAA (Kaartinen et al., 2004). In contrast, the NCC-specific deletion of the alternative BMP receptor BMPR1A does not affect cardiac NCC migration, but impairs endocardial cushion formation and consequently results in an unseptated OFT (Stottmann et al., 2004).

TGFβ2 appears to be particularly important for cardiac NCC-mediated vascular remodelling. Thus, addition of exogenous TGFβ2 to whole-embryo cultures causes OFT and aortic arch remodelling defects (Kubalak et al., 2002). Moreover, TGFβ2 knockout mice have defects in the development of several tissues, including the OFT and the aortic arch; in contrast, similar defects are not observed in TGFβ1 and TGFβ3 knockouts (Sanford et al., 1997).

TGFβ signalling may also have a cell autonomous role in cardiac NCCs. Thus, the loss of TGFβ receptor 2 (TGFβR2) in cardiac NCCs prevents their differentiation into myocytes and therefore perturbs remodelling of both the OFT and PAAs in mice (Wurdak et al., 2005). Furthermore, loss of the TGFβ receptor ALK5 in the NCC lineage also causes PAA and OFT defects by impairing post-migratory cardiac NCC survival (Wang et al., 2006a).

To date, twenty FGFs have been described, all of which are small, heparin-binding secreted proteins. Nevertheless, out of these, only FGF8 has been implicated in cardiac NCC development (Frank et al., 2002). Even though FGF8 deletion causes embryonic death at mid-gastrulation (Sun et al., 1999), FGF8 hypomorphic mice secrete enough FGF8 to survive gastrulation elucidating the role of this molecule in cardiac NCC function. Thus, these mice have defective cardiac NCC migration into the pharyngeal arches (Frank et al., 2002), as FGF8 is secreted by the pharyngeal ectoderm and endoderm as a guidance cue for migrating cardiac NCCs (Sato et al., 2011). It also promotes the survival of the cardiac NCCs that colonise the 4th PAAs (Abu-Issa et al., 2002, Macatee et al., 2003). Accordingly, the conditional FGF8 deletion in pharyngeal ectoderm impairs 4th PAA formation, whilst conditional deletion in the endoderm prevents OFT septation (Park et al., 2006).

VEGF-A is a secreted polypeptide most commonly studied in regard to its critical role in vasculogenesis, angiogenesis and arteriogenesis (see **1.2.1**). In addition, VEGF-A has been reported to act as a guidance cue for cranial NCCs that invade the 2nd PAAs to contribute to craniofacial tissues (McLennan et al., 2010). In contrast, VEGF-A is thought to not play a major role in cardiac NCC migration (Stalmans et al., 2003, Kirby and Hutson, 2010). Nevertheless, genetic studies in the mouse have implicated specific isoforms of VEGF-A in OFT and PAA remodelling. Thus, the exclusive expression of VEGF120 at the expense of VEGF164 and VEGF188 in *Vegfa*$^{120/120}$ mice, or the exclusive expression of VEGF188 at the expense of VEGF120 and VEGF164 in *Vegfa*$^{188/188}$ mice, has revealed an essential role for VEGF164 in OFT and PAA remodelling (Stalmans et al., 2003). Thus, similar cardiac and aortic arch malformations are observed in most *Vegfa*$^{120/120}$ and some *Vegfa*$^{188/188}$ mice, with the former suffering additional fatal cardiac defects. Aortic arch malformations include IAA type b, double aortic arch, right-sided aortic arch and different aberrations in the formation of the carotid and subclavian arteries, while cardiac defects arising from defective OFT septation included Tetralogy of Fallot, CAT, hypoplasia of the pulmonary trunk and VSDs (Stalmans et al., 2003).

Given that cardiac NCC migration is thought to be at least grossly normal in VEGF-A isoform-deficient mice (Stalmans et al., 2003, Kirby and Hutson, 2010), the mechanistic reasons for OFT and PAA defects in these mice are not well understood.

The prevailing model suggests that these defects are due to loss of VEGF164 signalling through NRP1 in OFT endothelium, because the complete absence of NRP1, or genetic ablation specifically of endothelial NRP1, impairs OFT and PAA remodelling (Kawasaki et al., 1999, Gu et al., 2003). However, I recently contributed to a study, which demonstrated that mice with a mutated NRP1 receptor unable to bind VEGF-A are viable (Fantin et al., 2014) (see **Chapter 3**), an observation that is not compatible with the hypothesis that VEGF-A signals through NRP1 in endothelium to enable OFT septation, as defective OFT septation should cause lethality at birth. It is, therefore, likely that VEGF-A signals in the OFT through another receptor, such as VEGFR2, and that endothelial NRP1 acts as a receptor for another ligand. However, prior to my thesis work, neither hypothesis had been tested experimentally (see **Chapter 3**).

SEMA3 proteins are secreted glycoproteins best known for their role in axon guidance (Rohm et al., 2000, Ruediger et al., 2013). One particular family member termed SEMA3C is secreted within the OFT and PAAs at the time when cardiac NCCs migrate into these tissues, and loss of SEMA3C causes CAT and IAA (Feiner et al., 2001). It has been proposed that SEMA3C acts as an attractive signal for cardiac NCCs, as knockdown of NRP1 in cardiac NCCs perturbs their migration in chick (Toyofuku et al., 2008). Agreeing with a similar role for SEMA3C in mammals, mice lacking semaphorin signalling through both NRP1 and NRP2 also have aortic arch and OFT defects (Gu et al., 2003). However, experimental proof for a role of NRPs in SEMA3C-induced cardiac NCC migration in mammals is still lacking.

1.5 Models of blood vessel development

Abnormal blood vessel growth or function is the cause of many prevalent, yet devastating diseases such as diabetic retinopathy or atherosclerosis. In addition, stimulating blood vessel growth to revascularise ischemic tissues, for example after stroke or myocardial infarction, has great therapeutic potential. In accordance, there is a great need to understand the cellular functions and signalling pathways involved in vascular biology. There are currently several mouse models, which are exquisitely suited to analyse particular aspects of vessel growth *in vivo*. In the following passages, I shall describe three of these models, which I have all used in my thesis: First, the embryonic hindbrain as a model to study embryonic angiogenesis; second, the retina as a model of postnatal developmental angiogenesis; and third, the oxygen-induced retinopathy (OIR) model as a method to study pathological angiogenesis.

1.5.1 Embryonic hindbrain

1.5.1.1 Hindbrain vascularisation

The mouse hindbrain is vascularised by angiogenesis in a highly stereotypical fashion (Ruhrberg and Bautch, 2013, Plein et al., 2015b). At E9.5, the first blood vessels enter the neuroectodermal tissue by sprouting from the underlying perineural vascular network. These sprouts break through the pial membrane and sprout radially into the hindbrain parenchyma in response to VEGF-A secreted by neural progenitors (Breier et al., 1992, Haigh et al., 2003, Raab et al., 2004). By E10.5, the vessel sprouts reach the subventricular zone, where they change their direction of growth by ~90 degrees to grow laterally. The vessels then continue sprouting additional vessels, which then fuse with adjacent sprouts forming a honey-comb shaped vascular network termed the subventricular vascular plexus (SVP) (Ruhrberg et al., 2002, Fantin et al., 2010) (**Figure 1.5A**). This vascular network can easily be imaged between E10.5 and E12.5 after dissecting the hindbrain, staining the endothelium with a lectin such as isolectin B4 (IB4) or antibodies against CD31 (PECAM), for example, and then flatmounting and imaging the hindbrain (**Figure 1.5A**), as published previously (Plein et al., 2015b, Fantin et al., 2013c) (see **Appendix** – co-authored publications).

1.5.1.2 Advantages of the hindbrain as a model system for angiogenesis

The embryonic mouse hindbrain provides several advantages as a model system to study angiogenesis. As described above, the hindbrain vasculature forms in a highly stereotypical fashion to generate a vascular plexus of a simple geometric nature, including a one dimensional (1D) pattern of radial vessels on the pial side, and a 2D network of SVP vessels on the ventricular side (Ruhrberg et al., 2002, Fantin et al., 2013c). This arrangement greatly facilitates the quantitation of vessel parameters, such as vessel number, diameter, branchpoints or filopodia number (Ruhrberg et al., 2002, Fantin et al., 2013c). In contrast, the vascularisation of organs such as the kidney and lung occurs in a 3D and less stereotypical fashion, complicating quantification.

In addition, the comparatively early vascularisation of the hindbrain from E9.5 onwards permits the analysis of mutants that are embryonic lethal, as long as they survive beyond E10.5. For example, mouse embryos lacking NRP1 are lethal around E12.5 on an outbred background (Kawasaki et al., 1999) and can be analysed easily with the hindbrain model (Gerhardt et al., 2004, Fantin et al., 2013a).

Another advantage of the hindbrain model is that the cellular interactions, which govern tissue vascularisation, are less complex than those in perinatal models. Accordingly, the angiogenic hindbrain environment predominantly contains neural progenitors alongside few neural subtypes and microglia. The angiogenic hindbrain also forms a particularly homogenous capillary bed suitable for accurate quantitative analysis, because arteriovenous differentiation and vascular remodelling occur after SVP formation.

1.5.2 Postnatal retina

1.5.2.1 Retinal vascularisation

Another well established model of developmental angiogenesis is the postnatal murine retina (Gariano and Gardner, 2005). Thus, in mice, the retina is vascularised by sprouting angiogenesis from postnatal day (P) 0 onwards, when vessels from the artery at the optic nerve head spread radially just underneath the inner limiting membrane, the vitreal surface of the retina (**Figure 1.5B**) (Connolly et

al., 1988). This is in contrast to humans, where retinal vascularisation begins at 36 weeks of gestation and is complete at birth (reviewed in Stahl et al., 2010). In contrast to the hindbrain, retinal angiogenesis and arterial specification occur concomitantly in the retina, resulting in the remodelling of the capillary bed soon after it has formed (Fruttiger, 2007). The extending angiogenic sprouts of the retina rely on astrocytes, which form a mesh preceding the vascular front and guide growing vessels by providing components of the ECM (Dorrell et al., 2009, Scott et al., 2010, Stenzel et al., 2011). The vascular network continues sprouting to form a dense planar network, which reaches the periphery of the retina around P7. This network also termed the primary plexus extends in a 2D fashion, as VEGF-A in the underlying layers is titrated by VEGFR2 expressed by the developing neurons (Okabe et al., 2014). Nevertheless, after P7 VEGFR2 expression in the underlying layers drops and the retinal vessels start sprouting into the deeper layers forming first the deep vascular plexus and then the intermediary plexus. All three plexi are completed by P21 (Milde et al., 2013). The primary plexus can easily be analysed after dissecting as published previously (Powner et al., 2012), staining vessels with a lectin such as IB4 or antibodies, and then flatmounting and imaging the retina (**Figure 1.5B**).

1.5.2.2 Advantages of the retina as a model system for postnatal angiogenesis

In comparison to the SVP of the hindbrain, the primary plexus of the retina develops in a 2D manner. This greatly facilitates the visualisation of the vasculature in flatmounted dissected retinas and the analysis of vascular phenotypes. Thus, vascular deficiencies can manifest as a reduced extension of the vascular plexus indicative of impaired EC proliferation or migration, as well as decreased branching suggesting defects in tip cell specification. In contrast to the hindbrain, in the retina arteriovenous specification occurs concomitantly with the formation of the capillary vessel plexus. Whilst this feature complicates the quantitation of angiogenic sprouting, it allows the analysis of arteriovenous differentiation. Thus, the retinal model has been used to demonstrate the importance of molecules such as SOX17 and the VEGF-A/NRP1 pathway for arteriovenous specification (Corada et al., 2013, Stalmans et al., 2002, Fantin et al., 2014). A specific feature of the murine retina as a model for angiogenesis is that vascularisation occurs postnatally, and thus this model

is not suitable for the analysis of mutants that are lethal antenatally. Nevertheless, certain genes for which the full knockout is embryonic lethal can be investigated postnatally by using tissue-or ligand-specific mutations, or deleting the gene postnatally (see **2.2.1.5** and **2.2.1.6**). For instance, *Nrp1*-nulls die at E12.5 (Kawasaki et al., 1999), whereas *Nrp1*$^{Vegfa/Vegfa}$ mutants survive until P14 (Fantin et al., 2014). Furthermore, endothelial-specific NRP1 mutants die perinatally (Gu et al., 2003); however, the postnatal deletion of endothelial NRP1 (*Pdgfb-Cre*^{ERT}*;Nrp1*$^{fl/fl}$) allowed the demonstration that NRP1 is required for angiogenesis in the postnatal retina (Raimondi et al., 2014).

The fact that the retina is vascularised postnatally also has the advantage that it allows the manipulation of vascular development with compounds and environmental factors. For instance, the retina has been used to show that Notch and ABL inhibitors are important for angiogenesis (Suchting et al., 2007, Raimondi et al., 2014). Furthermore, oxygen levels have been shown to affect retinal vascularisation by modifying VEGF-A levels (Shortt et al., 2004, McColm et al., 2004, Scott et al., 2010) (see **1.5.2.3**).

1.5.2.3 The retina as a model for pathological angiogenesis: Oxygen-induced retinopathy (OIR)

Besides being a model for normal angiogenesis, the mouse retina can also be used as a tool to investigate pathological angiogenesis. In the OIR model, P7 pups are subjected to hyperoxia (>80% oxygen) for five days, which results in the regression of the vessels within the central retina (vaso-obliteration) (**Figure 1.5C**). Thus, the increase in the partial pressure of oxygen results in vasoconstriction, as well as capillary regression to regulate oxygen levels. Subsequently, the pups are returned to normoxia (20% oxygen) for six days (P12-P17), which renders the vaso-obliterated area of the retina hypoxic and promotes the secretion of pro-angiogenic factors such as VEGF-A from Müller and glial cells (Ozaki et al., 1999). This excess of pro-angiogenic factors induces the formation of normal as well as abnormal neovascular tufts (**Figure 1.5C**) (Alon et al., 1995, Scott et al., 2010, Pierce et al., 1995). These vascular tufts extend into the normally avascular vitreous and resemble neovascular lesions associated with retinopathy of prematurity. Thus, premature

babies, which are born before their retinas are fully vascularised, are often placed into high oxygen chambers to provide adequate oxygenation despite their immature lungs (reviewed in Tin and Gupta, 2007). Nevertheless, as seen in the OIR model the high oxygen levels cause vaso-obliteration and thus often result in the formation of neovascular lesions once the infant is returned to ambient oxygen levels (Chen and Smith, 2007, Pau, 2008, Phelps, 1995).

The OIR model thus presents an excellent model to analyse vessel regression and hypoxia-induced vessel formation, which is relevant to human disease. Vessels can be analysed easily by staining with IB4 or antibodies against endothelial epitopes, flatmounting and imaging (**Figure 1.5C**).

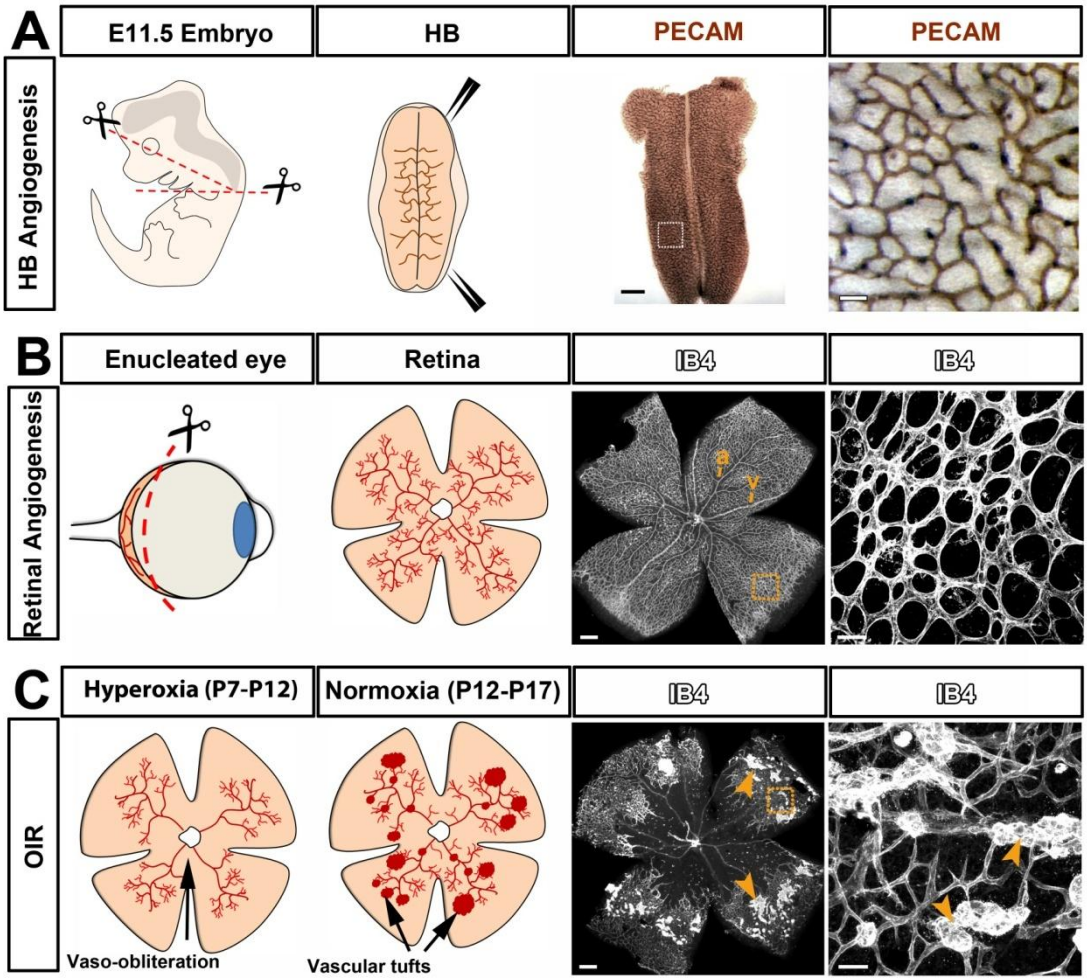

Figure 1.5. Mouse models of developmental and pathological angiogenesis

Hindbrain model: Schematic representation of hindbrain dissection from E12.5 embryo. Low and high magnification of E12.5 hindbrain immunolabelled for PECAM **(A)**. Retina model: Schematic representation of P7 eye dissection and retina. Low and high magnification of P7 retina immunolabelled with IB4 **(B)**. OIR model: Schematic representation of oxygen induced vaso-obliteration and vascular tufts formed in normoxia. Low and high magnification of P17 retina following OIR immunolabelled with IB4. Arrowheads indicate neovascular tufts. HB: hindbrain, a: artery, v: vein. Scale bars: 250 µm, 50 µm **(A)**; 200 µm, 20 µm **(B,C)**.

1.6 Aims of this Study

The formation of the vasculature is critical for life of higher vertebrates and relies on complex cellular as well as molecular interactions. The aims of my PhD research have been to contribute to our understanding of cardiovascular development by firstly investigating the role of the transmembrane receptor NRP1 in angiogenesis and cardiac OFT remodelling, and secondly by examining whether endothelial labelling of the *Csf1r-Cre* transgene indicates the contribution of a novel type of vascular precursor to angiogenesis.

Nrp1 knockout mice display severe cardiovascular defects, such as impaired angiogenesis and unseptated OFTs (see **1.2.3**) (Kawasaki et al., 1999). The main consensus by which NRP1 functions during angiogenesis was that endothelial NRP1 binds to VEGF-A, which enhances VEGF-A signalling through VEGFR2 (Soker et al., 2002). Nevertheless, NRP1 is also expressed by non-ECs (e.g. Tillo et al., 2015, Fantin et al., 2010). Furthermore, previous observations of mouse mutants with defective VEGF-A binding to NRP1 ($Nrp1^{Vegfa/Vegfa}$) by our group had revealed that these mice are viable; however, they demonstrated increased perinatal mortality. Thus, using cell type-specific NRP1 mouse mutants my first aim was to elucidate the function of non-endothelial NRP1 during vascular development by analysing the vascular phenotypes of these mice (see **Chapter 3**). In addition, I sought to investigate the cause underlying the reduced survival of $Nrp1^{Vegfa/Vegfa}$ mice after birth (see **Chapter 3**).

NRP1 mutants also display defective OFT remodelling, which was previously attributed to VEGF-A signalling through NRP1 on the OFT endothelium and cardiac NCC-derived NRP1 being essential for the SEMA3C-mediated migration of these cells into the OFT (Gu et al., 2003, Toyofuku et al., 2008). By analysing cell type- and ligand-specific *Nrp1* mutants, my second aim has been to understand the role of endothelial versus cardiac NCC-derived NRP1, and SEMA3C versus VEGF-A binding to NRP1 during OFT remodelling (see **Chapter 4**). Furthermore, by examining serial OFT sections of these mutants, I have sought to understand which specific aspect of OFT septation was defective, including endothelial fusion, endoMT and cardiac NCC migration.

Preliminary observations by Dr Fantin, a prior PhD student in the Ruhrberg lab, had shown that a *Csf1r-Cre* transgene could be used to lineage trace a subset of ECs. This finding was reminiscent of a previous publication by Kubota *et al*. (2011), which suggested that *P0-Cre* labelled the vascular endothelium, because the transgene was targeting a tissue-resident vascular progenitor (Kubota et al., 2011). Thus, my third aim was to substantiate Dr. Fantin's observations and relate them to the work of Kubota *et al*. (2011) (see **Chapter 5**). I, therefore, carried out *Csf1r-Cre* lineage tracing in two tissues undergoing developmental angiogenesis: the embryonic hindbrain and postnatal retina (see **1.5**). I further investigated the origin and reliability of endothelial lineage tracing with *Csf1r-Cre* by analysing CSF1R expression patterns and examining additional *Csf1r-Cre* transgenes and alternative lineage reporter alleles. Furthermore, I analysed whether macrophages contributed to the endothelium during angiogenesis by examining *Csf1r-Cre* labelling in mice lacking macrophages (*Pu.1*$^{-/-}$). Finally, I examined whether the *Csf1r-Cre* lineage trace labelled vascular precursor cells similar to those labelled by the *P0-Cre* transgene or isolated from the blood using EPC-specific markers.

Chapter 2 MATERIALS AND METHODS

2.1 Materials

2.1.1 General Laboratory Materials

All chemicals were obtained from Sigma Aldrich, except where indicated otherwise. Glassware was obtained from VWR International and plastic items were purchased from Corning or Nunc.

2.1.2 General Laboratory Solutions

Water was used after purification by a MilliRo 15 Water Purification System (Millipore) and, where necessary, water was further purified using the Milli-Q reagent Grade Water Ultrafiltration System (Millipore). RNAse and DNAse-free water was supplied by Sigma and absolute ethanol, methanol and isopropanol were obtained from Fischer Scientific.

1X PBS	137 mM NaCl, 3 mM KCl, 10 mM Na_2HPO_4, 1.8 mM KH_2PO_4, pH 7.2
4% PFA	4% (w/v) formaldehyde, prepared freshly from paraformaldehyde, in 1X PBS
1X PBT	1X PBS + 0.1% (v/v) Triton X-100
1X TE	10 mM Tris-HCl, 1 mM EDTA, pH 8.0
1X TAE	40 mM Tris-acetate, 1 mM EDTA, pH 8.0
1X TBS	25 mM Tris pH 7.5, 150 mM NaCl, 3 mM KCl

2.2 Methods

2.2.1 Animal Methods

All animal research was carried out according to institutional and United Kingdom Home Office guidelines.

2.2.1.1 Animal Maintenance and Husbandry

To generate embryos of a defined gestational age, mice were paired in the evening and the presence of a vaginal plug the following morning was defined as E0.5.

2.2.1.2 Genetic mouse strains

All mice were on mixed CD1 and C57Bl/6 genetic backgrounds. Please see **table 2.1** for details on the genetic mouse strains used.

Table 2.1: Genetic mouse strains and published reference

Genetic mutation	**Reference**
Nrp1-null (*Nrp1*$^{-/-}$)	(Kitsukawa et al., 1997)
Nrp1 flox (*Nrp1*$^{fl/fl}$)	(Gu et al., 2003)
Nrp1$^{Sema/Sema}$	(Gu et al., 2002)
Nrp1$^{Vegfa/Vegfa}$	(Fantin et al., 2014)
Nrp2-null (*Nrp2*$^{-/-}$)	(Giger et al., 2000)
Plxnd1-null (*Plxnd1*$^{-/-}$)	(Gitler et al., 2004)
Tie2-Cre	(Kisanuki et al., 2001)
Wnt1-Cre	(Jiang et al., 2000)
Nes-Cre	(Petersen et al., 2002)
Sm22a-Cre	(Holtwick et al., 2002)
Csf1r-Cre	(Deng et al., 2010)
Csf1r-eGFP	(Sasmono et al., 2003)
Csf1r-Cre^{ERT}	(Qian et al., 2011)
Pu.1 null (*Pu.1*$^{-/-}$)	(McKercher et al., 1996)
Vegfa$^{120/120}$	(Ruhrberg et al., 2002)
Vegfa^{LacZ}	(Miquerol et al., 1999)
Vegfa$^{fl/fl}$	(Gerber et al., 1999)
Sema3c flox (*Sema3c*$^{fl/fl}$)	Unpublished
Rosa$^{Yfp/Dta/LacZ}$	(Soriano, 1999, Srinivas et al., 2001, Ivanova et al., 2005)

2.2.1.3 Tissue-specific gene targeting

To delete genes in specific tissues, a genetic approach based on the *Cre/lox* recombination system was used (reviewed in Nagy, 2000). This method utilises the properties of the enzyme CRE recombinase, which was initially discovered in the P1 bacteriophage. This enzyme catalyses the recombination between its two 34 bp recognition sites, which are called *loxP* (locus of recombination) sites (Hamilton and Abremski, 1984). By flanking a DNA sequence with these sites, the enzyme is able to bind and create either an inversion or deletion of the sequence depending on the orientation of the *loxP* sites. This recombination can be made tissue-specific by creating a *Cre* transgene under the control of a tissue-specific promoter. Thus, the enzyme will only be expressed and sequence deletion will only occur in the cell type of interest. For instance, to delete *Nrp1* in ECs, mice with a *Cre* transgene under the control of the endothelial *Tie2* promoter (Kisanuki et al., 2001) were mated to mice, which were heterozygous for the *Nrp1*-null allele. The *Tie2-Cre;Nrp1*$^{+/-}$ offspring were then mated with mice homozygous for the "floxed" NRP1 allele (*Nrp1*$^{fl/fl}$) to generate *Tie2-Cre;Nrp1*$^{fl/-}$ mice.

2.2.1.4 Tissue-specific lineage trace

A similar approach was utilised to perform a tissue-specific lineage trace. In this case mice containing a *Cre* transgene such as *Tie2-Cre* or *Csf1r-Cre* were mated to mice possessing the *Rosa*^{Yfp} (Soriano, 1999) or *Rosa*^{LacZ} reporter allele. These alleles of the *Rosa* locus contain the sequence for the enhanced yellow fluorescent protein (*Yfp*) or β galactosidase enzyme (*lacZ)* downstream of a stop-cassette flanked by two *loxP* sites, which has been knocked in to the constitutively expressed *Rosa26* locus. Thus, YFP and β galactosidase are only expressed in cells once the *Cre* transgene has excised the stop codon. Furthermore, as this genetic event is permanent, the progeny of these cells are also YFP/ β galactosidase-positive.

2.2.1.5 Cre-mediated in vivo genetic ablation

In order to ablate a specific cell lineage, *Cre* transgenes such as *Csf1r-Cre* were crossed to mice containing the *Rosa*^{Dta} allele. Analogous to the *Rosa*^{Yfp} or *Rosa*^{LacZ} reporter, this allele only expresses the diphtheria toxin fragment A (DTA)

after *Cre*-mediated stop cassette excision (Ivanova et al., 2005). The expression of the toxin results in cell death and thus allows the *in vivo* ablation of a transgene-specific lineage (Breitman et al., 1990, Ivanova et al., 2005).

2.2.1.6 Temporally regulated Cre activation

To temporally control the expression of the *Csf1r-Cre*, we obtained mice containing the *Csf1r-Cre^{ERT}* transgene. This transgene consists of a *Cre* mutant murine oestrogen receptor (*ERT*) double-fusion protein (*Cre^{ERT}*) under the control of the *Csf1r* promoter (see **2.2.1.3**). Unlike the normal oestrogen receptor, which binds to 17'-oestradiol, the CRE^{ERT} recombinase binds to the synthetic compound 4-hydroxytamoxifen (tamoxifen) (Danielian et al., 1998). CRE^{ERT} is normally sequestered within the cytoplasm by the cytoplasmic protein, HSP90 (Mattioni et al., 1994, Picard, 1994); however, upon tamoxifen binding to the receptor, this interaction is prevented and thus allows the enzyme to translocate to the nucleus. Therefore, *Cre*-mediated DNA recombination will only occur once tamoxifen has been administered to the mouse. To analyse the postnatal lineage trace of *Csf1r-Cre^{ERT}*, I collaborated with Dr Alessandro Fantin, who prepared the tamoxifen solution by dissolving 4-OHT in absolute ethanol at 50 mg/ml and diluting it in peanut oil to 5 mg/ml. A volume of 25 µl per gram of body weight was injected intraperitoneally into *Csf1r-Cre^{ERT};Rosa^{Yfp}* pups from P4-P6.

2.2.1.7 Compound mutant mice

To generate compound *Nrp1$^{Sema/Sema}$;Nrp2$^{-/-}$* mouse mutants, mice heterozygous for the *Nrp1^{Sema}* mutation were crossed to mice heterozygous for the *Nrp2*-null allele. Subsequently, offspring heterozygous for both mutations were mated providing mice homozygous for both mutant alleles at a probability of 1/16. To generate *Wnt1-Cre;Nrp1$^{fl/fl}$;Nrp2$^{-/-}$* compound mutants, mice carrying the *Wnt1-Cre* transgene were mated the mice heterozygous for the *Nrp2*-null allele. The resulting offspring, which carried both the *Wnt1-Cre* and the *Nrp2*-null allele, were then mated to mice homozygous for the conditional *Nrp1* allele (*Nrp1$^{fl/fl}$*). By crossing offspring from this cross to *Nrp2$^{+/-}$;Nrp1$^{fl/+}$* compound mutants, *Wnt1-Cre;Nrp1$^{fl/fl}$Nrp2$^{-/-}$* were generated at a possibility of 1/16.

2.2.1.8 Genotyping of mouse strains

The majority of genotyping was performed by Laura Denti with the assistance of Andy Joyce and Valentina Senatore from the Ruhrberg group. Where conditional *Sema3c* (*Sema3c*$^{fl/fl}$) mice were used, genotyping was performed by Dr Amelie Calmont from Prof Pete Scambler's group (ICH, UCL). DNA was extracted either from embryonic tail snips or adult ear punches using a previously published method (Laird et al., 1991). Briefly, cells were lysed by incubating them overnight at 55°C with gentle agitation in 500 µl of lysis buffer (100 mM Tris-HCl pH 8.5, 5 mM EDTA, 0.2% SDS, 200 mM NaCl) with freshly added proteinase K (100 µg/ml). Following enzymatic digestion, DNA was precipitated by adding 1 ml of 100% ethanol, and collected following a 3 min centrifugation at 13000 rpm. DNA was resuspended in 70% ethanol and collected following another centrifugation using the aforementioned conditions. Subsequently, DNA was air-dried for 10 min at RT and reconstituted in 100 µl TBE buffer (2 mM Tris pH 8.0, 0.2 mM EDTA) for 5-30 min at 55°C.

The genomic DNA was amplified by PCR using primers specific to the DNA sequence of interest (see **table 2.2**) on a BioRad C1000 Touch Thermal Cycler. Per PCR reaction, 2 µl of DNA were added to 8 µl Megamix (Microzone, containing *Taq* polymerase, 1.1X reaction buffer, 220 µM dNTPs, loading dye) and 0.1 µg of both the forward and reverse primer using the relevant annealing temperature and number of amplification cycles (see **table 2.3**, **2.4**).

The PCR products were analysed using electrophoresis through a 2% (w/v) agarose (BDH Electran) in TAE gel containing 2 µl of nucleic acid staining solution, RedSafe (iNtRON). For each reaction, a negative control consisting of 2 µl sterile water instead of the DNA solution was used, as well as a positive control comprising of 2 µl previously validated DNA.

Table 2.2: Oligonucleotide primers used for genotyping

Gene	Primer	Sequence
Nrp1, *Nrp1^{fl}*	NP1Neo	5'-CGTGATATTGCTGAAGAGCTTGGC-3'
	NP1F	5'-CAATGACACTGACCAGGCTTATCATC-3'
	NP1R	5'-GATTTTTATGGTCCCGCCACATTTGTC-3'
Nrp1^{Sema}	P1	5'-AGGCCAATCAAAGTCCTGAAAGACAGTCCC-3'
	P2	5'-AAACCCCCTCAATTGATGTTAACACAGCCC-3'
Nrp1^{Vegfa}	Zac1	5'-ATTGCTGGGATTACAGGCGTGAACC-3'
	Zac2	5'-GTGTGCTGATCTGGGAAGGTAGGCAG-3'
	Zac3	5'-GGAGACGGGAGCAACCAGAGTGC-3'
Nrp2	NP2Neo	5'-CAGTGACAACGTCGAGCACAG-3'
	NP2F	5'-TCAGGACACGAAGTGAGAAGC-3'
	NP2R	5'-GCTCAATGTAGCTAAGTGGAGGG-3'
Plxnd1	PD1WF	5'-GGTTAAGGTCGAAGGTGAAGAGCTT-3'
	PD1WR	5'-ACCGCAGAACCGGTCACCGTGTT-3'
	PD1MF	5'-CTCTCGCCGCCTCC-3'
	PD1MR	5'-CCATTGCTCAGCGGTGCTGTCCATC-3'
Tie2-Cre	Tie2Pro	5'-CCCTGTGCTCAGACAGAAATGAGA-3'
	Cre2	5'-GTGGCAGATGGCGCGGCAACACCATT-3'
Wnt1-Cre	Wnt1F	5'-TAAGAGGCCTATAAGAGGCGG-3'
	Wnt12	5'-GTGGCAGATGGCGCGGCAACACCATT-3'
Nes-Cre	Nes8F1	5'-GAATACCCTCGCTTCAGCTC-3'
	CreB	5'-GCATTTTCCAGGTATGCTCAG-3'
Csf1r-Cre, *Csf1r-Cre^{ERT}* *Sm22a-Cre*	FMS-F	5'-GCCACCATGTGTCCGTGCTT-3'
	FMS-R	5'-ACCCAGAGCCCCCACAGATA-3'
Csf1r-eGFP	EGFP-F	5'-CCAGGAGCGCACCATCTTCT-3'
	EGFP-R	5'-GTAGTGGTTGTCGGGCAGCAG-3'
Pu.1	KO2	5'-GCCCCGGATGTGCTTCCCTTATCAAAC-3'

	920	5’-GCCCCGGATGTGCTTCCCTTATCAAAC-3’
Vegfa^{120}	Neo2	5’-CGCACGGGTGTTGGGTCGTTTGTTCGG-3’
	120F2	5’-CAGTCTATTGCCTCCTGACCTTCAGGGTC-3’
	120E2	5’-TTCAGAGCGGAGAAAGCATTTGTTTGTCCA-3’
Vegfa^{LacZ}	120R2	5’-CTTGCGTCCACACCGTCACATTAAGTCAC-3’
	V-WT	5’-ATGTGACAAGCCAAGGCGGTG-3’
	V-Ex8	5’-TGGCGATTTAGCAGCAGATA-3’
Vegfa^{fl}	V-LacZ	5’-GGTAGGGGTTTTTCACAGAC-3’
	VF-F	5’-CCTGGCCCTCAAGTACACCTT-3’
	VF-R	5’-TCCGTACGACGCATTTCTAG-3’
Sema3c^{fl}	SC-F	5’-GAATCTGGCAAAGGACGATG-3’
	SC-R	5’-GACCACTGGGCTTGAGAGAG-3’
Rosa$^{Yfp/LacZ/Dta}$	WT F1	5’-AAAGTCGCTCTGAGTTGTTAT-3’
	WT R1	5’-GGAGCGGGAGAAATGGATATG-3’
	KO R1	5’-GCGAAGAGTTTGTCCTCAACC-3’

Table 2.3: PCR parameters for specific primer pairs

Gene	Hot Start	Denaturing	Annealing	Extension	Cycles	End
Nrp1, *Nrp1^{fl}*	94°C, 3 min	94°C, 40 s	66°C,1 min	72°C, 1 min	35	72°C, 5 min
Nrp1^{Sema}	94°C, 3 min	94°C, 30 s	69°C,1 min	72°C, 1 min	35	72°C, 5 min
Nrp1^{Vegfa}	94°C, 3 min	94°C, 1 min	66°C, 30 s	72°C, 1 min	35	72°C, 5 min
Nrp2	94°C, 3 min	94°C, 1 min	66°C,1 min	72°C, 1 min	35	72°C, 5 min
Plxnd1	94°C, 3 min	94°C, 1 min	68°C,1 min	72°C, 1 min	35	72°C, 5 min
Tie2-Cre	94°C, 3 min	94°C, 1 min	67°C,1 min	72°C, 1 min	32	72°C, 5 min
Wnt1-Cre	94°C, 3 min	94°C, 40 s	62°C,1 min	72°C, 1.5 min	35	72°C, 5 min
Nes-Cre	94°C, 3 min	94°C, 1 min	62°C,1 min	72°C, 1 min	32	72°C, 5 min
Sm22a-Cre	94°C, 3 min	94°C, 1 min	62°C,1 min	72°C, 1.5 min	35	72°C, 5 min
Csf1r-Cre, *Csf1r-Cre^{ERT}*	94°C, 3 min	94°C, 1 min	61°C,1 min	72°C, 1.5 min	35	72°C, 5 min
Csf1r-eGFP	94°C, 3 min	94°C, 1 min	66°C, 1 min	72°C, 1.5 min	35	72°C, 5 min
Pu.1	94°C, 3 min	94°C, 40 s	60°C, 1 min	72°C, 2 min	35	72°C, 5 min
Vegfa^{120}	94°C, 3 min	94°C, 1 min	52°C, 1 min	72°C, 1 min	5	72°C, 5 min

			60°C, 1 min	72°C, 1 min	28	
Vegfa^{LacZ}	94°C, 3 min	94°C, 1 min	55° C,1 min	72°C, 1 min	35	72°C, 5 min
Vegfa^{fl}	94°C, 3 min	94°C, 1 min	52°C, 1 min 60°C, 1 min	72°C, 1 min 72°C, 1 min	5 28	72°C, 5 min
Sema3c^{fl}	94°C, 3 min	94°C, 1 min	62 C, 1 min	72°C, 1 min	35	72°C, 5 min
Rosa$^{Yfp/LacZ/Dta}$	94°C, 3 min	94°C, 1 min	61°C, 1 min	72°C, 1 min	35	72°C, 5 min

2.2.1.9 Tissue fixation

Pregnant dams were culled by cervical dislocation in accordance to Home Office and institutional animal guidelines. The gravid uterus was excised and placed in ice-cold 1X PBS. Using fine Dumont forceps, the embryos were dissected from the uterus and yolk sac. To remove hindbrains, embryos were dissected as published previously (Plein et al., 2015b, Fantin et al., 2013c). Retinal dissections were performed as outlined in (Pitulescu et al., 2010).

Retinas and embryonic tissue pre mid-gestation were fixed in 4% PFA for 2 h at 4°C, mid-embryonic and postnatal tissues were fixed overnight at 4°C. Following fixation, all samples were washed twice with 1X PBS for 5 min at RT to remove any residual PFA and either processed immediately or stored in 1X PBS at 4°C (short-term). Samples stored for the long-term were dehydrated down a methanol gradient comprised of 25%, 50% and 75% (v/v) absolute methanol in 1X PBT and then stored in 100% methanol at -80°C until use.

2.2.1.10 Oxygen-induced retinopathy (OIR)

The mouse model of OIR was performed as published previously (Connor et al., 2009). Briefly, P7 pups and their mothers were subjected to 80% oxygen for 5 days, which results in vaso-obliteration (Smith et al., 1994). At P12 mice were returned to normoxia (21%), which causes both normal vessel re-growth, as well as the formation of vascular tufts. Pups were culled at P17 for retinal dissection, as vascular tuft formation is maximal at this time point, before regressing between P17 and P25.

2.2.2 Immunolabelling

2.2.2.1 Cryosectioning

After fixation embryos were washed in 1X PBS and dehydrated in 20% sucrose in 1X PBS for cryoprotection. Once embryos had sunk in the solution, samples were placed into optimal cutting temperature embedding compound (OCT, Sakura Tissue-Tek) and rapidly frozen on dry ice. Following this step, samples were stored at -20°C for the short term (-80°C for long-term storage) or immediately

sectioned into 20 µm thick slices using a histology cryostat (Leica CM1850). The sections were collected on Superfrost Plus slides (VWR International), air-dried for an hour at RT and then either stored at -20°C or immediately processed for immunolabelling.

2.2.2.2 Vibratome sectioning

Pre-stained hindbrains were washed in 1X PBS and embedded in 3% molten agarose. After the agarose had set, samples were sectioned at 100 µm using the Vibratome 1000Plus Sectioning System (IntraCel). Sections were collected on glass slides and mounted using 90% (v/v) glycerol in 1X PBS.

2.2.2.3 Immunolabelling of wholemounts

Samples were initially washed with 1X PBT for 5 min at RT to permeabilise the tissue and allow antibody penetration. Samples to be stained with horseradish peroxidase (HRP)-tagged secondary antibodies were bleached with hydrogen peroxide (1% (v/v) H_20_2 in 1X PBT) for 30 min at RT to remove any endogenous peroxidases and washed twice with 1X PBT. Subsequently, samples were blocked using a blocking solution consisting of either 10% (v/v) NGS in 1X PBT or 10% (v/v) serum free block (Dako) in 1X PBT depending on the primary antibody used in the following steps (see **table 2.4**). After blocking, the primary antibody/ies were diluted in the aforementioned blocking solutions (see **table 2.4**) and applied to sections for 2 h at RT or overnight at 4°C. The antibody solution was removed and slides were washed 3 times with 1X PBT for 10 min each at RT. Secondary antibodies raised against the host animal of the primary antibody were diluted 1:200 in either 10% NGS or 10% serum free block (see **table 2.4** for primary antibody host species and appropriate blocking solutions). Sections were incubated with secondary antibody solution for 1 h at 4°C in the dark to protect fluorophores. Samples were washed 3 times with 1X PBS for 10 min and either post-fixed for 10 min with 4% PFA at RT or HRP-labelled samples were developed using diaminobenzidine (DAB)and hydrogen peroxide (SigmaFast) followed by post-fixing. Samples thinner than 50 µm were flatmounted directly with a glass cover slip on a glass slide using the SlowFade antifade reagent kit (Life Technologies). For samples thicker than 50 µm, such as the hindbrain, several layers of black electrical tape were stuck on a

glass slide. Using a scalpel, pockets of an appropriate size were cut and samples were placed inside and mounted using the SlowFade antifade reagent kit.

2.2.2.4 Immunolabelling of sections

Slides were initially washed with 1X PBS to remove the OCT. Using a PAP-PEN (Daido Sangyo) a hydrophobic barrier was drawn along the edge of the slide, which prevents loss of staining solution. Subsequent staining steps were performed, as detailed in **section 2.2.2.3**. Following the staining procedure, sections were mounted using Mowiol solution. Mowiol solution was made up by incubating 6 g of glycogen and 2.4 g of Mowiol 4-88 (Calbiochem) in 6 ml of water for 2 h at RT and then adding 12 ml of Tris (0.2 M, pH 8.5) and 2.5% (w/v) DABCO, and incubating for several hours at 55°C until dissolved.

2.2.2.5 Immunofluorescent staining of explants

Explants were washed twice with 1X PBS and fixed for 15 min on ice in 4% PFA. Samples were blocked using 10% NGS in 1X PBT for 30 min at RT and incubated in the primary antibody solution, which was prepared according to guidelines listed in **table 2.3** for 2 h at RT. After 3 10 min washes with 1X PBT at RT, the secondary antibody solution containing the antibody at a dilution of 1:200 was added to the explants for 1 h at RT. After 3 10 min washes with 1X PBS, samples were post fixed for 5 min with 4% PFA at RT. Using fine forceps, collagen gels were carefully removed from the 24-well plate and mounted on a glass slide using Mowiol solution.

2.2.2.6 BrdU labelling

To analyse cell proliferation *in vivo*, bromodeoxyuridine (BrdU, Sigma) was injected into mice. BrdU is a synthetic analogue of thymidine and thus gets incorporated during DNA synthesis of dividing cells. Pups were injected intraperitoneally with 300 mg/kg of BrdU (10 mg/ml) and culled at the required time. Immunostaining for BrdU was carried out at described in section **2.2.2.3**; however, the BrdU antibody can only access the BrdU after DNA has been denatured. Therefore, staining for BrdU first included a denaturation step, which constituted of serial incubations with 1 M HCl for 10 min on ice, followed by 2 M HCl for 10 min

at RT and then 10 min at 37°C. Subsequently, the acid was neutralised by incubating samples in borate buffer (0.1 M) for 10 min at RT. The denaturation step is damaging for many epitopes and thus immunostaining for other markers was performed first, followed by the acid treatment and then the BrdU antibody staining.

Table 2.4: Primary antibody parameters

Primary Antibody	Company	Dilution	Species	Secondary Antibody	Blocking Solution
IB4	Sigma	1:250	n/a (biotinylated)	strepdavidin	10% NGS in PBT
anti-BrdU	Abcam	1:200	rat	goat anti-rat	10% NGS in PBT
anti-activated CASPASE 3	Cell Signalling	1:200	rabbit	goat anti-rabbit	10% NGS in PBT
anti-CD45	Serotec	1:200	rat	goat anti-rat	10% NGS in PBT
anti-CSF1R	Santa Cruz	1:500	rabbit	goat anti-rabbit	10% NGS in PBT
anti-ENDOMUCIN	Santa Cruz	1:50	rat	goat anti-rat	10% NGS in PBT
anti-F4/80	Serotec	1:500	rat	goat anti-rat	10% NGS in PBT
anti-GFAP	Abcam	1:500	chick	goat anti-chick	10% NGS in PBT
anti-KIT	BD Biosciences	1:1000	rat/biotinylated	goat anti-rat/strepdavidin	10% NGS in PBT
anti-NG2	Millipore	1:200	rabbit	goat anti-rabbit	10% NGS in PBT
anti-NRP1	R&D Systems	1:100	goat	FAB anti-goat	10% Dako in PBT
anti-PECAM	BD Pharmingen	1:200	rat	goat anti-rat	10% NGS in PBT
FITC-conjugated	Sigma	1:40	n/a	n/a	10% NGS in PBT

anti-phalloidin					
anti-PLXNA2	R&D Systems	1:100	goat	FAB anti-goat	10% Dako in PBT
anti-PHH3	Millipore	1:400	rabbit	goat anti-rabbit	10% NGS in PBT
anti-SLUG	Cell Signalling	1:100	rabbit	goat anti-rabbit	10% NGS in PBT
cy3-conjugated anti-smooth muscle actin	Sigma	1:200	n/a	n/a	10% NGS in PBT
FITC-conjugated anti-smooth muscle actin	Sigma	1:200	n/a	n/a	10% NGS in PBT
anti-Sm22α	Abcam	1:200	rabbit	goat anti-rabbit	10% NGS in PBT
anti-VEGFR2	R&D Systems	1:200	goat	FAB anti-goat	10% Dako in PBT
anti-YFP	Aves	1:1000	chick	goat anti-chick	10% NGS in PBT
anti-YFP	MBL	1:500	rabbit	goat anti-rabbit	10% NGS in PBT

2.2.3 Xgal staining

Xgal staining was used to visualise the expression of the enzyme β-galactosidase in mice, which had the sequence for this enzyme (*lacZ*) inserted into a gene of interest. Embryos were collected and fixed for 30 min at 4°C. After fixation samples were washed 3 times with 0.02% (v/v) NP-40 in 1X PBS for 15 min at RT. The staining solution was made up freshly by adding the Xgal reagent (40 mg/ml in DMF) at a dilution of 1:40 to the staining buffer (5 mM $K_3Fe(CN)_6$, 5 mM $K_4Fe(CN)_6.3H_20$, 2 mM $MgCl_2$, 0.01% (v/v) sodium deoxycholate, 0.02% NP-40 in 1X PBS). The sample was incubated in the staining solution in the dark at 37°C until a sufficient staining intensity was achieved. To stop the reaction, samples were briefly washed in 1X PBS and post-fixed for 10 min in 4% PFA.

2.2.4 AP-binding assay

Plasmids containing AP only and VEGFA-AP were kindly provided by Prof Chenghua Gu.

2.2.4.1 AP-probe generation

HEK293 cells were transfected with plasmids containing the VEGFA-AP or AP sequence. Briefly, to transfect a 60% confluent T75 flask, 18.75 µg plasmid cDNA and 37.5 µl of Lipofectamine (Life Technologies) were each mixed with 750 µl of DMEM and incubated for 15 min at RT. Subsequently, both solutions were mixed together and incubated for 15 min at RT. Following the incubation, the previous medium was removed from the T75 flask, and cells were briefly washed with PBS. Subsequently, the transfection solution was diluted in a further 7.5 ml of DMEM and the solution added to the T75 flask. Cells were incubated with transfection solution for 4 h and subsequently the solution was replaced with normal growth medium. After 72 h, the medium containing the AP fusion protein was collected and used in subsequent experiments.

2.2.4.2 AP-probe binding

Following cryosectioning (see **2.2.2.1**) sections were briefly fixed with ice-cold methanol and washed 3 times with AP wash buffer (4 mM $MgCl_2$ in 1X PBS)

for 5 min at RT. Sections were then blocked using 10% (v/v) FBS in AP wash buffer for 30 min at RT and incubated overnight at 4°C with the medium containing the AP fusion protein. Sections were then washed 5 times with PBS for 5 min each at RT and the AP probe binding was fixed using 4% PFA for 5 min at RT and subsequently washed 3 times with PBS for 5 min each. Next, endogenous phosphatases were inactivated by incubating sections within coplin jars containing PBS for 3 h at 65°C. After washing with PBS twice, sections were first incubated with AP staining buffer (100 mM Tris pH 9.5, 100 mM NaCl, 5 mM $MgCl_2$) and then in AP staining buffer with 3.75 µl NBT and 3.5 µl BCIP per 1ml of buffer until the staining developed. Subsequently, the reaction was stopped by washing sections with PBS for 5 min and the staining was fixed using 4% PFA for 5 min. Finally, slides were mounted with a glass coverslip using glycerol.

2.2.5 *In situ* hybridisation

All solutions and equipment used during this protocol were kept RNase-free. Plasmid containing the SEMA3C probe sequence was provided by Jonathan Raper.

2.2.5.1 Bacterial culture of probe plasmid

2 µl of plasmid were added to 100 µl of chemically competent bacterial cells in a 1.5 ml Eppendorf tube and incubated on ice for 10 min. Subsequently, cells were heat shocked by placing tubes in a 42°C water bath for 45 s and then on ice for 10 s. 500 µl of LB medium (10 g/l bacto-tryptone, 5 g/l yeast extract, 10 g/l NaCl, pH 7.5) was added and cells were incubated at 37°C for 30 min. Bacterial culture was evenly spread over a sterile LB agar plate (LB medium,100 µg/ml ampicillin, 25 g/l agar) and incubated overnight at 37°C. The following day, a colony was picked using a 10 µl pipette tip and grown in 2 ml LB medium containing 100 µg/ml ampicillin for 12 h at 37°C.

2.2.5.2 Plasmid digestion

The plasmid was isolated from cultured bacterial cells by using the Qiagen Qiaprep Spin Miniprep kit according to manufacturer's instructions. Briefly, bacteria were pelleted by centrifuging tubes for 5 min at 12000 rpm and resuspended in 250

µl of cold P1 buffer. Subsequently, cells were lysed by adding 250 µl of P2 buffer and gently mixing the solutions. After no more than 5 min of lysis reaction time, 350 µl of the neutralizing buffer N3 was added and gently mixed. Next, tubes were centrifuged for 10 min at 13000 rpm and the supernatant was applied to a Qiaprep spin column. Columns were centrifuged for 1 min at 13000 rpm and washed by adding 750 µl PE buffer followed by a centrifugation for 1 min at 13000 rpm. Subsequently, columns were air-dried by centrifugation for 1 min at 13000 rpm. DNA was eluted by adding 50 µl of water to the column, centrifuging for 1 min at 13000 rpm and collecting the flow-through in a fresh 1.5 ml eppendorf.

Plasmid was linearised by digesting it with the appropriate restriction enzyme (New England Biolabs). Briefly, 2.5 µl of plasmid, 1 µl of restriction enzyme, 4 µl of 10X buffer, 4 µl of 10X BSA and 22 µl of water were incubated at 37°C for 2.5 h. DNA was extracted by phenol/chloroform extraction and resuspended in 16 µl of water. To validate plasmid, 1 µl of digested DNA was visualised alongside undigested plasmid by electrophoresis through a 2% (w/v) agarose (BDH Electran) in TAE gel containing 2 µl nucleic acid staining solution, RedSafe (iNtRON).

2.2.5.3 RNA probe synthesis

A DIG-labelled RNA probe was synthesised from linearised plasmid by incubating 14.5 µl of DNA, 2 µl of 10X buffer, 2 µl of 10X DIG, 1 µl of a promoter-specific reverse transcriptase enzyme and 0.5 µl RNAse inhibitor (Roche) for 2.5 h at 37°C. 1 µl of transcription product was visualised by performing electrophoresis through 2% (w/v) agarose (BDH Electran) in TAE gel containing 2 µl nucleic acid staining solution, RedSafe (iNtRON). RNA was precipitated by adding 300 µl absolute ethanol, 100 µl water, 8 µl 5 M LiCl and incubating at -80°C for 1 h. RNA was pelleted by high speed centrifugation at 4°C for 30 min, washed with 70% (v/v) ethanol and air-dried for 10 min at RT. RNA was resuspended in 40 µl water and stored at -80°C.

2.2.5.4 In situ hybridisation

Samples were fixed overnight in 4% PFA at 4°C and dehydrated for 4 h at 4°C in 20% (w/v) sucrose in 1X PBS. Samples were cryosectioned as described in

section 2.2.2.1, air-dried for 30 min at RT and placed into a wet chamber. Each section was incubated overnight at 65°C with 200 µl of hybridisation solution consisting of 1X Salt solution (200 mM NaCl, 5 mM EDTA, 10 mM Tris-HCl pH 7.5, 5 mM $NaH_2PO_4.7H_20$, 5 mM Na_2HPO_4), 0.1 mg/ml tRNA, 10% (w/v) Dextran sulphate, 1X Denhardts and 200 ng/ml of the RNA probe. Dehydration was avoided by placing RNAse-free cover slips on top of sections and sealing chamber with tape. Sections were washed 3 times for 30 min each in coplin jars containing pre-heated washing buffer consisting of 50% (v/v) formamide, 1X SSC pH 4.5, 0.1% (v/v) Tween-20 at 65°C. Subsequently, sections were washed twice for 30 min each with 1X MABT (100 mM maleic acid, 150 mM NaCl, 0.1% (v/v) Tween-20, pH 7.5) at RT and blocked with 500 µl of blocking solution consisting of 2% (w/v) blocking reagent (Roche), 10% (v/v) NSS in 1X MABT for 1 h at RT. Slides were incubated overnight with anti-DIG AP-conjugated antibody (Roche) diluted at 1:1500 in blocking solution at 4°C and washed 3 times for 15 min each in 1X MABT at RT. Sections were washed twice for 5 min each with NTMT (0.1 M NaCl, 0.1 M Tris-HCl pH 9.5, 0.05 M $MgCl_2$, 1% (v/v) Tween-20) and incubated in the dark with staining buffer (3.5 µl BCIP, 4.5 µl NBT per ml of NTMT) until sufficient staining intensity was achieved. The reaction was stopped by washing with water and post-fixed for 10 min with 4% PFA. Slides were mounted using the SlowFade antifade reagent kit.

2.2.6 *Ex vivo* endoMT assay

The endoMT assay was performed as published previously (Bai et al., 2013). Briefly, OFTs were dissected from E10.5 embryos and cultured with the endocardium facing downwards in DMEM Glutamax (Life Technologies) supplemented with 10% (v/v) FBS in a 24-well plate coated with 1 mg/ml collagen (BD Biosciences) at 37°C for 72 h. Explants were fixed on ice for 30 min with 4% PFA and stained with FITC-conjugated phalloidin to detect F-actin and DAPI to identify nuclei. In some experiments, explants were immunolabelled for YFP or PECAM. The extent of endoMT was quantified by counting cells contributing to the explant outgrowth. In some experiments, wildtype explants were cultured in growth medium containing low serum (1%) and treated with 400 ng/ml mouse SEMA3C (R&D Systems). *Nrp1*-null explants were cultured in medium supplemented with 1% or 10% serum in the presence or absence of 400 ng/ml SEMA3C.

2.2.7 Imaging

Fluorescently labelled samples were imaged using either an Olympus SZX16 fluorescent stereomicroscope equipped with a Micropublisher camera (Perkin-Elmer) or a LSM710 laser scanning confocal microscopes (Zeiss). Images were processed with Adobe Photoshop CS4 (AdobeSystems, Inc.).

2.2.8 Fluorescence-activated cell sorting (FACS)

Tissues were isolated and homogenised in ice-cold RPMI1640 medium (Life Technologies) containing 5% (v/v) FBS, 2.38 g/L HEPES and 1.5 g/L sodium hydrogen carbonate according to their tissue-specific requirements. Thus, spleens and yolk sacs were homogenised using a scalpel, whereas bone marrow cells were obtained by flushing RPMI buffer through isolated femurs using a 23 G needle syringe. Blood was collected in heparin-lined tubes (BD Biosciences) and erythrocytes were lysed by treating samples for 5 min with red blood cell lysis buffer before centrifuging at 1200 rpm for 5 min. The resulting supernatant was used for FACS analysis. To generate single cell suspensions, homogenates were passed through a 70 µm filter. Cell suspensions were incubated with Fc block (BD Biosciences) for 5 min at RT to prevent non-specific binding of antibodies. Samples were stained using the following directly conjugated antibodies (BD Biosciences): PECAM-APC, CD45-Brilliant Violet 570, KIT-PerCP-Cy5.5 and DAPI to identify dying or dead cells. Labelled cells were analysed with a BD LSR II flow cytometer (BD Biosciences). Samples from unstained controls and *Csf1r-Cre*–negative embryos were used to identify appropriate fluorescence voltage and gate parameters (Tung et al., 2007).

2.2.9 qRT-PCR

All solutions were maintained RNAse free.

2.2.9.1 RNA extraction

Total RNA was extracted from samples using the RNeasy Micro kit (Qiagen) according to manufacturer's instructions. Briefly, tissue samples were homogenised with a 23 G needle syringe in 350 µl of RLT lysis buffer containing β-

mercaptoethanol (10 µl/ml). An equal volume of 70% (v/v) ethanol was added to lysates and solutions were transferred to individual spin columns. RNA was transferred to membranes by centrifuging columns at 8500 rpm for 15 s. Subsequently, membrane-bound RNA was washed with 350 µl of RW1 buffer. Genomic DNA was removed by digestion with DNase 1 solution for 15 min at RT and a subsequent wash with 350 µl of RW1 buffer. Membrane-bound RNA was first washed with 500 µl of RPE buffer and then 80% (v/v) ethanol. Finally, RNA was eluted in 14 µl of RNAse free water.

2.2.9.2 Reverse transcription

First strand cDNA synthesis was performed using the SuperScript Transcriptase III kit (Invitrogen). For each reaction 500 ng of RNA, 250 ng of random primers, 1 µl of 10 mM dNTPs were mixed and the volume was adjusted to 13 µl with water. The mixtures were heated to 65°C for 5 min and chilled on ice for 1 min. 4 µl of 5X First-Strand Buffer, 1 µl of 0.1 M DTT, 1 µl of RNaseOUT and 1 µl of the enzyme SuperScript III (200 units/µl) were added to each sample. Subsequently, samples were incubated for 10 min at 25°C, 50 min at 42°C and 10 min at 70°C. Finally, cDNA quality and concentration was determined using a NanoDrop 1000 spectrometer (Thermo Scientific). Unless qPCR reactions were performed immediately after, cDNA was stored at -20°C.

2.2.9.3 qRT-PCR

qRT-PCR was performed on a 96-well plate using a 7900HT Fast Real-Time PCR System (Applied Biosystems). For each reaction 12.5 µl of Power SYBR Green PCR Master Mix (Applied Biosystems) were added to 250 ng of sample cDNA and 1.5 µM of the forward and reverse oligonucleotide primer, which were designed using the Primer3 software and synthesised to order by Sigma (see **table 2.5**). For each gene, the reaction was run in triplicate and for each primer pair a no template control was included. After a 10 min enzyme activation step at 95°C, 40 PCR cycles consisting of a 15 s denaturation step at 95°C followed by an annealing and extension step at 60°C were carried out. Data was collected using the Sequence Detector Software (SDS version 2.2; Applied Biosystems) and the presence of primer dimer formation was excluded by examining dissociation curves and DNA

amplification in no template controls. Expression levels were extrapolated from PCR data using DART-PCR software (Peirson et al., 2003) and normalised using *Gapdh* expression as a reference. Final data was presented as a fold change from control samples.

Table 2.5: Oligonucleotide primers designed for qRT-PCR

Gene	Primer	Sequence
Gapdh	G-F	5'-TGCGACTTCAACAGCAACTC-3'
	G-R	5'-CTTGCTCAGTGTCCTTGCTG-3'
Nrp1	Np-F	5'-GAAGGTGAAATCGGAAAAGG-3'
	Np-R	5'-GGTCTGTTGGTTTTGCACAG-3'
Slug	Sl-F	5'-TTCAACGCCTCCAAGAAGCC-3'
	Sl-R	5'-GGGTAAAGGAGAGTGGAGTGG-3'
Snail	Sn-F	5'-CCCAGTCGCGGAAGATCTT-3'
	Sn-R	5'-CAGTGGGAGCAGGAGAATGG-3'

2.2.10 Statistics

Results are expressed as mean ±s.d. For all statistical analyses, I used a 2-tailed, unpaired Student's *t* test. *P* values of less than 0.05 were considered significant.

Chapter 3 NRP1 IS REQUIRED IN ENDOTHELIUM, BUT DOES NOT FUNCTION EXCLUSIVELY AS A VEGF-A RECEPTOR DURING DEVELOPMENTAL ANGIOGENESIS

3.1 Introduction

NRP1 is critical for developmental angiogenesis, and endothelial *Nrp1* knockouts display similar vascular defects to full *Nrp1* knockouts (Kawasaki et al., 1999, Gu et al., 2003). However, the vascular defects of endothelial *Nrp1* mutants are less severe than those of full knockouts. It is therefore interesting that NRP1 is also expressed by multiple other cell types within the immediate environment of the developing vasculature such as macrophages and neurons (Fantin et al., 2010, Cariboni et al., 2011). To analyse if NRP1 has non-endothelial functions that complement endothelial NRP1 functions during developmental angiogenesis, Dr Alessandro Fantin and Dr Joaquim Vieria, former PhD students in the Ruhrberg group, decided to closely compare angiogenesis in the hindbrain of cell type-specific *Nrp1* knockouts affecting ECs, macrophages and neurons (see **1.5.1**). This project was already in progress when I started my PhD, and I contributed to it by repeating the experiments outlined below to generate statistically significant data (**Figure 3.1**, Figure 3.2,**Figure** 3.3). The results of this study were published in (Fantin et al., 2013a) (see **Appendix** – co-authored publications).

At the start of my PhD, the most widely accepted role for endothelial NRP1 during developmental angiogenesis had been attributed to the fact that NRP1 binds to VEGF164 to initiate complex formation with and therefore signalling through VEGFR2 (Soker et al., 2002). However, no study had formally investigated, whether NRP1 functioned as a VEGF-A receptor during angiogenesis *in vivo*. To address this question, we collaborated with Prof Ian Zachary (Rayne Institute, UCL), who had generated mice with a Y297A mutation in the VEGF-A binding b1 domain of the NRP1 receptor ($Nrp1^{Vegfa/Vegfa}$) (see **Figure 1.2**). This mutation abolished VEGF-A binding to NRP1, as demonstrated using VEGF-AP binding assays on $Nrp1^{Vegfa/Vegfa}$ hindbrains (Fantin et al., 2014). Unexpectedly, analysis of these mice revealed that mutants only displayed very mild defects in developmental angiogenesis. Thus, quantitation of vessel branchpoints in the SVPs of E12.5 $Nrp1^{Vegfa/Vegfa}$ hindbrains by Dr Alessandro Fantin revealed only a small reduction compared to wildtype

littermates (Fantin et al., 2014), which was in contrast to the severe vascular phenotype observed in *Nrp1*-nulls and *Tie2-Cre;Nrp1*$^{fl/-}$ mutants (see **Figure 3.1)**. Furthermore, unlike the *Nrp1*$^{-/-}$ and *Tie2-Cre;Nrp1*$^{fl/-}$ embryos which are embryonic lethal, *Nrp1*$^{Vegfa/Vegfa}$ mutants were viable at birth. Nevertheless, these mutants displayed a reduced birth weight and only 75% survival within the first two weeks after birth. My aim was to investigate the underlying cause of the increased mortality demonstrated by *Nrp1*$^{Vegfa/Vegfa}$ mice. The results of this analysis were published in (Fantin et al., 2014) (see **Appendix** – co-authored publications).

3.2 Results

3.2.1 NRP1 functions cell autonomously in endothelium to promote developmental angiogenesis

3.2.1.1 EC-specific NRP1 mutants display similar albeit milder vascular defects compared to Nrp1-nulls

The embryonic hindbrain is vascularised by angiogenic vessel sprouts, which enter from the pial side at E9.5 and branch to form the SVP from E10.5 onwards (Fantin et al., 2013c, Plein et al., 2015b). During this process, NRP1 is expressed on ECs, as well as several other cell types closely associated with the developing SVP, including tissue macrophages that promote vascular anastomosis and neuronal progenitors that secrete VEGF-A (Fantin et al., 2013b).

To discern the role of endothelial versus non-endothelial NRP1 during embryonic angiogenesis, Dr Fantin, and I isolated the hindbrains from endothelial-, macrophage-, and neuronal-specific *Nrp1* mutants, and visualised the SVPs by PECAM immunolabelling. We first examined the SVP in E12.5 *Nrp1*$^{-/-}$ hindbrains, which confirmed a prior report that the vascular network failed to form in *Nrp1*$^{-/-}$ hindbrains (Gerhardt et al., 2004); instead, vessel sprouts generated vascular tufts (clear arrowheads, **Figure 3.1D**). Furthermore, instead of branching within the subventricular zone, vessels formed rare interconnections within the deeper layers of the hindbrain (arrows, **Figure 3.1D**). We next compared this phenotype to hindbrains from endothelial-specific *Nrp1* knockouts by crossing the conditional *Nrp1*-null allele (*Nrp1*^{fl}) to mice carrying one *Nrp1*-null allele together with a well-established

endothelial-specific transgene, *Tie2-Cre*. This approach was used in a previous publication to efficiently delete *Nrp1* in the endothelium of the CNS (Gu et al., 2003). We decided to generate the endothelial-specific mutants on a $Nrp1^{fl/-}$ background, because this prior study had reported that *Nrp1* targeting was more efficient with one conditional *Nrp1*-null allele on a heterozygous, constitutive *Nrp1*-null background ($Nrp1^{fl/-}$) than with two conditional *Nrp1*-null alleles ($Nrp1^{fl/fl}$) (Gu et al., 2003).

In comparison to *Nrp1*-nulls, the SVPs of E12.5 *Tie2-Cre;*$Nrp1^{fl/-}$ mice displayed abnormal SVPs. For example, they contained vascular tufts similar to the ones observed in the hindbrain vasculature of *Nrp1*-nulls (clear arrowheads, **Figure 3.1C**). Surprisingly, however, the phenotype in the *Tie2-Cre;*$Nrp1^{fl/-}$ mutants appeared to be milder than in the full *Nrp1*-nulls. Thus, the *Tie2-Cre;*$Nrp1^{fl/-}$ hindbrains contained a few vascular branchpoints within the SVPs (clear arrows, **Figure 3.1C)**. Quantitation of the number branchpoints in mutant and control $Nrp1^{fl/-}$ hindbrains confirmed that there was a significantly reduced number of branchpoints in *Tie2-Cre;*$Nrp1^{fl/-}$ mutants (**Figure 3.1C**). We used $Nrp1^{fl/-}$ as a control, as we unexpectedly observed a reduction in branchpoints in $Nrp1^{fl/-}$ mice compared to $Nrp1^{fl/+}$ controls (**Figure 3.1E**). Nevertheless, we also demonstrated that *Tie2-CreNrp1*$^{fl/-}$ SVPs contained significantly more branchpoints than *Nrp1*-nulls suggesting that NRP1 expressed by non-ECs might be additionally required for developmental angiogenesis (**Figure 3.1E**).

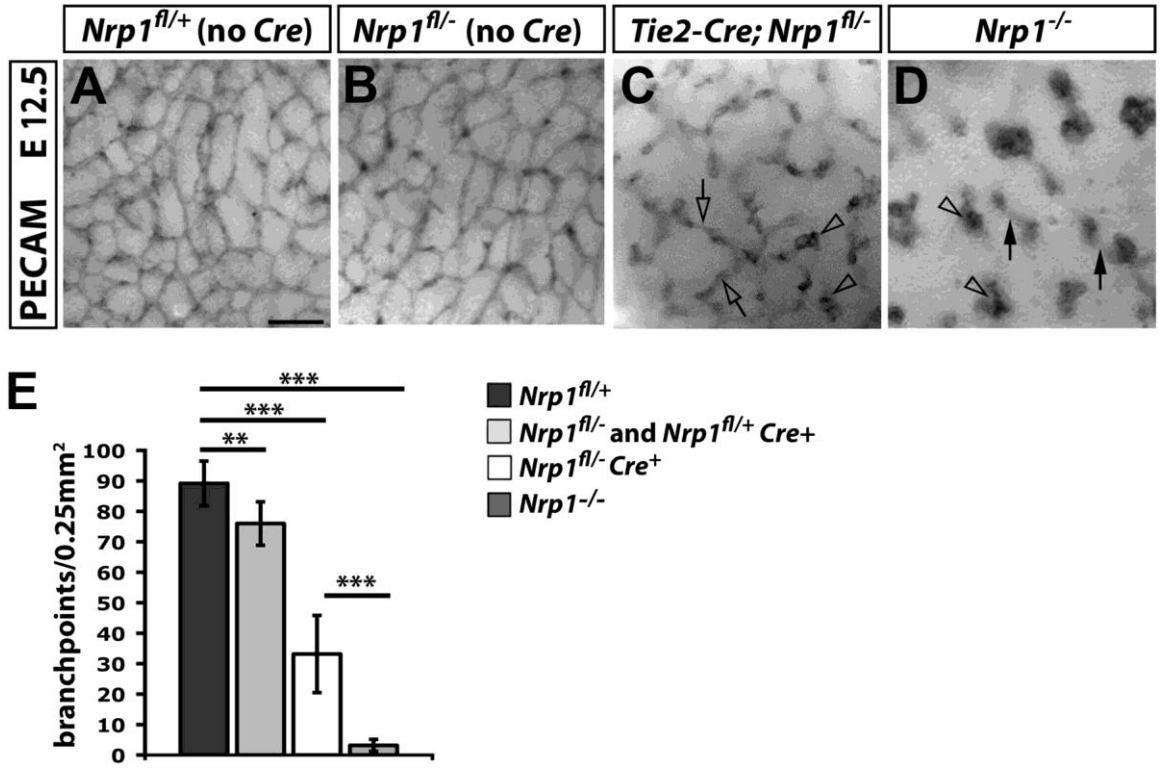

Figure 3.1 Endothelial NRP1 is required for developmental angiogenesis.

(A-D) E12.5 *Nrp1*$^{-/-}$, *Tie2-Cre;Nrp1*$^{fl/-}$, *Nrp1*$^{fl/-}$ and control hindbrains were immunolabelled for PECAM and the SVPs imaged. Clear arrowheads indicate examples of vascular tufts; clear arrows and solid arrows indicated examples of vascular interconnections in the SVP versus deeper brain layers, respectively. **(E)** Quantitation of SVP branchpoints in *Nrp1*$^{fl/+}$ (n= 12), *Nrp1*$^{fl/-}$ (n= 16), *Tie2-Cre;Nrp1*$^{fl/-}$ (n= 5) and *Nrp1*-null (n= 8) E12.5 hindbrains. Mean ± s.d.; the asterisks indicate p values; **≤ 0.001, ***≤ 0.0001. Scale bar: 100 μm.

3.2.1.2 Non EC-derived NRP1 is not required for developmental angiogenesis

To establish whether macrophage-derived NRP1 was required for developmental angiogenesis, we crossed *Nrp1*$^{fl/fl}$ mice carrying the conditional *Nrp1*-null allele to *Nrp1*$^{+/-}$ mice expressing the macrophage *Cre* transgene *Csf1r-Cre* (Deng et al., 2010). Analysis of E12.5 *Csf1r-Cre;Nrp1*$^{fl/-}$ and control hindbrains immunolabelled for PECAM revealed that the SVPs appeared normal compared to their control littermates (**Figure 3.2B**). Furthermore, quantitation of branchpoints demonstrated that the number of vessel branch points was similar between mutant and control hindbrains (**Figure 3.2C**).

To address whether NRP1 expressed by the neuronal progenitors was involved in embryonic angiogenesis, we crossed *Nrp1*$^{fl/fl}$ mice to *Nrp1*$^{+/-}$ mice carrying the transgene *Nes-Cre*, which had been used previously to efficiently target neuronal progenitors (Petersen et al., 2002). Having immunolabelled the hindbrains of the resulting *Nes-Cre;Nrp1*$^{fl/-}$ embryos and their control littermates for PECAM, we observed that the mutant SVPs displayed no vascular abnormalities (**Figure 3.3B**). Furthermore, quantitation of branchpoints revealed that there was no significant difference between mutants and controls (**Figure 3.3C**). Together with the lack of a phenotype in *Csf1r-Cre;Nrp1*$^{fl/-}$ mice, these results demonstrated that, whilst endothelial NRP1 is required for embryonic angiogenesis, macrophage- and neuronal-derived NRP1 is dispensable.

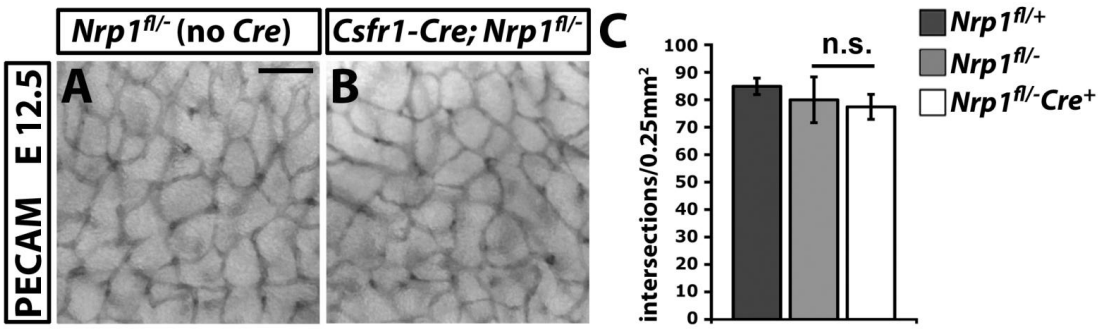

Figure 3.2 Macrophage-derived NRP1 is not required for developmental angiogenesis.

E12.5 *Csf1r-Cre;Nrp1*$^{fl/-}$ and control hindbrains were immunolabelled for PECAM and the SVP imaged **(A,B)**. Quantitation of SVP branchpoints in *Nrp1*$^{fl/+}$ (n= 6), *Nrp1*$^{fl/-}$ (n= 6) and *Csf1r-Cre;Nrp1*$^{fl/-}$ (n= 5) E12.5 hindbrains **(C)**. Mean ± s.d.; n.s., not significant. Scale bar: 100 μm.

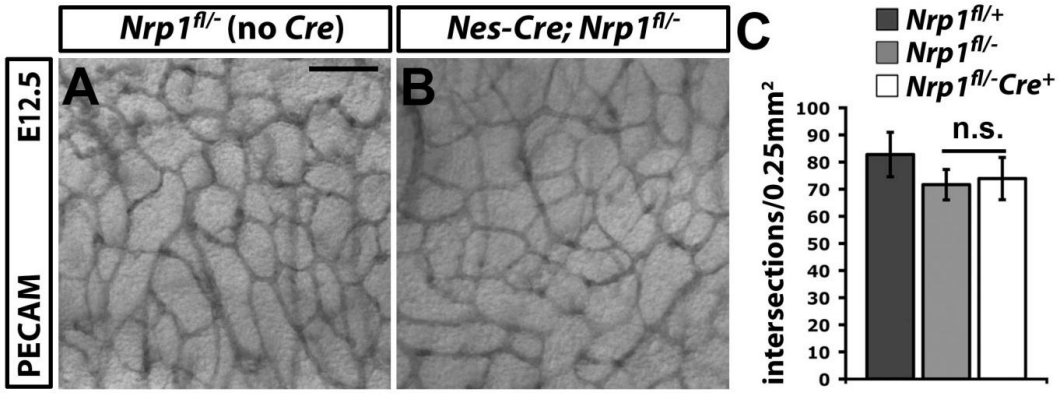

Figure 3.3 NRP1 derived from neuronal progenitors is not required for developmental angiogenesis.

E12.5 *Nes-Cre;Nrp1*$^{fl/-}$ and control hindbrains were immunolabelled for PECAM and the SVP imaged **(A,B)**. Quantitation of SVP branchpoints in *Nrp1*$^{fl/+}$ (n= 3), *Nrp1*$^{fl/-}$ (n= 5) and *Nes-Cre;Nrp1*$^{fl/-}$ (n= 8) E12.5 hindbrains **(C)**. Mean ± s.d.; n.s. not significant. Scale bar: 100 µm.

3.2.2 NRP1 does not function as an exclusive VEGF-A receptor during developmental angiogenesis

Nrp1$^{Vegfa/Vegfa}$ pups display a reduced body weight and an increased mortality rate compared to control litter mates (Fantin et al., 2014). To investigate the underlying cause of the increased mortality of these mutants, Dr Fantin and I, performed post-mortem examinations on *Nrp1*$^{Vegfa/Vegfa}$ mutants, which had deceased within the first two weeks after birth. This analysis revealed that mutants had enlarged hearts and blood-filled lungs indicative of congestive heart failure (Gavalas et al., 2003). To examine, whether heart development was defective in these mice, I analysed heart sections from P7 *Nrp1*$^{Vegfa/Vegfa}$ mice and control littermates after immunolabelling for endomucin, which visualises capillaries as well as veins, and SMA, which labels the SMCs surrounding the coronary arteries. This revealed that the myocardium from *Nrp1*$^{Vegfa/Vegfa}$ mice contained fewer endomucin^{+} capillaries (**Figure 3.4B,D**). In addition, the capillaries appeared abnormal and were particularly sparse within the subendomyocardium, consistent with reports that angiogenesis occurs in an epicardial-to-endocardial fashion (Tomanek, 1996). Furthermore, there were less SMA^{+} endomucin^{-} coronary arteries within mutant hearts compared to controls, whereas the number of veins was not affected (arrowheads, clear arrowheads, respectively, **Figure 3.4A,C**). Thus, VEGF-A signalling through NRP1 is required for normal vascularisation of the myocardium, which in turn is a requisite of proper cardiac function.

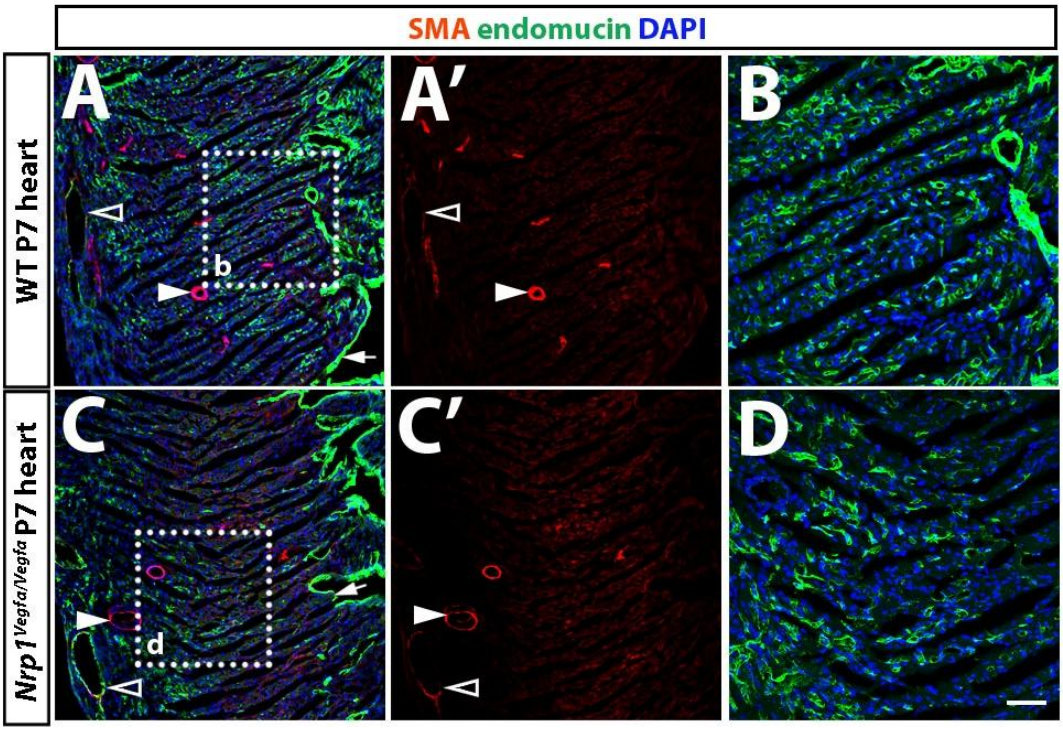

Figure 3.4 *Nrp1*$^{Vegfa/Vegfa}$ hearts display reduced myocardial vascularisation

Sections of *Nrp1*$^{Vegfa/Vegfa}$ and wildtype P7 hearts were immunolabelled for endomucin, SMA and counterstained with DAPI. Single SMA channel is shown in **(A',C')**. High magnification of areas indicated in **(A,C)** are shown in **(B,D)**. Solid arrowheads indicate SMA^{+}endomucin^{-} arteries, clear arrowheads SMA^{low}endomucin^{+} veins. Scale bar: 100 µm.

3.3 Discussion

Examination of endothelial versus non-endothelial NRP1 mutants demonstrated that all essential functions of NRP1 during embryonic angiogenesis are mediated within the endothelium, raising the question as to why the endothelial-specific *Nrp1* mutants display milder defects compared to the full *Nrp1* knockouts. Further investigation by our group demonstrated that this can be explained by the inefficient recombination of the *Tie2-Cre* transgene allowing unrecombined ECs to acquire tip cell properties and thus promote some residual angiogenesis (Fantin et al., 2013a, Gerhardt et al., 2004).

Whilst macrophage-derived NRP1 is dispensable for developmental angiogenesis, studies have shown that it is required for the attraction of pro-angiogenic macrophages during tumour angiogenesis (Casazza et al., 2013). Thus, tumours were found to secrete SEMA3A, which attracts NRP1-expressing macrophages and in turn promotes tumour vascularisation (Casazza et al., 2013). In contrast, no role for neuronal-derived NRP1 during developmental or pathological angiogenesis has been described to date; instead, this receptor is required for neuronal survival, migration and patterning (Tillo et al., 2015, Gu et al., 2003, Cariboni et al., 2011).

Analysis of $Nrp1^{Vegfa/Vegfa}$ hearts revealed that the vascularisation of the myocardium was defective in these mutants, suggesting that VEGF-A signalling through NRP1 is required for this process. This phenotype was similar to the defect displayed by $Vegfa^{120/120}$ mice, which also have a reduction in myocardial vascularisation resulting in an increased perinatal mortality (Carmeliet et al., 1999). The similarity of defects in myocardial vascularisation observed in $Nrp1^{Vegfa/Vegfa}$ and $Vegfa^{120/120}$ hearts suggests that the perinatal vascularisation of the myocardium depends on VEGF-A binding to NRP1. Future studies using conditional *Nrp1* and *Vegfa* mutants may wish to examine the cell type-specific requirements of these molecules. Furthermore, as the occurrence of enlarged hearts and blood-filled lungs can also be indicative of pulmonary deficiencies, future studies should also examine the lungs of $Nrp1^{Vegfa/Vegfa}$ mice to determine whether the decreased survival of these mutants might also be attributed to decreased lung vascularisation and/or branching.

3.4 Summary

At the beginning of my PhD the role of endothelial versus non-endothelial NRP1 had not yet been defined. My analysis confirmed that non-endothelial NRP1 was dispensable for developmental angiogenesis, whilst endothelial NRP1 was essential.

Furthermore, I demonstrated that *Nrp1*$^{Vegfa/Vegfa}$ mutants display impaired myocardial vascularisation, which presumably contributes to the occurrence of ischemic cardiomyopathy and thus increased perinatal mortality in these mice.

Chapter 4 NEURAL CREST-DERIVED SEMA3C ACTIVATES AN ENDOTHELIAL-TO-MESENCHYMAL TRANSITION THAT IS ESSENTIAL FOR CARDIAC OUTFLOW TRACT SEPTATION

4.1 Introduction

As detailed in the introduction, the OFT of the embryonic heart needs to septate and remodel to generate the base of the aorta and the pulmonary artery. This septation is essential for the formation of the double circulation that sustains adult mammalian life. Several prior studies have elucidated molecular signals that regulate the interactions of the three cell types involved in OFT remodelling, the ECs, the cardiac NCCs and the SHF-derived myocardium (see **1.4.3**). Yet, the precise molecular and cellular regulatory hierarchies remain ill-defined, and the sequence of events that enable vascular remodelling and septal bridge formation are not yet understood. Accordingly, NRP1 is essential for OFT remodelling (Kawasaki et al., 1999), but its precise function in this process has not been fully defined. Thus, previous studies suggested that VEGF-A signalling through endothelial NRP1 is essential for OFT remodelling, as the endothelial-specific deletion of *Nrp1* results in OFT defects (Gu et al., 2003, Zhou et al., 2012). Furthermore, mice lacking the NRP1-binding isoforms of VEGF-A ($Vegfa^{120/120}$) display defective OFT septation (Stalmans et al., 2003). Nevertheless, a recent publication that I contributed to (see **Chapter 3**) demonstrated that mice lacking the VEGF-A binding site in their NRP1 receptor ($Nrp1^{Vegfa/Vegfa}$) are viable, implying that another ligand must be signalling through the endothelial NRP1 (Fantin et al., 2014).

In addition, SEMA3C is known to be critical for OFT septation (Feiner et al., 2001) and studies have suggested that it is required to guide migrating cardiac NCCs into the OFT (Feiner et al., 2001, Kirby and Hutson, 2010). NRP1 is thought to function as a SEMA3C receptor in cardiac NCCs, where it is partially redundant with its homolog NRP2 (Toyofuku et al., 2008, Gu et al., 2003). To convey semaphorin signals in cardiac NCCs, it has been postulated that NRPs form a complex with a co-receptor termed PLXNA2, a member of the plexin family that is also expressed in cardiac NCCs (Brown et al., 2001). Nevertheless, a role for NRPs in cardiac NCCs has never been demonstrated directly for mammalian OFT

remodelling. Furthermore, another study showed that a different plexin, PLXND1, which binds SEMA3C and forms a receptor complex with NRPs, is required on the endothelium for OFT septation (Gitler et al., 2004). Thus, the tissue-specific functions, as well as the ligand requirements of NRP1 during OFT septation are not fully understood.

Given the conflicting results regarding NRP1's involvement in OFT remodelling, I have re-investigated the role of this receptor by taking advantage of tissue-specific *Nrp1* knockout mice. I have thus compared OFT development in mice lacking NRP1 in OFT endothelium (*Tie2-Cre;Nrp1*$^{fl/-}$) versus mice lacking NRP1 in cardiac NCCs (*Wnt1-Cre;Nrp1*$^{fl/fl}$). I have also investigated knockin mice with mutations in NRP1 that selectively target VEGF-A (*Nrp1*$^{Vegfa/Vegfa}$; (Fantin et al., 2014) versus SEMA3 (*Nrp1*$^{Sema/Sema}$; (Gu et al., 2003) binding to distinguish the relative contribution of both ligands to NRP1 signalling during OFT septation. Finally, I have also investigated tissue-specific ligand requirements using mice containing a conditional VEGF-A allele (*Vegfa*$^{fl/fl}$; (Gerber et al., 1999). To investigate tissue-specific SEMA3C knockout mice, I collaborated with Prof Peter Scambler at the Institute of Child Health (UCL), as his group had generated mice containing a conditional SEMA3C allele (*Sema3c*$^{fl/fl}$, unpublished).

I have examined these complementary mouse mutants by combining a variety of techniques, including detailed analyses of immunolabelled histological sections, comparison of gene expression, as well as the investigation of *in vitro* assays. Amelie Calmont, a postdoctoral research fellow in Prof Pete Scambler's group, contributed towards the analysis of *Wnt1-Cre;Sema3c*$^{fl/fl}$ mice.

4.2 Results

4.2.1 NRP1, not NRP2, has multiple essential roles during OFT remodelling

A prior study (Kawasaki et al., 1999) demonstrating that NRP1 is required for OFT remodelling, used ink injections to show that *Nrp1*-null mutants display defective OFT septation, a technique that does not reveal which aspect of OFT development is impaired. To analyse the OFT defect in *Nrp1*$^{-/-}$ mice in more detail, I cut serial, orthogonal (20 µm) sections of mutant and control E12.5 embryos and

stained them with the endothelial marker PECAM and the SMC marker SMA, as previous experiments from our lab as well as previous studies had demonstrated that SMA also labels the embryonic myocardium (Clement et al., 2007). By examining sections through the distal and proximal OFT at this time point, I was able to analyse endocardial cushion swelling and endothelial fusion, as well as myocardialisation of the septal bridge and valve formation (Compare **Figure 4.1A** with **Figure 4.1B-D**).

Using this experimental approach, I observed that none of the wildtypes (9/9), but all mutants (5/5) displayed a complete CAT, i.e. a lack of septation throughout the entire OFT (**Figure 4.1E**). In addition, I found that the proximal sections of mutant OFTs displayed disorganised endocardial cushions (asterisks, **Figure 4.1G**), which resulted in their abnormal orientation relative to the heart (dotted line, **Figure 4.1F**). Thus, wildtype OFTs contained two opposing endocardial cushions (asterisks, **Figure 4.1D**), whereas in mutants the endocardium associated with the myocardium in ectopic positions generating additional cushion "leaflets" or "fingers" (asterisks, **Figure 4.1G**). Furthermore, myocytes in the mutant OFTs failed to migrate towards the centre of the vessel; instead, these cells appeared to "stall" in the lateral part of the endocardial cushions (open arrowheads, **Figure 4.1E,L**). Finally, valve formation was completely absent in mutant OFTs (**Figure 4.1E**). In contrast, *Nrp2*$^{-/-}$ mutants did not show any defects in OFT remodelling (**Figure 4.1H-J,M**).

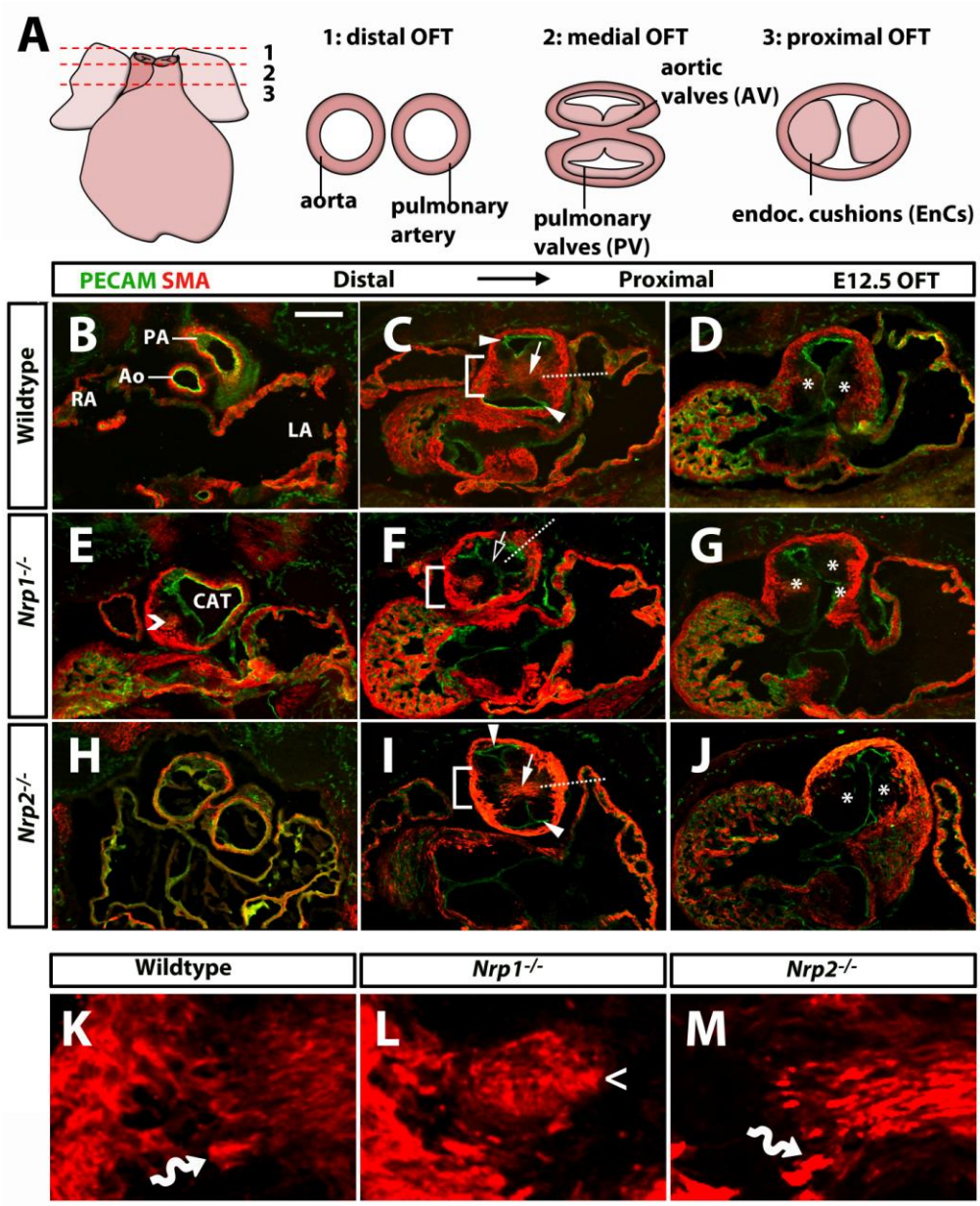

Figure 4.1. NRP1, not NRP2, is required for multiple steps of OFT remodelling.

Schematic representation of the E12.5 mouse OFT at distal (1), medial (2) and proximal (3) positions relative to the heart **(A)**. Serial sections of wildtype, *Nrp1*$^{-/-}$ and *Nrp2*$^{-/-}$ E12.5 OFTs immunolabelled for PECAM and SMA, and imaged at corresponding proximal, medial and distal levels **(B-J)**. Solid arrowheads indicate the septated endothelium, solid arrows demonstrate septal bridge myocardialisation and clear arrows the absence of septal bridge formation. Dotted lines indicate the angle of septal bridge formation and asterisks highlight endocardial cushion position. Magnification of areas indicated by brackets in **(C,F,I)** are shown in **(K-M).** Curly arrows label migrating myocytes and open arrowheads denote stalled myocytes. Scale bar: 200 µm.

4.2.2 Expression pattern of NRP1 during OFT remodelling

To understand how NRP1 might be required for the multiple steps in OFT septation, I examined the expression pattern of both NRP1 and NRP2 at E11.5 and E12.5. By labelling medial OFT sections of wildtype embryos with a previously validated antibody for NRP1 (Fantin et al., 2010) together with SMA and the vascular endothelial marker IB4, I found that NRP1 was expressed on the $IB4^+$ OFT endothelium at both E11.5 and E12.5 (arrowheads, **Figure 4.2A-B'**). Furthermore, NRP1 was expressed on migrating myocytes at E12.5, but not at E11.5, at which point myocytes migration has not yet begun (curly arrow, clear curly arrow, respectively, **Figure 4.2A-B'**). In contrast, there was no obvious NRP1 expression within the region occupied by the post-migratory cardiac NCCs (asterisk, **Figure 4.2B,B'**).

Analysis of wildtype OFT sections immunolabelled for NRP2, SMA and IB4 demonstrated that NRP2 and NRP1 expression overlapped only partially. Thus, unlike NRP1, NRP2 was only found on the OFT endothelium at E12.5. However, like NRP1 no NRP2 detection was found within myocytes at E11.5 (clear curly arrow, **Figure 4.2C,C'**) or in the septal bridge at E12.5 (asterisk, **Figure 4.2D,D'**). In addition, NRP2 was weakly expressed on migrating myocytes at E12.5 (curly arrow, **Figure 4.2D,D'**).

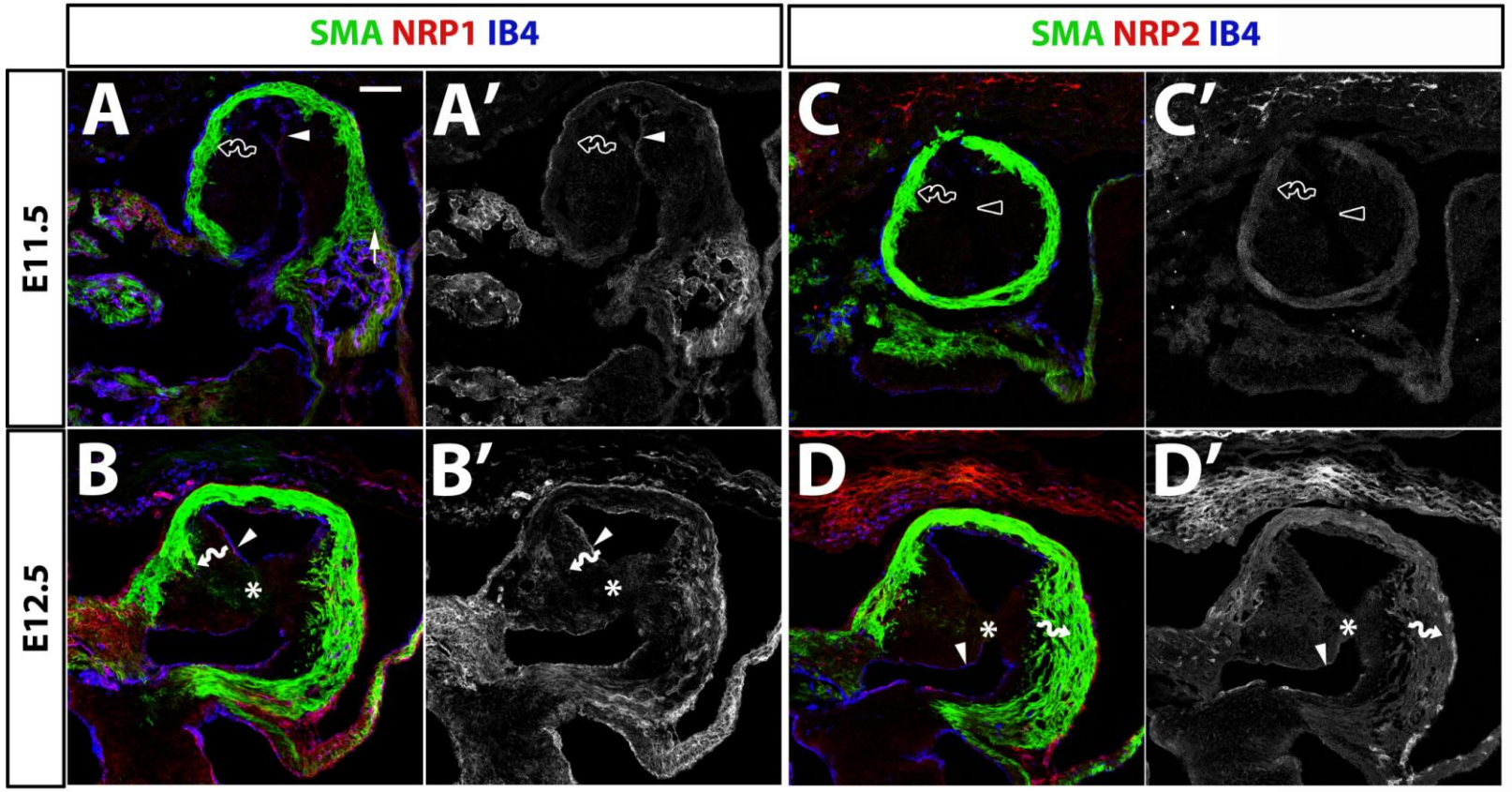

Figure 4.2. NRP1 and NRP2 expression in E11.5 and E12.5 OFT.

Medial OFT sections at E11.5 and E12.5 were immunolabelled for SMA and IB4 together with NRP1 **(A-B')** or NRP2 **(C,D')**; Solid arrowheads denote NRP expression within endothelium, curly arrows expression within migrating myocytes, whilst clear curly arrows indicate a lack of NRP expression in myocytes; asterisks highlight the lack of NRP expression within the septal bridge that is colonised by cardiac NCCs. Scale bar: 100 µm.

4.2.3 EndoMT and NCCs give rise to distinct parts of the OFT

To examine the cell-specific requirements for NRP1 in OFT septation, I performed a detailed analysis of mice lacking endothelial- versus NCC-derived NRP1. For this experiment, I first validated the *Tie2-Cre* and *Wnt1-Cre* transgenes as suitable tools for endothelial versus NCC targeting by crossing the transgene to the floxed $Rosa^{Yfp}$ reporter. YFP immunolabelling of serial sections through E12.5 OFTs from *Wnt1-Cre;*$Rosa^{Yfp}$ and *Tie2-Cre;*$Rosa^{Yfp}$ mice also allowed me to determine the relative positions of endothelial and NCC progeny via lineage tracing.

As expected, *Tie2-Cre* targeted the endothelium (arrowhead, **Figure 4.3H**), whereas *Wnt1-Cre* did not (clear arrowhead, **Figure 4.3D**). In addition, YFP staining revealed a substantial number of *Tie2-Cre*-labelled cells within the endocardial cushions of the OFT and, to a lesser extent, within the semilunar valves (curved arrow, **Figure 4.3G,H**), consistent with the occurrence of endoMT. Interestingly, the areas, where endoMT had occurred within the endocardial cushions, overlapped with the areas occupied by the cardiac NCCs (compare asterisk and curved arrow, **Figure 4.3C** and **Figure 4.3G**, respectively). Analysis of YFP labelling in *Wnt1-Cre;*$Rosa^{Yfp}$ OFTs showed that the progeny of cardiac NCCs formed the septal bridge (arrow, **Figure 4.3B**) and additionally made a major contribution to the two semilunar valve leaflets in the central part of the OFT (open arrowheads, **Figure 4.3A**). Thus, this analysis validated the suitability of both transgenes to target NRP1 in endothelium versus NCCs and confirmed the distinct contributions of ECs and cardiac NCCs to OFT remodelling.

4.2.4 NRP1 is not required for cardiac NCC migration into the OFT

Because a role for NRP1 in cardiac NCC migration had been reported previously in chick (Toyofuku et al., 2008), I compared the distribution of cardiac NCCs in wildtype and *Nrp1*-null OFTs with the cardiac NCC reporter *Wnt1-Cre;Rosa*^{LacZ} (Jiang et al., 2000) (**Figure 4.3I,J**). I observed that cardiac NCCs migrated through the PAAs and into the OFT in two prong-shaped streams, as expected (see schematic, **Figure 4.3K**); unexpectedly, however, the migration pattern was similar in both wildtype (n= 4) and *Nrp1*-null mutant (n= 3) mice (arrowheads, **Figure 4.3I,J**). This result established that cardiac NCCs do not require NRP1 to reach their target tissues and implies that the OFT phenotype of *Nrp1*$^{-/-}$ mutants is not caused by defective cardiac NCC migration.

4.2.5 NCC-derived NRP1 is not required for OFT septation in the mouse

Because the normal cardiac NCC migration pattern in *Nrp1*-nulls suggested that cardiac NCC-derived NRP1 was dispensable for OFT septation, even though previous studies had implied that it was required (Toyofuku et al., 2008), I examined the OFTs from *Wnt1-Cre;Nrp1*$^{fl/fl}$ mice. This genetic cross targets *Nrp1* efficiently in the NCC lineage, as *Wnt1-Cre;Nrp1*$^{fl/fl}$ mutants demonstrate severe defects in the sympathetic nervous system similar to those of full *Nrp1*$^{-/-}$ mice (Maden et al., 2012). Nevertheless, serial sections through E12.5 mutant and control OFTs demonstrated that, in contrast to the phenotype of *Nrp1*$^{-/-}$ mice, the OFTs of neural crest-specific NRP1 mutants were septated properly with a normal appearance and rotation of the endocardial cushions and typical myocardialisation of the septal bridge in 4/4 of mutants analysed (**Figure 4.4D-F**). As several ligands of NRP1 can also signal through NRP2, I crossed *Wnt1-Cre;Nrp1*$^{fl/fl}$ mutants onto a *Nrp2*-null background to address whether NRP2 was compensating for the lack of NRP1 in cardiac NCCs, as previously proposed (Gu et al., 2003, Toyofuku et al., 2008). However, 3/3 mutants examined also showed normal OFT septation, rotation and myocardialisation (**Figure 4.4G-I**). Thus, these findings established that contrary to prior hypotheses, NRP1 and NRP2 expression by cardiac NCCs is not required for OFT remodelling.

4.2.6 Endothelial NRP1 is essential for OFT septation in the mouse

Like the original studies demonstrating a requirement for NRP1 during OFT remodelling (Kawasaki et al., 1999), ink injections were also used to demonstrate that mice lacking NRP1 in the vascular endothelium (*Tie2-Cre;Nrp1*$^{fl/-}$) have defective OFT septation (Gu et al., 2003, Zhou et al., 2012). My histological approach confirmed this finding; thus, serial sections immunolabelled for PECAM and SMA showed that 6/6 *Tie2-Cre;Nrp1*$^{fl/-}$ mutants had defective OFT septation (**Figure 4.4J-L)**. In addition, I was also able to demonstrate that the defects included septation failure both in the proximal and distal part of the OFT, as well as disorganised endocardial cushion formation and impaired myocardialisation (**Figure 4.4J-L)**. Taken together with my analysis of the NCC-specific NRP1 mutants, these observations suggest that all essential NRP1 signalling during OFT remodelling takes place in the vascular endothelium.

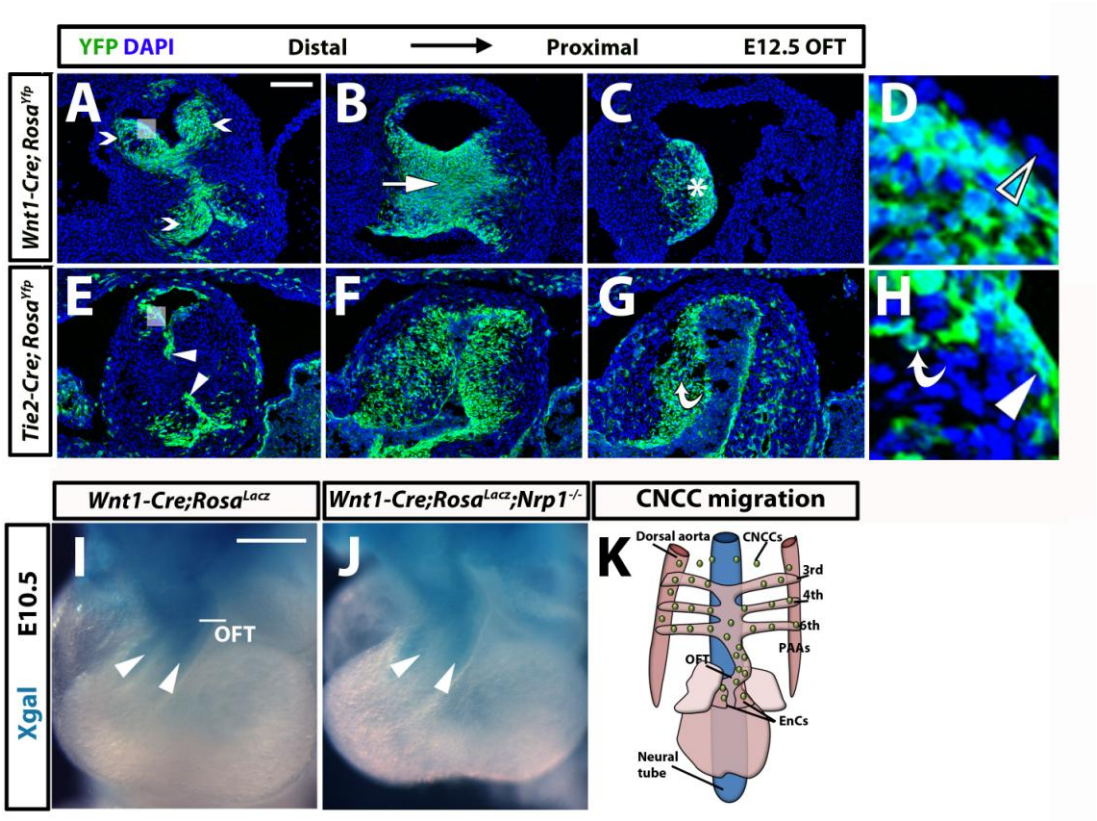

Figure 4.3. NRP1 is not required for cardiac NCC migration into the OFT.

Serial sections of *Tie2-Cre;Rosa*^{Yfp} and *Wnt1-Cre;Rosa*^{Yfp} E12.5 OFTs at corresponding distal, medial and proximal levels immunolabelled for YFP and counterstained with DAPI (**A-H**). Arrows indicate the contribution of cardiac NCCs to the septal bridge, whereas the open arrowheads highlight the contribution to the valves. Insets show a higher magnification of the valves, where arrowheads show the targeting or absence of targeting of the endothelium (full arrowhead and clear arrowhead, respectively) and curved arrows indicate endoMT within the valves. Wholemount Xgal staining of *Wnt1-Cre;Rosa*^{LacZ} E10.5 OFTs on a wildtype or *Nrp1*-null background; arrowheads indicate the paired streams of migrating cardiac NCCs **(I,J)**. Schematic representation of cardiac NCC migration at E10.5 (**K**). Cardiac NCCs (green) migrate from neural tube (blue), along PAAs and into OFT in two streams. CNCC: Cardiac NCCs. Scale bars: 100 µm **(A-H)**, 200 µm **(I,J)**.

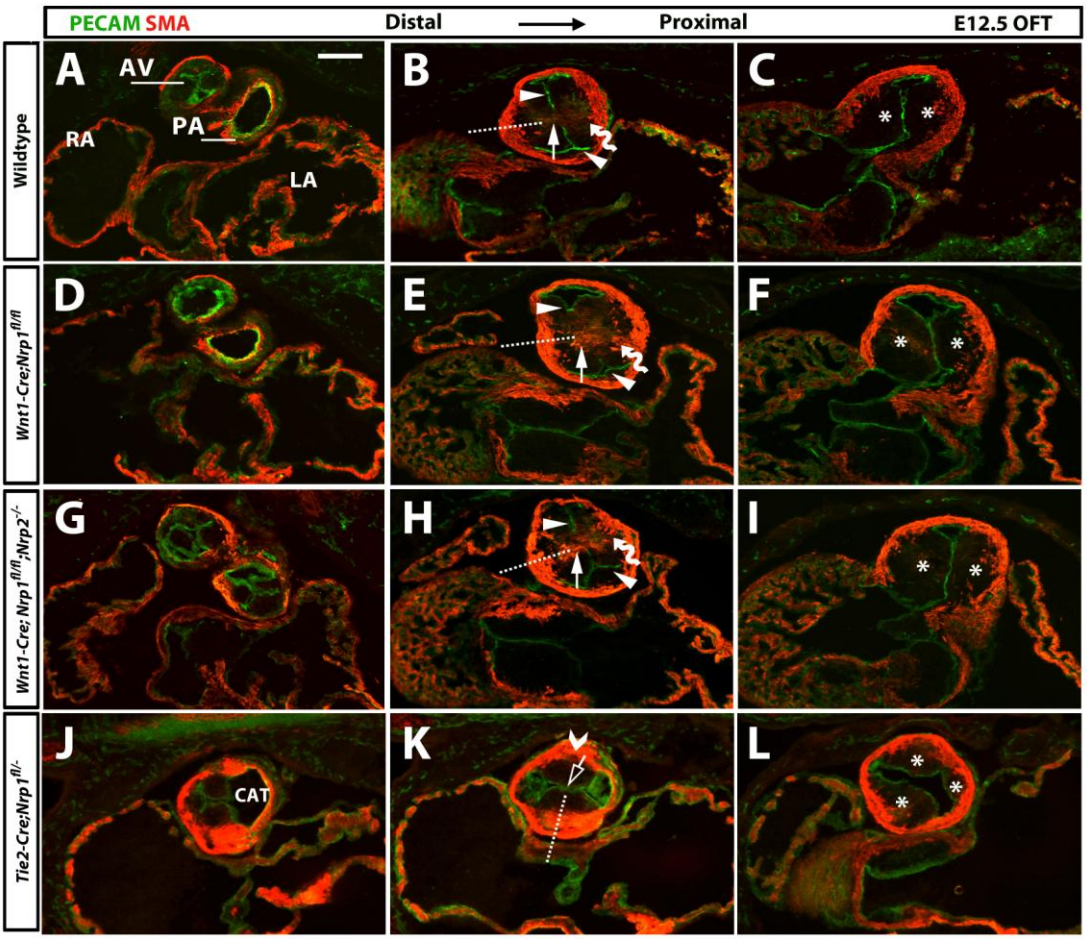

Figure 4.4. Endothelial, not NCC-derived NRP1 is required for OFT septation.

Serial sections of wildtype **(A-C)**, *Wnt1-Cre;Nrp1*$^{fl/-}$**(D-F)**, *Wnt1-Cre;Nrp1*$^{fl/fl}$*;Nrp2*$^{-/-}$**(G-I)** and *Tie2-Cre;Nrp1*$^{fl/-}$ **(J-L)** E12.5 OFTs immunolabelled for PECAM and SMA. Solid arrowheads indicate the septated endothelium, solid arrows demonstrate septal bridge myocardialisation and clear arrows the absence of septal bridge formation. Curly arrows denote migrating myocytes and open arrowheads stalled myocytes. Dotted lines indicate the angle of septal bridge formation and asterisks highlight endocardial cushion position. Scale bar: 200 µm.

4.2.7 Cardiac NCC-derived VEGF-A is not important for OFT remodelling

VEGF-A has been shown to be an important NRP1 ligand for OFT septation. Thus, prior studies observed that *Vegfa*$^{120/120}$ mice, which express only VEGF120 at the expense of the heparin/NRP-binding isoforms of VEGF-A (Stalmans et al., 2003), had OFT septation defects. Furthermore, another study observed that mice lacking NRP1 in the endothelium display defective OFT septation (Gu et al., 2003). As previous studies had suggested that NRP1's only role in the endothelium is to enhance VEGF-A signalling through its receptor, VEGFR2, the phenotype of these mice was interpreted as evidence for an essential role of VEGF-A signalling through NRP1 in OFT remodelling (Gu et al., 2003). However, neither study was able to directly address the role of VEGF-A as a NRP1 ligand in OFT development, because a mouse mutant defective in VEGF-A binding to NRP1 was not available at the time; moreover, the *Vegfa* expression pattern had not been analysed to determine whether NCCs provide an important source of this growth factor for OFT remodelling. To investigate, which ligand is required to signal to the endothelial NRP1 during OFT remodelling, I decided to first analyse the expression of VEGF-A within the OFT.

Using an established *Vegfa*^{LacZ} reporter mouse (Miquerol et al., 1999), I observed weak VEGF-A expression by the OFT endothelium within the valve leaflets, and strong expression by the SHF-derived myocardial OFT cuff at E12.5 (arrowhead and curly arrow, respectively, **Figure 4.5A-C**). In contrast, VEGF-A appeared to be absent from the area occupied by cardiac NCCs (arrow, **Figure 4.5B**).

As the defects in great vessel remodelling observed in *Vegfa*$^{120/120}$ mutants are reminiscent of the phenotype found in mice with defective cardiac NCC behaviour, I decided to investigate whether cardiac NCCs are an essential source of VEGF-A. Thus, I introduced the *Wnt1-Cre* transgene into mice with a conditional *Vegfa*-null allele (*Vegfa*$^{fl/fl}$; (Gerber et al., 1999). In agreement with the lack of obvious *Vegfa* expression in OFT NCCs, 3/3 *Wnt1-Cre;Vegfa*$^{fl/fl}$ embryos revealed normal OFT septation (arrow, **Figure 4.5G-I**).

To address, whether VEGF-A binds to cardiac NCCs during OFT remodelling, I labelled E12.5 serial sections with an AP-tagged VEGF-A probe. This analysis revealed that VEGF-A binds strongly to the OFT endothelium (arrowheads,

Figure 4.5J-L). In addition, VEGF-A also bound to cells undergoing endoMT in the semilunar valves (curly arrows, **Figure 4.5J,K**). In contrast, no VEGF-A binding was observed within the myocardial cuff and septal bridge (open arrowheads, arrow, respectively, **Figure 4.5J,K**). Together, these findings demonstrated that cardiac NCCs do not express VEGF-A to induce OFT septation; instead, the SHF-derived cells appeared to be the major source of VEGF-A. Furthermore, VEGF-A mainly bound to ECs, but not to cardiac NCCs suggesting that the functions of VEGF-A are mainly within the endothelium. The observation that VEGF-A also bound strongly to cells undergoing endoMT implies that VEGF-A might play a role in endocardial cushion and semilunar valve formation.

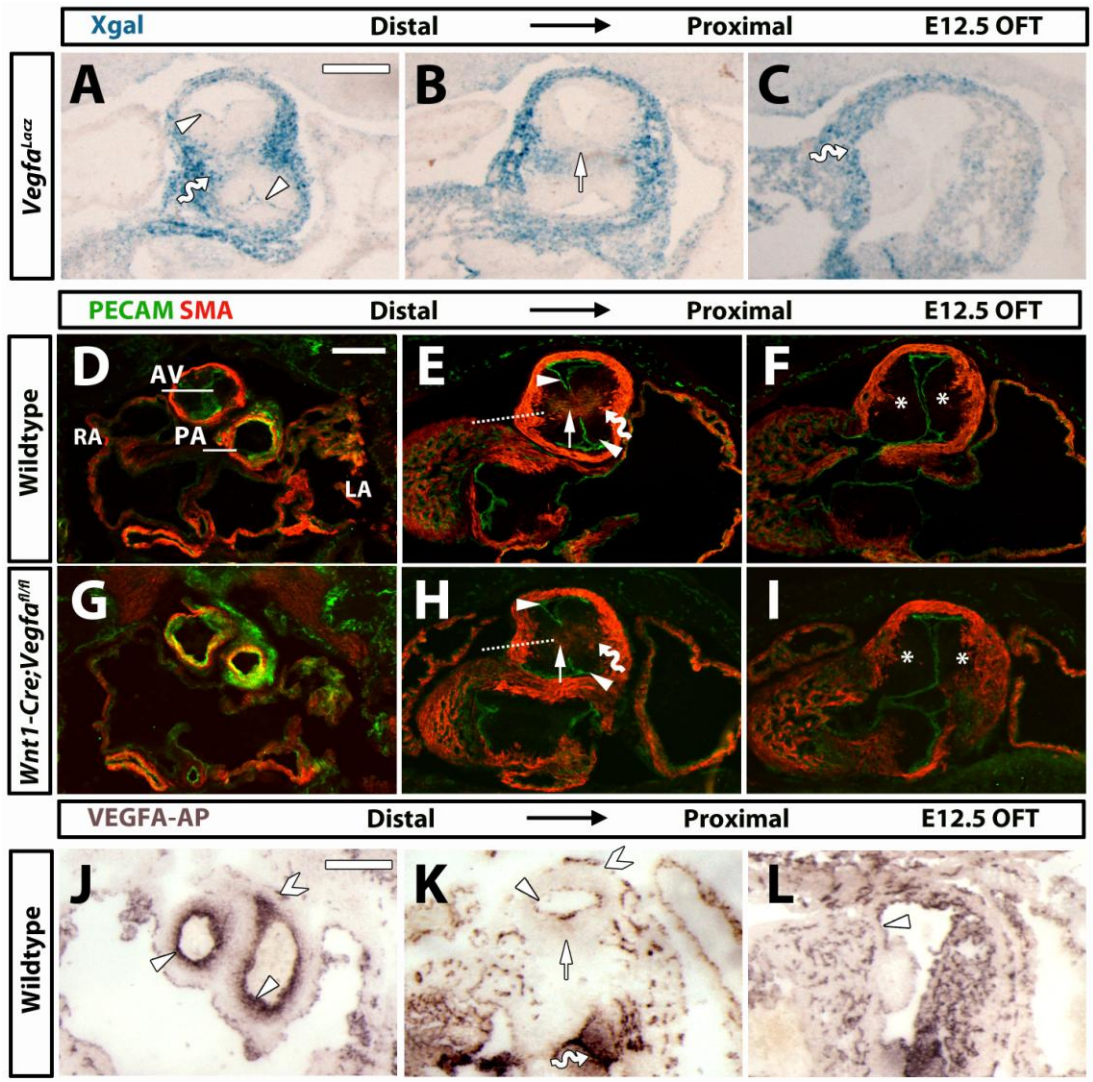

Figure 4.5. Cardiac NCCs are not an essential source of VEGF-A for OFT remodelling.

Serial sections through E12.5 *Vegfa*^{LacZ} OFTs stained with Xgal **(A-C)**. Arrowheads indicate *Vegfa* expression on OFT endothelium, arrow highlights lack of *Vegfa* expression in the septal bridge area; curly arrows indicate *Vegfa* expression on the OFT myocardium. Serial sections of wildtype and *Wnt1-Cre;Vegfa*$^{fl/fl}$ E12.5 OFTs immunolabelled for PECAM and SMA **(D-I)**. Arrowheads indicate the septated endothelium and arrows highlight septal bridge myocardialisation. Dotted lines indicate the angle of septal bridge formation, curly arrows migrating myocytes and asterisks highlight endocardial cushion position. Serial sections through E12.5 wildtype OFTs labelled with a VEGFA-AP probe **(J-L)**. Arrowheads indicate VEGF-A binding to the OFT endothelium, arrows highlight lack of binding within in the septal bridge area; curly arrows indicate VEGF-A binding to cells undergoing endoMT, whereas open arrowheads label lack of binding to the myocardial cuff. Scale bars: 200 µm.

4.2.8 VEGF-A signalling through NRPs is dispensable for OFT septation

To examine whether the defects observed in *Nrp1*-null and *Tie2-Cre;Nrp1*$^{fl/-}$ were caused by a lack of VEGF-A signalling through NRP1, I first compared the OFT phenotype of *Vegfa*$^{120/120}$ mice to the phenotype observed in *Nrp1*-null mice by analysing serial sections through the E12.5 OFTs.

In contrast to the phenotype observed in *Nrp1*-null mice, *Vegfa*$^{120/120}$ OFTs showed normal endocardial cushion organisation (asterisk, **Figure 4.6F**). Furthermore, endothelial fusion took place in *Vegfa*$^{120/120}$ OFTs, albeit only in the distal segment in 1/4 mutants analysed (clear arrow, arrow **Figure 4.6D,E**), whereas all *Nrp1*-null mutants displayed a complete lack of OFT septation. In addition, the pulmonary segment of the OFT appeared hypoplastic and lacked semilunar valves in 1/4 *Vegfa*$^{120/120}$ mutants analysed (open arrowhead, **Figure 4.6D**), whereas 2/4 of *Vegfa*$^{120/120}$ mutants displayed no OFT phenotype (data now shown), which agreed with the partially penetrant heart defects described in *Vegfa*$^{120/120}$ mice in previous studies (Stalmans et al., 2003), but differed from the defect observed in *Nrp1*-null mutants. This analysis therefore revealed that the *Vegfa*$^{120/120}$ and *Nrp1*-null mutant phenotypes are different, which implies that the defective OFT septation in *Nrp1*$^{-/-}$ mice is not caused by a lack of VEGF-A signalling through NRP1

To confirm that VEGF-A signalling through NRP1 is indeed dispensable for OFT remodelling, I took advantage of mice with a knockin mutation that impairs VEGF-A binding to NRP1 (Fantin et al., 2014), designated here as *Nrp1*$^{Vegfa/Vegfa}$ mutants (see **Chapter 3**). Immunolabelling of serial sections for PECAM and SMA revealed that septation, OFT rotation and myocardialisation were normal in 4/4 *Nrp1*$^{Vegfa/Vegfa}$ mutants examined (**Figure 4.6G-I**). Moreover, 3/3 *Nrp1*$^{Vegfa/Vegfa}$ mice on a *Nrp2*-null background also had normal OFT septation, rotation and myocardialisation (**Figure 4.6J-L**), excluding the possibility that a lack of defect in *Nrp1*$^{Vegfa/Vegfa}$ mutants is caused by NRP2 compensating for the *Nrp1*^{Vegfa} mutation. Thus, contrary to prior hypotheses, endothelial NRP1 does not act as a VEGF-A receptor during OFT septation.

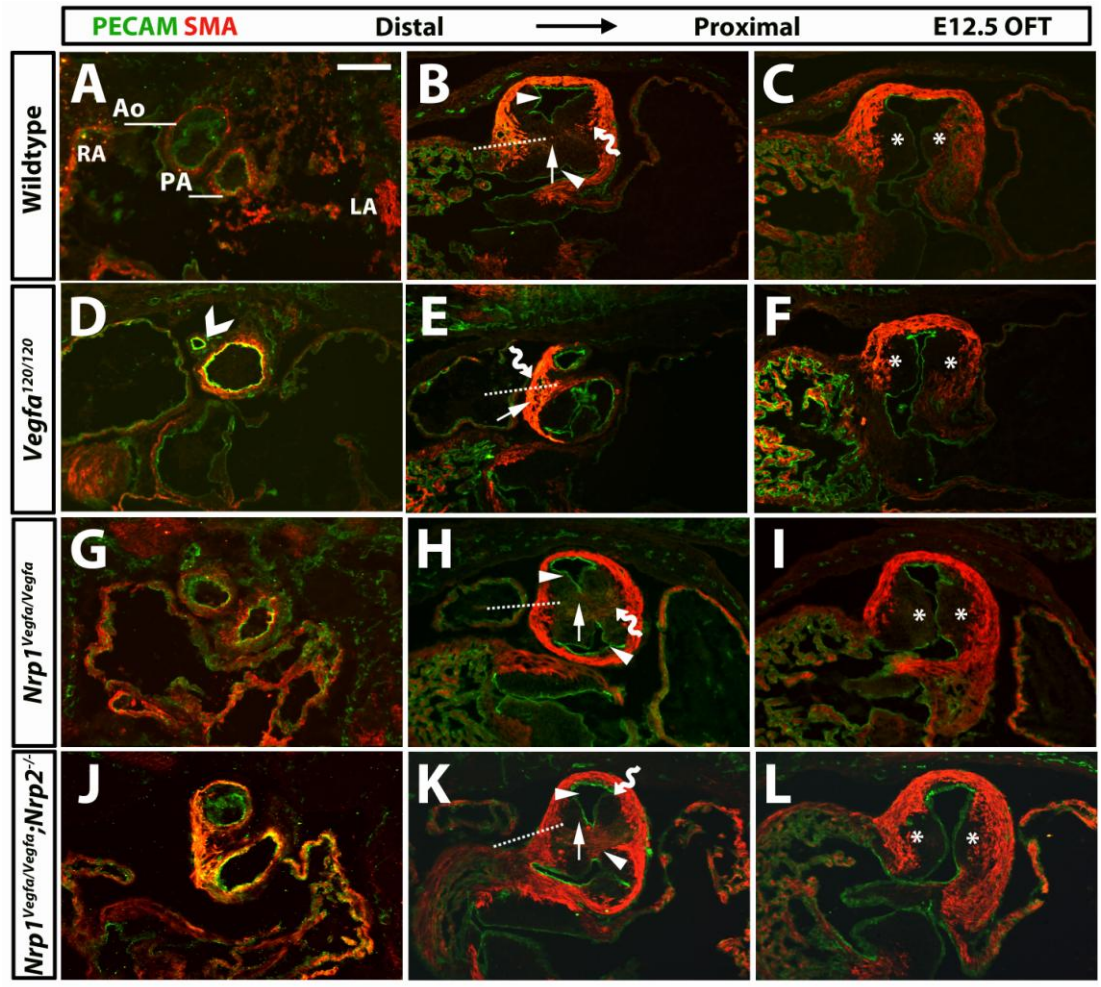

Figure 4.6. VEGF-A signalling through NRPs is dispensable for OFT remodelling.

Serial sections of wildtype **(A-C)**, *Vegfa*$^{120/120}$ **(D-F)**, *Nrp1*$^{Vegfa/Vegfa}$ **(G-I)** and *Nrp1*$^{Vegfa/Vegfa}$*;Nrp2*$^{-/-}$ **(J-L)** E12.5 OFTs immunolabelled for PECAM and SMA. Solid arrowheads indicate the septated endothelium, solid arrows highlight septal bridge myocardialisation and clear arrows the absence of septal bridge formation. Dotted lines indicate the angle of septal bridge formation, curly arrows migrating myocytes, asterisks highlight endocardial cushion position and open arrow heads denote a hypoplastic pulmonary artery. Scale bar: 200 μm.

4.2.9 The expression pattern of VEGFR2 suggests a role for this VEGF-A receptor in OFT remodelling

To investigate whether VEGFR2 functions as the critical VEGF-A receptor during OFT remodelling, I examined VEGFR2 expression in E12.5 OFTs by immunolabelling serial sections for VEGFR2, SMA and IB4. This experiment demonstrated that VEGFR2 was strongly expressed by OFT ECs (arrowhead, **Figure 4.7A,B,D**). In addition, VEGFR2 appeared to be expressed by ECs undergoing endoMT and thus invading the endocardial cushions (curly arrow, **Figure 4.7D,D'**), which agreed with my observation that the VEGFA-AP probe binds to ECs as well as cells adjacent to the endothelium in E12.5 OFT (see **Figure 4.5**). However, I observed no VEGFR2 staining within the septal bridge that contains cardiac NCCs (arrow, **Figure 4.7E,E'**). This finding also agreed with the VEGFA-AP binding pattern in the OFT (see **Figure 4.5**). Altogether, the pattern of VEGFR2 expression is consistent with VEGF-A signalling though endothelial VEGFR2 during OFT septation. Because *Vegfr2*-null mice are embryonic lethal by E9.5 (Shalaby et al., 1995), future studies could ablate endothelial VEGFR2 at E10.5 with an inducible *Cre/LoxP* approach (see **2.2.1.6**), followed by analysis of OFT remodelling in the mutants.

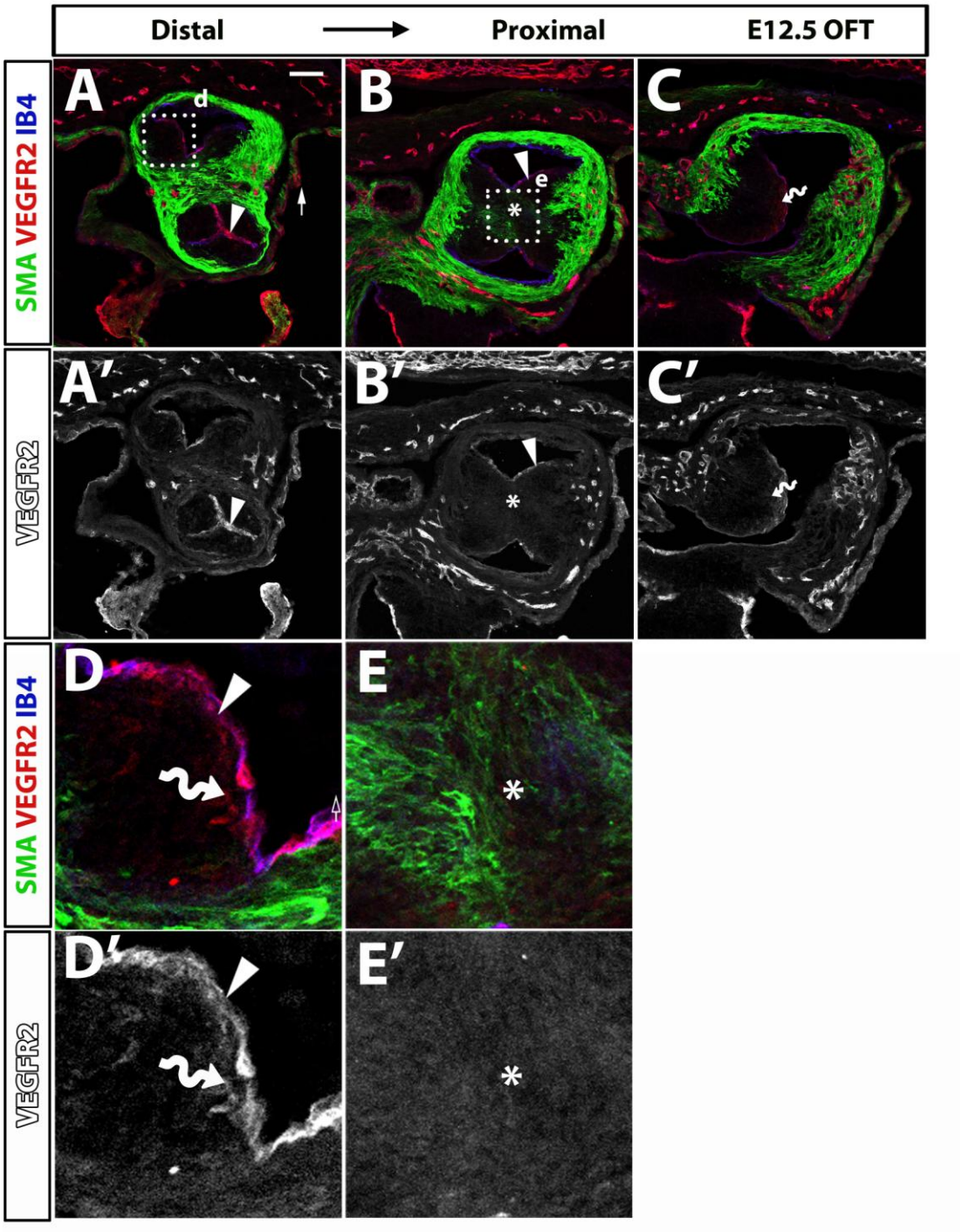

Figure 4.7. VEGFR2 is only expressed on EC lineage in the OFT.

(A-C) Serial sections of wildtype E12.5 OFTs immunolabelled for SMA, VEGFR2 and IB4. **(D-E')** Magnification of indicated areas in **(A)** and **(B)**. Solid arrowheads indicate expression on endothelium; whereas asterisks highlight lack of expression in septal bridge. Curly arrows label expression in cells undergoing endoMT. Scale bar: 100 μm.

4.2.10 SEMA3C is expressed by myocardial cuff cells and cardiac NCCs in the septal bridge

Given my observation that VEGF-A signalling through NRP1 is dispensable for OFT remodelling, I next investigated whether SEMA3C might be the ligand that is required by endothelial NRP1 for OFT septation. I chose to focus on SEMA3C, as genetic knockout studies had shown that SEMA3C is essential for OFT septation (Feiner et al., 2001, Gitler et al., 2004); however, its precise function during this process had not yet been established. To gain an understanding into the role of SEMA3C during OFT remodelling, I first analysed SEMA3C expression by *in situ* hybridisation. In agreement with prior findings (High et al., 2009, Feiner et al., 2001), I found that *Sema3c* was strongly expressed within the myocardial cuff that surrounds the aortic segment of the OFT and in the area where cardiac NCCs are located (arrowhead and arrow, respectively, **Figure 4.8A-C)**. Prior studies interpreted this expression pattern as an indication that SEMA3C attracts cardiac NCC into the OFT (Feiner et al., 2001, Toyofuku et al., 2008). In contrast, other studies hypothesised that *Sema3c* may also be expressed by cardiac NCCs themselves (High et al., 2009, Vallejo-Illarramendi et al., 2009). To resolve this controversy, I performed *Sema3c in situ* hybridisation on E12.5 OFT sections from *Wnt1-Cre;Rosa*^{Yfp} embryos. This analysis suggested that *Sema3c* is expressed by a subpopulation of cells in the cardiac NCC lineage (arrows, **Figure 4.8D,D'**). Double immunolabelling of sections from *Wnt1-Cre;Rosa*^{Yfp} embryos for YFP and PLXNA2, an established marker for a subset of postmigratory cardiac NCCs in the OFT (Brown et al., 2001), showed that the position of the SEMA3C-expressing subpopulation corresponded to that of cardiac NCCs expressing PLXNA2 (compare areas indicated with arrows in **Figure 4.8D** with **Figure 4.8E**).

To demonstrate directly that cardiac NCCs are a source of SEMA3C, we collaborated with Prof Pete Scambler at the UCL Institute of Child Health (ICH), who had generated mice with a conditional *Sema3c*-null allele (*Sema3c*$^{fl/fl}$) and bred them to *Wnt1-Cre* mice. Dr Calmont, a postdoctoral research fellow in his group, performed *in situ* hybridisation for *Sema3c* on *Wnt1-Cre;Sema3c*$^{fl/fl}$ OFTs to show that *Sema3c* expression was abolished in the septal bridge at E12.5 (asterisk, **Figure 4.8G**), demonstrating that they had generated a cardiac NCC-specific *Sema3c* knockout and further that cardiac NCCs do indeed provide a source of SEMA3C in

the OFT. In contrast, *Wnt1-Cre*;*Sema3c*$^{fl/fl}$ mutants preserved *Sema3c* expression in the myocardial cuff (arrowhead, **Figure 4.8G**), which is of SHF origin. Together, these findings raised the possibility that SEMA3C, rather than attracting cardiac NCCs into the OFT, is instead secreted by cardiac NCCs to promote OFT septation.

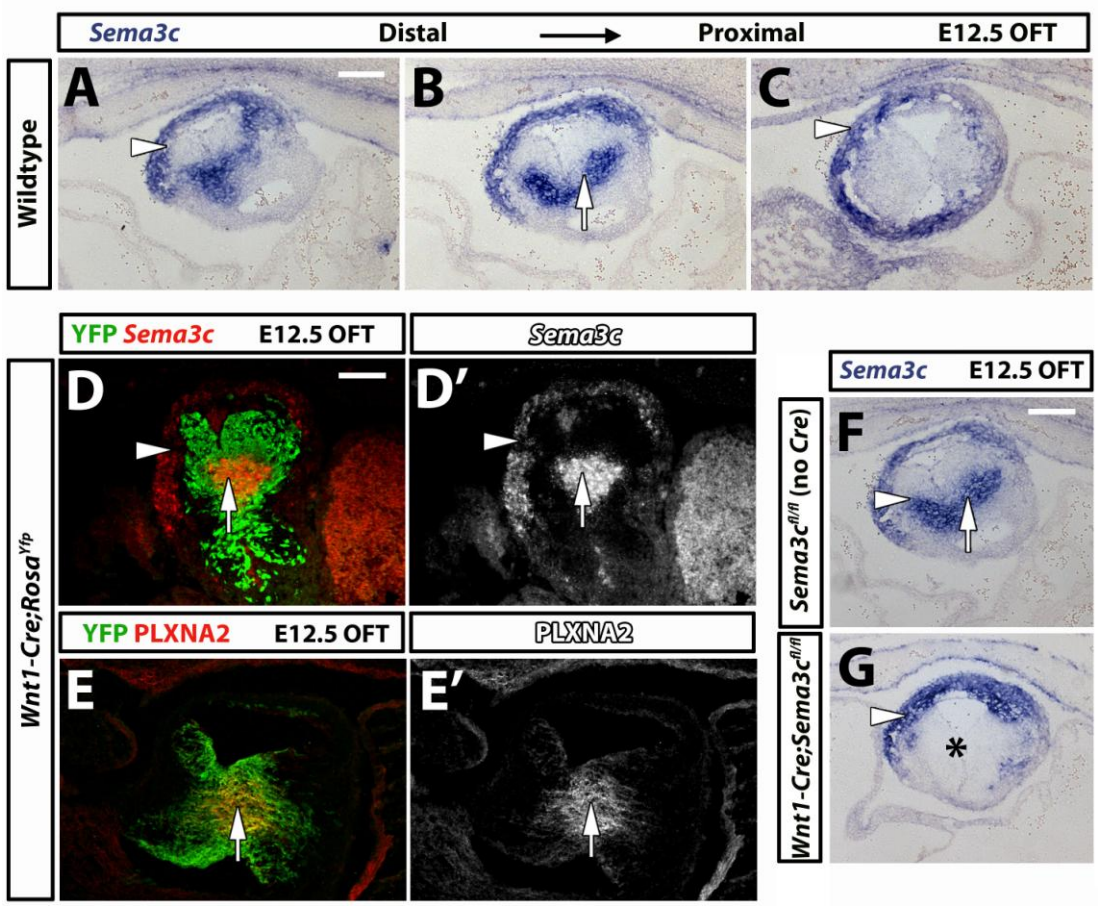

Figure 4.8. Cardiac NCCs are a source of SEMA3C within the OFT.

Sema3c in situ hybridisation of serial sections through E12.5 OFTs **(A-C)**. White arrowheads indicate *Sema3C* expression within the myocardial cuff and arrows *Sema3c* expression in the septal bridge area. **(D-E')** E12.5 *Wnt1-Cre;Rosa*^{Yfp} OFT sections were immunolabelled for YFP and counter-stained after *in situ* hybridisation for *Sema3c* **(D,D')** or double labelled for PLXNA2 **(E,E')**. White arrowheads highlight SEMA3C expression in the myocardial cuff; arrows indicate partial co-localisation of SEMA3C or PLXNA2 with YFP. E12.5 *Wnt1-Cre;Rosa*^{Yfp} OFT sections from *Sema3c*$^{fl/fl}$ mice lacking or containing *Wnt1-Cre* were labelled by *in situ* hybridisation for *Sema3c* **(F,G)**. Solid arrowheads indicate SEMA3C expression within the myocardial cuff, arrows indicate SEMA3C expression in the septal bridge and asterisks demonstrate absent SEMA3C expression due to genetic deletion of *Sema3c* within the cardiac NCCs. Scale bar: 100 µm.

4.2.11 Cardiac NCC-derived SEMA3C is essential for proximal OFT septation

Having established that cardiac NCCs are a source of SEMA3C within the OFT, Amelie and I next investigated whether SEMA3C secreted by these cells is important for OFT remodelling. Immunolabelling of E12.5 serial sections through *Wnt1-Cre;Sema3c*$^{fl/fl}$ OFTs for PECAM and SMA revealed that septation was defective in the proximal OFT of 20/20 mutants examined (clear arrow, **Figure 9B**), whereas the septal bridge did form distally in 18/20 mutants analysed (not shown). In the proximal OFT a lack of septation was accompanied by impaired myocyte migration, which instead appeared to stall within the endocardial cushions in the peripheral OFT (compare open arrowheads, **Figure 4.9B** with **Figure 4.9E**). Thus, the phenotype within the proximal OFT was reminiscent of the defect observed in the proximal segment of *Nrp1*$^{-/-}$ and *Tie2-Cre;Nrp1*$^{fl/-}$ OFTs (compare **Figure 4.1** and **Figure 4.4**), suggesting that in this part of the vessel SEMA3C is required to signal to endothelial NRP1 for normal remodelling to occur.

4.2.12 SEMA3C signalling through NRP1 promotes NCC-dependent septal bridge formation

To test the hypothesis that SEMA3C signals through NRP1 to enable proximal OFT septation, I cut serial sections through the OFT of E12.5 mice with a mutated version of NRP1 unable to bind to SEMA3s (*Nrp1*$^{Sema/Sema}$; (Gu et al., 2003) and immunolabelled them for PECAM and SMA. As observed in prior studies, these mice displayed normal OFT remodelling. Nevertheless, SEMA3C is known to bind to NRP1 and NRP2 (Chen et al., 1998) and thus NRP2 is able to compensate for NRP1. To analyse whether SEMA3C signalling through either NRP is essential for OFT septation, I generated *Nrp1*$^{Sema/Sema}$ mice on a *Nrp2*-null background, *Nrp1*$^{Sema/Sema}$*;Nrp2*$^{-/-}$. I cut serial sections through the E12.5 OFTs of *Nrp1*$^{Sema/Sema}$*;Nrp2*$^{-/-}$ mutants and labelled them for PECAM and SMA to compare them to mutants lacking NCC-derived SEMA3C. This analysis showed that 3/3 *Nrp1*$^{Sema/Sema}$*;Nrp2*$^{-/-}$ OFTs showed similar anatomical defects as the *Wnt1-Cre;Sema3c*$^{fl/fl}$ mutants, including a failure of proximal OFT septation (clear arrow, **Figure 4.10**) that was accompanied by impaired myocardialisation. This observation is consistent with the idea that cardiac NCC-derived SEMA3C signals through NRP enable OFT septation.

Because PLXND1 is a known co-receptor for NRP1 and mice lacking endothelial PLXND1 have OFT defects (Gitler et al., 2004), I also analysed OFTs of *Plxnd1*$^{-/-}$ mice. This analysis revealed that 3/3 *Plxnd1*$^{-/-}$ mutants displayed a completely unseptated OFT, similar to endothelial *Nrp1*-null mutants (compare **Figure 4.10G-I** with **Figure 4.4J-L**). In addition, the *Plxnd1*$^{-/-}$ phenotype within the proximal OFT also phenocopied that observed in all other mutants deficient in SEMA3C or NRP1 signalling analysed thus far (see **Figures 4.1**, **4.9**).

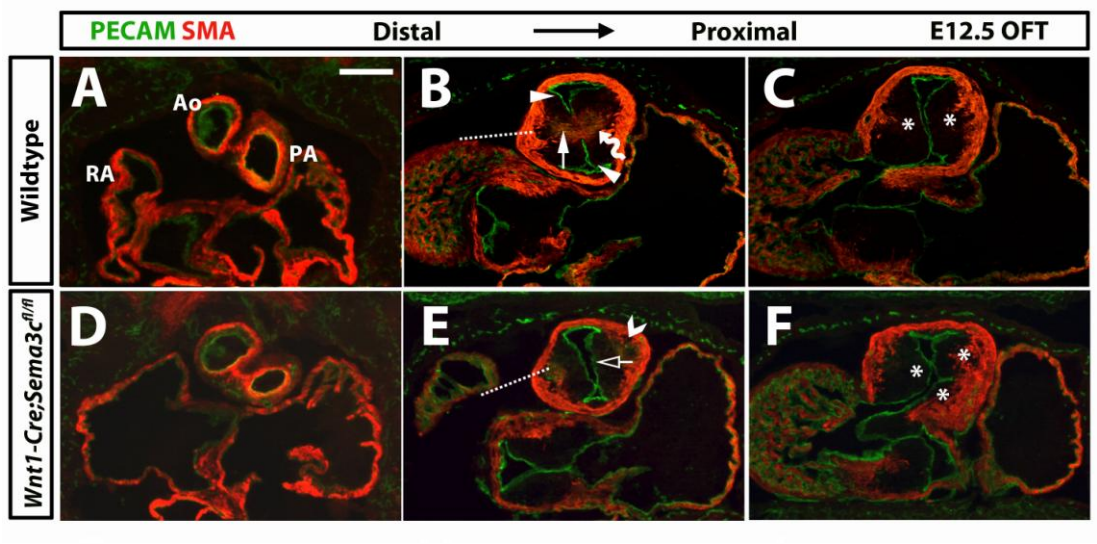

Figure 4.9. Cardiac NCC-derived SEMA3C is required for proximal OFT septation.

Serial sections of wildtype **(A-C)** and *Wnt1-Cre;Sema3c*$^{fl/fl}$ **(D-F)** E12.5 OFTs immunolabelled for PECAM and SMA. Solid arrowheads indicate the septated endothelium; solid arrows demonstrate septal bridge myocardialisation, clear arrows the absence of septal bridge formation and open arrowheads indicate stalled myocytes. Dotted lines indicate the angle of septal bridge formation, curly arrows label migrating myocytes and asterisks highlight endocardial cushion position. Scale bar: 200 µm.

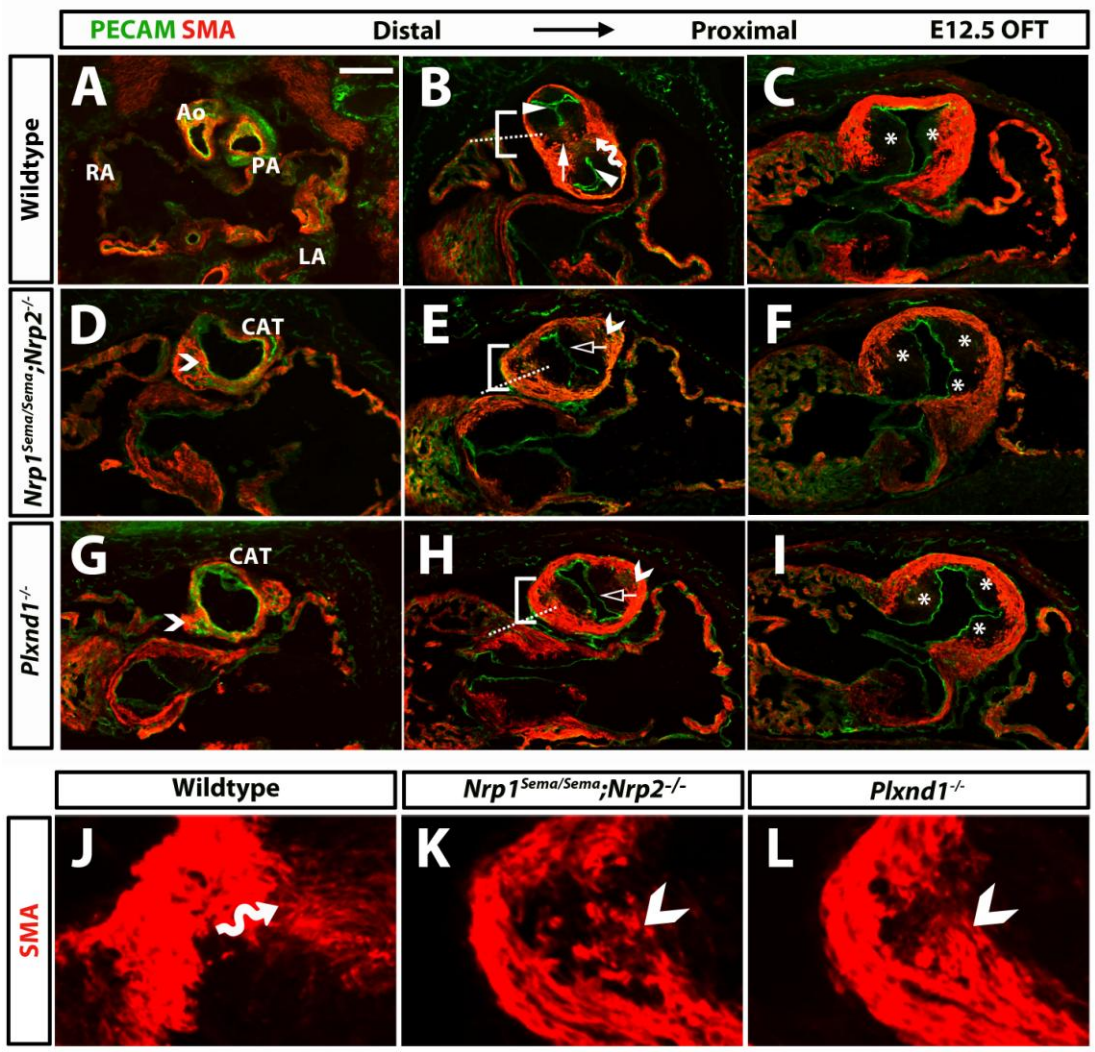

Figure 4.10. SEMA3C signals through NRP1 and PLXND1 to regulate OFT septation.

Serial sections of wildtype **(A-C)**, *Nrp1*$^{Sema/Sema}$*;Nrp2*$^{-/-}$ **(D-F)** and *Plxnd1*$^{-/-}$ **(G-I)** E12.5 OFTs, immunolabelled for PECAM and SMA. Solid arrowheads indicate the septated endothelium; solid arrows highlight septal bridge myocardialisation and clear arrows the absence of septal bridge formation. Dotted lines indicate the angle of septal bridge formation and asterisks highlight endocardial cushion position. Curly arrows label migrating myocytes and open arrowheads denote stalled myocytes. Scale bar: 200 µm.

4.2.13 SEMA3C signalling through NRP1 and PLXND1 promotes NCC-dependent septal bridge formation

Having established that SEMA3C signalling through the endothelial NRP/PLXND1 complex is important for proximal OFT septation, I next sought to elucidate the mechanism underlying the observed defect. Thus, I analysed cardiac NCC behaviour in mice with defective NRP1 signalling by immunolabelling E12.5 OFT sections with the cardiac NCC marker PLXNA2 (High et al., 2009). This analysis revealed that at this stage cardiac NCCs had migrated towards the centre of the OFT for septal bridge formation (arrow, **Figure 4.11A**). Moreover, the entry of cardiac NCCs into the septal bridge appeared to precede the invasion of myocytes from the myocardial cuff into this area, and invading myocytes seemed to orientate themselves towards the cardiac NCCs (curved arrow, **Figure 4.11A**). These findings suggest a role for cardiac NCCs in attracting myocytes into the bridge area to initiate the process of myocardialisation.

PLXNA2 immunostaining showed that cardiac NCCs had reached the OFT in *Nrp1*-null and endothelial *Nrp1*-null mutants (arrowheads, **Figure 4.11B,C**). This observation agreed with the *Wnt1-Cre* lineage trace I had performed at E10.5 in *Nrp1*-null mutants, which demonstrated that NRP1 was not required for cardiac NCC migration into the OFT (see above, **Figure 4.3**). However, $PLXNA2^{+}$ NCCs remained separated in two lateral columns both in *Nrp1*-null and endothelial *Nrp1*-null OFTs, rather than fusing in a central position as seen in wildtypes (arrowheads, **Figure 4.11B,C)**. The location of the cardiac NCCs in the mutants corresponded to the position of the two NCC prongs seen at earlier stages in wildtypes, indicating a failure of translocation to the central area (see above, **Figure 4.3**).

In addition to a failure of cardiac NCCs moving into the central bridge area, *Nrp1*-null and endothelial *Nrp1*-null mutants showed defective myocyte migration. Thus, myocytes were no longer orientated towards the central area of the OFT like in wildtypes, but appeared to orientate themselves towards the mispositioned cardiac NCCs in the *Nrp1* mutants (curly arrows, **Figure 4.11B,C**), providing further evidence for the hypothesis that cardiac NCCs attract myocytes into the bridge area to initiate the process of myocardialisation.

The findings above are consistent with the idea that NRP1 is dispensable for cardiac NCC attraction into the OFT, but is required within the OFT for NCC guidance from a lateral area into a central position and the ensuing attraction of myocytes for septal bridge formation. In agreement with this model, and demonstrating that the NRP1 ligand directing cardiac NCC translocation is SEMA3C rather than VEGF-A, NCC migration into the central OFT was normal in mice lacking VEGF-A signalling through NRPs (*Nrp1*$^{Vefa/Vegfa}$*;Nrp2*$^{-/-}$), but absent in mice lacking semaphorin signalling through neuropilins (*Nrp1*$^{Sema/Sema}$*;Nrp2*$^{-/-}$) (**Figure 4.11D,E**, respectively). Moreover, mice lacking NCC-derived SEMA3C also lacked central NCC localisation, with NCCs located in two lateral columns and abnormal myocyte migration towards the stalled NCCs (**Figure 4.11F**).

To investigate how ablation of SEMA3C/NRP1 signalling in the OFT affects the behaviour of the total cardiac NCC population, including cardiac NCCs which do not express SEMA3C or PLXNA2, I introduced the *Wnt1-Cre;Rosa*^{Yfp} reporter into *Nrp1*-null mice and in collaboration with Prof Scambler into *Sema3c*$^{fl/fl}$ mice. I subsequently analysed OFT sections of E12.5 *Wnt1-Cre;Rosa*^{Yfp}*;Nrp1*$^{-/-}$ or *Wnt1-Cre;Rosa*^{Yfp}*;Sema3c*$^{fl/fl}$ embryos stained for YFP and the early SMC marker SM22α. As observed with PLXNA2 and Xgal staining, the YFP analysis suggested that a similar amount of cardiac NCCs had migrated into the OFT of *Nrp1*$^{-/-}$ mice and wildtype littermates (**Figure 4.12B,E**). However, despite having reached the OFT, most YFP^{+} cells in mutants had failed to translocate into the central area at E12.5 (arrowheads, **Figure 4.12E**). This defect was also present in the proximal OFT of *Wnt1-Cre;Rosa*^{Yfp}*;Sema3c*$^{fl/fl}$ mutants (**Figure 4.12H**). These observations suggest that the SEMA3C-expressing cardiac NCCs are able to influence the behaviour of the entire cardiac NCC population in the OFT. Whereas NCC-derived SEMA3C was essential for cardiac NCC relocalisation in the proximal OFT, cardiac NCCs had successfully migrated into the central area in the distal OFT of *Wnt1-Cre;Rosa*^{Yfp}*;Sema3c*$^{fl/fl}$ mutants, similar to wildtype littermates (**Figure 4.12G**). This observation agrees with the incomplete penetrance of OFT septation within the distal OFTs of the *Wnt1-Cre;Sema3c*$^{fl/fl}$ and *Nrp1*$^{Sema/Sema}$*;Nrp2*$^{-/-}$ mutants and suggests that NRP1 might have an additional role within the distal OFT.

All together, these findings demonstrate that semaphorin, not VEGF-A signalling through NRP1 is a major driving force underlying NCC-mediated OFT septation. Moreover, they imply that SEMA3C signals to endothelial NRP1 to promote cardiac NCC migration towards the centre of the proximal OFT, which then leads to myocyte invasion and therefore the formation of a myocardialised septal bridge.

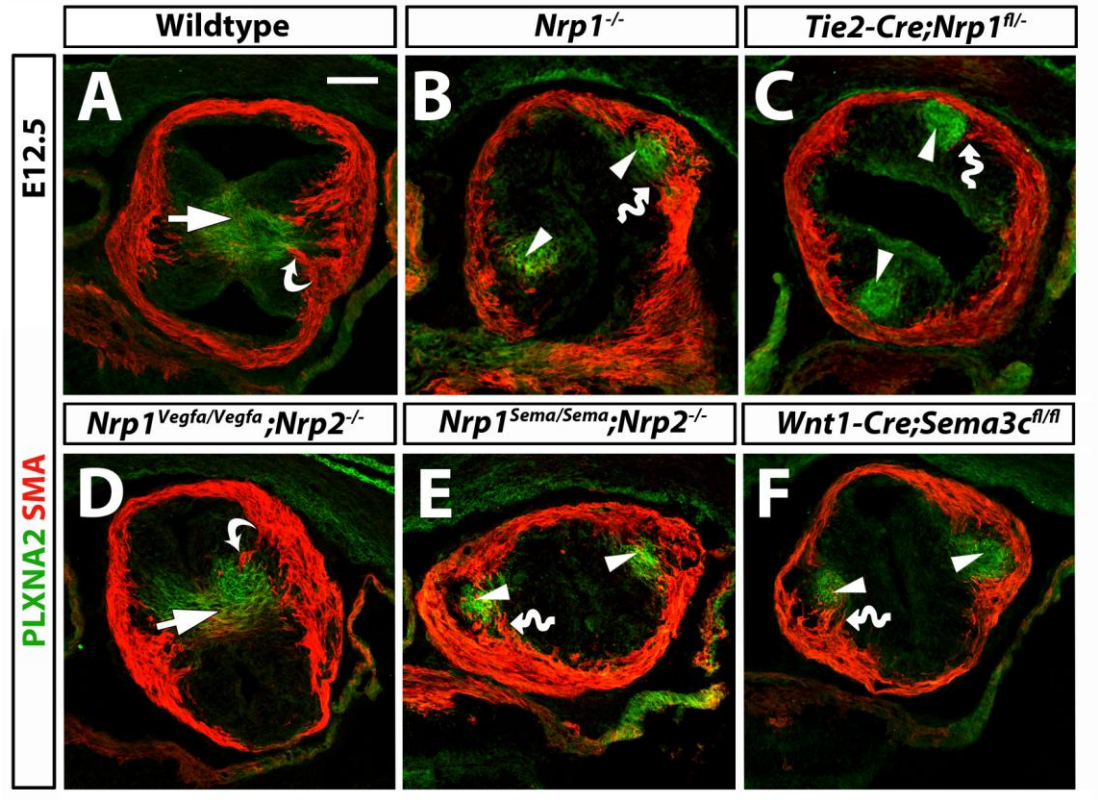

Figure 4.11. SEMA3C signals through NRP1 to promote the fusion of the SEMA3C expressing cardiac NCCs and promote the myocardialisation of the septal bridge.

E12.5 OFT sections of the indicated genotypes were labelled for PLXNA2 and SMA. Arrows indicate the central position of cardiac NCCs in the septal bridge that is present in the wildtype OFT and the OFT of mice lacking VEGF-A signalling through neuropilins; arrowheads highlight the abnormal lateral position of $PLXNA2^{+}$ cardiac NCCs in all other mutant genotypes. Curved arrows denote myocytes migrating to the central NCCs, curly arrows those migrating towards abnormal lateral NCCs. Scale bar: 100 µm.

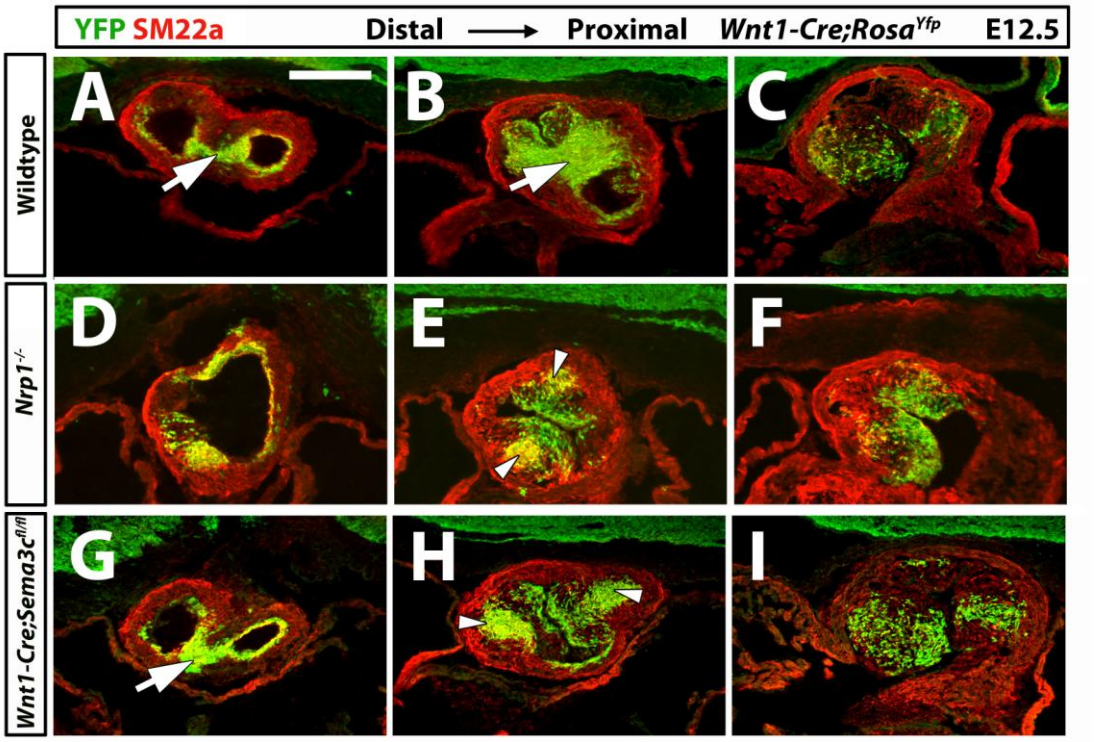

Figure 4.12. NCC-derived SEMA3C is required for cardiac NCC fusion and septal bridge myocardialisation in the proximal OFT.

E12.5 OFT sections from wildtype **(A-C)**, *Nrp1*$^{-/-}$ **(D-F)** and *Sema3c*$^{fl/fl}$ **(G-I)** mice containing the *Wnt1-Cre;Rosa*^{Yfp} reporter were co-labelled for YFP and SM22α. Arrows indicate cardiac NCCs in the septal bridge of the control and distal mutant OFT, the arrowheads highlight abnormal lateral positioning of cardiac NCCs in the mutant OFT. Note that the failure of NCCs to re-localise in the proximal OFT is similar in both *Nrp1*$^{-/-}$ and *Wnt1-Cre;Sema3c*$^{fl/fl}$ mutants, but only *Nrp1*-nulls show defective OFT rotation, as indicated by the position of the arrowheads relative to the atria. Scale bar: 200 µm.

4.2.14 NRP1 is not required for cardiac NCC survival or proliferation within the OFT

Prior studies have shown that deletion of the BMP receptor ALK2 or the TGF β receptor ALK5 increase NCC apoptosis within the OFT and cause OFT defects (Kaartinen et al., 2004, Wang et al., 2006a). In addition, loss of the retinoid X receptor alpha promotes apoptosis in the endocardial cushions and therefore compromises OFT remodelling (Kubalak et al., 2002). Conversely, loss of FOX1P reduces apoptosis in the endocardial cushions and also causes OFT septation defects (Wang et al., 2004). I therefore investigated whether apoptosis was affected in mutants lacking NRP1 by immunolabelling E11.5 OFT sections for activated caspase 3 (aCAS3) (Porter and Janicke, 1999, Sabine et al., 2012). Because the OFT phenotype in NRP1 mutants is already overt at E12.5, apoptosis should be present prior to this stage, if it were the underlying cause. However, consistent with previous studies (Sharma et al., 2004, Barbosky et al., 2006), we observed little apoptosis in the OFT at E11.5 (**Figure 4.13A**). Furthermore, there was no significant difference in the number of apoptotic cells between *Nrp1*-null mutants and control OFTs (**Figure 4.13B**, n= 3 each). Defects in proliferation can also cause OFT defects. Thus, deletion of the BMP type 1 receptor in NCCs reduces proliferation in the endocardial cushions and causes defective OFT remodelling (Nomura-Kitabayashi et al., 2009). To examine whether proliferation was affected in *Nrp1*-null embryos, I immunolabelled E11.5 OFT sections for the proliferation marker phosphohistone H 3 (pHH3) (Hendzel et al., 1997, Tapia et al., 2006). However, there was no significant difference in the number of proliferating cells between *Nrp1*-null mutants and control OFTs (**Figure 4.13C**,**D**, n= 3 each).

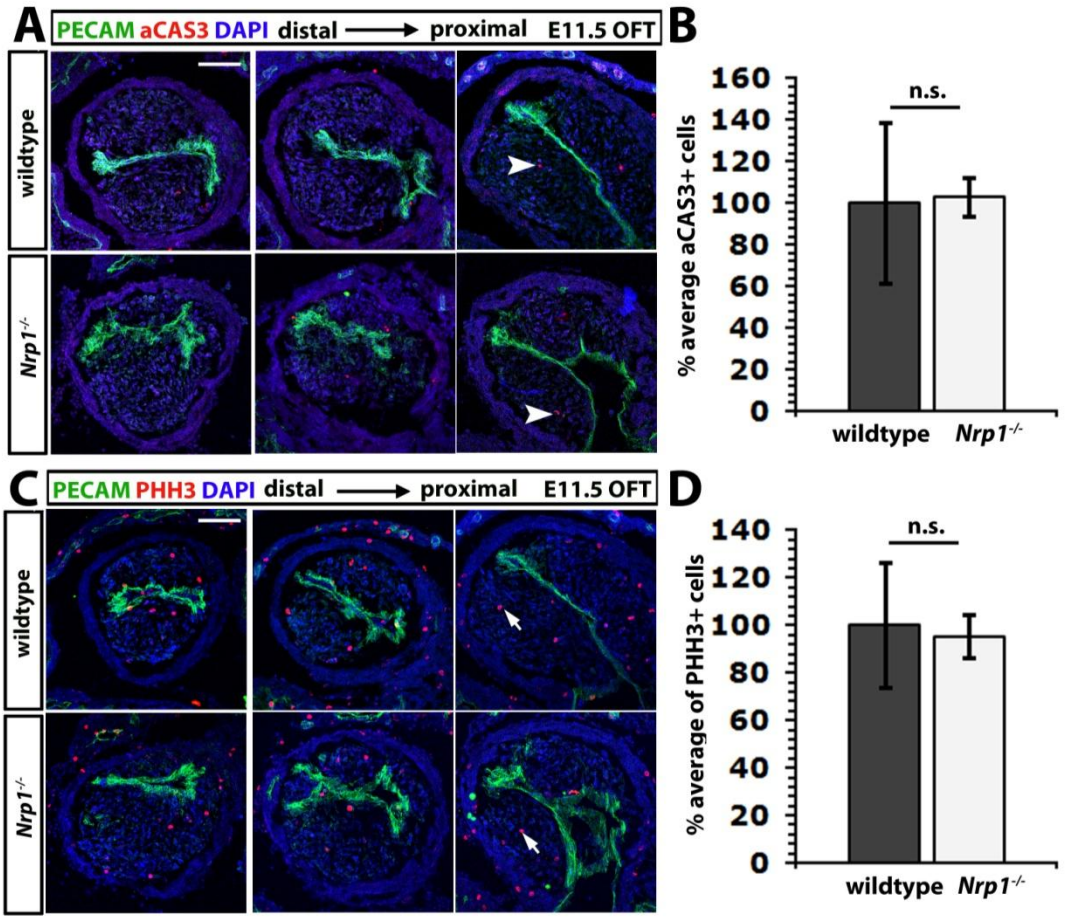

Figure 4.13. NRP1 is not required for cardiac NCC survival or proliferation.

Sections through E11.5 OFTs from *Nrp1*-nulls and wildtype littermates were immunolabelled for PECAM, DAPI and aCAS3 or pHH3, respectively. Arrowheads indicate aCAS3^{+} and arrows pHH3^{+} cells. **(B,D)**. Quantitation of aCAS3^{+} or pHH3^{+} cells in the proximal OFT of *Nrp1*-nulls (n= 3) and control littermates (n= 3). Mean ± s.d., n.s., not significant. Scale bar: 100 µm **(A,C)**.

.

4.2.15 SEMA3C signals through NRP1 to induce endoMT in the OFT in vitro

My analyses had revealed that mice with impaired SEMA3C/NRP1 signalling display disorganised endocardial cushions and lack proximal OFT septation, two processes known to rely on endoMT (Bai et al., 2013, Ma et al., 2013, Timmerman et al., 2004). This observation raised the possibility that cardiac NCC-derived SEMA3C signalling through endothelial NRP1 is essential to induce normal levels of endoMT in the OFT. I therefore investigated next, how the onset of endoMT relates to the timing of cardiac NCC immigration into the OFT, and asked, whether cardiac NCC-derived SEMA3C signalling through endothelial NRP1 is essential for endoMT in the OFT.

To determine the onset of endoMT within the OFT, I immunolabelled E10.5 *Tie2-Cre;Rosa*^{Yfp} OFT sections for YFP and PECAM. This analysis showed that the PECAM^{+} endothelium was effectively labelled by YFP, but that only few single cells around the endothelium were YFP^{+} suggesting that endoMT was only just beginning at this stage (arrowhead and arrow, respectively, **Figure 4.14A,A'**). Similar analysis of sections through E10.5 *Wnt1-Cre,Rosa*^{Yfp} OFTs confirmed that cardiac NCCs had already colonised the OFT at this stage (arrow, **Figure 4.14B,B'**), consistent with my wholemount stains (**Figure 4.3**) and as previously shown (Jiang et al., 2000, Epstein et al., 2000). Even though the *Tie2-Cre;Rosa*^{Yfp} OFT at E10.5 contained only few single cells that were YFP^{+} and lacked PECAM expression, it contained many such cells at E12.5 (arrowhead, **Figure 4.14C,C'**). Together, these observations suggest that endoMT is induced around E10.5, coincident with cardiac NCC migration into the OFT, and has produced many cushion cells by E12.5.

To investigate if SEMA3C induces endoMT in the OFT in a NRP1-dependent manner, I used an established explant assay (Bai et al., 2013). In this assay, OFT tissue from E10.5 embryos is explanted and the ensuing endoMT is measured as F-actin^{+} cellular outgrowth. To confirm that this assay is a good model of endoMT in the OFT, I first explanted E10.5 *Tie2-Cre;Rosa*^{Yfp} OFT tissue, because endoMT was only just beginning at this stage (see above, **Figure 4.14A**). Consistent with the idea that the outgrowing cells arise through endoMT, I found that the vast majority of these outgrowth cells were YFP^{+} (arrowheads, **Figure 4.15A**). Importantly, the outgrowth cells lacked PECAM expression **(**arrowhead, **Figure 4.15B,B'**), similar to cells that have undergone endoMT *in vivo* (**Figure 4.14C,C'**). These findings

confirmed that the OFT explant assay recapitulates key features of endoMT. Furthermore, the lack of PECAM expression in the cellular outgrowth also validated that these cells were not forming angiogenic sprouts, as found in aortic rings when they are cultured on collagen (Baker et al., 2012). To determine whether endoMT depends on NCC-derived SEMA3C and NRP1, I first investigated whether SEMA3C was able to induce endoMT by culturing E10.5 serum-starved wildtype explants with 400 ng/ml recombinant SEMA3C and comparing it to untreated explants (n= 3 each; **Figure 4.16A,B**). I chose this amount of SEMA3C, as previous studies had validated that this concentration can elicit a biological response (Vadivel et al., 2013).This revealed that SEMA3C significantly increased cellular outgrowth by approx. 180% (n= 3 each, p≤ 0.01; **Figure 4.16I**). To investigate whether the lack of NCC-derived SEMA3C affected endoMT, Amelie Calmont used the explant assay on E10.5 *Wnt1-Cre;Sema3c*$^{fl/fl}$ OFT tissue mice (**Figure 4.16C,D**). She observed significantly reduced outgrowth in mutant compared to control explants (*Sema3c*$^{fl/+}$ n= 14 versus *Wnt1-Cre;Sema3c*$^{fl/fl}$ n= 6, p≤ 0.01; **Figure 4.16I**). I next examined whether endoMT was also deficient in *Nrp1*-nulls. I, thus, explanted E10.5 OFT tissue from wildtype and *Nrp1*-null mutants (**Figure 4.16E,F**) and observed that outgrowth was significantly reduced in mutant compared to control explants (*Nrp1*$^{+/+}$ n= 4 versus *Nrp1*$^{-/-}$ n= 5, p≤ 0.001; **Figure 4.16J**). To determine directly if the SEMA3C-mediated induction of endoMT was NRP1-dependent, I next treated OFT explants from *Nrp1*-null mutants and littermate controls with SEMA3C (**Figure 4.16D,E**). This experiment demonstrated that SEMA3C promoted outgrowth in wildtype, but not in *Nrp1*-null mutant explants. Thus, the amount of cellular outgrowth remained reduced in *Nrp1*-nulls compared to wildtype littermates (n= 3 each; p≤ 0.05; **Figure 4.16J**). Furthermore, the amount the cellular outgrowth was reduced by in *Nrp1*-nulls treated with SEMA3C, was not significantly changed from the amount outgrowth was reduced by in untreated *Nrp1* mutants (p> 0.05). Together, these experiments showed that cardiac NCC-derived SEMA3C promotes endoMT in the OFT via NRP1.

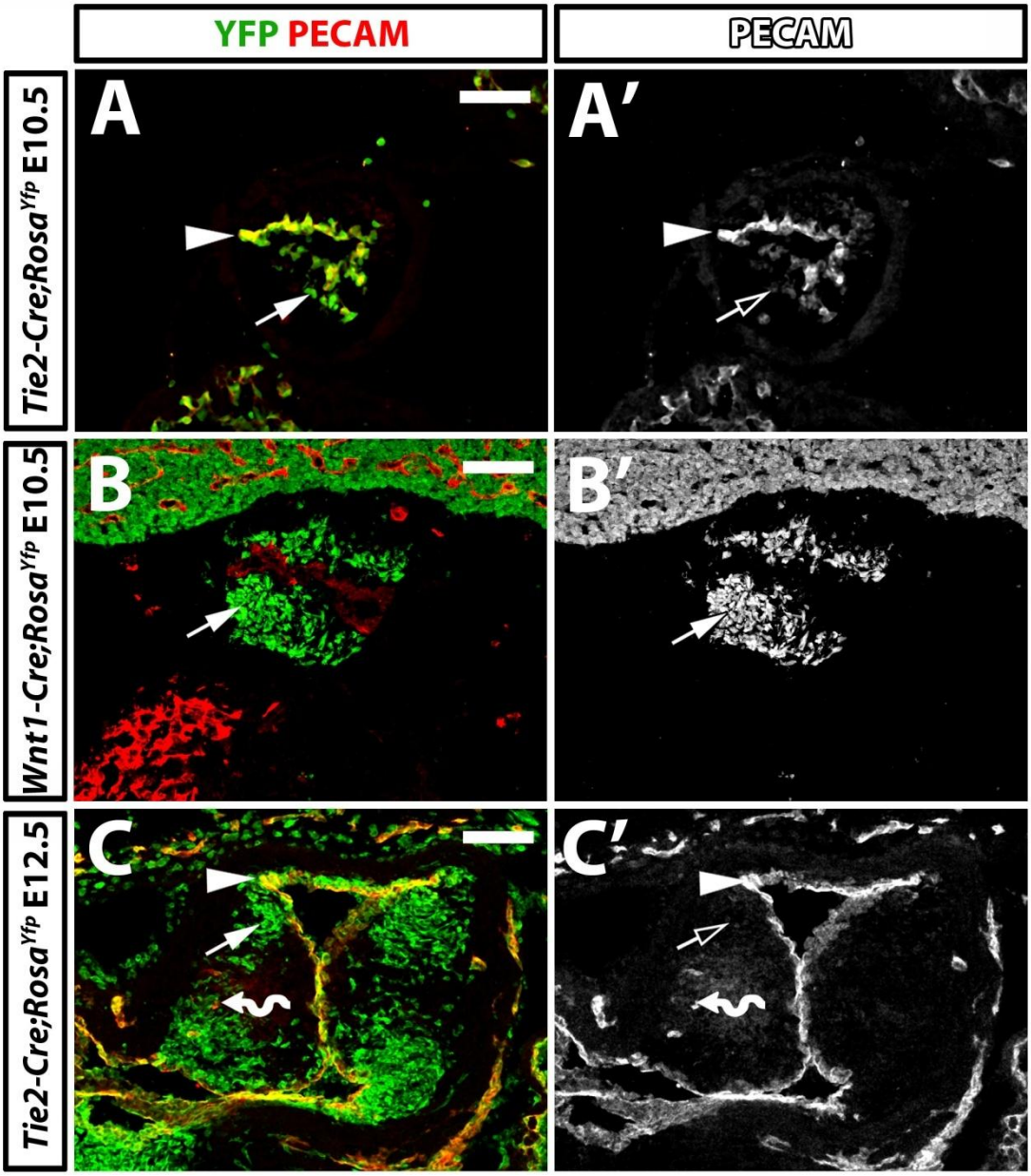

Figure 4.14. EndoMT occurs after OFT colonisation by NCCs.

Sections of E10.5 and E12.5 *Tie2-Cre;Rosa*^{Yfp} and 10.5 *Wnt1-Cre;Rosa*^{Yfp} OFTs immunolabelled for YFP and PECAM. Arrowheads indicate endothelial targeting of YFP at E10.5 and E12.5. The solid arrows in **(A,C)** highlight mesenchymal cells of endothelial origin, which are targeted by *Tie2-Cre*, whereas the clear arrow in **(C')** indicates a lack of PECAM expression in these cells. The solid arrow in **(B,B')** denotes *Wnt1-Cre*-labelled NCCs that have colonised the OFT. Curly arrows highlight PECAM^{+} capillaries within the OFT. Scale bars: 100 µm.

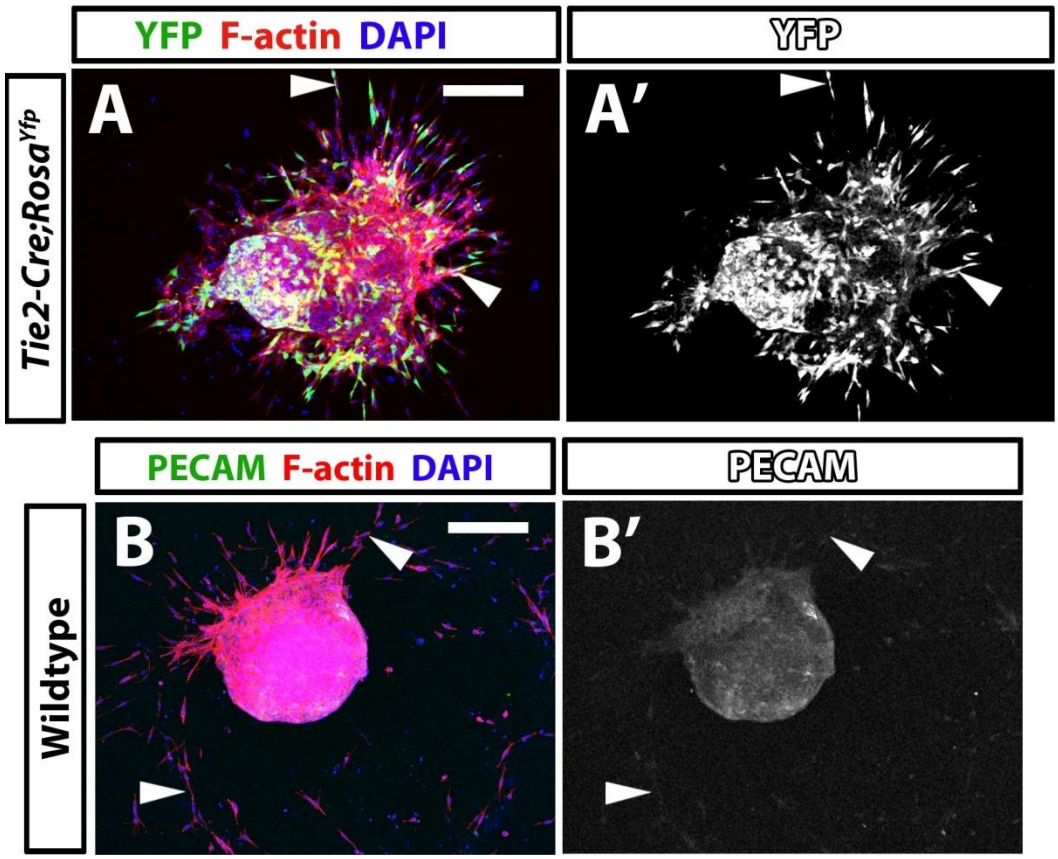

Figure 4.15. E10.5 OFT explants recapitulate endoMT.

E10.5 *Tie2-Cre;Rosa*^{Yfp} and wildtype OFTs immunolabelled for YFP **(A,A')** or PECAM **(B,B')**, F-actin and DAPI. Arrowheads label cells, which have undergone endoMT and are targeted by *Tie2-Cre* **(A,A')** or lack PECAM **(B,B')**. Scale bars: 200 µm.

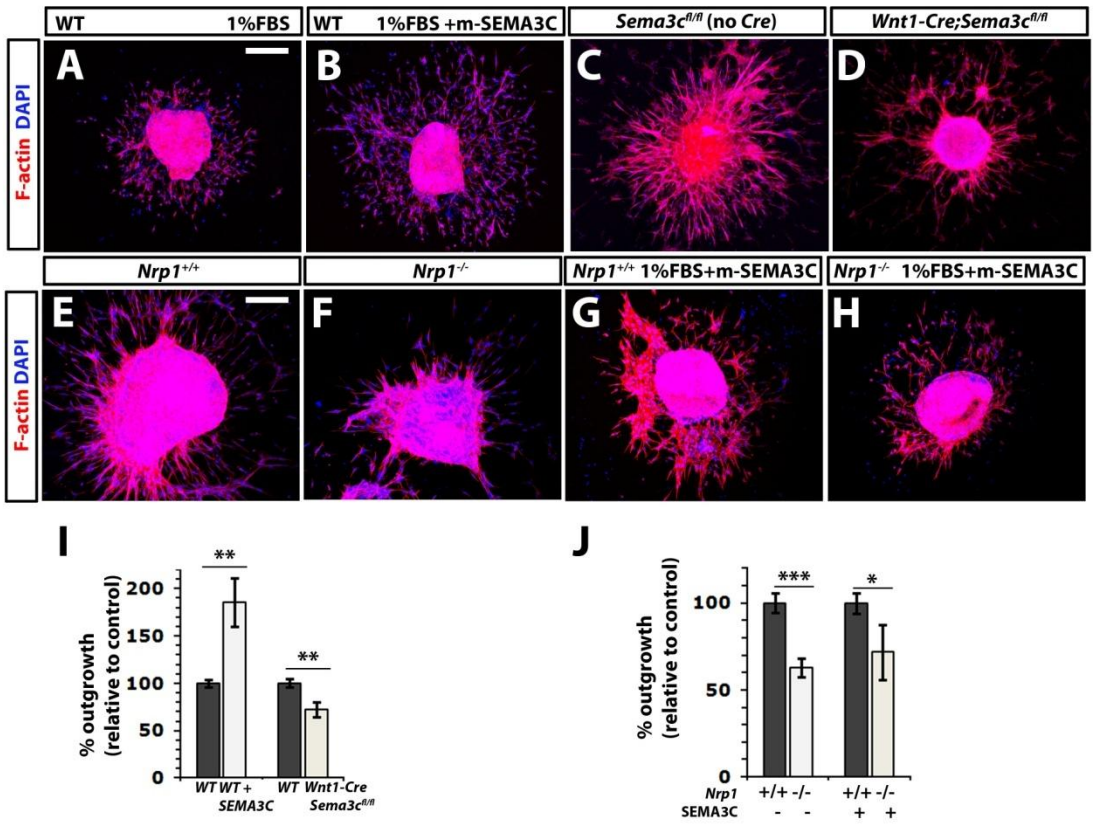

Figure 4.16. SEMA3C induces endoMT through NRP1.

E10.5 wildtype, *Wnt1-Cre;Sema3c*$^{fl/fl}$ and *Nrp1*-null OFTs were cultured for 72 h with **(B,G,H)** or without 400 ng/ml SEMA3C **(A,C-F)**, and immunolabelled for F-actin and counterstained with DAPI. The number of F-actin^{+}DAPI^{+} emigrated cells per explant was quantitated **(I,J)**. Mean ± s.d.; the asterisks indicate p values; *≤ 0.05, **≤ 0.01, ***≤ 0.001; n.s., not significant. Scale bars: 200 µm.

Reduced endoMT in the OFT of mice lacking SEMA3C or NRP1 in vivo

To confirm that NRP1 is required for endoMT *in vivo*, I investigated the expression of two genes, *Slug* and *Snail,* which encode transcription factors important for endoMT (Niessen et al., 2008, Leong et al., 2007). Quantitative PCR analysis revealed that *Slug* and *Snail* expression was reduced in *Nrp1*-null mice compared to control littermates on *Nrp1*-null and control E10.5 OFTs. Thus, as expected, *Nrp1* expression was reduced in *Nrp1*-null mutants; moreover, *Slug* was also significantly reduced in mutants compared to littermate controls (**Figure 4.17A**; n= 3 each, $p \leq 0.05$). Furthermore, *Snail* also appeared reduced in mutants, albeit this analysis did not reach statistical significance presumably due to the variability of gene expression and low n number (**Figure 4.17A**; n= 3 each, $p > 0.05$). Similarly, *Slug* was significantly reduced in the E10.5 OFTs from *Wnt1-Cre;Sema3c*$^{fl/fl}$ mutants compared to control littermates, whereas *Snail* appeared reduced, albeit without significance (**Figure 4.17B**; controls lacking *Cre* n= 3; *Wnt1-Cre;Sema3c*$^{fl/fl}$ n= 7; $p \leq 0.01$, $p > 0.05$, respectively).

I next validated this finding by performing immunostaining of serial OFT sections for SLUG and PECAM at E11.25, when endoMT is in progress. By comparing *Tie2-Cre;Nrp1*$^{fl/-}$ and control sections, I found that there were fewer SLUG^{+} single cells immediately adjacent to the OFT endothelium in mutants compared to littermate controls (arrowheads, **Figure 4.18A**). Instead, many SLUG^{+} cells appeared to be retained within the OFT endothelium (arrow, **Figure 4.18D**). This observation raised the possibility that the defective induction of the endoMT programme at E10.5 results in the retention of cells that are normally destined for endoMT within the OFT endothelium. Reduced *Slug* expression at E10.5 and the abnormal distribution of SLUG^{+} cells at E11.25 predicted fewer mesenchymal cells of endothelial origin in the absence of endothelial NRP1 activation. To test this idea, I analysed cells that had arisen by endoMT in the E12.5 OFT through lineage tracing with the *Tie2-Cre;Rosa*^{Yfp} transgene. Consistent with impaired endoMT, immunostaining of serial sections showed fewer YFP^{+}PECAM^{-} cells in the endocardial cushions in 3/3 mutants compared to controls (**Figure 4.18B**). Taken together, these observations show that endothelial NRP1 is required for endoMT *in vivo*.

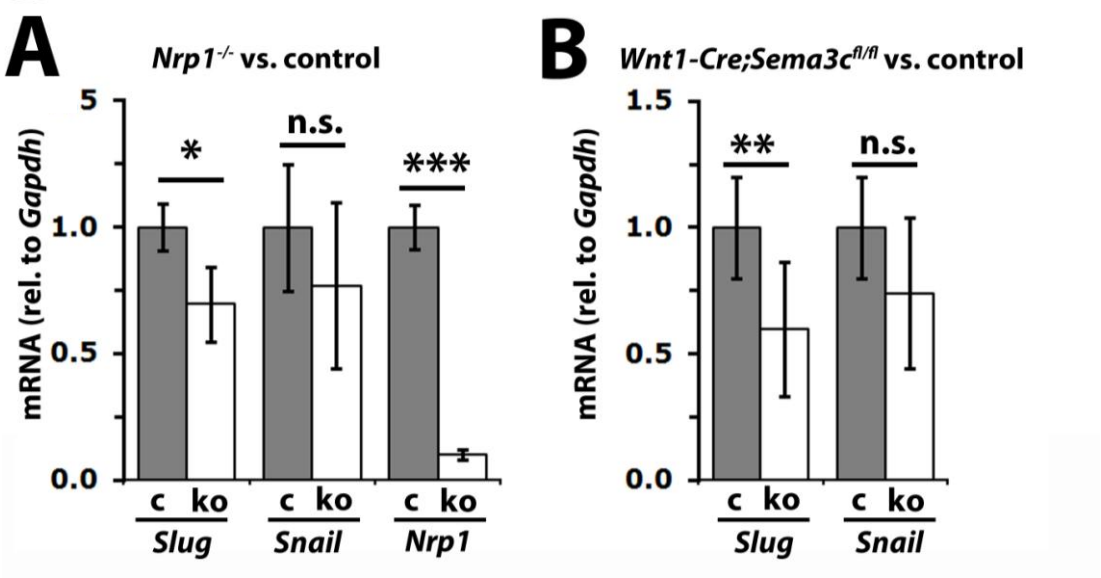

Figure 4.17. Reduction of endoMT markers *Snail* and *Slug* in *Nrp1*-null and *Wnt1-Cre;Sema3c$^{fl/fl}$* OFTs.

Quantitation of *Nrp1*, *Slug* and *Snail* mRNA expression relative to GAPDH in E10.5 OFTs from *Nrp1$^{-/-}$* (n= 3, grey bars) and control litter mates (n= 3, white bars) by SybrGreen qPCR **(A)**. Quantitation of *Slug* and *Snail* mRNA expression relative to *Gapdh* in E10.5 OFTs from *Wnt1-Cre;Sema3c$^{fl/fl}$* (n= 7, grey bars) and control litter mates (n= 3, white bars) by SybrGreen qPCR **(B)**. Mean ± s.d.; the asterisks indicate p values; *≤ 0.05, **≤ 0.01 ***≤ 0.001; n.s., not significant.

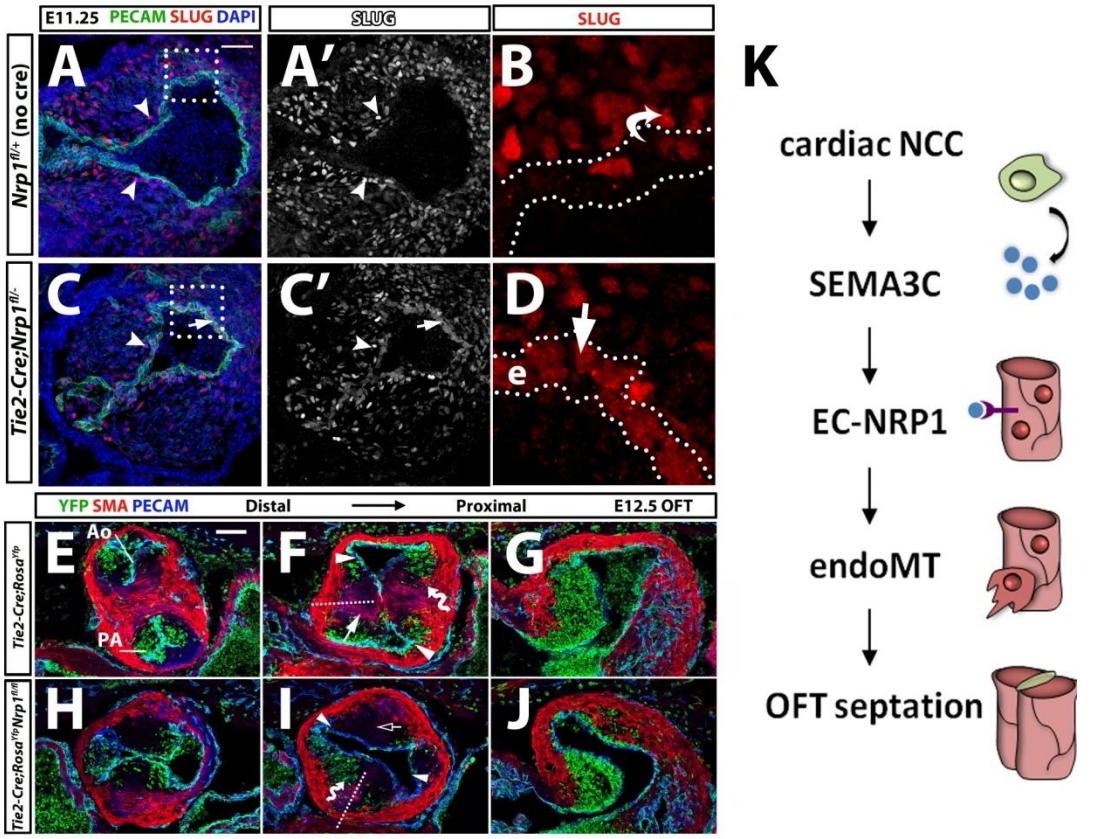

Figure 4.18. NRP1 is required for endoMT *in vivo*.

Serial sections of *Tie2-Cre;Nrp1*$^{fl/-}$ and control E11.25 OFTs stained with PECAM and SLUG. Arrowheads indicate cells expressing SLUG in the OFT; curved arrow in high magnification illustrates endoMT, whereas arrows shows SLUG^{+} cells retained in the endothelium. Dotted lines outline the endothelium (e) **(A-D)**. Serial sections of *Tie2-Cre;Rosa*^{Yfp} E12.5 OFTs on a *Nrp1*$^{fl/+}$ and *Nrp1*$^{fl/-}$ background at corresponding distal, medial and proximal levels immunolabelled for YFP, SMA and PECAM. Solid arrowheads indicate the septated endothelium and solid arrows septal bridge myocardialisation; clear arrows highlight the absence of septal bridge formation in mutants. Dotted lines indicate the angle of septal bridge formation **(E-J)**. Schematic representation of SEMA3C induced endoMT. Cardiac NCCs (green) secrete SEMA3C (blue), which binds to endocardial NRP1 (purple) and induces endoMT resulting in NCC clustering and septal bridge formation **(K)**. Scale bars: 50 µm **(A-D)**, 100 µm **(E-J)**.

4.3 Discussion

Even though the importance of NRP1 for OFT remodelling and therefore cardiovascular function has been recognised for more than a decade (Kawasaki et al., 1999), its mechanism of action was not previously understood. A widely accepted hypothesis postulated that NRP1 contributes to OFT remodelling in a dual fashion: firstly, by enabling the SEMA3C-mediated attraction of NRP1-expressing cardiac NCCs into the OFT, and secondly, by acting as a VEGF-A receptor in NRP1-expressing OFT endothelium to induce an unidentified endothelial function. By taking advantage of a previously unavailable repertoire of tissue-specific and ligand-selective *Nrp1* mutants and analysing them through both *in vivo* and *in vitro* approaches, I, together with my collaborators, was able to overhaul the prior working model and identify novel roles for NRP1 during OFT septation. Firstly, I found that neither NRP1 nor NRP2 are required to guide cardiac NCCs into the OFT. Secondly, I demonstrated that endothelial NRP1 is not required as a receptor for VEGF-A during OFT remodelling, but that it instead binds to SEMA3C, which is essential for this process. Thirdly, I identified a hitherto unrecognised role for NCC-derived SEMA3C and endothelial NRP1 in promoting endoMT in the OFT and therefore the generation of mesenchymal cells for the endocardial cushions. Finally, I found that SEMA3C signalling through NRP1 is required for the fusion of the bilateral cardiac NCC columns in the central OFT to enable the formation and myocardialisation of the septal bridge that separates the emerging aortic and pulmonary trunks.

Out of all SEMA3s the only SEMA3 known to be a critical factor for OFT septation is SEMA3C (reviewed in Worzfeld and Offermanns, 2014), as *Sema3c*$^{-/-}$ mice display CAT (Feiner et al., 2001). Thus genetic knockouts of SEMA3A, which binds to NRP1 with strong affinity, display enlarged atria, but otherwise show no defects in vascular development (Behar et al., 1996). In contrast to SEMA3A, SEMA3C binds both NRPs with similar affinity (Chen et al., 1997, Chen et al., 1998), and therefore the occurrence of CAT in *Nrp1*$^{Sema/Sema}$*;Nrp2*$^{-/-}$, but not *Nrp1*$^{Sema/Sema}$ mice, supports the idea that SEMA3C acts on cells that express both NRPs. In common with their well-characterised role as axon guidance cues, it was suggested that these SEMA3C-dependent cells are cardiac NCCs (Gu et al., 2003, Toyofuku et al., 2008), which require SEMA3C to migrate into the OFT. In accordance with this prior model, mice with cardiac NCCs lacking NRP1 and NRP2

should show impaired cardiac NCC migration into the OFT and therefore defective OFT septation, similar to *Sema3c*-null mice. To test this idea, I analysed *Wnt1-Cre;Nrp1*$^{fl/fl}$*;Nrp2*$^{-/-}$ mice, where *Wnt1-Cre* was shown to effectively delete NRP1 within the cardiac NCCs in studies analysing the development of the sympathetic nervous system (Maden et al., 2012). However, in disagreement with the previous model, *Wnt1-Cre;Nrp1*$^{fl/fl}$*;Nrp2*$^{-/-}$ mutants had normal OFT septation, excluding the possibility that SEMA3 signalling through NRPs is required for cardiac NCC immigration into the OFT of the developing mouse. My finding disagreed with prior studies in chick, in which siRNA-mediated targeting of NRP1 impaired cardiac NCC migration (Toyofuku et al., 2008). This discrepancy might be due to species differences in cardiac NCC behaviour. In support of this idea, the misregulation of SDF1 or its receptor CXCR4 perturbs cardiac NCC migration in chick (Escot et al., 2013), whereas mouse mutants showed only mild anomalies, such as ventricular septal defects (Tachibana et al., 1998, Nagasawa et al., 1996). Alternatively, the siRNA-mediated knockdown technology used for the chick studies may have sensitised NCCs in such a manner that they became more prone to developmental defects caused by NRP1 knockdown.

In contrast to *Wnt1-Cre;Nrp1*$^{fl/fl}$*;Nrp2*$^{-/-}$ mice, *Tie2-Cre;Nrp1*$^{fl/-}$ mutants fully recapitulated the defects I had observed in *Nrp1*-null mice. This finding suggested that all major NRP1-dependent steps during OFT remodelling are orchestrated by endothelial NRP1. Furthermore, my NRP2 expression analysis showed that NRP2 is also expressed on the endothelium demonstrating that instead of the cardiac NCCs, ECs could be the cells requiring SEMA3C signals during OFT remodelling. However, I also found expression of NRP1 and NRP2 within the migrating myocytes s within the OFT (**Figure 4.2**), raising the possibility that NRPs might play an additional role in OFT development by guiding myocytes during myocardialisation.

Given the essential role of NRP1 in OFT septation, it is not immediately obvious why NRP2 is able to compensate for the loss of SEMA3 binding to NRP1, as observed for mice carrying the *Nrp1*$^{Sema/Sema}$ mutation (Gu et al., 2003), whilst it is unable to compensate for the lack of NRP1 in *Nrp1*$^{-/-}$ or *Tie2-Cre;Nrp1*$^{fl/-}$ mice. One possibility is that NRP2 and NRP1 form a heterodimer, in which both NRPs function redundantly as receptors for SEMA3C (**Figure 4.19A**). In agreement, heterodimer

formation has been demonstrated in Cos7 cells *in vitro*, where NRP1 and NRP2 pre-assemble in a ligand-independent fashion (e.g. Chen et al., 1997, Chen et al., 1998, Takahashi et al., 1998). In a heterodimeric complex, NRP2 may be sufficient to bind SEMA3C even if the semaphorin binding domain of NRP1 is disrupted; however, the remainder of the NRP1 receptor, which is present in *Nrp1*$^{Sema/Sema}$ mice but absent in *Nrp1*$^{-/-}$, may be indispensable for downstream signalling (**Figure 4.19B**,**C**). For example, NRP1 may be absolutely required to transduce appropriate signals for OFT septation, with NRP2 being unable to compensate for this function. In support of this model, *Nrp2*$^{-/-}$ mutants do not display defects in OFT remodelling (Chen et al., 2000), even though NRP2 can rescue the *Nrp1*^{Sema} mutation (Gu et al., 2003).

NRP1 signalling in OFT endothelium appears to depend on the recruitment of a signal transducing co-receptor (**Figure 4.19A**), because mice lacking the cytoplasmic tail of the NRP1 receptor are viable and are therefore unlikely to have OFT defects (Fantin et al., 2011). This co-receptor is likely PLXND1, because both NRP1 and NRP2 form complexes with PLXND1, and PLXND1 enhances SEMA3C binding to NRP-expressing Cos7 cells (Gitler et al., 2004). Moreover, *Plxnd1* knockouts recapitulate the OFT phenotype observed in NRP1 and SEMA3C knockout mice (**Figure 4.10**). Furthermore, studies reported that endothelial-specific deletion of PLXND1, similar to the endothelial deletion of NRP1, result in OFT defects (Zhang et al., 2009), supporting the hypothesis that the essential function of such a NRP1/PLXND1 complex receptor occurs in OFT endothelium.

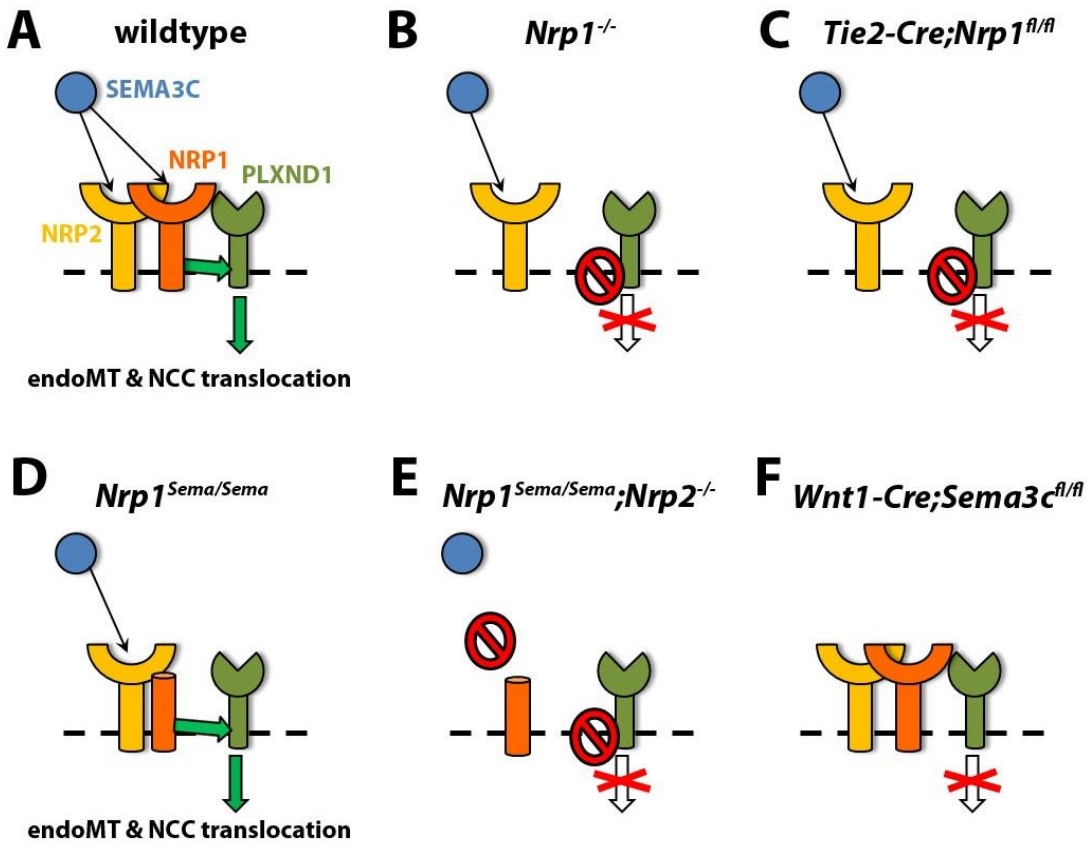

Figure 4.19. Working model of SEMA3C signalling through NRPs and PLXND1 to induce endoMT in the OFT.

In wildtypes, SEMA3C binds to NRP1 and the complex transduces signals through PLXND1 to induce endoMT and NCC translocation **(A)**. Signalling is impaired in EC-specific and full *Nrp1*-nulls, as the NRP1 receptor cannot activate PLXND1 **(B,C)**. In *Nrp1*$^{Sema/Sema}$ mice, SEMA3C signals through NRP2, perhaps because it binds to NRP1 but induces PLXND1 activation through NRP2 **(D**; not that I have not specifically investigated this possibility**)**. In *Nrp1*$^{Sema/Sema}$;*Nrp2*$^{-/-}$ OFTs, SEMA3C cannot induce endoMT as there is no receptor binding site **(E)**, whereas in *Wnt1-Cre*,*Sema3c*$^{fl/fl}$ endoMT is not induced, because SEMA3C is not secreted by NCCs **(F)**.

I also tested the prior hypothesis that NRP1 acts as a VEGF-A receptor in OFT endothelium (Gu et al., 2003). This hypothesis was an extrapolation of *in vitro* findings, in which NRP1 forms a complex with VEGFR2 in ECs to enhance VEGF-A signalling through VEGFR2 (e.g. Soker et al., 2002). However, the importance of this pathway has so far only been demonstrated *in vivo* for arteriogenesis, where NRP1 tethers a VEGF-bound NRP1/VEGFR2 complex to an intracellular trafficking machinery that ensures the enrichment of activated VEGFR2 in signalling endosomes (Lanahan et al., 2013). In contrast, the results presented here show that mice lacking VEGF-A binding to NRP1 have normal OFT remodelling, even in the absence of NRP2. This finding was particularly unexpected, because $Vegfa^{120/120}$ mice lacking the NRP1-binding VEGF164 isoform have defective OFT septation (Stalmans et al., 2003). My observations therefore imply that the phenotype of $Vegfa^{120/120}$ mice is not linked to NRP1's ability to bind VEGF-A. Instead, impaired ECM retention of VEGF120, known to be responsible for vascular patterning defects in other tissues (Ruhrberg et al., 2002), may also contribute to the OFT defect of $Vegfa^{120/120}$ mice. In this context, future studies may wish to investigate whether $Vegfa^{LacZ/LacZ}$ mice, which have increased VEGF-A levels (Miquerol et al., 1999), display OFT defects reminiscent of the defect observed in $Vegfa^{120/120}$.

To determine the specific role of SEMA3C signalling through NRP1 in OFT remodelling, I collaborated with Prof Pete Scambler (ICH, UCL) who had generated a conditional *Sema3c*-null mouse. We were able to delete SEMA3C expression from the cardiac NCCs by mating these mutants to mice expressing the *Wnt1-Cre* transgene. Using this genetic approach in combination with expression studies, we found that *Sema3c* is expressed by cardiac NCCs. This finding disagrees with the prior hypothesis that SEMA3C is an attractive cue for NCCs to migrate into the OFT, but supports a role for SEMA3C as a signal secreted by NCCs. In agreement with the idea that myocardial cuff derived-SEMA3C is not sufficient for OFT septation, the NCC-specific deletion of *Gata6*, which drives SEMA3C expression, causes OFT defects (Lepore et al., 2006).

Even though SEMA3C was not required for the colonisation of the OFT by cardiac NCCs, the cells were indirectly affected by loss of endothelial SEMA3C/NRP1 signalling once they had reached the OFT. Thus, cardiac NCCs

were abnormally positioned in paired columns in the lateral parts of the endocardial cushions, in locations where NCCs are located in both wildtypes and mutants at earlier stages (see **Figure 4.3**). These observations suggest that the process by which NCCs normally fuse in the central OFT at E12.5 to enable formation of the septal bridge had failed in the mutants.

The incomplete penetrance of distal, as opposed to proximal OFT septation defects observed in *Wnt-1;Sema3c*$^{fl/fl}$ and *Nrp1*$^{Sema/Sema}$*;Nrp2*$^{-/-}$ mice may be due to a number of factors. Thus, variability in my analyses may be secondary to less than 100% efficient *Cre*-mediated targeting of *Sema3c*. In addition, the ligand binding mutation may have residual activity. Additionally, the variation may be secondary to stochastic or genetic background effects. Previous reports of *Sema3c*-null mutants described partially penetrant (75%) and partially expressed (i.e. incomplete) OFT septation defects (Feiner et al., 2001). Indeed previous studies showed that postnatal mortality of *Sema3c*-null mice was 50% lower on a C57Bl6 background (Feiner et al., 2001). In contrast, both *Nrp1*-null and *Tie2-Cre;Nrp1*$^{fl/-}$ mice displayed CAT in all mutant OFTs analysed, which implies that there is an additional, SEMA3C/VEGF-A-independent pathway involved in OFT remodelling, which is less susceptible to genetic perturbations. Evidence for such a pathway was provided in a recent study by our lab, which showed that NRP1 is required for postnatal angiogenesis due to its role in regulating the cytoskeleton of ECs through ABL (Raimondi et al., 2014). Such a pathway seems plausible, as the cytoskeletal remodelling of the endothelium is known to be critical for OFT remodeling (Sakabe et al., 2006).

Previous studies as well as our endothelial lineage tracing have shown that endoMT contributes significantly to the endocardial cushions of the proximal OFT. Moreover, mice with reduced BMP signalling, a known inducer of endoMT, lack proximal septation (Delot et al., 2003), a defect similar to that observed in *Wnt1-Cre;Sema3c*$^{fl/fl}$ mutants. To address whether SEMA3C/NRP1 signalling promotes endoMT in the OFT, Amelie and I used an explant assay which showed that SEMA3C induced endoMT, that NCC-derived SEMA3C and NRP1 were both required for endoMT, and that loss of endoMT in NRP1 mutants could not be rescued by exogenous SEMA3C. Furthermore, expression of the transcription factor

SLUG, which is a known marker of endoMT (Niessen et al., 2008, Leong et al., 2007), as well as the process of endoMT, was markedly reduced in the OFTs of mice lacking endothelial NRP1. The finding that SLUG was down-regulated in mutants with defective SEMA3C/NRP1 signalling agreed with recent studies, which showed that the enhanced expression of SEMA3C (Herman and Meadows, 2007) or NRP1 (Peng et al., 2014) in cancer cells results in an increased level of tumour invasiveness- a process in which tumour cells acquire mesenchymal properties reminiscent of endoMT. Thus, SEMA3C-dependent NRP1 signalling may represent a conserved mechanism that promotes the conversion of cells bound into non-invasive epithelial or endothelial monolayers into migratory single cells.

The SHF has been found to be a source for several molecules, which are required for endoMT in the OFT such as FGF8 (Frank et al., 2002, Park et al., 2006) and BMP4 (McCulley et al., 2008, Liu et al., 2004, Bai et al., 2013). Furthermore, loss of notch signalling in the SHF was shown to reduce FGF8 and BMP4 secretion, and this was accompanied by impaired cardiac NCC immigration and endoMT and caused failure of OFT septation (High et al., 2009). These prior studies concluded that SHF-derived mesoderm communicates with both cardiac NCCs and ECs to induce OFT septation. In contrast, my study has revealed an additional mechanism by which the endothelium is able to instruct the cardiac NCCs and thereby contribute to OFT remodelling. Thus, I have shown that a subpopulation of cardiac NCCs secretes SEMA3C to instruct the $NRP1^{+}$ endocardium to undergo endoMT during OFT morphogenesis. Further work will therefore be necessary to determine how the endothelial SEMA3C/NRP1 pathway we have identified interacts with or complements notch, FGF8 and BMP4 signalling in the OFT. Interestingly, defective endoMT observed within the OFT cushions of the notch, FGF8 and BMP4 mutants is also accompanied with faulty migration of cardiac NCCs, reinforcing the link between endoMT and NCC relocalisation.

4.4 Summary

In this chapter I have investigated OFT development in tissue-specific knockout mice to compare the requirement of NRP1 in OFT endothelium versus cardiac NCCs. I have also examined the relative contribution of both ligands to

NRP1 signalling during OFT septation by analysing NRP1 knockin mice with mutations that selectively target VEGF-A versus SEMA3. Unexpectedly, this analysis revealed that NRP1 expression by cardiac NCCs and VEGF-A binding to NRP1 are both dispensable for OFT remodelling, even when NRP2 is additionally ablated. Instead, I found that loss of endothelial NRP1 was sufficient to recapitulate the complete OFT phenotype of *Nrp1*-null mice and that NRP1 served as a receptor for SEMA3C in ECs. Thus, working in collaboration with a Prof Pete Scambler's group, we found that cardiac NCCs, contrary to prior hypotheses, do not respond to SEMA3C, but instead provide an essential source of SEMA3C and that NCC-derived SEMA3C promotes endoMT, a prerequisite for septal bridge formation. I also found that SEM3C signalling through NRP1 in endothelium indirectly causes cardiac NCC relocalisation within the OFT, another requirement for septal bridge formation in the proximal OFT. These findings demonstrate a mechanism by which cardiac NCCs communicate with OFT endothelium to orchestrate the septation of the embryonic OFT and therefore the separation of the arterial and pulmonary circulation for life after birth.

I have, thus, replaced a previous model of NRP signalling to illustrate the complexity of developmental events that ensure proper OFT septation and involve multiple signalling events between the contributing cell lineages. Unravelling these interactions at the molecular and cellular level in mouse models will inform our interpretation of human genetic data obtained from patients with congenital heart defect patients, where a heterozygous single gene mutation is rarely found to be causative. In support of the idea that defective NRP1 signalling also contributes to human congenital heart disease, recent GWAS studies have shown that a non-synonymous single nucleotide polymorphism (SNP) in the oligomerisation domain of *NRP1* sequence is associated with Tetralogy of Fallot (Cordell et al., 2013).

Chapter 5 *CSF1R-CRE* TARGETS A SUBPOPULATION OF ENDOTHELIAL CELLS THAT CONTRIBUTES TO DEVELOPMENTAL AND PATHOLOGICAL ANGIOGENESIS

5.1 Introduction

Even though vasculogenesis mainly gives rise to the first embryonic and extra-embryonic vessels and the remaining vascular network largely arises through angiogenic sprouting, several studies have suggested that angioblast-like endothelial precursors might contribute to the growth of organ-specific vessel beds in the embryo and to vascular repair in the adult (Nishikawa et al., 1998, Gehling et al., 2000). The adult precursors have been termed endothelial progenitor cells (EPCs) and were first described by Asahara *et al.*, who isolated single cells with the ability to differentiate into EC *in vitro* and *in vivo* from adult human peripheral blood (Asahara et al., 1997). These circulating EPCs were proposed to play a role in adult vascular homeostasis and repair by inserting into the blood vessel endothelium in response to endothelial injury or dysfunction, for example during atherosclerosis (Asahara et al., 1997, Hill et al., 2003). Furthermore, studies have suggested that these cells might contribute to pathological angiogenesis, for instance during tumour vascularisation (Plummer et al., 2013, Nolan et al., 2007, Mellick et al., 2010).

Despite several other studies since demonstrating that single cells within the blood or other tissues have the potential to differentiate into ECs *in vitro* and contribute to vascular growth *in vivo* (Quirici et al., 2001, Peichev et al., 2000, Gehling et al., 2000), the lack of a definite marker of EPCs has created controversy regarding the origin and nature of these cells. For example, it has been suggested that EPCs are derived from a stem cell population within the bone marrow and released into the blood stream, as transplanted murine bone marrow was shown to give rise to ECs in the host mouse (Asahara et al., 1999).

Some studies have implied that the putative bone marrow-derived EPC precursor is of hematopoietic origin. Thus, the bone marrow contains hematopoietic stem cells (HSCs), which are the main source of all postnatal blood cells (Pietras et al., 2011). After isolation from the bone marrow using markers such as CD133 and

VEGFR2, these HSCs can differentiate into ECs *in vitro* and contribute to vessel growth *in vivo* (Ria et al., 2008, Reyes et al., 2002). Nevertheless, CD133 and VEGFR2 are not exclusively expressed by HSCs, and some studies have postulated that they are also expressed by EPCs (Peichev et al., 2000, Salven et al., 2003). Therefore, these experiments do not conclusively show whether EPCs are derived from a hematopoietic precursor. In fact, another study observed that $CD133^+$ cells, which were also positive for the hematopoietic marker CD45 (Nakano et al., 1990, Van Craenenbroeck et al., 2013), did not differentiate into ECs *in vitro*, whereas $CD133^+CD45^-$ cells did develop into ECs, suggesting that EPCs are not of hematopoietic origin (Case et al., 2007).

In addition to the bone marrow, some papers have argued the existence of tissue-resident EPCs. For example, in the retina, which is not vascularised until after birth, several studies have described stellate precursors that precede the growing vasculature and were proposed to function as angioblasts (Ashton, 1970, Kretzer et al., 1984). A recent genetic study using *Cre/LoxP* lineage tracing has provided compelling evidence for spindle-shaped cells that differentiate into ECs *in vitro* and contribute to the retinal vasculature (Kubota et al., 2011).

Furthermore, several studies have suggested that the endothelium itself can give rise to EPCs that enter the blood stream and maintain vascular homeostasis and contribute to tissue remodelling and repair (Alvarez et al., 2008, Ingram et al., 2005). These cells, termed endothelial colony forming cells (ECFCs), differ from normal ECs in their proliferative and colony forming potential and were initially observed within the aorta (Schwartz and Benditt, 1976, Schwartz and Benditt, 1977). Since then, ECFCs have also been described within the microvasculature of several organs such as the lung (Schniedermann et al., 2010, Alvarez et al., 2008).

Finally, some studies have postulated that macrophages may function as EPCs by transdifferentiating into ECs that contribute to vessel growth. For instance, it was reported that macrophages express endothelial markers and adopt an endothelial morphology to contribute to tumour angiogenesis (McKenney et al., 2001, Yan et al., 2011). Furthermore, some studies reported that overexpression of the angiogenic molecules pleiotrophin or VEGF-A caused macrophages to express endothelial

markers such as VEC or CD31 and to form vascular structures both *in vitro* and *in vivo*, which may suggest vascular mimicry (Yeh et al., 1998, Chen et al., 2009a, Yan et al., 2011). Finally, as monocytes/macrophages are known to promote vascular growth by releasing pro-angiogenic factors such as VEGF-A or VEGF-C (McLaren et al., 1996, Tammela et al., 2005), they can also act as pro-angiogenic accessory cells that home to sites of active angiogenesis to create a pro-angiogenic environment (Grunewald et al., 2006).

Considering the vast number of studies that differ in the molecular definition and proposed origin of EPCs (reviewed in Timmermans et al., 2009), the existence and function of these cells have remained contentious, with several studies suggesting that EPCs do not exist, but instead constitute pro-angiogenic monocytes that do not transdifferentiate into ECs (Rohde et al., 2006, Rehman et al., 2003). Nevertheless, considering the extensive evidence for a role of EPCs in both adult blood vessel formation and vascular homeostasis, it appears to me more likely that EPCs comprise a heterogeneous group of precursor cells, which can be found in different niches such as the bone marrow, vascular wall and blood and differ in their expression of markers as well as functional contribution to vascular repair and perhaps homeostasis.

Our group has recently become interested in the role of EPCs, as previous observations by Dr Alessandro Fantin from our group observed an unusual type of EC that expresses CRE recombinase under the control of the promoter of *Csf1r* (*Csf1r-Cre*) (Deng et al., 2010), when he analysed the role of macrophages during developmental angiogenesis in the mouse. Thus, to observe the targeting efficiency of the *Csf1r-Cre* transgene in tissue macrophages, he introduced this gene into mice carrying a floxed $Rosa^{Yfp}$ reporter (Srinivas et al., 2001). As expected, he observed many YFP^{+} macrophages, for example in the E11.5 hindbrain (Fantin et al., 2010). Unexpectedly, however, he also observed YFP^{+} cells that resembled ECs within the vasculature of E11.5 hindbrains (A. Fantin, unpublished). This observation raised the possibility that the *Csf1r-Cre* transgene was expressed in ECs or, alternatively, that the progeny of cells expressing the *Csf1r-Cre* transgene at some point in their development subsequently incorporated into the endothelium. My aim was to

investigate the nature and origin of these *Csf1r-Cre*-targeted ECs and to understand whether they contribute to vascular development.

5.2 Results

5.2.1 *Csf1r-Cre* labels ECs during embryonic angiogenesis

To confirm Dr Fantin's observations of endothelial targeting with *Csf1r-Cre*, I initially analysed E10.5 *Csf1r-Cre;Rosa*^{Yfp} hindbrains. At this time point, angiogenic sprouts have reached the subventricular side of the tissue and formed a vascular network termed the SVP (Fantin et al., 2013c, Plein et al., 2015b) (see **Chapter 3**). To visualise *Csf1r-Cre* targeting within hindbrains, I labelled them for YFP and the vessel/macrophage marker isolectin B4 (IB4) (Fantin et al., 2010, Sorokin and Hoyt, 1992). I also included the macrophage marker F4/80 (Austyn and Gordon, 1981, Rogove et al., 2002) to accurately distinguish ECs and yolk sac-derived macrophages, which are known to migrate into the subventricular zone from E10.5 onwards to interact with endothelial tip cells and promote vessel anastomosis (Fantin et al., 2010). As published previously (Deng et al., 2010, Fantin et al., 2013a), I confirmed that *Csf1r-Cre* targets almost all IB4^{+} and F4/80^{+} macrophages, (arrowhead, **Figure 5.1B**). In addition, I observed that YFP was sporadically expressed, albeit less strongly, in a small number of cells within the blood vessels, as previously seen by Dr Fantin. These cells did not appear to have the rounded morphology of circulating cells, but instead they resembled ECs in their elongated cell morphology (arrow, **Figure 5.1B**). Furthermore, they were not positive for F4/80, suggesting that these cells were macrophages adopting an endothelial morphology, as reported in previous studies of pathological angiogenesis (Scavelli et al., 2008).

Quantitation of the number of YFP^{+} macrophages (defined as IB4^{+}F4/80^{+} single cells) and ECs (defined as IB4^{+}F4/80^{-} vessel-bound cells) revealed that approximately 20% of YFP^{+} cells were ECs (**Figure 5.1G**). As the number of YFP^{+} ECs was relatively low at E10.5, I next analysed *Csf1r-Cre* labelling in hindbrains at later stages. At E11.5, the number of YFP^{+} macrophages as well as *Csf1r-Cre;Rosa*^{Yfp}-labelled ECs had roughly doubled (**Figure 5.1C**,**G**). By E12.5, the

number of *Csf1r-Cre;Rosa*^{Yfp}-targeted macrophages in the SVP had decreased. This finding agreed with prior studies, which showed that the amount of macrophages peaks at E11.5, when vascular anastomosis takes place, but that macrophages appear to move to deeper hindbrain layers after this stage (Fantin et al., 2010). In contrast to the decrease in macrophages in the subventricular zone, the amount of YFP^{+} ECs had increased by roughly 2.5 fold (**Figure 5.1E,G**).

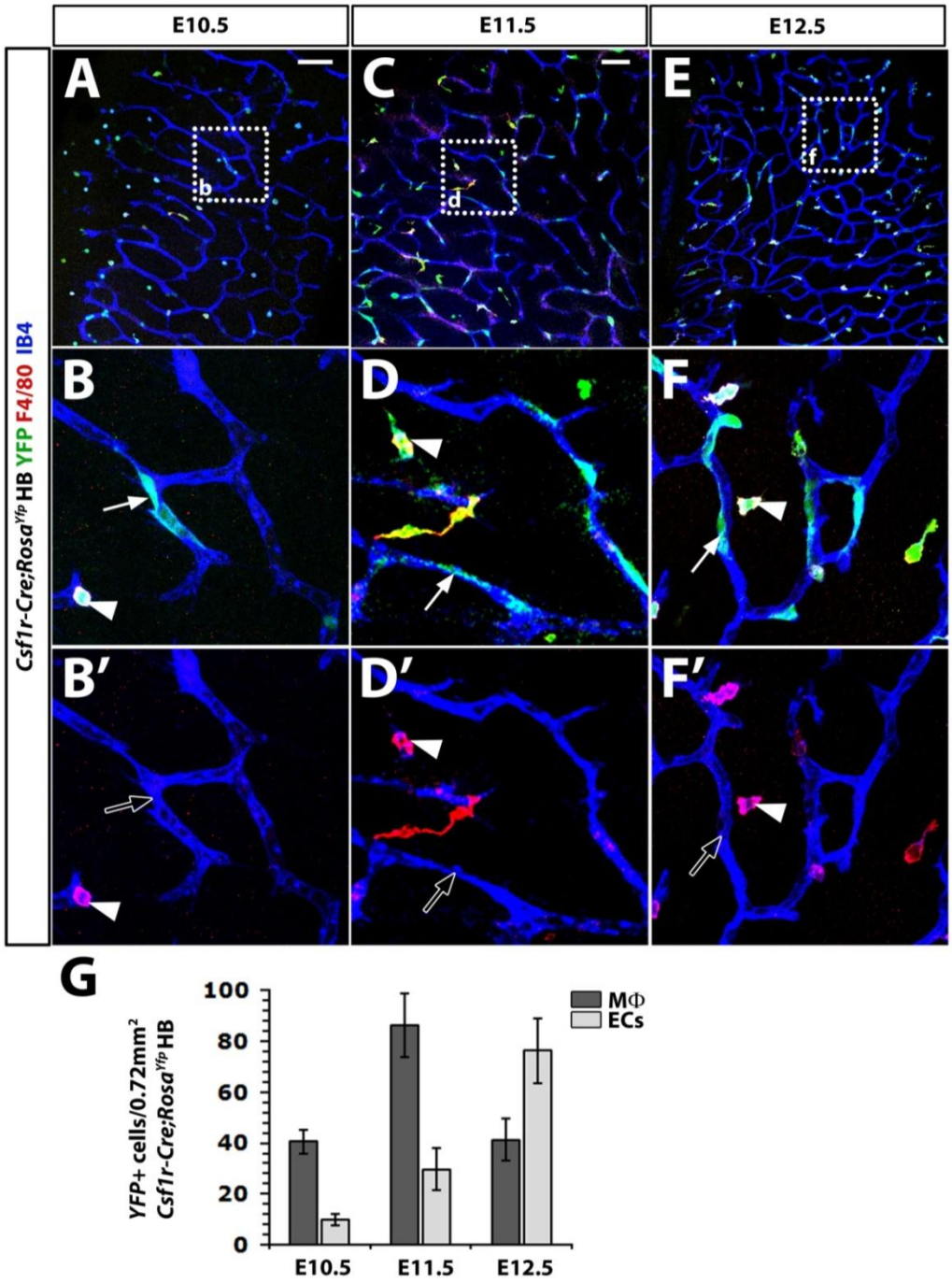

Figure 5.1. *Csf1r-Cre;Rosa*^{Yfp} targets ECs during embryonic hindbrain angiogenesis.

E10.5, E11.5 and E12.5 *Csf1r-Cre;Rosa*^{Yfp} hindbrains were wholemount labelled for YFP, F4/80 and IB4. High magnification of the boxed areas indicated in **(A,C,E)** are shown in **(B,D,F)** and in **(B',D',F')** without the green channel. Arrowheads indicate *Cre*-targeted macrophages, arrows highlight *Cre*-targeted ECs and clear arrows denote unlabelled endothelium. The density of YFP^{+} macrophages (MΦ) and ECs in *Csf1r-Cre;Rosa*^{Yfp} hindbrains was determined, where macrophages were defined as IB4^{+}F4/80^{+} single cells and ECs as IB4^{+}F4/80^{-} cells within vessels **(G)**. Mean ± s.d., n= 3 each. Scale bars: 100 μm **(A)**, 50 μm **(C)**.

Having established that the *Csf1r-Cre;Rosa*^{Yfp}-labelled cells within the hindbrain vasculature did not express F4/80 and did not morphologically resemble macrophages, I next investigated whether the *Csf1r-Cre;Rosa*^{Yfp}-targeted vascular cells were located within the endothelium or were surrounding the endothelium like pericytes. Pericytes are mural cells that are embedded within the basement membrane of the vessel (reviewed in Armulik et al., 2011). The close spatial association of pericytes and ECs within blood vessels makes it difficult to discern between these two cell types in z stack confocal projections. Furthermore, pericytes are recruited to angiogenic sprouts in the brain as soon as they are formed (Abramsson et al., 2007) and would therefore be associated with SVP vessels at all time points analysed. To overcome these challenges in assigning an EC versus pericyte identity to the *Csf1r-Cre;Rosa*^{Yfp}-targeted vascular cells, I stained *Csf1r-Cre;Rosa*^{Yfp} E12.25 hindbrains for YFP together with the pericyte marker NG2 (Ozerdem et al., 2001) and the vessel/macrophage marker IB4, acquired confocal scans and generated both z stack projections and x/y or y/z optical slices. Using this method, I confirmed that the hindbrain vasculature was extensively covered by NG2^{+} pericytes (wavy arrows, **Figure 5.2B**), which were never YFP^{+}. These NG2^{+} pericytes wrapped around the vessels (solid wavy arrow, **Figure 5.2C**,**D**), whilst NG2^{-}YFP^{+} cells were integrated into the endothelium (clear wavy arrow, solid arrow, **Figure 5.2C-D**).

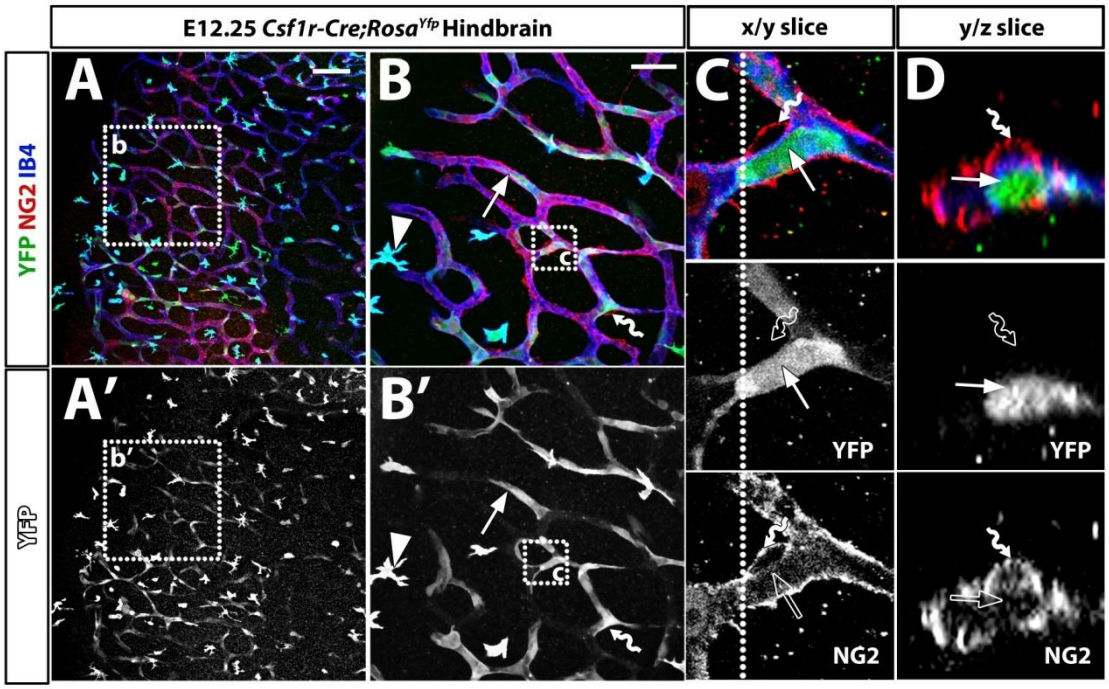

Figure 5.2 *Csf1r-Cre;Rosa*^{Yfp} targets ECs, not pericytes in the mouse embryo hindbrain.

E12.25 *Csf1r-Cre;Rosa*^{Yfp} hindbrain tissue was wholemount labelled for YFP, the pericyte marker NG2 and IB4 **(A,B)**. The projection of a confocal z stack is shown in **(A)**, with a higher magnification of the boxed area in **(A)** in **(B)**, and the corresponding single channel for YFP in (**A',B'**). A single optical x/y section from the boxed area in **(B)** is displayed in **(C)**, and a y/z cross-section through the z stack at the level indicated with a dotted line in **(C)** is shown in **(D)**. Corresponding single channels for YFP and NG2 are shown, as indicated. Arrowheads indicate *Cre*-targeted macrophages, wavy arrows NG2^{+} pericytes and arrows YFP^{+} endothelium. Clear wavy arrows highlight a lack of YFP expression in pericytes, whereas the clear arrow shows a lack of NG2 in the YFP^{+} ECs. Note that the YFP^{+} EC (arrow) lines the vessel, whilst the NG2^{+} pericyte (wavy arrow) is located on the outside. Scale bars: 100 µm **(A)**, 50 µm **(B)**.

5.2.2 *Csf1r-Cre* labels ECs during postnatal angiogenesis

Having confirmed the endothelial identity of the *Csf1r-Cre;Rosa*^{Yfp}-labelled cells, I next investigated whether *Csf1r-Cre;Rosa*^{Yfp} also targeted ECs in other tissues undergoing angiogenesis. I thus analysed YFP expression in the *Csf1r-Cre;Rosa*^{Yfp} retina, as this tissue is a well established postnatal model of angiogenesis (Fruttiger, 2007, Stahl et al., 2010) (see **1.5.2.1**). In the murine retina, vascularisation begins immediately after birth, when vessels enter the most superficial retinal layer from the optic nerve head. Between P0 and P7, these vessels extend from this central point to cover the entire inner layer of the retina with an elaborate vascular network before sprouting into the deeper layers to form the deep and then the intermediate vascular plexus in the second and third weeks after birth (Connolly et al., 1988, Milde et al., 2013). I first investigated P4 *Csf1r-Cre;Rosa*^{Yfp} retinas by staining them for YFP and IB4 together with F4/80. Analysis of YFP expression demonstrated that at this time point *Csf1r-Cre;Rosa*^{Yfp} targeted nearly all F4/80^{+} retinal macrophages, but there was no apparent YFP expression in ECs either in the more mature vessels of the central retina or the nascent vessels at the vascular front (arrowhead, clear arrow, **Figure 5.3B,C**). I next investigated whether *Csf1r-Cre;Rosa*^{Yfp} targeted ECs in the retina at P7 by staining for YFP, F4/80 and IB4. This analysis demonstrated that, in contrast to retinas at P4, YFP was expressed by a large number of ECs within the central retina (arrow, **Figure 5.3E**). I also observed YFP expression in ECs of nascent vessels at the vascular front (arrow, **Figure 5.3F**). Similar observations had previously been made by Dr Fantin, demonstrating their reliability.

Interestingly, *Csf1r-Cre;Rosa*^{Yfp} did not only label macrophages and ECs in the angiogenic retina, but also labelled stellate cells that were mainly located at the vascular front. This observation was intriguing, because several early studies had reported cells with a spindle-shaped morphology at the retinal vascular front and suggested that they contribute as angioblasts to retinal vascular growth (Ashton, 1970, Kretzer et al., 1984, Okuno et al., 2011). However, the existence of such retinal angioblasts is contentious; for example, it has been suggested that they are immature astrocytes (see discussion).

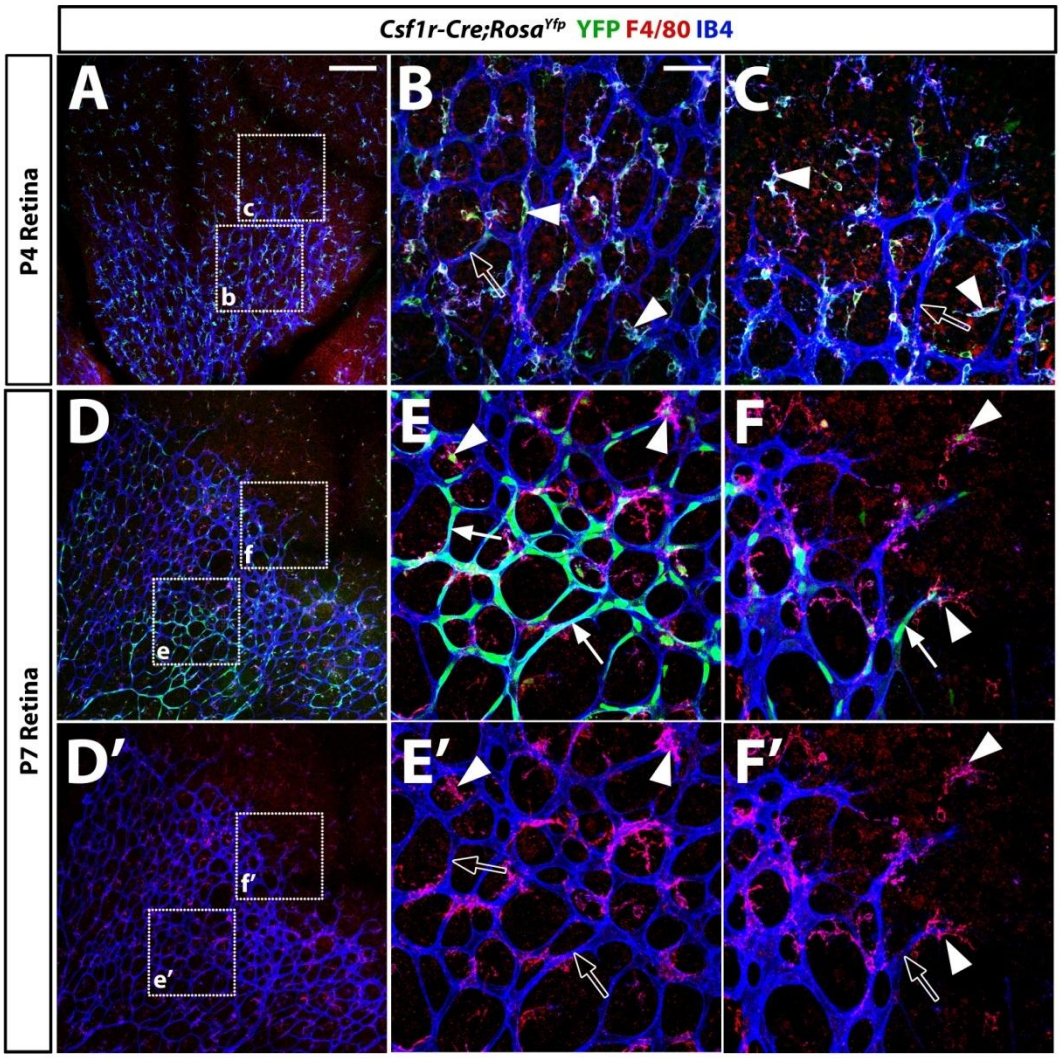

Figure 5.3. *Csf1r-Cre;Rosa*^{Yfp} labels ECs during postnatal angiogenesis.

P4 and P7 *Csf1r-Cre;Rosa*^{Yfp} retinas were wholemount labelled for YFP, the macrophage marker F4/80 and IB4. High magnification of boxed areas in **(A,D)** are shown in **(B,C** and **E,F)**, respectively. The F4/80 and IB4 channels of images **(D-F)** are shown in **(D'-F')**. Arrowheads indicate *Cre*-targeted macrophages, solid arrows YFP^{+} and clear arrows YFP^{-} endothelium. Scale bars: 200 µm **(A)**, 50 µm **(B)**.

In comparison to the vascularisation of the hindbrain, pericytes are recruited to the nascent vessels in the retina and are thus present from P0 (Fruttiger, 2002). To establish whether YFP expression within retinal blood vessels indicated endothelial rather than pericyte targeting, I labelled *Csf1r-Cre;Rosa*^{Yfp} retinas at P4 and P7 for YFP, NG2 and IB4. In agreement with my findings in the hindbrain, I did not observe YFP^{+} pericytes at either time point (clear wavy arrows, **Figure 5.4C,E,F**).

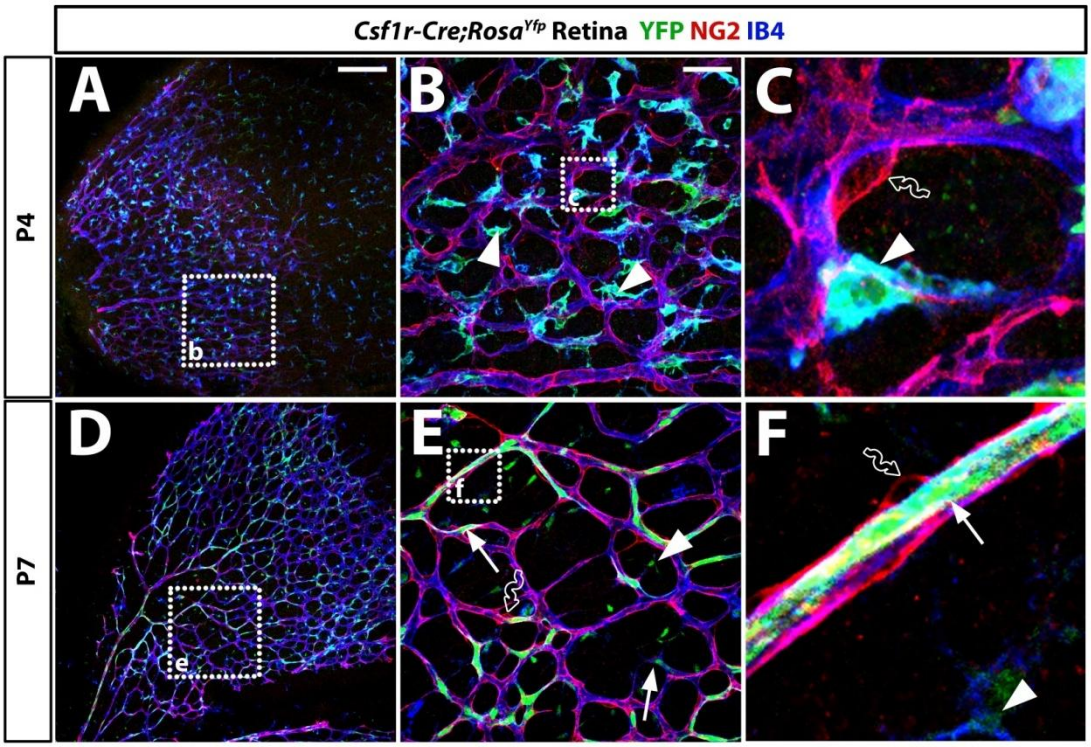

Figure 5.4. *Csf1r-Cre;Rosa*^{Yfp} targets ECs, not pericytes in the postnatal retina.

P4 and P7 *Csf1r-Cre;Rosa*^{Yfp} retinas were wholemount labelled for YFP, NG2 and IB4. High magnification of the boxed areas in **(A,D)** and in **(B,E)** are shown in **(B,E)** and **(C,F)**, respectively. Arrowheads indicate *Cre*-targeted macrophages, arrows YFP^{+} endothelium and clear wavy arrows YFP^{-}NG2^{+} pericytes. Scale bars: 200 µm **(A)**, 50 µm **(B)**.

5.2.3 *Csf1r-Cre;Rosa^{Yfp}* labels spindle-shaped cells at the vascular front, which are not astrocytes

Because it has been suggested that stellate cells at the retinal vascular front are immature astrocytes (Fruttiger, 2002) and that *Csf1r* mRNA is expressed in a subpopulation of astrocytes (Sawada et al., 1993), Dr Fantin and I investigated whether the *Csf1r-Cre;Rosa^{Yfp}*-labelled spindle-shaped cells at the vascular front are indeed astrocytes. For this experiment, we labelled P7 *Csf1r-Cre;Rosa^{Yfp}* retinas for YFP, IB4 and the astrocyte marker glial fibrillary acid protein (GFAP) (Dyer et al., 2000). This revealed that *Csf1r-Cre* did target IB4^{-} cells at the vascular front that were non-endothelial and non-myeloid in character (clear wavy arrow, **Figure 5.5B'**,**C'**). Some of these cells were GFAP^{+} and thus constituted astrocytes (wavy arrow, **Figure 5.5B'''**). Nevertheless, there were other IB4^{-}, spindle-shaped cells at the vascular front that were not GFAP^{+}, suggesting that not all stellate cells targeted by *Csf1r-Cre* are astrocytes (double arrow, **Figure 5.5C''**). These cells may be astrocyte precursors that have not yet begun to express GFAP (see discussion). Alternatively, they may comprise stellate cells that are vascular precursors, perhaps similar to those identified by Kubota *et al.* (Kubota et al., 2011).

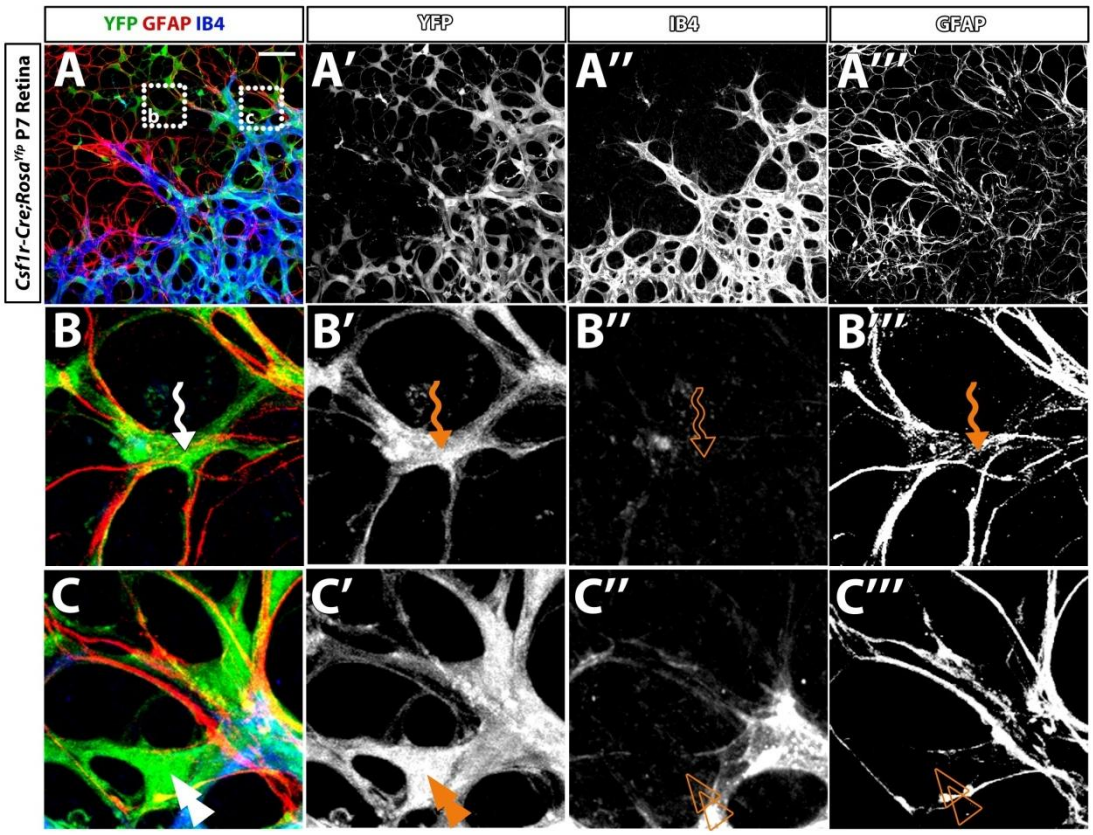

Figure 5.5. *Csf1r-Cre;Rosa*^{Yfp} labels both GFAP^{+} and GFAP^{-} spindle-shaped cells at the retinal vascular front.

P7 *Csf1r-Cre;Rosa*^{Yfp} retinas were wholemount labelled for YFP, IB4, and the astrocyte marker GFAP. The single YFP channel is shown in **(A'-C')**, single IB4 channel in **(A''-C'')** and single GFAP channel in **(A'''-C''')**. High magnification of areas indicated in **(A-A'')** are shown in **(B-B'')** and **(C-C'')**. Wavy arrows label YFP^{+}GFAP^{+} and double arrows YFP^{+} GFAP^{-} spindle-shaped cells. Scale bar: 50 µm **(A)**. Image courtesy of Dr Fantin.

5.2.4 *Csf1r-Cre*-targeted ECs do not express CSF1R or *Csf1r-eGFP*

The endothelial YFP expression might reflect the existence of *Csf1r-Cre;Rosa*^{Yfp}-labelled single cells that insert into the endothelium to complement sprouting angiogenesis in the hindbrain and retina. Alternatively, *Csf1r-Cre;Rosa*^{Yfp} labelling of the endothelium might reflect CSF1R expression by ECs, even though, to date, endothelial expression of CSF1R has not been described. In contrast, ECs are known to be a source of the CSF1R ligand, CSF1 (He et al., 2012).To investigate whether CSF1R is expressed by ECs in the embryonic hindbrain, I labelled E11.5 *Csf1r-Cre;Rosa*^{Yfp} hindbrains for YFP, IB4 and CSF1R. As expected, macrophages were positive for both CSF1R and YFP (arrowhead, **Figure 5.6A-B''**); however, none of the YFP^{+} ECs in the hindbrain expressed CSF1R (solid and clear arrow, **Figure 5.6B-B''**). I made similar observations in the retina (not shown).

As certain genes such as the gene encoding the myelin protein P0 are only transcribed and not translated during early stages of development (Kubota et al., 2011) and a recent paper detected CSF1R expression in the neural linage by *in situ* hybridisation but not immunolabelling (Luo et al., 2013), I next investigated if the *Csf1r* promoter can drive gene expression in ECs. For this experiment, I took advantage of the *Csf1r-eGFP* transgene (Sasmono et al., 2003), in which GFP expression faithfully recapitulates *Csf1r* gene expression (Abtin et al., 2014, Chen et al., 2011a, Lin et al., 2006). This transgene contains an *eGFP* construct fused to the *Csf1r* promoter and it thus labels cells in which the *Csf1r* promoter is currently active, in contrast to the *Csf1r-Cre;Rosa*^{Yfp} transgene, which labels the *Csf1r-Cre* lineage, including cells that activated the *Csf1r* promoter at some point in their development independently of whether they activate it presently.

By staining E11.5 *Csf1r-eGFP* hindbrains and retinas for GFP, CSF1R and IB4, using the same method employed to label *Csf1r-Cre;Rosa*^{Yfp} tissues, I observed that that all GFP^{+} cells were also CSF1R^{+} and thus macrophages (**Figure 5.6D,F**). In contrast, there was no GFP labelling of ECs (**Figure 5.6D,F**), similar to the lack of CSF1R immunolabelling. Together, these observations suggest that CSF1R is neither expressed at protein nor mRNA level in hindbrain endothelium. Future work should include an analysis by *in situ* hybridisation for *Csf1r* mRNA to validate this finding.

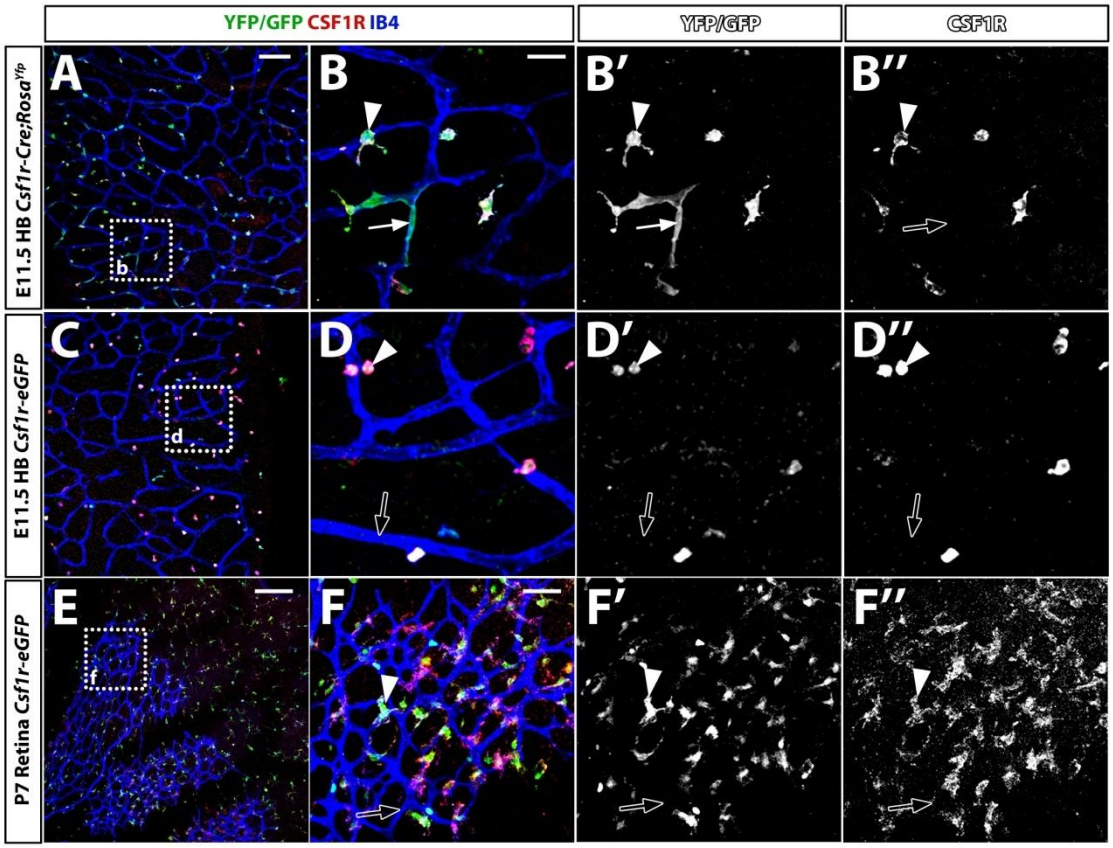

Figure 5.6. *Csf1r-Cre;Rosa*^{Yfp} targeted, YFP^{+} ECs do not express CSF1R.

E11.5 *Csf1r-Cre;Rosa*^{Yfp} **(A-B'')** and *Csf1r-eGFP* hindbrains **(C-D'')** and P7 retinas **(E-F'')** were wholemount labelled for YFP, CSF1R and IB4. High magnifications of the boxed areas indicated in **(A,C,E)** are shown in **(B,D,F)** together with the corresponding single channels for YFP **(B',D',F')** and CSF1R **(B'',D'',F'')**, respectively. Arrowheads indicate CSF1R^{+} macrophages, solid arrows YFP^{+} ECs and clear arrows a lack of either YFP **(F',H')** or CSF1R **(C'',F'',H'')** expression. HB: hindbrain. Scale bars: 100 µm **(A)**, 50 µm **(B,F)**, 200 µm **(E)**.

5.2.5 Unregulated *Rosa^{Yfp}* activation cannot explain the presence of *Csf1r-Cre* targeted ECs in the retina

Because other labs using *Csf1r-Cre* in combination with the *Z/EG* reporter transgene (Novak et al., 2000) did not report endothelial targeting (Stefater et al., 2011), I next asked whether YFP$^+$ labelling of ECs in *Csf1r-Cre;Rosa^{Yfp}* mice is an artefact caused by spontaneous recombination within the endothelium, independently of *Cre* expression and CRE-mediated excision of the *Rosa^{Yfp}* stop cassette. To address this possibility, I analysed YFP expression in hindbrains from E11.5 *Csf1r-Cre;Rosa^{Yfp}* embryos lacking the *Cre* transgene, but carrying the *Rosa^{Yfp}* allele. This experiment showed that, YFP expression depended on the presence of CRE (**Figure 5.7D**), demonstrating that *Rosa^{Yfp}* is only activated following the expression of *Csf1r-Cre* and that it is therefore a faithful reporter of *Cre* expression.

To confirm this finding, I also investigated YFP expression in *Rosa^{Yfp}* mice expressing *Cre* under the control of another transgene, *Sm22a-Cre*, which targets vascular myocytes (Solway et al., 1995, Lepore et al., 2005) and pericytes (Anastasia et al., 2014, Daniel et al., 2012). I, thus, labelled P7 *Sm22a-Cre;Rosa^{Yfp}* retinas for YFP, IB4 and the smooth muscle marker SMA and compared them to P7 retinas from *Csf1r-Cre;Rosa^{Yfp}* mice stained for YFP, NG2 and IB4. As expected, *Sm22a-Cre;Rosa^{Yfp}* retinas expressed YFP strongly in the SMA$^+$ myocytes of the artery (**Figure 5.8D**) as well as in the perivascular cells surrounding the capillaries (wavy arrows, **Figure 5.8E-F''**). I did not, however, observe any EC-targeting in these retinas (clear arrows, **Figure 5.8E-F''**). In contrast, the *Csf1r-Cre;Rosa^{Yfp}* retinas displayed extensive endothelial *Cre*-targeting with no apparent YFP expression in pericytes (solid arrows and clear wavy arrows, respectively, **Figure 5.8A-C''**). Together, these experiments suggest that endothelial YFP expression is not due to the unspecific recombination of the *Rosa^{Yfp}* reporter. It also suggests that the *Rosa^{Yfp}* knockin allele is a more sensitive reporter than the Z/EG transgene.

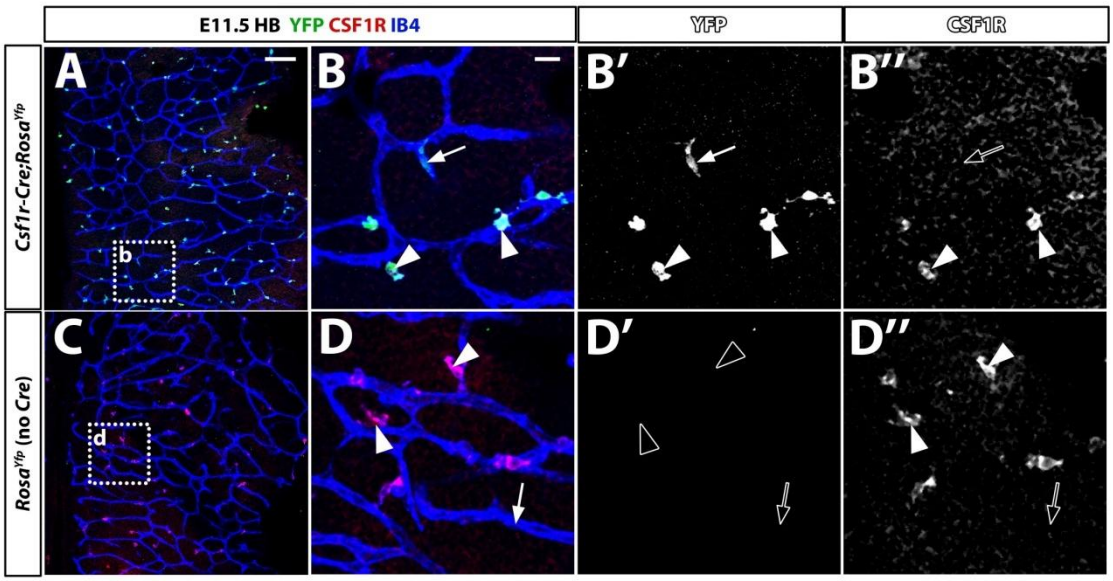

Figure 5.7. *Rosa*^{Yfp} is not activated unspecifically in *Csf1r-Cre*-negative E11.5 hindbrains.

E11.5 *Csf1r-Cre;Rosa*^{Yfp} *Cre*-positive and *Cre*-negative hindbrains were wholemount labelled for YFP, CSF1R and IB4. Higher magnification of the boxed areas in **(A,C)** are shown in **(B,D)** together with the corresponding single channels for YFP in **(B',D')** and CSF1R **(C'',D'')**. Solid arrowheads and arrows in **(B')** indicate *Cre*-targeted macrophages and ECs, respectively, whereas clear arrowheads and arrows in **(D')** highlight the absence of YFP in macrophages or ECs, respectively, in *Cre*-negative hindbrains. HB: hindbrain. Scale bars: 100 µm **(A)**, 20 µm **(B)**.

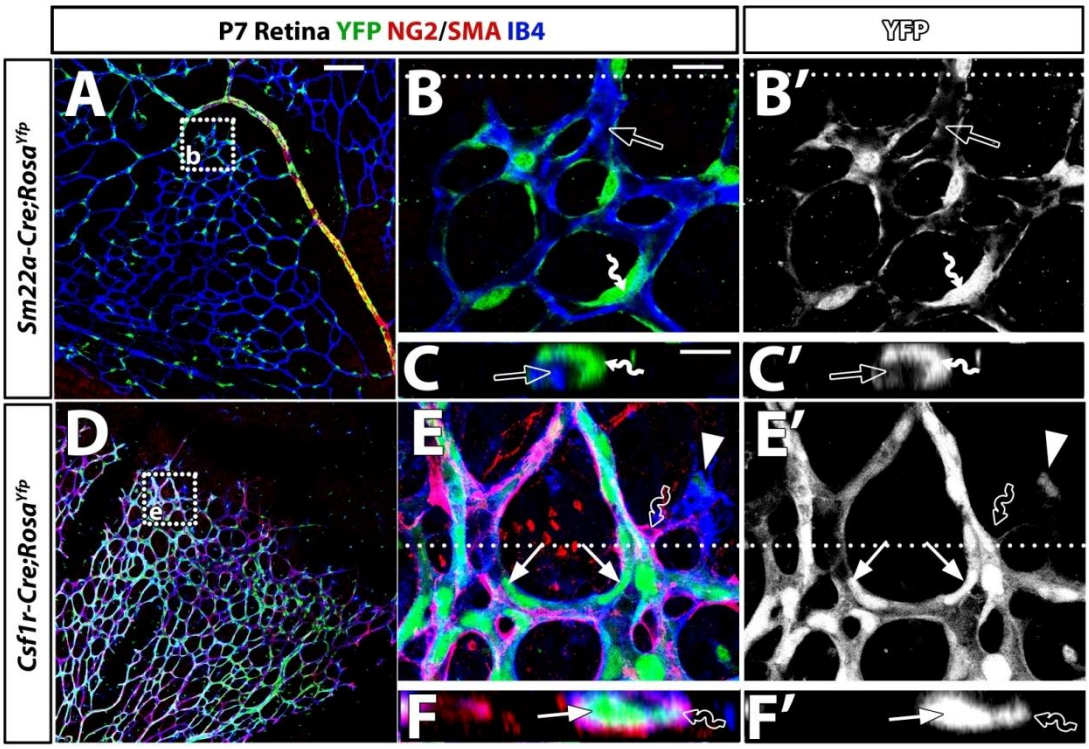

Figure 5.8. *Sm22a-Cre* targeting of the *Rosa*^{Yfp} reporter yields YFP^{+} mural cells but not ECs, whilst *Csf1r-Cre* targeting yields YFP^{+} ECs but not mural cells.

P7 *Sm22a-Cre;Rosa*^{Yfp} and *Csf1r-Cre;Rosa*^{Yfp} retinas were wholemount labelled for YFP, IB4 and SMA or NG2. Higher magnification of the boxed areas in **(A,D)** are shown in **(B,E)**, respectively. The dotted lines in **(B,E)** indicate the position of the high magnification y/z cross-sections shown in **(C,F)**. **(B,C,E,F)** are shown as a single YFP channel in **(B',C',E',F')**. Arrowheads indicate *Cre*-targeted macrophages, solid arrows YFP^{+} and clear arrows YFP^{-} endothelium. Solid wavy arrows highlight YFP^{+} and clear wavy arrows YFP^{-} pericytes. Scale bars: 200 μm **(A)**, 25 μm **(B)**, 10 μm **(C)**.

5.2.6 *Csf1r-Cre;Rosa^{Yfp}*-labelled ECs are not of macrophage origin

Having established that *Csf1r-Cre;Rosa^{Yfp}*-targeting of ECs during embryonic and postnatal angiogenesis does not reflect endogenous CSF1R expression, and that it is not caused by ectopic activation of the *Csf1r* promoter in the transgene or a "leaky" *Rosa^{Yfp}* locus, it appears likely that YFP^{+} ECs are derived from *Csf1r-Cre*-targeted cells that are recruited into the vasculature during the process of angiogenesis. To identify the origin of these hypothetical *Csf1r-Cre;Rosa^{Yfp}*-labelled progenitor cells, I first asked if they were derived from tissue macrophages (see **1.3.3**). Thus, tissue macrophages are known to promote developmental and pathological angiogenesis (Fantin et al., 2010, Nakao et al., 2005, Lewis et al., 1995, Wu et al., 2012), and several studies have suggested that this is partly due to their ability to transdifferentiate into ECs *in vitro* and contribute to tumour vascularisation (Chen et al., 2009a, Scavelli et al., 2008).

To address whether *Csf1r-Cre;Rosa^{Yfp}*-labelled ECs in the hindbrain were indeed derived from macrophages inserting into the angiogenic endothelium, Dr Fantin crossed *Csf1r-Cre;Rosa^{Yfp}* mice onto a *Pu.1*-null background. PU.1 is a member of the *Ets* family of transcription factors that is critical for myeloid and lymphoid differentiation, and mice with a mutation abolishing the DNA binding domain of this gene are therefore deficient in macrophages (McKercher et al., 1996, Scott et al., 1994). Dr Fantin's initial analysis of E11.5 *Csf1r-Cre;Rosa^{Yfp};Pu.1$^{-/-}$* and control hindbrains labelled for YFP and IB4 had suggested that YFP^{+} ECs were still present in mice lacking macrophages. To confirm this finding, I labelled E11.5 *Csf1r-Cre;Rosa^{Yfp}* hindbrains on a *Pu.1$^{+/+}$* versus *Pu.1$^{-/-}$* background for YFP and IB4 together with F4/80. This experiment confirmed a lack of macrophages in the hindbrain of *Pu.1$^{-/-}$* embryos and further showed that YFP expression was retained in a subset of ECs in the *Pu.1*-null mutants (arrows, **Figure 5.9D**). Quantitation of the number of YFP^{+} ECs on a *Pu.1*-null versus wildtype background demonstrated that the amount of YFP^{+} ECs was unaffected by the loss of macrophages (**Figure 5.9E**). Together, these observations suggest that the YFP^{+} ECs in *Csf1r-Cre;Rosa^{Yfp}* hindbrains are not macrophage-derived.

Unfortunately, *Pu.1*-null mutants die perinatally due to their compromised immune system (McKercher et al., 1996), and I was therefore not able to determine whether the *Csf1r-Cre;Rosa*^{Yfp}-labelled ECs contributing to retinal vascularisation are also of non-macrophage origin.

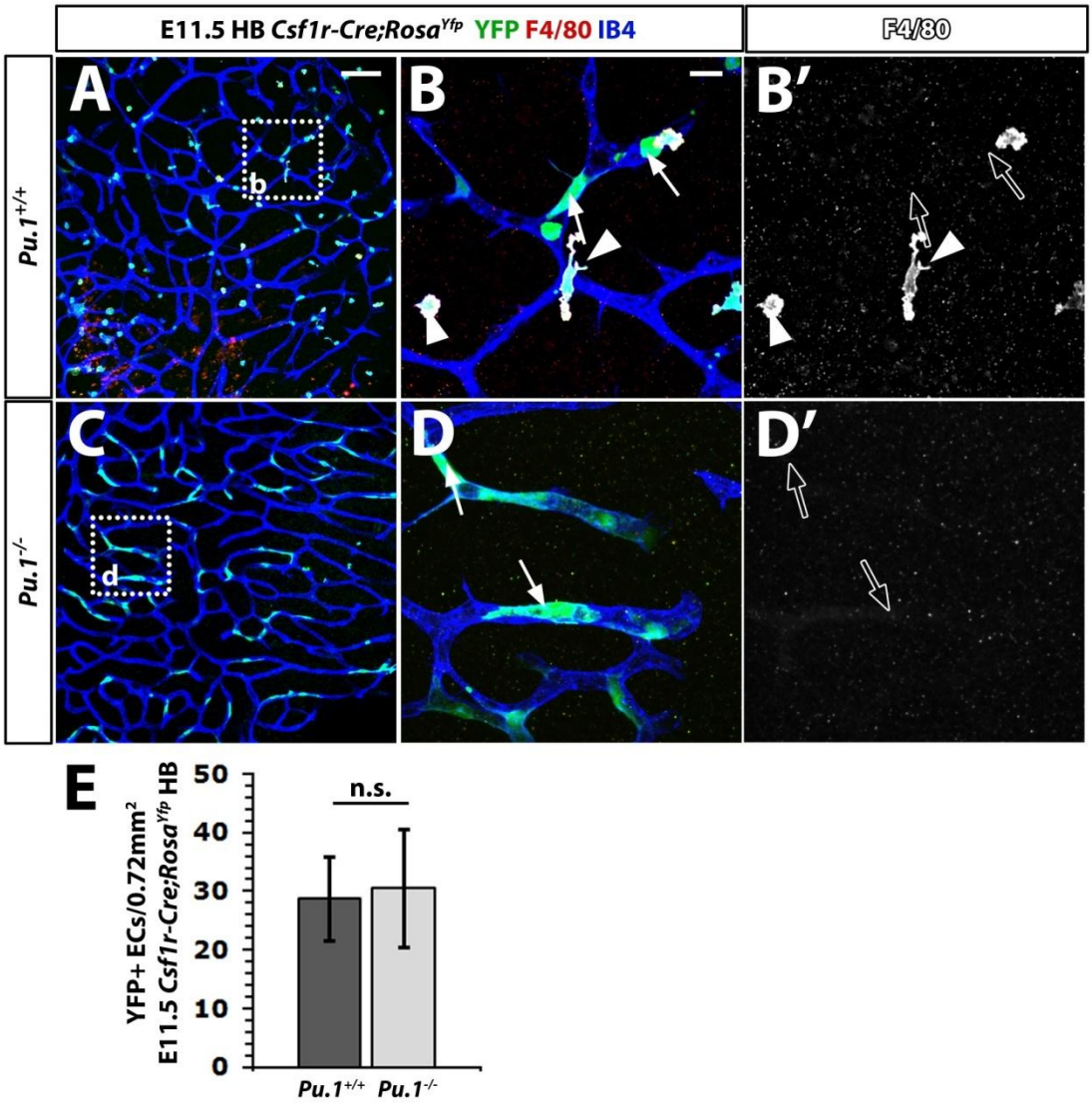

Figure 5.9. *Csf1r-Cre;Rosa*^{Yfp}-targeted ECs are not macrophage-derived.

E11.5 *Csf1r-Cre;Rosa*^{Yfp} hindbrains on a *Pu.1*$^{+/+}$ **(A-B')** and *Pu.1*$^{-/-}$ **(C-D')** background were wholemount labelled for YFP, F4/80 and IB4. High magnification of boxed areas indicated in **(A,C)** are shown in **(B,D)** and as a single F4/80 channel in **(B',D')**. Arrowheads indicate *Cre*-targeted macrophages and arrows YFP^{+} endothelium. Note the absence of F4/80 in YFP^{+} endothelium. Quantitation of YFP^{+} ECs in 0.72 mm^{2} of E11.5 *Csf1r-Cre;Rosa*^{Yfp} hindbrains on a *Pu.1*$^{+/+}$ (n= 4) and *Pu.1*$^{-/-}$ (n= 4) background **(E)**. Mean ± s.d.; n.s., not significant. HB: hindbrain. Scale bars: 100 µm **(A)**, 20 µm **(B)**.

5.2.7 Postnatal induction of *Csf1r-Cre* results in YFP$^+$ ECs

To understand if *Csf1r-Cre;Rosa*^{Yfp}-targeted ECs in the angiogenic retina are derived from an embryonic or postnatal *Csf1r-Cre*-labelled progenitor, I used mice containing the tamoxifen-inducible transgene *Csf1r-Cre*^{ERT} (Qian et al., 2011). This transgene enables the spatiotemporal control of *Cre*-mediated gene recombination, because *Csf1r-Cre*^{ERT} is only active in cells expressing the *Csf1r* promoter after tamoxifen administration (see **2.2.1.6**) (Mattioni et al., 1994, Picard, 1994). Dr Fantin and I injected *Csf1r-Cre*^{ERT}*;Rosa*^{Yfp} pups with tamoxifen from P4 to P6, collected retinas at P7 or P21, and stained them for YFP, F4/80 and IB4. Unexpectedly, even though macrophages expressed CSF1R (**Figure 5.6E**) and were abundant in the retina at both stages, tamoxifen induction led to the targeting of only a small number of macrophages at P7 and P21 (arrowhead, **Figure 5.10B,D**). Low frequency targeting of retinal macrophages was likely explained by tamoxifen's inability to effectively cross the blood-retinal barrier (Noguchi et al., 1988) to reach the retinal macrophages, which under physiological conditions are mostly tissue-resident microglia rather than being derived from circulating monocytes (Caicedo et al., 2005). The sparse YFP$^+$ macrophages may, thus, be derived from tissue-resident microglia exposed to a small local source of tamoxifen that entered the retina across leaky patches of blood-retina-barrier. Alternatively, the targeted cells may be derived from extravasated monocytes that were targeted whilst still in the circulation. In support of this possibility, a low number of blood-derived monocytes were shown to be present in the healthy adult retina (Caicedo et al., 2005).

Even though tamoxifen normally targets ECs with good efficiency due to their ready exposure to blood-borne agents (e.g. Pitulescu et al., 2010, Raimondi et al., 2014), there was no YFP expression apparent in ECs of P7 retinas (n= 4). By P21, however, some YFP$^+$ ECs were present in the retinal vasculature, albeit at a low frequency, alongside a few YFP$^+$ macrophages (arrowhead and arrow, respectively, **Figure 5.10D**). Because CSF1R is not usually expressed in retinal ECs (see **Figure 5.6**), the presence of YFP$^+$ ECs in *Csf1r-Cre*^{ERT}*;Rosa*^{Yfp} mice suggests that the YFP$^+$ ECs are derived from a CSF1R-expressing precursor. Moreover, the fact that EC-targeting was achieved with two independently generated transgenic lines, *Csf1r-Cre*^{ERT} and *Csf1r-Cre*, argues against unspecific *Cre* activation caused by host

regulatory elements at the transgene integration site, because both transgenes should have randomly inserted into different genomic loci. In the absence of CSF1R expression by retinal ECs (**Figure 5.6F**), endothelial targeting by constitutive *Csf1r-Cre* in the retina therefore implies the existence of an endothelial progenitor that expresses CSF1R, whilst postnatal targeting by *Csf1r-Cre*^{ERT} additionally shows that the progenitor population persists postnatally.

A study investigating the *P0-Cre* lineage trace had demonstrated that *P0-Cre*-labelling of the endothelium is caused by *P0*-expressing stellate cells at the retinal vascular front (Kubota et al., 2011). Analysis of *Csf1r-Cre;Rosa*^{Yfp} retinas had revealed cells with a similar morphology at the vascular front suggesting that *Csf1r-Cre* might also label tissue-resident vascular precursors. Thus, the low frequency of YFP^{+} ECs might reflect the small amount of tamoxifen that enters the retinal parenchyma and reaches the tissue-resident progenitors. Nevertheless, given the delay between the induction of *Cre*^{ERT} and the appearance of YFP^{+} ECs in the retina, the *Csf1r-Cre*-labelled progenitors most likely do not arise locally within the retina, but elsewhere in the body and are subsequently recruited into the retina, presumably from the blood. For example, they might arise in the bone marrow from a precursor that releases progeny, in analogy to HSCs giving rise to circulating monocytes that can invade tissues and differentiate in accordance with local requirements. To support this hypothesis, further experiments should address whether the bone marrow is efficiently and immediately targeted in *Csf1r-Cre*^{ERT}*;Rosa*^{Yfp} mice after tamoxifen administration.

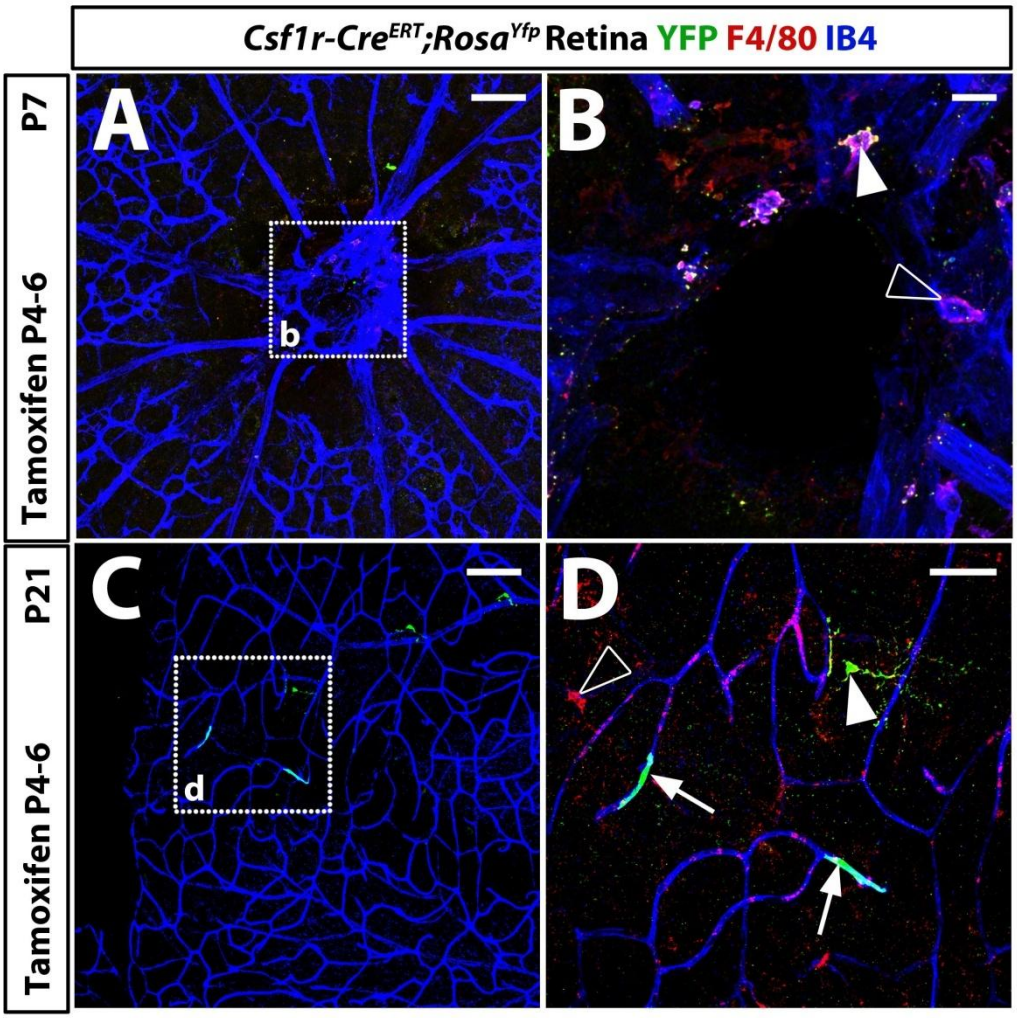

Figure 5.10. Postnatal induction of *Csf1r-Cre^{ERT}* yields YFP^{+} retinal ECs.

P7 and P21 retinas from *Csf1r-Cre^{ERT};Rosa^{Yfp}* mice that were injected with tamoxifen from P4 to P6 to induce *Cre*-recombination were wholemount labelled for YFP, F4/80 and IB4, and flatmounted **(A-D)**. High magnification of the boxed areas indicated in **(A,C,E)** are shown in **(B,D,F)**, respectively. Solid arrowheads indicate *Cre*-targeted macrophages, clear arrowheads non-recombined macrophages and arrows YFP^{+} ECs. Scale bars: 100 µm **(A,C)**, 20 µm **(B)**, 50 µm **(D)**.

5.2.8 A *Csf1r-Cre*-targeted cell population in blood and bone marrow expresses previously published markers of endothelial progenitors.

Given my observations, which suggested that *Csf1r-Cre* labelled circulating vascular precursors that contribute to postnatal vascular development, I next investigated whether *Csf1r-Cre* targeted cells in the bone marrow and blood that resembled previously published endothelial progenitor populations within the adult mouse bone marrow (e.g. Asahara et al., 1999) (see **1.1.2.4**). I, thus, immunolabelled the bone marrow of *Csf1r-Cre;Rosa*^{Yfp} adult mice with antibodies for YFP and the proto-oncogene KIT (CD117), which is a marker for hematopoietic stem cells but has also been used as a marker of endothelial progenitors (e.g. Suzuki et al., 2014, Fang et al., 2012, Dentelli et al., 2007). I found that YFP labelled numerous cells within the bone marrow, of which a subset was also KIT^{+} (open arrowheads, **Figure 5.11B**).

Because KIT also labels hematopoietic progenitors in the bone marrow (Shin et al., 2014) and *Csf1r-Cre* targets myeloid precursors, which are present in the bone marrow (Akashi et al., 2000), I next sought to distinguish hematopoietic progenitors from non-hematopoietic cells by FACS on adult *Csf1r-Cre;Rosa*^{Yfp} bone marrow cells stained for KIT and the hematopoietic marker CD45 (e.g. Case et al., 2007). Analysis of the FACS-sorted cells according to the gating strategies outlined in (**Figure 5.11C-E**) revealed that the majority of bone marrow cells from *Csf1r-Cre;Rosa*^{Yfp} mice was CD45^{+} and therefore hematopoietic (80%), whereas the CD45^{-} (non-hematopoietic) population constituted roughly 20% of bone marrow cells (**Figure 5.11C**,**F**). I next quantitated the number of KIT^{+} cells in these two populations and found that 2.8% of hematopoietic cells and only 0.5% of CD45^{-} cells were positive for this progenitor marker (**Figure 5.11D**,**G**). This observation agreed with previous studies showing that CD45^{-} progenitors are rare within the bone marrow (Kucia et al., 2005). Strikingly, almost all of the non-hematopoietic KIT^{+} progenitors were YFP^{+} (**Figure 5.11G**), consistent with the idea that *Csf1r-Cre;Rosa*^{Yfp} does indeed label cells akin to previously described bone marrow-resident EPCs (e.g. Case et al., 2007).

Intriguingly, *Csf1r-Cre;Rosa*^{Yfp} also appeared to label almost all (99%) of the hematopoietic progenitors within the bone marrow. As the myeloid precursors only constitute a subset of all bone marrow progenitors (Akashi et al., 2000), this result implied that *Csf1r-Cre* labelled haematopoietic progenitors other than those that give rise to myeloid cells. In agreement, 98.1% of all blood cells were YFP^{+} in *Csf1r-Cre;Rosa*^{Yfp} adults (**Figure 5.11H**). These results agree with prior observations that *Csf1r-Cre;Rosa*^{Yfp} labels non-myeloid hematopoietic cells such as T lymphocytes (Deng et al., 2010).

I next investigated by FACS whether the peripheral blood also contained *Csf1r-Cre;Rosa*^{Yfp}-labelled KIT^{+}CD45^{-} cells. As expected, most of the blood cells were CD45^{+} and therefore part of the hematopoietic lineage (98.4%) (**Figure 5.11I)**. The remaining 1.6% CD45^{-} cells contained a small fraction of KIT^{+} cells (0.15%) (**Figure 5.11I**). Strikingly, all of these cells were YFP^{+}, i.e. targeted by *Csf1r-Cre;Rosa*^{Yfp} (**Figure 5.11J**)**.** These results show that *Csf1r-Cre* labels a population of non-haematopoietic progenitor cells within the peripheral blood, albeit the number of these cells is much lower than in the bone marrow. Previous studies have suggested that the number of EPCs correlates with the level of neoangiogenesis (see **1.1.2.4**) (Gill et al., 2001, Massa et al., 2005). Accordingly, the number of EPCs is thought to be low when the endothelium is mostly quiescent, which is usually the case in the adult (Heiss et al., 2005). In contrast, the number of these cells is thought to increase in response to endothelial injury, following myocardial infarction, for example (Massa et al., 2005). Thus, future studies should analyse whether the number of YFP^{+}KIT^{+}CD45^{-} cells is higher in pups with ongoing postnatal angiogenesis or adults with induced neovascularisation.

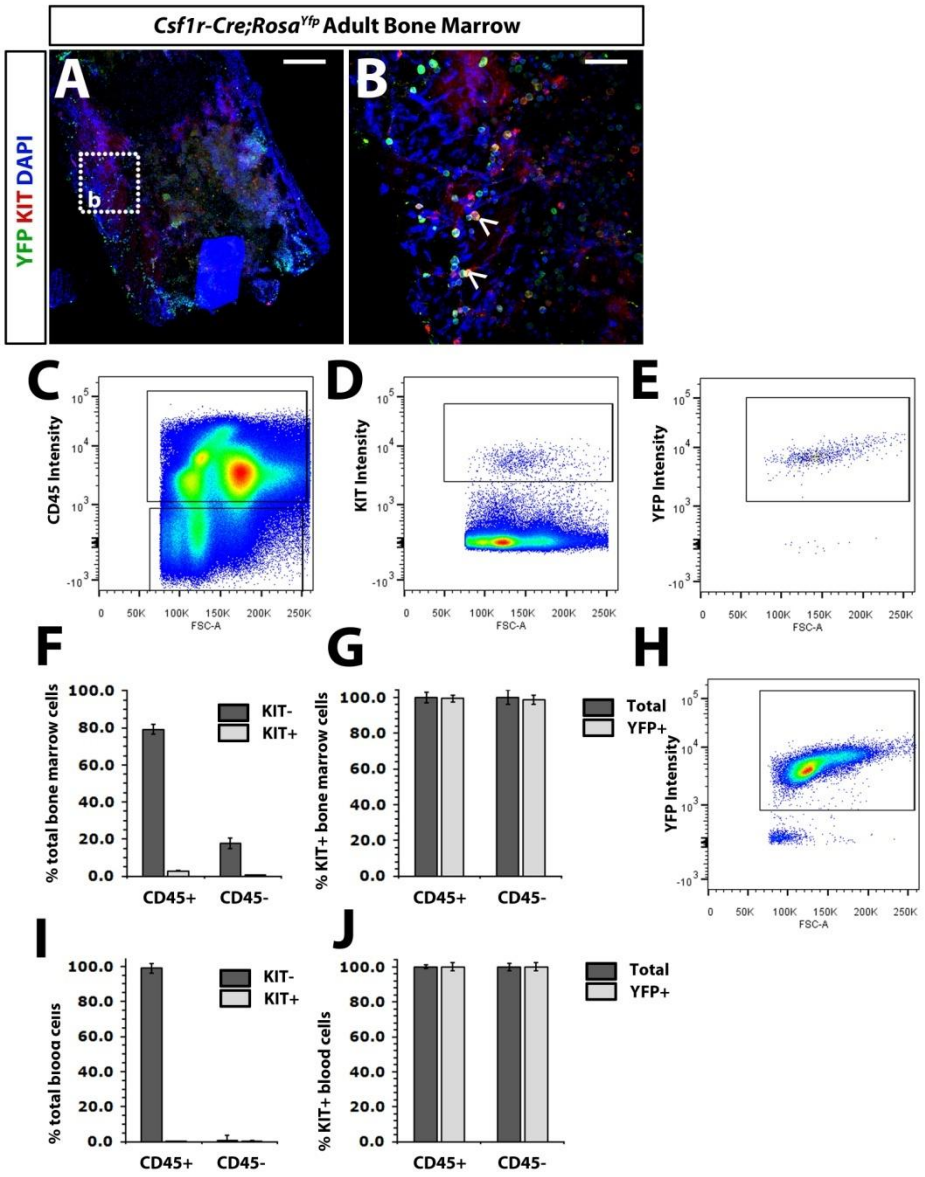

Figure 5.11. *Csf1r-Cre;Rosa*^{Yfp} targets cells expressing KIT in bone marrow and blood.

Adult *Csf1r-Cre;Rosa*^{Yfp} bone marrow sections were immunolabelled for YFP and the progenitor marker KIT and counterstained with DAPI **(A,B)**. A high magnification of the boxed area in **(A)** is shown in **(B)**. Open arrowheads indicate KIT^{+}YFP^{+} cells. FACS analysis of adult *Csf1r-Cre;Rosa*^{Yfp} bone marrow (n= 2) **(C-G)** and blood **(H-J)**. Gating strategy for the intensity of CD45 **(C)**, KIT **(D)** and YFP **(E)**. Quantitation of indicated bone marrow and blood cell populations **(F,G)** and **(I,J)**, respectively. Scatter plot showing *Csf1r-Cre;Rosa*^{Yfp}-labelling of blood cells **(H)**. Mean ± s.d. Scale bars: 200 µm **(A)**, 50 µm **(B)**.

5.2.9 *Csf1r-Cre* targets ECs during pathological angiogenesis

To investigate whether *Csf1r-Cre*-targeted progenitors also contribute to pathological angiogenesis, I used the OIR model (Smith et al., 1994) on *Csf1r-Cre;Rosa*^{Yfp} pups (see **1.5.2.3**). OIR is a useful tool to examine vascular pathologies in the retina, as the sequential exposure of neonatal mice to hyperoxia and then normoxia causes the formation of pathologic neovascular tufts similar to those seen in diseases such as retinopathy of prematurity (Chen and Smith, 2007) or diabetic retinopathy (Archer, 1976).

OIR was performed as published previously (Connor et al., 2009) (see **Chapter 2**). Briefly, *Csf1r-Cre;Rosa*^{Yfp} pups were placed into a high oxygen chamber (>80% oxygen) from P7 until P12, which caused the vessels within the central retina to regress. They were then returned to normoxia (20% oxygen), which resulted in the formation of normal vessels as well as neovascular tufts within the central retinas (Lange et al., 2009). As the number of tufts peaks at P17, I collected the retinas at P17 and labelled them for YFP and IB4 together with CD45, which labels all cells of the haematopoietic system including macrophages. Analysis of YFP expression within these retinas revealed a large number of *Csf1r-Cre*-targeted cells in the OIR-induced vascular tufts (**Figure 5.12A,B**). Many of these cells were CD45^{+} macrophages (arrowheads, **Figure 5.12A,B**), consistent with prior reports that monocytes recruited from the blood closely associate with OIR-induced neovascular tufts (Ritter et al., 2006, Naug et al., 2000, Shen et al., 2007). In addition, YFP was present in a large number of ECs within the vascular tufts, suggesting that *Csf1r-Cre* had targeted ECs or their progenitors (**Figure 5.12B**,**B'**). Strikingly, *Csf1r-Cre;Rosa*^{Yfp}-labelling of ECs appeared to be more prevalent within the tuft vessels than in healthy-looking neighbouring vessels (compare **Figure 5.12B** and **C**), however I have yet to formally quantitate this.

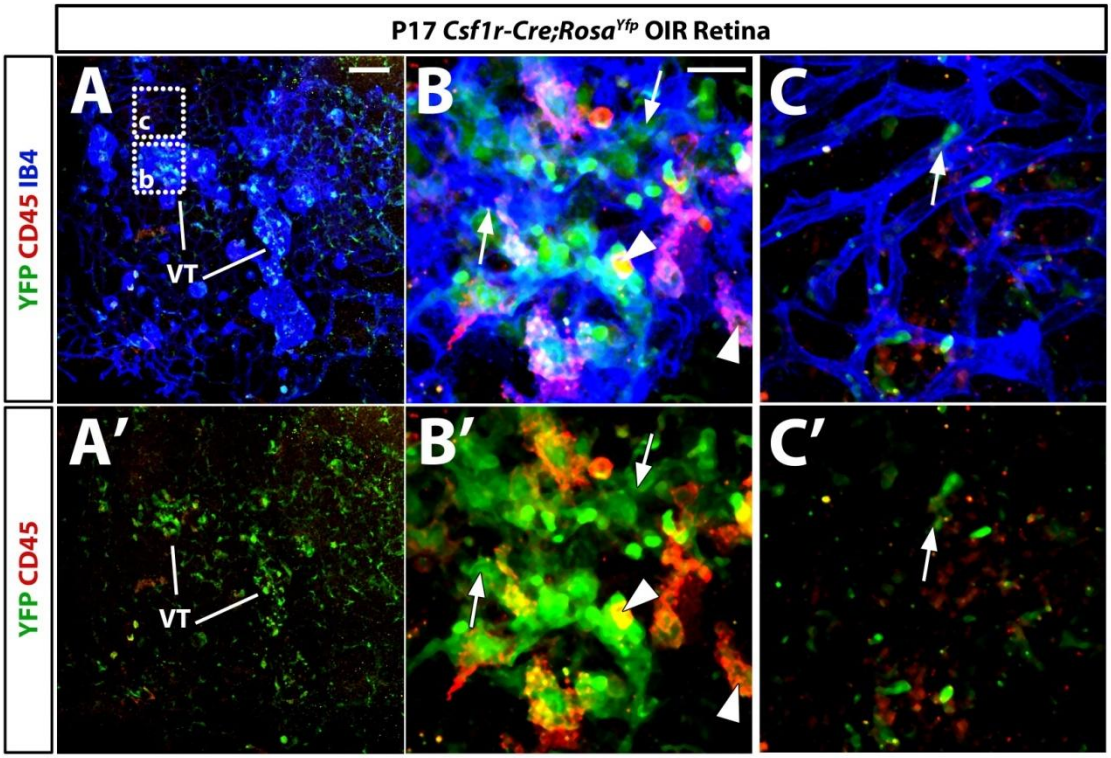

Figure 5.12. *Csf1r-Cre;Rosa*^{Yfp}-targeted cells contribute to pathological angiogenesis.

P17 *Csf1r-Cre;Rosa*^{Yfp} retinas with pathological angiogenesis due to OIR were wholemount labelled for YFP, IB4 and CD45. High magnification of the indicated boxed areas in **(A)** are shown in **(B,C)**. The YFP and CD45 channels of **(A-C)** are shown in **(A'-C')**. Arrows highlight YFP^{+} ECs and arrowheads *Cre*-targeted macrophages within the neovascular tufts (VTs). Scale bars: 100 µm **(A)**, 20 µm **(B)**.

5.2.10 *Csf1r-Cre*-labelled ECs in the neovascular tufts caused by OIR are derived from recruited vascular precursors, not proliferating ECs

The increased number of YFP^+ ECs within the vascular tufts could be caused either by enhanced proliferation of YFP^+ ECs within the neovascular lesions or by an increased recruitment of YFP^+ cells into the vascular tufts. To distinguish these possibilities, I first measured endothelial proliferation by injecting pups with bromodeoxyuridine (BrdU) each day from P13 to P16, i.e. for 4 days after their return from hyperoxia to normoxia (see **2.2.2.6**). Immunostaining of P17 retinas for BrdU revealed moderate levels of proliferation throughout the retinal endothelium. Intriguingly, the amount of $BrdU^+$ cells did not appear to be higher within the vascular tufts than in the healthy-looking vessels outside the lesion, even though they contained a higher number of YFP^+ ECs. This result was surprising, because excessive endothelial proliferation in response to VEGF-A secreted from myeloid cells and astrocytes was previously suggested to be responsible for vascular tuft formation in OIR (Naug et al., 2000). Even more surprising, most *Csf1r-Cre;Rosa*^{Yfp}-labelled ECs appeared to be $BrdU^-$ (arrows, **Figure 5.13B'**,**B''**), suggesting that they had not arisen from proliferating ECs. Together, these results suggest that the bulk of ECs in OIR-induced vascular tufts may be derived from recruited vascular progenitors rather than local EC proliferation. Nevertheless, further quantitative experiments are required to validate this hypothesis (see **Chapter 6**).

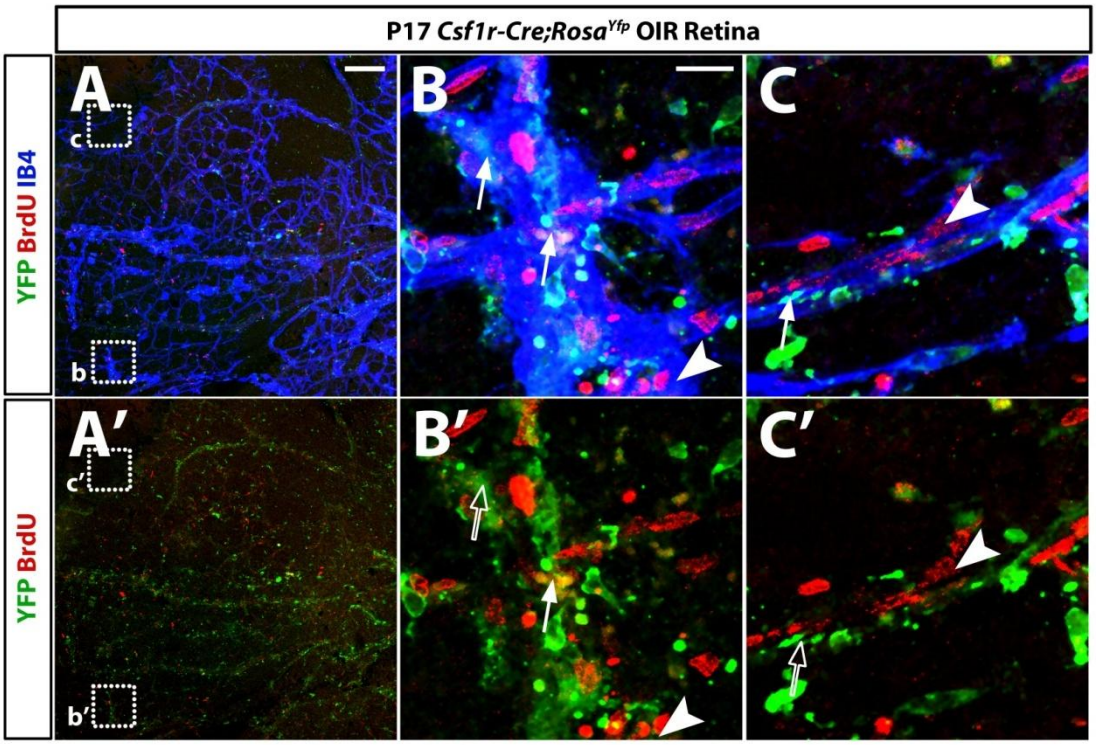

Figure 5.13. YFP$^+$ ECs in neovascular tufts are not proliferating.

P17 *Csf1r-Cre;Rosa^{Yfp}* retinas with neovascular tufts due to OIR were wholemount labelled for YFP, IB4 and BrdU. High magnification of the indicated boxed areas indicated in **(A)** are shown in **(B,C)**. The YFP and BrdU channels of **(A-C)** are show in **(A'-C')**. Arrows highlight YFP$^+$BrdU$^-$ ECs and arrowheads indicate YFP$^-$BrdU$^+$ ECs. Scale bars: 100 µm **(A)**, 20 µm **(B)**.

5.2.11 *Csf1r-Cre*-targeted ECs and cells resembling vascular precursors emerge in the yolk sac

Having established that *Csf1r-Cre;Rosa*^{Yfp} labels a putative vascular progenitor population in embryonic and postnatal mice, I next investigated the origin of these cells within the embryo. The first ECs of the mouse conceptus arise in the yolk sac at E7.5 and are derived from angioblasts, which are generated in the mesoderm of the posterior primitive streak (reviewed in Ferkowicz and Yoder, 2005) and migrate into the yolk sac to enable vasculogenesis (Risau and Flamme, 1995) (see **1.1.2.1**). To address whether *Csf1r-Cre* targets these initial ECs, I stained E7.5 *Csf1r-Cre;Rosa*^{Yfp} embryos and their extra-embryonic membranes for YFP and the earliest known endothelial marker VEGFR2 (Flamme et al., 1995). However, this analysis failed to detect any YFP^{+}VEGFR2^{+} cells in the primitive vascular plexus of the yolk sac (clear arrow, **Figure 5.14A,B**), which suggests that *Csf1r-Cre;Rosa*^{Yfp} does not label the earliest angioblasts; instead, I observed that giant trophoblast cells (GTCs) were labelled by *Csf1r-Cre;Rosa*^{Yfp} (curved arrow, **Figure 5.14B**) at this stage, consistent with their known expression of CSF1R (Jokhi et al., 1993, Ovchinnikov et al., 2010, Ide et al., 2002).

In addition to being the site where the first ECs differentiate and aggregate into blood vessels, the yolk sac is also the tissue where the first blood cells are generated (see **1.3**). This first wave of haematopoiesis occurs around E7.5 and mainly gives rise to primitive erythroid cells (Yoder et al., 1997a,), whereas from E8.25 onwards a subset of macrophages arises within the yolk sac, which colonise the embryo and give rise to the tissue-resident macrophages (Schulz et al., 2012) (see **1.3.3.2**). In agreement with CSF1R's role in myeloid differentiation, I did not detect any single YFP^{+} cells in the yolk sac at E7.5 (**Figure 5.14A,B),** whilst at E8.5 the VEGFR2^{+} vessels within the C*sf1r-Cre;Rosa*^{Yfp} yolk sacs contained many round YFP^{+} cells (arrowhead, **Figure 5.14D**,**E**). These cells presumably constituted the myeloid progenitors (see **1.3.1**); however some of these cells might have also comprised the earliest circulating vascular precursors. In agreement with the fact that vascular precursors are present in the yolk sac at this stage, *Csf1r-Cre;Rosa*^{Yfp} also labelled a small number of cells that resembled ECs due to their flat morphology, and these cells appeared less bright for YFP (arrow, **Figure 5.14D**,**E**), similar to what was observed for YFP^{+} ECs in the hindbrain (e.g. **Figure 5.1**). By E9.5 the number

of YFP$^+$ round cells within the yolk sac vasculature had substantially increased (arrowhead, **Figure 5.14G**). In addition and consistent with the notion that vascular precursors are emerging within the yolk sac at this stage, the number of ECs had also increased (arrow, **Figure 5.14G)**.

To analyse whether all of the YFP$^+$ round cells within the vasculature of *Csf1r-Cre;Rosa^{Yfp}* yolk sacs constituted early yolk-sac derived macrophages or whether they in fact also comprised embryonic endothelial progenitors, I repeated my analysis in *Csf1r-Cre;Rosa^{Yfp}* mice on a *Pu.1*-null background, which lack cells of the myeloid lineage (see **Figure 5.15**). Analysis of 8.5 *Csf1r-Cre;Rosa^{Yfp};Pu.1$^{-/-}$* yolk sacs labelled for YFP and VEGFR2 revealed that the number of small round YFP$^+$ cells was reduced in these mutants, presumably due to the lack of myeloid progenitors in the yolk sac. Nevertheless, a small number of round YFP$^+$ cells persisted in the *Pu.1$^{-/-}$* mutant yolk sacs (arrowhead, **Figure 5.15B**) and had increased by E9.5 (arrowhead, **Figure 5.15D**). In addition, I observed a similar number of flatter YFP^{dim} cells within the endothelium of *Pu.1$^{-/-}$* embryos compared to *Pu.1$^{+/+}$* yolk sacs, which again agreed with my analysis in the *Csf1r-Cre;Rosa^{Yfp};Pu.1$^{-/-}$* E11.5 hindbrains (arrows, **Figure 5.15D**).

To determine whether the YFP$^+$ round cells in *Csf1r-Cre;Rosa^{Yfp};Pu.1$^{-/-}$* yolk sacs expressed markers associated with a precursor identity, I labelled E9.5 *Csf1r-Cre;Rosa^{Yfp};Pu.1$^{-/-}$* yolk sacs for YFP and KIT, which has been published as a marker of EPCs (e.g. Suzuki et al., 2014, Fang et al., 2012, Dentelli et al., 2007). This revealed that all round cells were indeed KIT$^+$ (arrowhead, **Figure 5.15E,F**), indicating that they might constitute vascular precursors. To investigate this hypothesis further, I FACS-sorted E9.0 *Csf1r-Cre;Rosa^{Yfp}* yolk sacs labelled for KIT, CD31 (to distinguish YFP$^+$ ECs), and CD45 to label haematopoietic cells (**Figure 5.15G**). This revealed that the majority (75%) of all YFP$^+$ cells was CD45$^+$, which agreed with the idea that *Csf1r-Cre;Rosa^{Yfp}* labels the myeloid cells emerging within the yolk sac. Out of the remaining CD45$^-$ cells, a subset (5% of total YFP$^+$ cells) was CD31$^+$KIT$^-$ and thus presumably constituted the bona fide ECs, as these cells do not express KIT (see **Figure 5.15)**. Intriguingly, *Csf1r-Cre* also labelled a population of KIT$^+$CD31$^+$ cells (~18%), which most likely constituted the vascular precursors and the round YFP$^+$ cells that persisted in the *Pu.1*-null mice. Nevertheless, as a study

suggested that some immature macrophages are still generated in the yolk sac on a *Pu.1*-null background (Olson et al., 1995, Lichanska et al., 1999) and these cells might not express CD45 but KIT, further experiments should analyse whether these cells express other early myeloid genes such as the gene encoding myeloperoxidase (Olson et al., 1995).

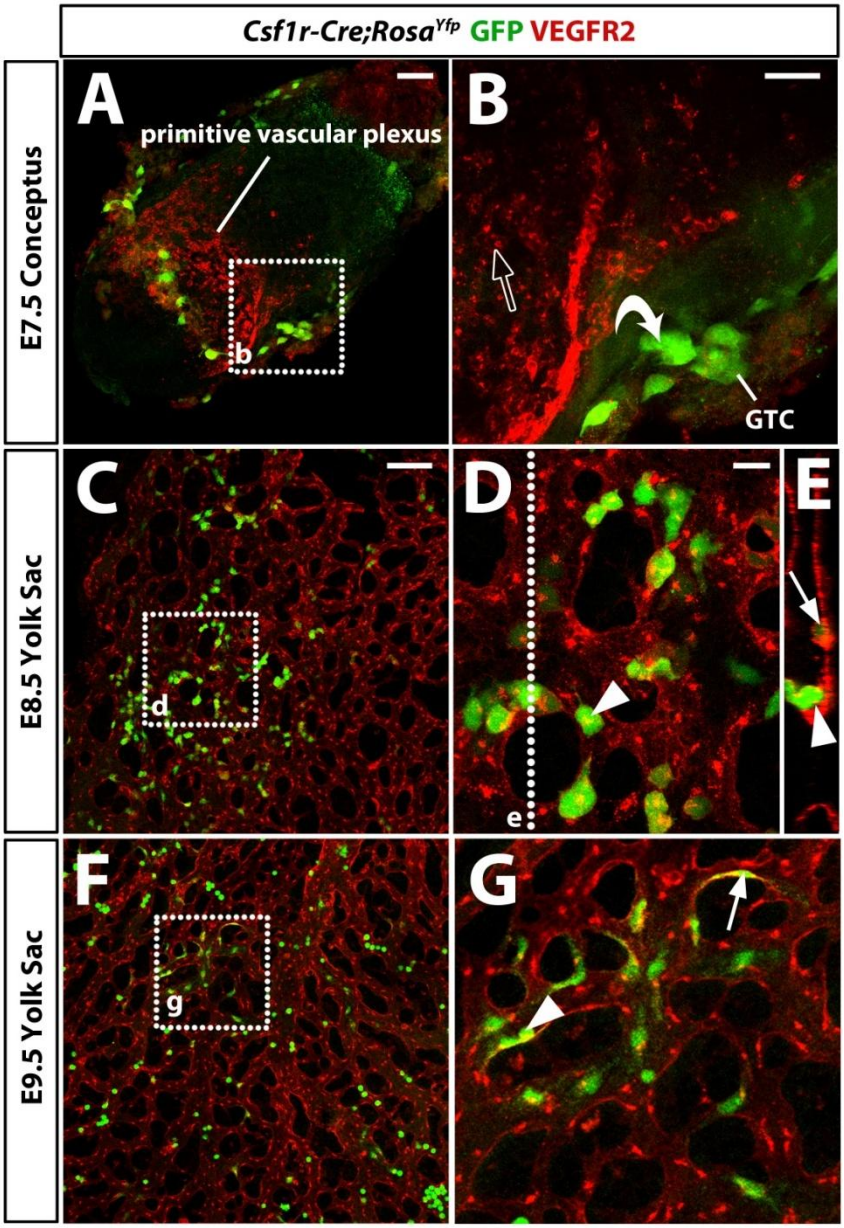

Figure 5.14. *Csf1r-Cre;Rosa*^{Yfp} labels ECs in the yolk sac.

E7.5 **(A,B)**, E8.5 **(C-E)** and E9.5 **(F-G)** *Csf1r-Cre;Rosa*^{Yfp} yolk sacs were wholemount immunolabelled for YFP and VEGFR2. High magnification of boxed areas indicated in **(A,C,F)** are shown in **(B,D,G)**, respectively. A cross-section through the confocal z stack projection in **(D)** is shown in **(E)**. The dotted line **(e)** indicates the level of cross-section. The clear arrow highlights the lack of YFP expression in ECs and the curved arrow *Csf1r-Cre;Rosa*^{Yfp}-labelled giant trophoblast cells (GTCs). Arrowheads highlight YFP^{+}, round cells and solid arrows YFP^{dim} flattened cells within the yolk sac vasculature. Scale bars: 100 µm **(A,C)**, 50 µm **(B)**, 20 µm **(D)**.

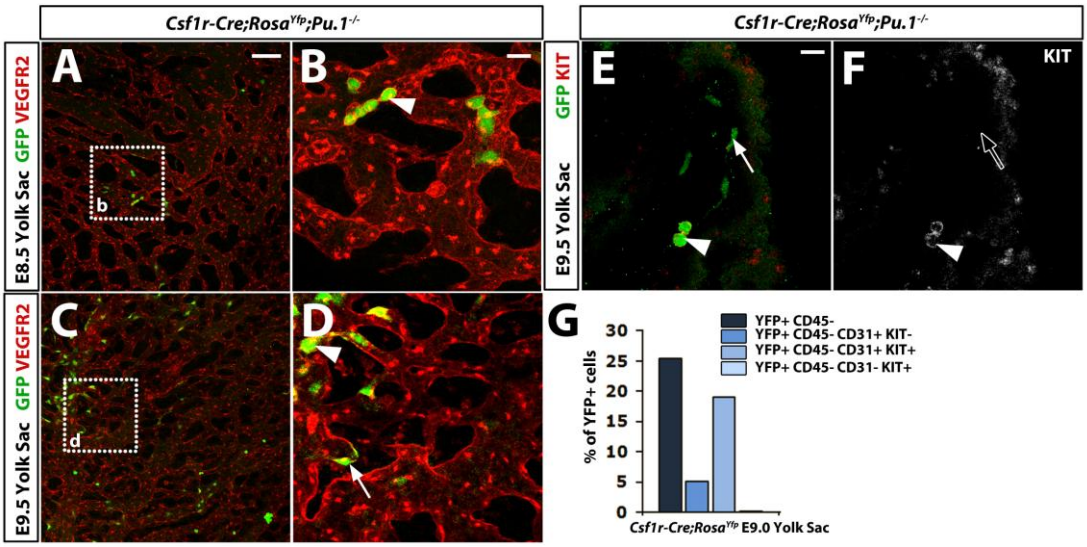

Figure 5.15. *Csf1r-Cre;Rosa^{Yfp}* labels non myeloid-derived cells and ECs in yolk sac.

E8.5 and E9.5 *Csf1r-Cre;Rosa^{Yfp};Pu.1$^{-/-}$* yolk sacs were immunolabelled for YFP and VEGFR2 or KIT. High magnification of boxed areas indicated in **(A,C)** are shown in **(B,D)**, respectively. A KIT single channel of **(E)** is shown in **(F)**. Arrowheads highlight YFP^{+}KIT^{+} round cells and solid arrows YFP^{dim} flattened cells within the yolk sac vasculature. The clear arrow indicates a lack of KIT expression in a YFP^{dim} cell. FACS analysis of a E9.0 *Csf1r-Cre;Rosa^{Yfp}* yolk sac labelled for CD45, CD31 and KIT **(G)**. Scale bars: 100 µm **(A)**, 20 µm **(B,E)**.

5.2.12 *Csf1r-Cre*-targeted cells, which are not macrophage-derived, also contribute to lymphatic endothelium

The lymphatic vasculature is a unidirectional network of blind-ended vessels, which absorbs excess interstitial fluid from the periphery and returns it to the veins, thus maintaining interstitial fluid homeostasis (reviewed in Schulte-Merker et al., 2011). The lymphatic system also provides a conduit for patrolling lymphatic cells and therefore presents an important component of the immune system (reviewed in Liao and Padera, 2013). Similar to blood vessels, lymphatic vessels consist of a specialised endothelial layer that is covered by mural cells. The lymphatic ECs resemble blood vessel ECs in their morphology and apical-basal polarity; however, they differ in their specialised junctions, which allow the pressure-dependent absorption of the interstitial fluid (Leak and Burke, 1966).

The lymphatic vasculature is first formed when venous cells acquire lymphatic properties and sprout from the cardinal vein (Srinivasan et al., 2007). The migrating lymphatic ECs then coalesce in areas, where VEGF-C is expressed by the mesenchyme, and form lymph sacs (Karkkainen et al., 2004). This process occurs at several positions along the anterior–posterior axis and results in the formation of the jugular, medial, and axial lymph sacs. Lymphatic vessels then sprout from the lymph sacs to give rise to the lymphatic vascular network (**Figure 5.16A**). The process of lymphatic sprouting, lymphangiogenesis, has many similarities to angiogenesis (reviewed in Adams and Alitalo, 2007). Thus, in both cases vessels led by tip and then stalk cells sprout from pre-existing ones (Xu et al., 2010, Gerhardt et al., 2003, Fantin et al., 2013a). Furthermore, in comparison to blood vessels, bone marrow-derived lymphatic EPCs are thought to be involved in pathological lymph vessel growth (Lee et al., 2010, Kerjaschki et al., 2006). In addition, a recent publication has suggested that KIT^+ cells derived from the hemogenic endothelium contribute to the development of the mesenteric lymphatic vessels (Stanczuk et al., 2015). Nevertheless, a study has reported that myeloid cells also contribute to the lymphatic endothelium during tumour lymphangiogenesis (Zumsteg et al., 2009).

To investigate whether *Csf1r-Cre;Rosa*^{Yfp}-labelled cells contribute to lymphatic vascular development, I sectioned through the jugular lymph sacs (JLS) of E15.5 *Csf1r-Cre;Rosa*^{Yfp} embryos on a wildtype and *Pu.1*-null background, and

labelled them for YFP, IB4 and the lymphatic/venous marker NRP2 (Lin et al., 2010, Xu et al., 2010, Yuan et al., 2002). In the *Pu.1*$^{+/+}$ sections, YFP expression was observed in cells within the lymph (asterisk, **Figure 5.16C-D'**); additionally, YFP was also expressed within the lymphatic endothelium of the JLS as well as the superficial lymphatics (SLs) (arrow, **Figure 5.16D,D'**). In *Pu.1*$^{-/-}$ mice, no YFP^{+} lymph was apparent (delta symbol, **Figure 5.16E-F'**); nevertheless, *Csf1r-Cre;Rosa*^{Yfp}-targeting of the lymphatic endothelium persisted (arrows, **Figure 5.16E-F'**).

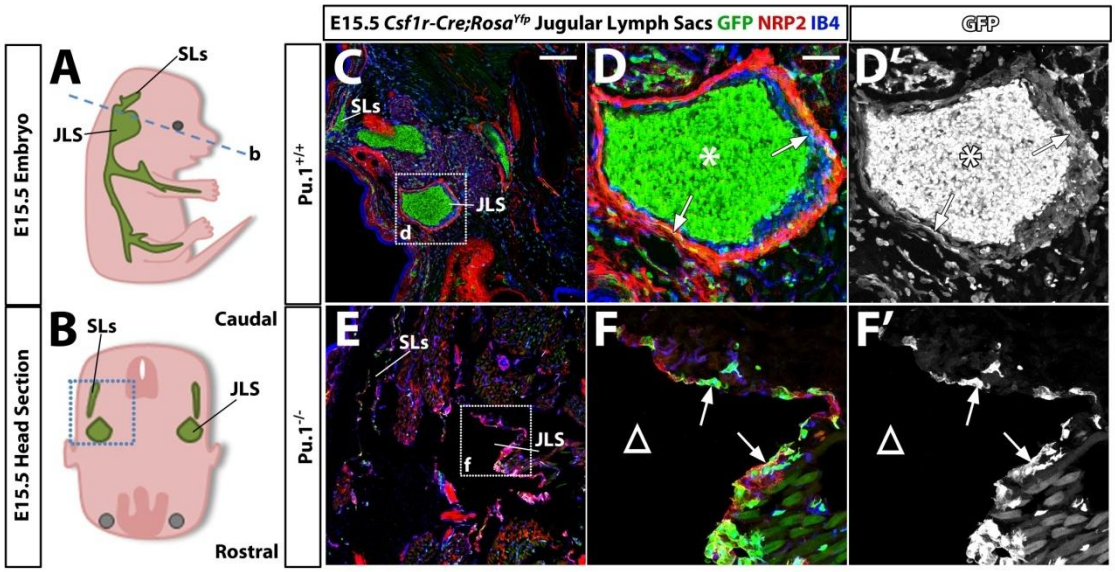

Figure 5.16. *Csf1r-Cre*-targeted cells, which are not macrophage-derived, contribute to jugular lymph sac endothelium.

Schematic representation of the superficial lymphatics (SLs) and jugular lymph sac (JLS) (green) **(A)** and a transverse section through the lymphatics within the head **(B)** in an E15.5 embryo. **(C-F)** Transverse sections of E15.5 *Csf1r-Cre;Rosa*^{Yfp} embryos on a *Pu.1*$^{+/+}$ **(C-D')** or *Pu.1*$^{-/-}$ **(E-F')** background at the level of the JLSs were labelled for YFP, the lymph/vein marker NRP2 and IB4. High magnification of boxed areas in **(C,E)** are shown in **(D,E)** and as a GFP single channel in **(D',F')**. Arrows indicate YFP^{+} endothelium within the JLS, the asterisk the *Cre*-targeted lymph and the delta the absence of lymph targeting on a *Pu.1*$^{-/-}$ background. Scale bars: 200 µm **(C)**, 50 µm **(D)**.

I next investigated whether *Csf1r-Cre;Rosa*^{Yfp}-targeting of ECs is also present in other lymphatic beds by labelling E17.5 skin from *Csf1r-Cre;Rosa*^{Yfp}*;Pu.1*$^{-/-}$ embryos for YFP, NRP2 and the venous/capillary marker endomucin (Liu et al., 2001, Kuhn et al., 2002). As observed for the JLSs, YFP expression could be found in the lymphatic endothelium of *Pu.1*$^{-/-}$ dermal lymphatics (arrows, **Figure 5.17A,B,B'**). Interestingly, the targeting of the endothelium appeared to be higher in the E17.5 skin than the E15.5 JLS, suggesting that EC incorporation continues throughout lymphangiogenesis, as observed in the hindbrain and retina for blood vascular angiogenesis.

I next investigated whether CSF1R was expressed by the lymphatic ECs. Staining of E17.5 *Csf1r-eGFP* skin for GFP, NRP2 and endomucin showed that CSF1R was widely expressed by macrophages (defined as CSF1R^{+} single cells), but not by lymphatic ECs (arrowhead, clear arrows, respectively, **Figure 5.17C,D,D'**). Whilst I have not yet conducted a thorough time course, this finding raised the possibility that a *Csf1r-Cre*-targeted vascular precursor contributes to lymphangiogenesis, similar to what I observed for blood vascular angiogenesis.

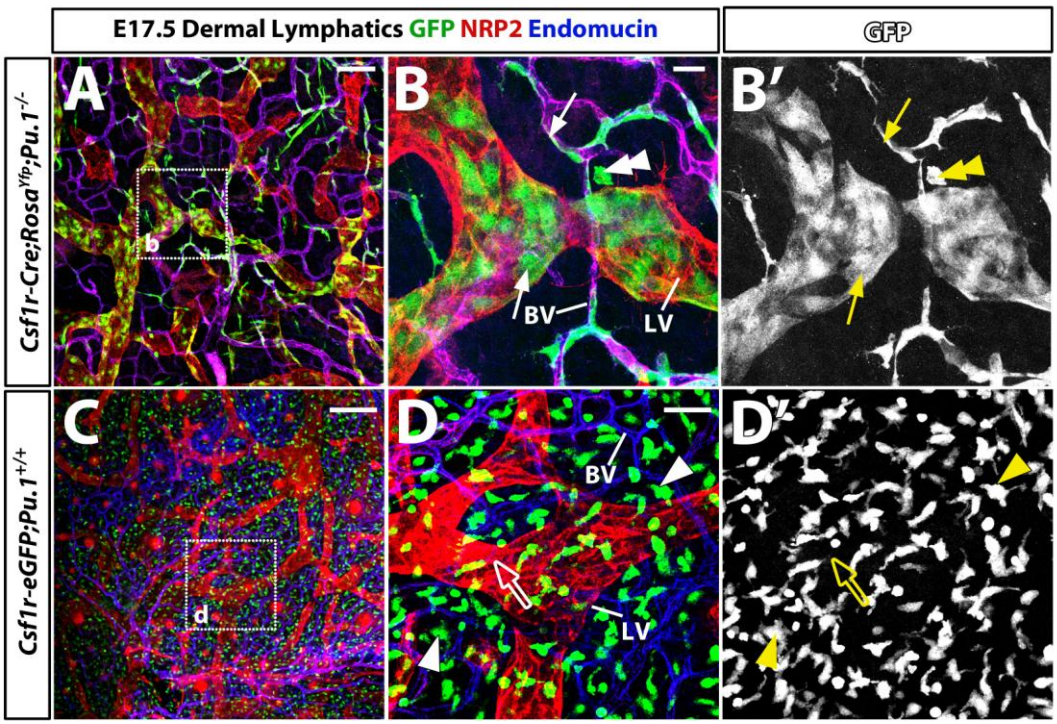

Figure 5.17. *Csf1r-Cre;Rosa*^{Yfp}-targeted ECs of non-macrophage origin contribute to lymphatic endothelium in the skin.

E17.5 skin from *Csf1r-Cre;Rosa*^{Yfp} mice on a macrophage-deficient *Pu.1*$^{-/-}$ background **(A-B')** and from *Csf1r-eGFP* mice **(C-D')** was labelled for YFP/GFP, NRP2 and the vascular marker endomucin. High magnification of boxed areas in **(A,C)** are shown in **(B,D)** and as a single YFP channel in **(C',D')**. The solid arrows indicate YFP^{+} ECs and the double arrow a rare single, YFP^{+} cells in the tissue, possibly macrophage-like despite the *Pu.1* deletion. The arrowheads highlight examples of GFP^{+} macrophages and the clear arrows GFP^{-} endothelium. L: Lymphatic vessel, BV: Blood vessel. Scale bars: 100 µm **(A)**, 200 µm **(B)**, 20 µm **(C)**, 50 µm **(D)**.

5.2.13 *Csf1r-Cre*-mediated cell death induction causes embryonic lethality by E10.5

To understand the significance of *Csf1r-Cre*-targeted vascular precursors for embryonic vascular development, I introduced the *Csf1r-Cre* transgene into mice with a floxed $Rosa^{Dta}$ knockin allele (Ivanova et al., 2005). Analogous to the $Rosa^{Yfp}$ reporter, this allele expresses the diphtheria toxin fragment A (DTA) only after *Cre*-mediated stop cassette excision, which results in cell death and thus allows *in vivo* *Cre*-specific cell ablation (Breitman et al., 1990). By generating embryos, which expressed the $Rosa^{Dta}$ allele under the control of the *Csf1r-Cre* transgene, I was therefore hoping to observe vascular development in mice lacking the myeloid lineage, as well as the *Csf1r-Cre*-labelled vascular precursor cells.

As the $Rosa^{Dta}$ allele contains a *Yfp* allele, which is constitutively expressed, I was unable to validate the *Csf1r-Cre;*$Rosa^{Dta}$ targeting efficiency. Nevertheless, analysis of the number of *Csf1r-Cre;*$Rosa^{Dta}$ embryos in litters from $Rosa^{Dta}$ females crossed to *Csf1r-Cre* males revealed that no mutant embryos survived past E10.5, and already at E9.5, the mutants were noticeably smaller and developmentally delayed compared to their wildtype littermates (**Figure 5.18A,C,E**). This early embryonic lethality was unexpected, as the number of ECs labelled by *Csf1r-Cre;*$Rosa^{Yfp}$ is fairly low at this stage (see **Figure 5.18**). Furthermore, deletion of the myeloid lineage is known to only result in death perinatally (McKercher et al., 1996). Instead, the early lethality suggested placental insufficiency. In agreement, CSF1R is known to be expressed by GTCs (giant trophoblast cells), which are crucial for embryo implantation and post-implantation placental modulation (Jokhi et al., 1993, Ovchinnikov et al., 2010). It would therefore be of interest to analyse the placenta of these mutants.

To understand whether vascular development was affected in these mutants, I could therefore only study early vascular development up to E9.5. Thus, I immunolabelled the embryos and yolk sacs from E9.5 *Csf1r-Cre;*$Rosa^{Dta}$ mutants and their wildtype littermates for VEGFR2. In wildtype embryos and yolk sacs, VEGFR2 staining revealed an extensive network of vessels. In the mutants, vessels also formed in the embryo and yolk sac; however, they seemed much less remodelled. This vascular phenotype varied in its severity. Thus, one mutant

displayed a vascular phenotype that was likely due to a developmental delay of 1d, and the vasculature in one mutant yolk sac was abnormal resembling a sheet of ECs rather than a network of vessels (**Figure 5.18F**). Thus, I could not obtain any evidence that the *Csf1r-Cre*-targeted vascular precursors are important for early angiogenesis.

Future work will be needed to establish the significance of losing the vascular precursor for hindbrain and retinal angiogenesis or lymphangiogenesis. As a recent publication showed that CSF1R expression in the GTCs is achieved by a promoter region distinct from the one driving myeloid CSF1R expression (Ovchinnikov et al., 2010), it might be possible to generate a *Cre* driver that targets vascular precursors independently of GTC. This line could then be used to investigate whether embryonic development is affected in mice where DTA is expressed under the control of the *Csf1r* promoter without the trophoblast-specific sequence.

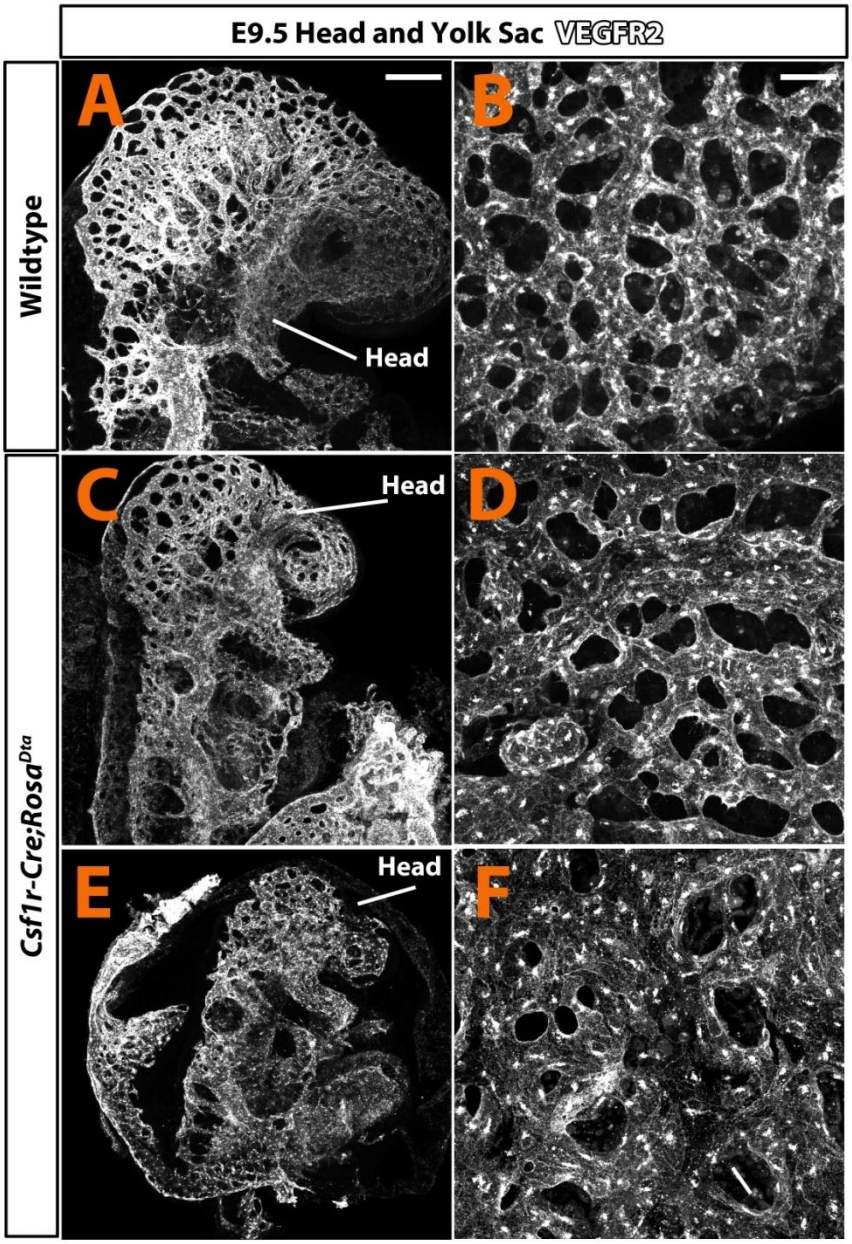

Figure 5.18. Diphtheria toxin A-mediated deletion of cells targeted by *Csf1r-Cre* results in substantial developmental delay at E9.5 and embryonic lethality by E10.5.

E9.5 *Csf1r-Cre;Rosa*^{Dta} and wildtype control embryos **(A,C,E)** and their yolk sacs **(B,D,F)** were wholemount immunolabelled for VEGFR2. Note the developmental delay in *Csf1r-Cre;Rosa*^{Dta} mutants. Scale bars: 200 µm **(A)**, 50 µm **(B)**.

5.3 Discussion

Ever since the first description of EPCs in the peripheral human blood by Asahara *et al*., there has been great controversy regarding the origin and function of these cells (Asahara et al., 1997). Some studies have postulated that cells from several sources such as the bone marrow or endothelium can give rise to circulating vascular precursor cells that contribute to blood vessel growth or repair *in vivo* (Quirici et al., 2001, Peichev et al., 2000, Gehling et al., 2000). Other studies have dismissed the notion of EPCs completely, suggesting that prior *in vitro* findings are, for instance, experimental artefacts with no biological relevance (Rohde et al., 2007, Prokopi et al., 2009), or that the pro-angiogenic cells observed *in vivo* are in fact pro-angiogenic monocytes (e.g. Rohde et al., 2006, Rehman et al., 2003). It has proven difficult to resolve the EPC controversy to a large part, because of the lack of a definite marker of such cells (reviewed in Timmermans et al., 2009). Accordingly, many studies aiming to demonstrate the nature or function of these cells have differed in their isolation procedures and molecular definition. This has greatly impaired the advancement of this field and, therefore, there is currently no consensus regarding the role or even existence of EPCs.

I may have provided evidence for the existence of a population of vascular progenitors with the help of genetic tools, independently of identifying a definite EPC marker. Thus by analysing the lineage trace of the *Csf1r-Cre* transgene, I identified a subpopulation of ECs in both blood and lymphatic vessels that is likely derived from *Csf1r-Cre*-labelled vascular precursors. Thus, I demonstrated that *Csf1r-Cre* labels cell populations that share molecular and morphological characteristics with cells previously referred to as EPCs or vascular progenitors, e.g. *Csf1r-Cre*-labelled cells in the blood and bone marrow that are $KIT^{+}CD45^{-}$, and *Csf1r-Cre*-labelled spindle-shaped cells in the retina that are $GFAP^{-}$ (see below, and **Figures 5.5**, **5.11** and **5.12)**. In addition, having excluded that *Csf1r-Cre*-mediated lineage tracing of a subset of ECs with the $Rosa^{Yfp}$ is caused by endothelial *Csf1r* or ectopic CRE expression, or that is caused by unspecific spontaneous $Rosa^{Yfp}$ recombination (see **Figures 5.6-5.8**), the most likely explanation for the endothelial targeting with *Csf1r-Cre* is that these cells are derived from *Csf1r-Cre*-labelled

vascular progenitors. Below, I will discuss the evidence for this suggestion in more detail.

My analysis revealed that *Csf1r-Cre*-labelled ECs persist on a macrophage-deficient background (see **Figure 5.9**), implying that these progenitors are not of myeloid origin, at least during embryonic angiogenesis. This was surprising, as the only cells targeted by *Csf1r-Cre* and linked to EC differentiation described to date are macrophages (Schmeisser et al., 2001). For example, macrophages can adopt an endothelial morphology and contribute to tumour vascularisation (Chen et al., 2009a, Scavelli et al., 2008). Nevertheless, my observation that *Csf1r-Cre* labels a non-myeloid progenitor population during developmental angiogenesis agrees with other studies, which have, in principle, shown that *Csf1r* is not exclusively expressed by cells of the myeloid lineage (Sawada et al., 1993, Luo et al., 2013). Thus, it was recently shown that the *Csf1r* gene is expressed by astrocytes as well as adult neurons, albeit only at mRNA level (Luo et al., 2013). Whilst I have excluded that the ECs lineage traced by *Csf1r-Cre* are of macrophage origin during embryonic angiogenesis, I would still need to examine whether the *Csf1r-Cre*-labelled ECs during pathological angiogenesis are also not myeloid-derived, for example, by showing that other macrophage-specific *Cre*-lines such as *LysM-Cre* (Clausen et al., 1999) do not lineage trace ECs in neoangiogenic vessel beds.

My analysis of CSF1R expression has thus far not detected any endothelial *Csf1r* expression in any of the developing tissues examined (e.g. **Figures 5.6, 5.15**). Accordingly, these experiments imply the existence of *Csf1r-Cre*-labelled vascular progenitors that at some point express *Csf1r*. These vascular progenitors appear to also exist postnatally, because I observed YFP^+ retinal ECs after the postnatal induction of *Csf1r-Cre*^{ERT} expression with tamoxifen (see **Figure 5.10**). Moreover, my preliminary analysis (n= 1) identified *Csf1r* expression in an EPC-like $CD31^+CD45^-KIT^+YFP^+$ cell population isolated from the P10 *Csf1r-Cre;Rosa*^{Yfp} brain (data not shown). Together, these experiments suggest that *Csf1r* is expressed by cells that serve as vascular precursors, but they would have to be repeated to derive a firm conclusion.

Whether CSF1R has a functional role in *Csf1r-Cre*-labelled vascular progenitors and/or their offspring is presently not clear. To address this possibility, one can attempt to draw inferences from the EPC literature; however, there is currently much controversy on this topic. On the one hand, some studies have suggested that CSF1 signalling through CSF1R induces EPC mobilisation, because CSF1 promotes tumour vascularisation (Eubank et al., 2003, Okazaki et al., 2005). On the other hand, this pro-angiogenic effect may in fact be caused by CSF1 acting on pro-angiogenic monocytes, but this possibility has not yet been addressed.

Alternatively, CSF1R signalling might not play a functional role in EPCs at all, in analogy to the gene encoding the myelination protein P0, which is expressed in mesenchymal stem cells (Hagedorn et al., 1999) and vascular progenitors (Kubota et al., 2011), albeit only at mRNA level. Generally speaking, a gene may be part of a transcriptional programme consisting of some genes that are functionally required and therefore translated into protein, as well as other genes that are not required and whose translation may be actively suppressed, for example by inhibitory RNA. The dispensable expression of these genes might have persisted throughout evolution when their protein products are not harmful. Alternatively, if the protein products are of an evolutionary disadvantage, mRNA expression from these genes might have been able to persist because means have evolved to repress their translation. To investigate these hypotheses, future studies could, for instance, compare *Csf1r* mRNA and CSF1R protein expression in *Csf1r-Cre*-tagged progenitors after FACS sorting *Pu.1*-null embryos to obtain $YFP^{+}CD45^{-}KIT^{+}$ non-endothelial (i.e. $CD31^{-}$) cells.

The finding that *Csf1r-Cre* labels a subset of ECs of non-myeloid origin raises the question of how reliable the *Csf1r-Cre* transgene is as a tool to distinguish roles for floxed target genes in macrophages versus ECs. For example, our group used this transgene to demonstrate that macrophage-derived NRP1 was not required for developmental angiogenesis, whilst endothelial NRP1 was essential (Fantin et al., 2013a) (see **Chapter 3**). Despite *Csf1r-Cre* targeting most macrophages, it targets only a subset of ECs at the relevant developmental stages (see **Chapter 3**). In contrast, deletion of endothelial NRP1 using the *Tie2-Cre* transgene, which targets most ECs and tissue macrophages (Kisanuki et al., 2001), recapitulated the severe

vascular defects displayed by *Nrp1*-null embryos (Fantin et al., 2013a, Kawasaki et al., 1999). Thus, the comparative analysis of *Csf1r-Cre;Nrp1*$^{fl/-}$ and *Tie2-Cre;Nrp1*$^{fl/-}$ embryos suggested an exclusive role of NRP1 in ECs rather than in macrophages during angiogenesis.

Other studies have used the *Csf1r-Cre* transgene to investigate whether VEGFR1 is required by macrophages to regulate retinal vascularisation (Stefater et al., 2011). Thus at P18, *Csf1r-Cre;Flt*$^{fl/+}$ mice demonstrate a higher vessel density in the deeper retinal plexi than their wildtype littermates. However, in my preliminary analysis (n= 1), I found that at P21, *Csf1r-Cre* extensively targeted ECs in all three retinal plexi, including the deep plexus (data not shown). Accordingly, if *Csf1r-Cre* were to delete *Flt* in the retinal endothelium in addition to macrophages, then it could not be excluded that an endothelial deletion of *Flt* was contributing or even responsible for the *Csf1r-Cre;Flt*$^{fl/+}$ phenotype reported by Stefater *et al.* (2011). In fact, VEGFR1 is known to play a role in endothelial VEGF-A signalling (Gille et al., 2001, Kanno et al., 2000, Autiero et al., 2003b).

Given the widespread use of the *Csf1r-Cre* transgene as a tool that is meant to selectively target macrophages at postnatal stages, it is surprising that the endothelial targeting by this transgene has not been reported in previous studies (e.g. Stefater et al., 2011, Gordon et al., 2010, Deng et al., 2010). One explanation might be that other studies did not notice the endothelial targeting of this transgene, because of the type of analysis used, e.g. FACS of blood cells (Deng et al., 2010). It is also conceivable that others using immunostaining to visualise YFP expression were not able to discern labelled ECs from vessel-associated macrophages (e.g. Stefater et al., 2011).

An alternative explanation why endothelial targeting with *Csf1r-Cre* was previously missed might be that the reporter transgenes used in prior studies are less readily expressed in ECs than the *Rosa*^{Yfp} allele, which I have used in my experiments. Thus, other studies investigating *Csf1r-Cre*-targeting in the retina and lymphatics have used the *Z/EG* reporter allele (Novak et al., 2000, Stefater et al., 2011, Gordon et al., 2010). As *Rosa*^{Yfp} is a knockin allele into the constitutively expressed *Rosa26* locus (Soriano, 1999) (see **2.2.1.4**), it is possible that the *Rosa26*

locus is more accessible to CRE recombinase in ECs than the *Z/EG* transgene, whose integration site into the genome is not well defined (Novak et al., 2000). For example, in zebrafish the insertion of transgenes into different loci within the genome resulted in varying levels of transgene activation (Feng et al., 2001). To test the hypothesis that *Csf1r-Cre*-labelling of endothelium depends of the recombination reporter used, one could directly compare *Z/EG*- and $Rosa^{Yfp}$-mediated labelling with *Csf1r-Cre* and possibly other, well-established endothelial transgenes such as *Tie2-Cre* (Kisanuki et al., 2001).

Another explanation for our observation of EC-targeting, in contrast to reports from other laboratories using this line, is that the *Csf1r-Cre* transgene has been subject to epigenetic drift or is affected by genetic background differences in different host laboratories. Disagreeing with this hypothesis, I observed EC targeting also with freshly imported $Csf1r\text{-}Cre^{ERT}$ mice from the JAX laboratories (see **Figure 5.10**). To address whether EC labelling is somehow facilitated in the $Rosa^{Yfp}$ mice, future work could investigate whether endothelial labelling also occurs in $Csf1r\text{-}Cre^{ERT}$ mice crossed to other, freshly imported reporter mice. However, my preliminary analysis (n= 2) using *Csf1r-Cre* mice crossed to $Rosa^{Tomato}$ mice (Madisen et al., 2010) imported from a lab elsewhere at UCL suggested that this is not the case (data not shown).

My analysis of the $Csf1r\text{-}Cre;Rosa^{Yfp}$ lineage trace in the developing retina identified stellate cells at the vascular front, raising the question, as to whether they are in any way related to the stellate retinal cells described in prior reports. Thus, several studies postulated that spindle-shaped cells contribute to retinal vascular growth by vasculogenesis (Ashton, 1970, Kretzer et al., 1984). However, another study found that these stellate cells did not express the well-established EC and angioblast marker VEGFR2, but instead were positive for the astrocyte marker, PDGFRα (Fruttiger, 2002). Thus, the idea of spindle-shaped angioblasts within the retina was mostly dismissed, and any pro-angiogenic role of spindle-shaped retinal cells may have reflected astrocyte functions in guiding the growing retinal vasculature (Scott et al., 2010, Stenzel et al., 2011).

Nevertheless, a recent paper provided compelling evidence for tissue-resident vascular precursors with a stellate morphology in the murine retina (Kubota et al., 2011). This study used *P0-Cre* lineage tracing to identify stellate cells at the vascular front with the potential to differentiate into ECs *in vitro* and further showed that *P0-Cre*-labelled cells contributed to vessel growth in the retina (Kubota et al., 2011). The *Csf1r-Cre*-labelled cells at the vascular front resembled these *P0-Cre*-labelled retinal EPCs in their position relative to the growing retinal vessels as well as their stellate morphology. In addition, similar to the *P0-Cre*-labelled stellate cells (Kubota et al., 2011), the *Csf1r-Cre*-labelled spindle-shaped cells were negative for the astrocyte marker GFAP, suggesting that they are not astrocytes. However, because GFAP may only label mature astrocytes (Fruttiger, 2002), it would be important to use another astrocyte marker such as PDGFRα (Fruttiger et al., 1996). This analysis was already performed for the *P0-Cre*-labelled cells, which were shown not to express PDGFRα (Kubota et al., 2011).

All together, the fact that *Csf1r-Cre* labels retinal ECs and stellate cells at the vascular front agrees with the idea that *Csf1r-Cre* targets a tissue-resident vascular precursor population similar to the one described by Kubota *et al.* (2011). Further experiments are therefore warranted to demonstrate that *Csf1r-Cre* and *P0-Cre* label the same type of spindle-shaped cells. For example, it could be examined whether there is *Csf1r* expression in *P0-Cre*-labelled vascular precursors and vice versa. In addition, it would be of interest to investigate whether the *Csf1r-Cre*-specific deletion of *Vegfr2* results in a vascular phenotype, because the *P0-Cre*-mediated deletion of *Vegfr2* impaired retinal vascularisation (Kubota et al., 2011). This experiment would provide evidence that *Csf1r-Cre* labels a vascular progenitor similar to *P0-Cre*, as VEGFR2 is not expressed by macrophages or astrocytes.

Previous studies have suggested that adult lymphatic and blood vessel EPCs are derived from a non-hematopoietic progenitor population within the bone marrow, which release endothelial precursors into the blood (Religa et al., 2005, Lee et al., 2010, Case et al., 2007). In addition, several studies demonstrated that circulating KIT^+ cells are able to differentiate into ECs (Sandstedt et al., 2014, Fang et al., 2012, Russell and Brown, 2014). Interestingly, my analysis of the adult bone marrow and blood revealed that *Csf1r-Cre;Rosa*^{Yfp} indeed labelled almost all of the non-

hematopoietic ($CD45^-$) KIT^+ cells in the bone marrow as well as the blood. Moreover, YFP^+ ECs only appeared a few days after tamoxifen induction in the retina of *Csf1r-Cre^{ERT};Rosa^{Yfp}* pups, a finding that is consistent with *Csf1r-Cre*-labelled cells having been recruited from the blood into the retinal vasculature, rather than having been derived from an already tissue-resident precursor. Of course this finding does not exclude that the tissue-resident precursors inactivate the *Csf1r* promoter, but maintain or upregulate *P0* expression once they have left the blood stream to enter tissues. Alternatively, tissue-resident precursors may express *Csf1r*, but are not able to give rise to ECs immediately following tamoxifen administration, because tamoxifen fails to effectively cross the postnatal blood-retinal barrier. In agreement, only a small number of microglia within the retinal parenchyma was targeted by *Csf1r-Cre^{ERT}* after tamoxifen administration (see **Figure 5.10**), even though this transgene enables efficient tamoxifen-mediated recombination in other tissues (e.g. DeFalco et al., 2014, Qian et al., 2011).

Given my observations in the bone marrow and retina, the vascular progenitor pool might thus be comprised of a bone marrow-derived (EPC-like) population, as well as a tissue-resident (stellate) cell population, a notion that would support the plethora of studies that have argued for the existence of either of these two populations (reviewed in Basile and Yoder, 2014). In analogy to the roles of tissue resident-macrophages versus bone marrow-derived monocytes, tissue-resident progenitors might have a role in vascular homeostasis, whilst the bone marrow-derived populations might play a larger role in pathological angiogenesis. It would therefore be interesting to see whether transplantation of the YFP^+ putative bone marrow-derived EPCs from *Csf1r-Cre;Rosa^{Yfp}* mice into wildtype mice with irradiated bone marrow gives rise to YFP^+ ECs in angiogenic vessel beds.

Unfortunately, I was unable to determine, whether *Csf1r-Cre*-labelled vascular precursors are required for developmental vascular growth due to the early lethality of embryos in which the *Csf1r-Cre* lineage has been ablated. Thus, *Csf1r-Cre;Rosa^{Dta}* embryos died by E10.5 (see **Figure 5.18**). This cannot be due to the loss of macrophages, as macrophage-deficient embryos survive until birth (McKercher et al., 1996). In addition, lethality was unlikely to be caused by the loss of ECs, because only few ECs are targeted by *Csf1r-Cre* at this stage (data not shown). Instead, the

early embryonic death is most likely caused by the ablation of trophoblast cells, which express CSF1R (Jokhi et al., 1993) and are critical for normal placentation (reviewed in Hu and Cross, 2010), although I have not formally investigated this possibility.

Given that I observed a moderate contribution of *Csf1r-Cre*-labelled ECs to embryonic blood vessel growth, but higher contribution to perinatal or pathological angiogenesis; it seems likely that these cells play a larger role in scenarios where blood vessels grow more rapidly than is possible by an upregulation of EC proliferation alone. To investigate this hypothesis further, one would need to quantitate the amount of *Csf1r-Cre*-targeted ECs in developmental and pathological vessels, measure the growth rate of the endothelium during angiogenesis and relate it to the proliferation rate. Nevertheless, in support of the notion that proliferation alone is not sufficient for normal angiogenesis to occur, a paper analysing the number of proliferating cells in the retina at P5 demonstrated that a surprisingly small number of ECs were $PHH3^{+}$ (Rocha et al., 2014).

5.4 Summary

In this chapter, using the macrophage-specific transgene *Csf1r-Cre* crossed to the $Rosa^{Yfp}$ reporter, I have provided evidence for the existence of a *Csf1r-Cre*-labelled vascular precursor that contributes to embryonic and postnatal blood vessel growth. Thus, I have demonstrated that *Csf1r-Cre* labels ECs and that this is not caused by endothelial CSF1R or ectopic *Csf1r-Cre* or $Rosa^{Yfp}$ expression. Furthermore, using macrophage-deficient mice, I have revealed that the *Csf1r-Cre*-labelled precursors are not derived from the myeloid lineage; instead, analysis of immunolabelled bone marrow and blood, as well as tamoxifen-inducible *Csf1r-Cre* mice suggested that *Csf1r-Cre* labels an adult bone marrow-derived population, which circulates in the blood. Importantly, *Csf1r-Cre*-targeted ECs were also found to contribute to pathological angiogenesis in the OIR model of retinal neoangiogenesis, suggesting that targeting the *Csf1r-Cre*-labelled precursors may be of therapeutic interest. However, future work is required to demonstrate that isolated *Csf1r-Cre*-targeted vascular precursors are indeed able to differentiate into ECs and required for developmental and pathological vessel growth (see **Chapter 6**).

Chapter 6 FINAL CONCLUSIONS AND FUTURE WORK

6.1 Summary of Conclusions and Final Remarks

During my PhD, my aims have been to understand the role of NRP1 during vascular development and OFT remodelling and to investigate why a lineage trace with the transgene *Csf1r-Cre* labels the vascular endothelium.

My NRP1 research has firstly contributed to two studies by demonstrating that NRP1 expressed by non-ECs is dispensable for developmental angiogenesis and that VEGF-A signalling through NRP1 is required for myocardial vascularisation, respectively. Furthermore, my project examining OFT remodelling uncovered an essential and exclusive role for NRP1 within the endothelium, where it binds to cardiac NCC-derived SEMA3C to enable endoMT and NCC relocalisation for the septation of the OFT.

My analysis of *Csf1r-Cre;Rosa*^{Yfp} mice has provided considerable evidence for the existence of a *Csf1r-Cre*-labelled vascular precursor that contributes to embryonic blood and lymphatic vessel growth as well as postnatal vessel growth. I have excluded that *Csf1r-Cre* activity is caused by ectopic *Cre* expression or unspecific *Rosa*^{Yfp} reporter activity. Moreover, I have demonstrated that this putative vascular precursor contributes to pathological neovascularisation within the retina.

My findings have made a significant contribution towards the field of vascular biology. As such, my work investigating NRP1 signalling has so far contributed to two peer-reviewed primary research papers (Fantin et al., 2014, Fantin et al., 2013a), two peer-reviewed review articles (Plein et al., 2015a, Plein et al., 2014) and two method articles (Plein et al., 2015b, Fantin et al., 2013c) (see **Appendix** – co-authored publications). Furthermore, a manuscript outlining my findings regarding the role of NRP1 in OFT remodelling has been accepted for publication pending revision. I hope that upon completion of the additional experiments outlined in (see **6.2**), the demonstration that *Csf1r-Cre* is a reliable marker of vascular precursors should also yield a publication.

6.2 Future Work

6.2.1 Signalling pathways downstream of SEMA3C/NRP1 during endoMT

Having established that SEMA3C induces endoMT through NRP1, future work could investigate the downstream signalling pathways that enable this process. Thus, future experiments could analyse, which pathways are activated in SEMA3C-treated primary ECs and investigate whether siRNA-mediated NRP1 knockdown affects this activation in a PLXND1-dependent fashion. Moreover, to identify targets of SEMA3C/NRP1 signalling, immunoblotting could be used to investigate changes in protein phosphorylation and translation, whereas changes in gene transcription in candidate pathways could be examined by qPCR. In particular, it is known that endoMT relies on multiple signalling pathways such as the TGFβ and DLL4/Notch pathway (reviewed in Lamouille et al., 2014), and both of these pathways have previously shown to interact with NRP1 (Sorensen et al., 2009, Glinka et al., 2011).

6.2.2 Role of endoMT in cardiac NCC translocation

Defective SEMA3C/NRP signalling was found to impair endoMT both *in vitro* and *in vivo* and prevented the translocation of the bilateral cardiac NCC streams towards the lumen of the vessel. However, it is currently not clear if and in what way these two processes are linked. Thus, future work may wish to examine, whether endoMT-derived mesenchymal cells displace the cardiac NCCs thus pushing them towards the OFT lumen, or, whether they secrete molecules that mobilise the cardiac NCCs. For example, mesenchymal cells derived from the endothelium could be isolated from *Tie2-Cre;Rosa*^{Yfp} OFTs by sorting for YFP^{+}F4/80^{-}CD31^{-} cells. Subsequently, mRNA expression could be analysed by RNAseq and potential chemoattractants tested *in vitro* using NCC cultures (Etchevers, 2011).

6.2.3 Additional roles of NRP1 during OFT remodelling

Analysis of ligand-specific NRP1 mutants revealed that whilst VEGF-A signalling through NRP1 is dispensable, SEMA3C signalling through NRPs is required for OFT remodelling. Nevertheless, the OFTs of *Nrp1*$^{Sema/Sema}$*;Nrp2*$^{-/-}$ mice mostly displayed milder defects than *Nrp1*-null and *Tie2-Cre;Nrp1*$^{fl/-}$ mice. In particular, *Nrp1*$^{-/-}$ OFTs always displayed a complete CAT, whereas

Nrp1$^{Sema/Sema}$*;Nrp2*$^{-/-}$ and *Wnt1-Cre;Sema3c*$^{fl/fl}$ embryos consistently lacked proximal septation, but only occasionally lacked distal septation. This observation suggests that there might be additional NRP1-dependent roles during OFT remodelling. In accordance, a recent publication by our group has demonstrated that NRP1 is activated by the ECM component fibronectin, which in turn activates ABL and thus paxillin-mediated focal adhesion turnover and also cytoskeletal remodelling. Fibronectin is expressed by cardiac NCC within the OFT, and mice deficient in fibronectin exhibit defective OFTs (Mittal et al., 2013, Dai et al., 2013). It is, therefore, conceivable that fibronectin/NRP1 signalling might also exert an essential function during OFT remodelling. Alternatively, the milder phenotype observed in *Nrp1*$^{Sema/Sema}$*;Nrp2*$^{-/-}$ mice might stem from residual ligand binding activity. Thus, future experiments could used AP-tagged SEMA3C probes to determine whether SEMA3C binding to NRPs in primary ECs from *Nrp1*$^{Sema/Sema}$*;Nrp2*$^{-/-}$ mice is completely abolished.

6.2.4 Contribution of *Csf1r-Cre*-labelled precursors to vascular endothelium

To demonstrate that *Csf1r-Cre* does indeed label cells with the ability to differentiate into ECs and contribute to neovascular growth, three experiments (outlined below) should be performed on the two putative vascular precursor populations. Thus, the *Csf1r-Cre*-targeted retinal stellate cells (see **Figure 5.5**), which resemble the vascular precursors described by Kubota *et al*. (2011), could be isolated from retinas using FACS to isolate $YFP^{+}CD31^{-}F4/80^{-}PDGFR\alpha^{-}$ cells. The potential bone marrow-derived vascular precursors could be isolated from bone marrow and blood using FACS to isolate $YFP^{+}KIT^{+}CD45^{-}$ cells. These cell populations could then be used for further experiments.

Firstly, to investigate whether the FACS-sorted vascular precursors are able to give rise to ECs *in vitro*, the cells could be cultured in endothelial growth medium and the generation of EC colonies assessed, as performed in previous studies (Kubota et al., 2011, Case et al., 2007). Secondly, the FACS-isolated vascular precursors could be injected into the tail vein of *Csf1r-Cre*-negative littermates. Following, the induction of neovascularisation using models such as the ear wound healing assay (Raimondi et al., 2014) or laser-induced CNV (Lambert et al., 2013), the presence of

YFP^+ ECs within the neovascular lesions should be assessed. Thirdly, live imaging of explants, e.g. yolk sac (Jones et al., 2008) or retina (Sawamiphak et al., 2010), could be used to visualise the possible integration of the YFP^+ vascular precursors into the endothelium as opposed to demonstrate ECs being not YFP^+ only because of previously undetected sporadic endothelial *Cre* expression. Retinal explants would be suitable if *Csf1r-Cre* does indeed label tissue-resident vascular progenitors similar to those described by Kubota *et al.* (2011). To investigate the potential of circulating vascular precursors, $YFP^+KIT^+CD45^-$ blood cells would have to be added to the explants, although this would only work if they normally extravasate and then incorporate from the tissue side, rather than incorporating from the luminal side.

6.2.5 Expression profile of *Csf1r-Cre*-labelled vascular precursors

To address whether the *Csf1r-Cre*-labelled KIT^+CD45^- vascular precursors constitute bone marrow-derived circulating EPCs similar to those that have been described in other studies (Case et al., 2007, Nolan et al., 2007, Park et al., 2014), future work should analyse the expression of other previously published markers of these cells. Thus, circulating $YFP^+KIT^+CD45^-$ cells could be isolated from the adult blood using FACS to measure the expression of markers such as CD133 (Hilbe et al., 2004, Gehling et al., 2000), VEGFR2 (Friedrich et al., 2006, Peichev et al., 2000) and CD34 (Yang et al., 2011, Peichev et al., 2000). To address whether the *Csf1r-Cre*-labelled stellate cells within the retina resemble the *P0-Cre*-labelled tissue-resident vascular precursors described by Kubota *et al*. (2011), $YFP^+F4/80^-CD31^-$ $PDGFR\alpha^-$ cells could be isolated using FACS to measure the expression of mRNA for P0, VEGFR2 and CXCR4, which are all expressed by the *P0-Cre*-labelled vascular precursors (Kubota et al., 2011).

6.2.6 Requirement of *Csf1r-Cre*-labelled precursors to vascular growth

Given the early embryonic lethality of mice lacking *Csf1r-Cre*-labelled cells (see **Figure 5.17**), which is presumably caused by the ablation of CSF1R-expressing trophoblasts, it is currently not clear whether *Csf1r-Cre*-labelled vascular precursors are essential for developmental or pathological angiogenesis. Future work should, therefore, attempt to generate a *Csf1r-Cre* allele that spares trophoblast cells, or analyse $Csf1r\text{-}Cre^{ERT};Rosa^{Dta}$ mice, in which the *Cre* could be activated during late

gestation when CSF1R is no longer required by trophoblast cells (Jokhi et al., 1993). The use of *Csf1r-Cre*^{ERT}*;Rosa*^{Dta} mice would also help determine whether the *Csf1r-Cre*-labelled vascular precursors are essential for pathological vessel growth, which would be of great therapeutic interest (see **1.1.2.4**).

BIBLIOGRAPHY

ABRAMSSON, A., KURUP, S., BUSSE, M., YAMADA, S., LINDBLOM, P., SCHALLMEINER, E., STENZEL, D., SAUVAGET, D., LEDIN, J., RINGVALL, M., LANDEGREN, U., KJELLEN, L., BONDJERS, G., LI, J. P., LINDAHL, U., SPILLMANN, D., BETSHOLTZ, C. & GERHARDT, H. 2007. Defective N-sulfation of heparan sulfate proteoglycans limits PDGF-BB binding and pericyte recruitment in vascular development. *Genes Dev,* 21**,** 316-31.

ABTIN, A., JAIN, R., MITCHELL, A. J., ROEDIGER, B., BRZOSKA, A. J., TIKOO, S., CHENG, Q., NG, L. G., CAVANAGH, L. L., VON ANDRIAN, U. H., HICKEY, M. J., FIRTH, N. & WENINGER, W. 2014. Perivascular macrophages mediate neutrophil recruitment during bacterial skin infection. *Nat Immunol,* 15**,** 45-53.

ABU-ISSA, R., SMYTH, G., SMOAK, I., YAMAMURA, K. & MEYERS, E. N. 2002. Fgf8 is required for pharyngeal arch and cardiovascular development in the mouse. *Development,* 129**,** 4613-25.

ADAMS, R. H. & ALITALO, K. 2007. Molecular regulation of angiogenesis and lymphangiogenesis. *Nat Rev Mol Cell Biol,* 8**,** 464-78.

ADAMS, R. H., WILKINSON, G. A., WEISS, C., DIELLA, F., GALE, N. W., DEUTSCH, U., RISAU, W. & KLEIN, R. 1999. Roles of ephrinB ligands and EphB receptors in cardiovascular development: demarcation of arterial/venous domains, vascular morphogenesis, and sprouting angiogenesis. *Genes Dev,* 13**,** 295-306.

AICHER, A., RENTSCH, M., SASAKI, K., ELLWART, J. W., FANDRICH, F., SIEBERT, R., COOKE, J. P., DIMMELER, S. & HEESCHEN, C. 2007. Nonbone marrow-derived circulating progenitor cells contribute to postnatal neovascularization following tissue ischemia. *Circ Res,* 100**,** 581-9.

AKASHI, K., TRAVER, D., MIYAMOTO, T. & WEISSMAN, I. L. 2000. A clonogenic common myeloid progenitor that gives rise to all myeloid lineages. *Nature,* 404**,** 193-7.

ALON, T., HEMO, I., ITIN, A., PE'ER, J., STONE, J. & KESHET, E. 1995. Vascular endothelial growth factor acts as a survival factor for newly formed retinal vessels and has implications for retinopathy of prematurity. *Nat Med,* 1**,** 1024-8.

ALVAREZ, D. F., HUANG, L., KING, J. A., ELZARRAD, M. K., YODER, M. C. & STEVENS, T. 2008. Lung microvascular endothelium is enriched with progenitor cells that exhibit vasculogenic capacity. *Am J Physiol Lung Cell Mol Physiol,* 294**,** L419-30.

ANASTASIA, A., DEINHARDT, K., WANG, S., MARTIN, L., NICHOL, D., IRMADY, K., TRINH, J., PARADA, L., RAFII, S., HEMPSTEAD, B. L. & KERMANI, P. 2014. Trkb signaling in pericytes is required for cardiac microvessel stabilization. *PLoS One,* 9**,** e87406.

ANDERSON, M. K., WEISS, A. H., HERNANDEZ-HOYOS, G., DIONNE, C. J. & ROTHENBERG, E. V. 2002. Constitutive expression of PU.1 in fetal hematopoietic progenitors blocks T cell development at the pro-T cell stage. *Immunity,* 16**,** 285-96.

ANDERSON, R. H., WEBB, S., BROWN, N. A., LAMERS, W. & MOORMAN, A. 2003. Development of the heart: (3) formation of the ventricular outflow tracts, arterial valves, and intrapericardial arterial trunks. *Heart,* 89**,** 1110-8.

APPLETON, B. A., WU, P., MALONEY, J., YIN, J., LIANG, W. C., STAWICKI, S., MORTARA, K., BOWMAN, K. K., ELLIOTT, J. M., DESMARAIS, W., BAZAN, J. F., BAGRI, A., TESSIER-LAVIGNE, M., KOCH, A. W., WU, Y., WATTS, R. J. & WIESMANN, C. 2007. Structural studies of neuropilin/antibody complexes provide insights into semaphorin and VEGF binding. *EMBO J,* 26**,** 4902-12.

ARA, T., TOKOYODA, K., SUGIYAMA, T., EGAWA, T., KAWABATA, K. & NAGASAWA, T. 2003. Long-term hematopoietic stem cells require stromal cell-derived factor-1 for colonizing bone marrow during ontogeny. *Immunity,* 19**,** 257-67.

ARAI, F., HIRAO, A., OHMURA, M., SATO, H., MATSUOKA, S., TAKUBO, K., ITO, K., KOH, G. Y. & SUDA, T. 2004. Tie2/angiopoietin-1 signaling regulates hematopoietic stem cell quiescence in the bone marrow niche. *Cell,* 118**,** 149-61.

ARCECI, R. J., KING, A. A., SIMON, M. C., ORKIN, S. H. & WILSON, D. B. 1993. Mouse GATA-4: a retinoic acid-inducible GATA-binding transcription factor expressed in endodermally derived tissues and heart. *Mol Cell Biol,* 13**,** 2235-46.

ARCHER, D. B. 1976. Neovascularization of the retina. *Trans Ophthalmol Soc U K,* 96**,** 471-93.

ARMULIK, A., GENOVE, G. & BETSHOLTZ, C. 2011. Pericytes: developmental, physiological, and pathological perspectives, problems, and promises. *Dev Cell,* 21**,** 193-215.

ARRAS, M., ITO, W. D., SCHOLZ, D., WINKLER, B., SCHAPER, J. & SCHAPER, W. 1998. Monocyte activation in angiogenesis and collateral growth in the rabbit hindlimb. *J Clin Invest,* 101**,** 40-50.

ASAHARA, T., MASUDA, H., TAKAHASHI, T., KALKA, C., PASTORE, C., SILVER, M., KEARNE, M., MAGNER, M. & ISNER, J. M. 1999. Bone marrow origin of endothelial progenitor cells responsible for postnatal vasculogenesis in physiological and pathological neovascularization. *Circ Res,* 85**,** 221-8.

ASAHARA, T., MUROHARA, T., SULLIVAN, A., SILVER, M., VAN DER ZEE, R., LI, T., WITZENBICHLER, B., SCHATTEMAN, G. & ISNER, J. M. 1997. Isolation of putative progenitor endothelial cells for angiogenesis. *Science,* 275**,** 964-7.

ASHTON, N. 1970. Retinal angiogenesis in the human embryo. *Br Med Bull,* 26**,** 103-6.

AUFFRAY, C., FOGG, D., GARFA, M., ELAIN, G., JOIN-LAMBERT, O., KAYAL, S., SARNACKI, S., CUMANO, A., LAUVAU, G. & GEISSMANN, F. 2007. Monitoring of blood vessels and tissues by a population of monocytes with patrolling behavior. *Science,* 317**,** 666-70.

AUSTYN, J. M. & GORDON, S. 1981. F4/80, a monoclonal antibody directed specifically against the mouse macrophage. *Eur J Immunol,* 11**,** 805-15.

AUTIERO, M., LUTTUN, A., TJWA, M. & CARMELIET, P. 2003a. Placental growth factor and its receptor, vascular endothelial growth factor receptor-1: novel targets for stimulation of ischemic tissue revascularization and inhibition of angiogenic and inflammatory disorders. *J Thromb Haemost,* 1**,** 1356-70.

AUTIERO, M., WALTENBERGER, J., COMMUNI, D., KRANZ, A., MOONS, L., LAMBRECHTS, D., KROLL, J., PLAISANCE, S., DE MOL, M., BONO,

F., KLICHE, S., FELLBRICH, G., BALLMER-HOFER, K., MAGLIONE, D., MAYR-BEYRLE, U., DEWERCHIN, M., DOMBROWSKI, S., STANIMIROVIC, D., VAN HUMMELEN, P., DEHIO, C., HICKLIN, D. J., PERSICO, G., HERBERT, J. M., SHIBUYA, M., COLLEN, D., CONWAY, E. M. & CARMELIET, P. 2003b. Role of PlGF in the intra- and intermolecular cross talk between the VEGF receptors Flt1 and Flk1. *Nat Med,* 9**,** 936-43.

BAI, Y., WANG, J., MORIKAWA, Y., BONILLA-CLAUDIO, M., KLYSIK, E. & MARTIN, J. F. 2013. Bmp signaling represses Vegfa to promote outflow tract cushion development. *Development,* 140**,** 3395-402.

BAKER, M., ROBINSON, S. D., LECHERTIER, T., BARBER, P. R., TAVORA, B., D'AMICO, G., JONES, D. T., VOJNOVIC, B. & HODIVALA-DILKE, K. 2012. Use of the mouse aortic ring assay to study angiogenesis. *Nat Protoc,* 7**,** 89-104.

BAMFORTH, S. D., CHAUDHRY, B., BENNETT, M., WILSON, R., MOHUN, T. J., VAN MIEROP, L. H., HENDERSON, D. J. & ANDERSON, R. H. 2013. Clarification of the identity of the mammalian fifth pharyngeal arch artery. *Clin Anat,* 26**,** 173-82.

BARBOSKY, L., LAWRENCE, D. K., KARUNAMUNI, G., WIKENHEISER, J. C., DOUGHMAN, Y. Q., VISCONTI, R. P., BURCH, J. B. & WATANABE, M. 2006. Apoptosis in the developing mouse heart. *Dev Dyn,* 235**,** 2592-602.

BASILE, D. P. & YODER, M. C. 2014. Circulating and tissue resident endothelial progenitor cells. *J Cell Physiol,* 229**,** 10-6.

BATLINER, J., BUEHRER, E., FEDERZONI, E. A., JENAL, M., TOBLER, A., TORBETT, B. E., FEY, M. F. & TSCHAN, M. P. 2012. Transcriptional regulation of MIR29B by PU.1 (SPI1) and MYC during neutrophil differentiation of acute promyelocytic leukaemia cells. *Br J Haematol,* 157**,** 270-4.

BECKER, P. M., WALTENBERGER, J., YACHECHKO, R., MIRZAPOIAZOVA, T., SHAM, J. S., LEE, C. G., ELIAS, J. A. & VERIN, A. D. 2005. Neuropilin-1 regulates vascular endothelial growth factor-mediated endothelial permeability. *Circ Res,* 96**,** 1257-65.

BECKMAN, D. A., BRENT, R. L. & LLOYD, J. B. 1996. Sources of amino acids for protein synthesis during early organogenesis in the rat. 4. Mechanisms before envelopment of the embryo by the yolk sac. *Placenta,* 17**,** 635-41.

BEHAR, O., GOLDEN, J. A., MASHIMO, H., SCHOEN, F. J. & FISHMAN, M. C. 1996. Semaphorin III is needed for normal patterning and growth of nerves, bones and heart. *Nature,* 383**,** 525-8.

BELAOUSSOFF, M., FARRINGTON, S. M. & BARON, M. H. 1998. Hematopoietic induction and respecification of A-P identity by visceral endoderm signaling in the mouse embryo. *Development,* 125**,** 5009-18.

BENEDITO, R., ROCHA, S. F., WOESTE, M., ZAMYKAL, M., RADTKE, F., CASANOVAS, O., DUARTE, A., PYTOWSKI, B. & ADAMS, R. H. 2012. Notch-dependent VEGFR3 upregulation allows angiogenesis without VEGF-VEGFR2 signalling. *Nature,* 484**,** 110-4.

BERGWERFF, M., VERBERNE, M. E., DERUITER, M. C., POELMANN, R. E. & GITTENBERGER-DE GROOT, A. C. 1998. Neural crest cell contribution to the developing circulatory system: implications for vascular morphology? *Circ Res,* 82**,** 221-31.

BERSE, B., BROWN, L. F., VAN DE WATER, L., DVORAK, H. F. & SENGER, D. R. 1992. Vascular permeability factor (vascular endothelial growth factor) gene is expressed differentially in normal tissues, macrophages, and tumors. *Mol Biol Cell,* 3**,** 211-20.

BERTRAND, J. Y., KIM, A. D., VIOLETTE, E. P., STACHURA, D. L., CISSON, J. L. & TRAVER, D. 2007. Definitive hematopoiesis initiates through a committed erythromyeloid progenitor in the zebrafish embryo. *Development,* 134**,** 4147-56.

BLANCO, R. & GERHARDT, H. 2013. VEGF and Notch in tip and stalk cell selection. *Cold Spring Harb Perspect Med,* 3**,** a006569.

BOLAT, F., KAYASELCUK, F., NURSAL, T. Z., YAGMURDUR, M. C., BAL, N. & DEMIRHAN, B. 2006. Microvessel density, VEGF expression, and tumor-associated macrophages in breast tumors: correlations with prognostic parameters. *J Exp Clin Cancer Res,* 25**,** 365-72.

BONDUE, A. & BLANPAIN, C. 2010. Mesp1: a key regulator of cardiovascular lineage commitment. *Circ Res,* 107**,** 1414-27.

BONDUE, A., LAPOUGE, G., PAULISSEN, C., SEMERARO, C., IACOVINO, M., KYBA, M. & BLANPAIN, C. 2008. Mesp1 acts as a master regulator of multipotent cardiovascular progenitor specification. *Cell Stem Cell,* 3**,** 69-84.

BRADE, T., PANE, L. S., MORETTI, A., CHIEN, K. R. & LAUGWITZ, K. L. 2013. Embryonic heart progenitors and cardiogenesis. *Cold Spring Harb Perspect Med,* 3**,** a013847.

BREIER, G., ALBRECHT, U., STERRER, S. & RISAU, W. 1992. Expression of vascular endothelial growth factor during embryonic angiogenesis and endothelial cell differentiation. *Development,* 114**,** 521-532.

BREITMAN, M. L., ROMBOLA, H., MAXWELL, I. H., KLINTWORTH, G. K. & BERNSTEIN, A. 1990. Genetic ablation in transgenic mice with an attenuated diphtheria toxin A gene. *Mol Cell Biol,* 10**,** 474-9.

BROTHERTON, T. W., CHUI, D. H., GAULDIE, J. & PATTERSON, M. 1979. Hemoglobin ontogeny during normal mouse fetal development. *Proc Natl Acad Sci U S A,* 76**,** 2853-7.

BROWN, C. B., FEINER, L., LU, M. M., LI, J., MA, X., WEBBER, A. L., JIA, L., RAPER, J. A. & EPSTEIN, J. A. 2001. PlexinA2 and semaphorin signaling during cardiac neural crest development. *Development,* 128**,** 3071-80.

BURRI, P. H. & DJONOV, V. 2002. Intussusceptive angiogenesis--the alternative to capillary sprouting. *Mol Aspects Med,* 23**,** S1-27.

BYRNE, P. V., GUILBERT, L. J. & STANLEY, E. R. 1981. Distribution of cells bearing receptors for a colony-stimulating factor (CSF-1) in murine tissues. *J Cell Biol,* 91**,** 848-53.

CABALLERO, S., SENGUPTA, N., AFZAL, A., CHANG, K. H., LI CALZI, S., GUBERSKI, D. L., KERN, T. S. & GRANT, M. B. 2007. Ischemic vascular damage can be repaired by healthy, but not diabetic, endothelial progenitor cells. *Diabetes,* 56**,** 960-7.

CADUFF, J. H., FISCHER, L. C. & BURRI, P. H. 1986. Scanning electron microscope study of the developing microvasculature in the postnatal rat lung. *Anat Rec,* 216**,** 154-64.

CAI, C. L., LIANG, X., SHI, Y., CHU, P. H., PFAFF, S. L., CHEN, J. & EVANS, S. 2003. Isl1 identifies a cardiac progenitor population that proliferates prior to differentiation and contributes a majority of cells to the heart. *Dev Cell,* 5**,** 877-89.

CAI, H. & REED, R. R. 1999. Cloning and characterization of neuropilin-1-interacting protein: a PSD-95/Dlg/ZO-1 domain-containing protein that interacts with the cytoplasmic domain of neuropilin-1. *J Neurosci,* 19**,** 6519-27.

CAICEDO, A., ESPINOSA-HEIDMANN, D. G., PINA, Y., HERNANDEZ, E. P. & COUSINS, S. W. 2005. Blood-derived macrophages infiltrate the retina and activate Muller glial cells under experimental choroidal neovascularization. *Exp Eye Res,* 81**,** 38-47.

CARIBONI, A., DAVIDSON, K., DOZIO, E., MEMI, F., SCHWARZ, Q., STOSSI, F., PARNAVELAS, J. G. & RUHRBERG, C. 2011. VEGF signalling controls GnRH neuron survival via NRP1 independently of KDR and blood vessels. *Development,* 138**,** 3723-33.

CARMELIET, P., FERREIRA, V., BREIER, G., POLLEFEYT, S., KIECKENS, L., GERTSENSTEIN, M., FAHRIG, M., VANDENHOECK, A., HARPAL, K., EBERHARDT, C., DECLERCQ, C., PAWLING, J., MOONS, L., COLLEN, D., RISAU, W. & NAGY, A. 1996. Abnormal blood vessel development and lethality in embryos lacking a single VEGF allele. *Nature,* 380**,** 435-9.

CARMELIET, P., NG, Y. S., NUYENS, D., THEILMEIER, G., BRUSSELMANS, K., CORNELISSEN, I., EHLER, E., KAKKAR, V. V., STALMANS, I., MATTOT, V., PERRIARD, J. C., DEWERCHIN, M., FLAMENG, W., NAGY, A., LUPU, F., MOONS, L., COLLEN, D., D'AMORE, P. A. & SHIMA, D. T. 1999. Impaired myocardial angiogenesis and ischemic cardiomyopathy in mice lacking the vascular endothelial growth factor isoforms VEGF164 and VEGF188. *Nat Med,* 5**,** 495-502.

CAROTTA, S., DAKIC, A., D'AMICO, A., PANG, S. H., GREIG, K. T., NUTT, S. L. & WU, L. 2010. The transcription factor PU.1 controls dendritic cell development and Flt3 cytokine receptor expression in a dose-dependent manner. *Immunity,* 32**,** 628-41.

CARTER, A. M. 2012. Evolution of placental function in mammals: the molecular basis of gas and nutrient transfer, hormone secretion, and immune responses. *Physiol Rev,* 92**,** 1543-76.

CASAZZA, A., LAOUI, D., WENES, M., RIZZOLIO, S., BASSANI, N., MAMBRETTI, M., DESCHOEMAEKER, S., VAN GINDERACHTER, J. A., TAMAGNONE, L. & MAZZONE, M. 2013. Impeding macrophage entry into hypoxic tumor areas by Sema3A/Nrp1 signaling blockade inhibits angiogenesis and restores antitumor immunity. *Cancer Cell,* 24**,** 695-709.

CASE, J., MEAD, L. E., BESSLER, W. K., PRATER, D., WHITE, H. A., SAADATZADEH, M. R., BHAVSAR, J. R., YODER, M. C., HANELINE, L. S. & INGRAM, D. A. 2007. Human CD34+AC133+VEGFR-2+ cells are not endothelial progenitor cells but distinct, primitive hematopoietic progenitors. *Exp Hematol,* 35**,** 1109-18.

CHAKROBORTY, D., CHOWDHURY, U. R., SARKAR, C., BARAL, R., DASGUPTA, P. S. & BASU, S. 2008. Dopamine regulates endothelial progenitor cell mobilization from mouse bone marrow in tumor vascularization. *J Clin Invest,* 118**,** 1380-9.

CHEN, H., BAGRI, A., ZUPICICH, J. A., ZOU, Y., STOECKLI, E., PLEASURE, S. J., LOWENSTEIN, D. H., SKARNES, W. C., CHEDOTAL, A. & TESSIER-LAVIGNE, M. 2000. Neuropilin-2 regulates the development of selective cranial and sensory nerves and hippocampal mossy fiber projections. *Neuron,* 25**,** 43-56.

CHEN, H., CAMPBELL, R. A., CHANG, Y., LI, M., WANG, C. S., LI, J., SANCHEZ, E., SHARE, M., STEINBERG, J., BERENSON, A., SHALITIN, D., ZENG, Z., GUI, D., PEREZ-PINERA, P., BERENSON, R. J., SAID, J., BONAVIDA, B., DEUEL, T. F. & BERENSON, J. R. 2009a. Pleiotrophin produced by multiple myeloma induces transdifferentiation of monocytes into vascular endothelial cells: a novel mechanism of tumor-induced vasculogenesis. *Blood,* 113**,** 1992-2002.

CHEN, H., CHEDOTAL, A., HE, Z., GOODMAN, C. S. & TESSIER-LAVIGNE, M. 1997. Neuropilin-2, a novel member of the neuropilin family, is a high affinity receptor for the semaphorins Sema E and Sema IV but not Sema III. *Neuron,* 19**,** 547-59.

CHEN, H., HE, Z., BAGRI, A. & TESSIER-LAVIGNE, M. 1998. Semaphorin-neuropilin interactions underlying sympathetic axon responses to class III semaphorins. *Neuron,* 21**,** 1283-90.

CHEN, H., WANG, S., ZHANG, J., REN, X., ZHANG, R., SHI, W., LV, Y., ZHOU, Y., YAN, X., CHEN, L., HE, L., ZHANG, B., NAN, X., YUE, W., LI, Y. & PEI, X. 2014. A novel molecule Me6TREN promotes angiogenesis via enhancing endothelial progenitor cell mobilization and recruitment. *Sci Rep,* 4**,** 6222.

CHEN, J. & SMITH, L. E. 2007. Retinopathy of prematurity. *Angiogenesis,* 10**,** 133-40.

CHEN, J., STAHL, A., KRAH, N. M., SEAWARD, M. R., DENNISON, R. J., SAPIEHA, P., HUA, J., HATTON, C. J., JUAN, A. M., ADERMAN, C. M., WILLETT, K. L., GUERIN, K. I., MAMMOTO, A., CAMPBELL, M. & SMITH, L. E. 2011a. Wnt signaling mediates pathological vascular growth in proliferative retinopathy. *Circulation,* 124**,** 1871-81.

CHEN, M. J., LI, Y., DE OBALDIA, M. E., YANG, Q., YZAGUIRRE, A. D., YAMADA-INAGAWA, T., VINK, C. S., BHANDOOLA, A., DZIERZAK, E. & SPECK, N. A. 2011b. Erythroid/myeloid progenitors and hematopoietic stem cells originate from distinct populations of endothelial cells. *Cell Stem Cell,* 9**,** 541-52.

CHEN, M. J., YOKOMIZO, T., ZEIGLER, B. M., DZIERZAK, E. & SPECK, N. A. 2009b. Runx1 is required for the endothelial to haematopoietic cell transition but not thereafter. *Nature,* 457**,** 887-91.

CHITTENDEN, T. W., CLAES, F., LANAHAN, A. A., AUTIERO, M., PALAC, R. T., TKACHENKO, E. V., ELFENBEIN, A., RUIZ DE ALMODOVAR, C., DEDKOV, E., TOMANEK, R., LI, W., WESTMORE, M., SINGH, J. P., HOROWITZ, A., MULLIGAN-KEHOE, M. J., MOODIE, K. L., ZHUANG, Z. W., CARMELIET, P. & SIMONS, M. 2006. Selective regulation of arterial branching morphogenesis by synectin. *Dev Cell,* 10**,** 783-95.

CLAUSEN, B. E., BURKHARDT, C., REITH, W., RENKAWITZ, R. & FORSTER, I. 1999. Conditional gene targeting in macrophages and granulocytes using LysMcre mice. *Transgenic Res,* 8**,** 265-77.

CLEMENT, S., STOUFFS, M., BETTIOL, E., KAMPF, S., KRAUSE, K. H., CHAPONNIER, C. & JACONI, M. 2007. Expression and function of alpha-smooth muscle actin during embryonic-stem-cell-derived cardiomyocyte differentiation. *J Cell Sci,* 120**,** 229-38.

CONNOLLY, S. E., HORES, T. A., SMITH, L. E. & D'AMORE, P. A. 1988. Characterization of vascular development in the mouse retina. *Microvasc Res,* 36**,** 275-90.

CONNOR, K. M., KRAH, N. M., DENNISON, R. J., ADERMAN, C. M., CHEN, J., GUERIN, K. I., SAPIEHA, P., STAHL, A., WILLETT, K. L. & SMITH, L. E. 2009. Quantification of oxygen-induced retinopathy in the mouse: a model of vessel loss, vessel regrowth and pathological angiogenesis. *Nat Protoc,* 4**,** 1565-73.

CORADA, M., ORSENIGO, F., MORINI, M. F., PITULESCU, M. E., BHAT, G., NYQVIST, D., BREVIARIO, F., CONTI, V., BRIOT, A., IRUELA-ARISPE, M. L., ADAMS, R. H. & DEJANA, E. 2013. Sox17 is indispensable for acquisition and maintenance of arterial identity. *Nat Commun,* 4**,** 2609.

CORDELL, H. J., TOPF, A., MAMASOULA, C., POSTMA, A. V., BENTHAM, J., ZELENIKA, D., HEATH, S., BLUE, G., COSGROVE, C., GRANADOS RIVERON, J., DARLAY, R., SOEMEDI, R., WILSON, I. J., AYERS, K. L., RAHMAN, T. J., HALL, D., MULDER, B. J., ZWINDERMAN, A. H., VAN ENGELEN, K., BROOK, J. D., SETCHFIELD, K., BU'LOCK, F. A., THORNBOROUGH, C., O'SULLIVAN, J., STUART, A. G., PARSONS, J., BHATTACHARYA, S., WINLAW, D., MITAL, S., GEWILLIG, M., BRECKPOT, J., DEVRIENDT, K., MOORMAN, A. F., RAUCH, A., LATHROP, G. M., KEAVNEY, B. D. & GOODSHIP, J. A. 2013. Genome-wide association study identifies loci on 12q24 and 13q32 associated with tetralogy of Fallot. *Hum Mol Genet,* 22**,** 1473-81.

CORTES, F., DEBACKER, C., PEAULT, B. & LABASTIE, M. C. 1999. Differential expression of KDR/VEGFR-2 and CD34 during mesoderm development of the early human embryo. *Mech Dev,* 83**,** 161-4.

CREAZZO, T. L., GODT, R. E., LEATHERBURY, L., CONWAY, S. J. & KIRBY, M. L. 1998. Role of cardiac neural crest cells in cardiovascular development. *Annu Rev Physiol,* 60**,** 267-86.

DAI, X., JIANG, W., ZHANG, Q., XU, L., GENG, P., ZHUANG, S., PETRICH, B. G., JIANG, C., PENG, L., BHATTACHARYA, S., EVANS, S. M., SUN, Y., CHEN, J. & LIANG, X. 2013. Requirement for integrin-linked kinase in neural crest migration and differentiation and outflow tract morphogenesis. *BMC Biol,* 11**,** 107.

DAI, X. M., RYAN, G. R., HAPEL, A. J., DOMINGUEZ, M. G., RUSSELL, R. G., KAPP, S., SYLVESTRE, V. & STANLEY, E. R. 2002. Targeted disruption of the mouse colony-stimulating factor 1 receptor gene results in osteopetrosis, mononuclear phagocyte deficiency, increased primitive progenitor cell frequencies, and reproductive defects. *Blood,* 99**,** 111-20.

DANIEL, C., LUDKE, A., WAGNER, A., TODOROV, V. T., HOHENSTEIN, B. & HUGO, C. 2012. Transgelin is a marker of repopulating mesangial cells after injury and promotes their proliferation and migration. *Lab Invest,* 92**,** 812-26.

DANIELIAN, P. S., MUCCINO, D., ROWITCH, D. H., MICHAEL, S. K. & MCMAHON, A. P. 1998. Modification of gene activity in mouse embryos in utero by a tamoxifen-inducible form of Cre recombinase. *Curr Biol,* 8**,** 1323-6.

DE BRUIJN, M. F., SPECK, N. A., PEETERS, M. C. & DZIERZAK, E. 2000. Definitive hematopoietic stem cells first develop within the major arterial regions of the mouse embryo. *EMBO J,* 19**,** 2465-74.

DE FALCO, S., GIGANTE, B. & PERSICO, M. G. 2002. Structure and function of placental growth factor. *Trends Cardiovasc Med,* 12**,** 241-6.

DE VRIES, L., LOU, X., ZHAO, G., ZHENG, B. & FARQUHAR, M. G. 1998. GIPC, a PDZ domain containing protein, interacts specifically with the C terminus of RGS-GAIP. *Proc Natl Acad Sci U S A,* 95**,** 12340-5.

DEFALCO, T., BHATTACHARYA, I., WILLIAMS, A. V., SAMS, D. M. & CAPEL, B. 2014. Yolk-sac-derived macrophages regulate fetal testis vascularization and morphogenesis. *Proc Natl Acad Sci U S A,* 111**,** E2384-93.

DEKOTER, R. P. & SINGH, H. 2000. Regulation of B lymphocyte and macrophage development by graded expression of PU.1. *Science,* 288**,** 1439-41.

DELOT, E. C., BAHAMONDE, M. E., ZHAO, M. & LYONS, K. M. 2003. BMP signaling is required for septation of the outflow tract of the mammalian heart. *Development,* 130**,** 209-20.

DENG, B., WEHLING-HENRICKS, M., VILLALTA, S. A., WANG, Y. & TIDBALL, J. G. 2012. IL-10 triggers changes in macrophage phenotype that promote muscle growth and regeneration. *J Immunol,* 189**,** 3669-80.

DENG, L., ZHOU, J. F., SELLERS, R. S., LI, J. F., NGUYEN, A. V., WANG, Y., ORLOFSKY, A., LIU, Q., HUME, D. A., POLLARD, J. W., AUGENLICHT, L. & LIN, E. Y. 2010. A novel mouse model of inflammatory bowel disease links mammalian target of rapamycin-dependent hyperproliferation of colonic epithelium to inflammation-associated tumorigenesis. *Am J Pathol,* 176**,** 952-67.

DENTELLI, P., ROSSO, A., BALSAMO, A., COLMENARES BENEDETTO, S., ZEOLI, A., PEGORARO, M., CAMUSSI, G., PEGORARO, L. & BRIZZI, M. F. 2007. C-KIT, by interacting with the membrane-bound ligand, recruits endothelial progenitor cells to inflamed endothelium. *Blood,* 109**,** 4264-71.

DEWERCHIN, M. & CARMELIET, P. 2012. PlGF: a multitasking cytokine with disease-restricted activity. *Cold Spring Harb Perspect Med,* 2.

DIEZ-ROUX, G., ARGILLA, M., MAKARENKOVA, H., KO, K. & LANG, R. A. 1999. Macrophages kill capillary cells in G1 phase of the cell cycle during programmed vascular regression. *Development,* 126**,** 2141-7.

DIRKX, A. E., OUDE EGBRINK, M. G., WAGSTAFF, J. & GRIFFIOEN, A. W. 2006. Monocyte/macrophage infiltration in tumors: modulators of angiogenesis. *J Leukoc Biol,* 80**,** 1183-96.

DORRELL, M. I., AGUILAR, E., JACOBSON, R., YANES, O., GARIANO, R., HECKENLIVELY, J., BANIN, E., RAMIREZ, G. A., GASMI, M., BIRD, A., SIUZDAK, G. & FRIEDLANDER, M. 2009. Antioxidant or neurotrophic factor treatment preserves function in a mouse model of neovascularization-associated oxidative stress. *J Clin Invest,* 119**,** 611-23.

DOWNS, K. M. & HARMANN, C. 1997. Developmental potency of the murine allantois. *Development,* 124**,** 2769-80.

DRAKE, C. J. 2003. Embryonic and adult vasculogenesis. *Birth Defects Res C Embryo Today,* 69**,** 73-82.

DRAKE, C. J. & FLEMING, P. A. 2000. Vasculogenesis in the day 6.5 to 9.5 mouse embryo. *Blood,* 95**,** 1671-9.

DYER, C. A., KENDLER, A., JEAN-GUILLAUME, D., AWATRAMANI, R., LEE, A., MASON, L. M. & KAMHOLZ, J. 2000. GFAP-positive and myelin marker-positive glia in normal and pathologic environments. *J Neurosci Res,* 60**,** 412-26.

DYER, M. A., FARRINGTON, S. M., MOHN, D., MUNDAY, J. R. & BARON, M. H. 2001. Indian hedgehog activates hematopoiesis and vasculogenesis and

can respecify prospective neurectodermal cell fate in the mouse embryo. *Development,* 128**,** 1717-30.
DZIERZAK, E. 2003. Ontogenic emergence of definitive hematopoietic stem cells. *Curr Opin Hematol,* 10**,** 229-34.
DZIERZAK, E. & SPECK, N. A. 2008. Of lineage and legacy: the development of mammalian hematopoietic stem cells. *Nat Immunol,* 9**,** 129-36.
EHLING, J., BARTNECK, M., WEI, X., GREMSE, F., FECH, V., MOCKEL, D., BAECK, C., HITTATIYA, K., EULBERG, D., LUEDDE, T., KIESSLING, F., TRAUTWEIN, C., LAMMERS, T. & TACKE, F. 2014. CCL2-dependent infiltrating macrophages promote angiogenesis in progressive liver fibrosis. *Gut,* 63**,** 1960-71.
EISENBERG, L. M. & MARKWALD, R. R. 1995. Molecular regulation of atrioventricular valvuloseptal morphogenesis. *Circ Res,* 77**,** 1-6.
ENGLEKA, K. A., MANDERFIELD, L. J., BRUST, R. D., LI, L., COHEN, A., DYMECKI, S. M. & EPSTEIN, J. A. 2012. Islet1 derivatives in the heart are of both neural crest and second heart field origin. *Circ Res,* 110**,** 922-6.
EPSTEIN, J. A., LI, J., LANG, D., CHEN, F., BROWN, C. B., JIN, F., LU, M. M., THOMAS, M., LIU, E., WESSELS, A. & LO, C. W. 2000. Migration of cardiac neural crest cells in Splotch embryos. *Development,* 127**,** 1869-78.
ERSKINE, L., REIJNTJES, S., PRATT, T., DENTI, L., SCHWARZ, Q., VIEIRA, J. M., ALAKAKONE, B., SHEWAN, D. & RUHRBERG, C. 2011. VEGF signaling through neuropilin 1 guides commissural axon crossing at the optic chiasm. *Neuron,* 70**,** 951-65.
ESCOT, S., BLAVET, C., HARTLE, S., DUBAND, J. L. & FOURNIER-THIBAULT, C. 2013. Misregulation of SDF1-CXCR4 signaling impairs early cardiac neural crest cell migration leading to conotruncal defects. *Circ Res,* 113**,** 505-16.
ESPINOSA-HEIDMANN, D. G., CAICEDO, A., HERNANDEZ, E. P., CSAKY, K. G. & COUSINS, S. W. 2003a. Bone marrow-derived progenitor cells contribute to experimental choroidal neovascularization. *Invest Ophthalmol Vis Sci,* 44**,** 4914-9.
ESPINOSA-HEIDMANN, D. G., SUNER, I. J., HERNANDEZ, E. P., MONROY, D., CSAKY, K. G. & COUSINS, S. W. 2003b. Macrophage depletion diminishes lesion size and severity in experimental choroidal neovascularization. *Invest Ophthalmol Vis Sci,* 44**,** 3586-92.
ETCHEVERS, H. 2011. Primary culture of chick, mouse or human neural crest cells. *Nat Protoc,* 6**,** 1568-77.
EUBANK, T. D., GALLOWAY, M., MONTAGUE, C. M., WALDMAN, W. J. & MARSH, C. B. 2003. M-CSF induces vascular endothelial growth factor production and angiogenic activity from human monocytes. *J Immunol,* 171**,** 2637-43.
EVANS, I. M., YAMAJI, M., BRITTON, G., PELLET-MANY, C., LOCKIE, C., ZACHARY, I. C. & FRANKEL, P. 2011. Neuropilin-1 signaling through p130Cas tyrosine phosphorylation is essential for growth factor-dependent migration of glioma and endothelial cells. *Mol Cell Biol,* 31**,** 1174-85.
EVANS, R. 1977a. The effect of azathioprine on host cell infiltration and growth of a murine fibrosarcoma. *Int J Cancer,* 20**,** 120-8.
EVANS, R. 1977b. Effect of X-irradiation on host-cell infiltration and growth of a murine fibrosarcoma. *Br J Cancer,* 35**,** 557-66.

FADINI, G. P., DASSIE, F., ALBIERO, M., BOSCARO, E., ALBANO, I., MARTINI, C., DE KREUTZENBERG, S. V., AGOSTINI, C., AVOGARO, A., VETTOR, R. & MAFFEI, P. 2014. Endothelial progenitor cells are reduced in acromegalic patients and can be restored by treatment with somatostatin analogs. *J Clin Endocrinol Metab,* 99**,** E2549-56.

FANG, S., WEI, J., PENTINMIKKO, N., LEINONEN, H. & SALVEN, P. 2012. Generation of functional blood vessels from a single c-kit+ adult vascular endothelial stem cell. *PLoS Biol,* 10**,** e1001407.

FANTIN, A., HERZOG, B., MAHMOUD, M., YAMAJI, M., PLEIN, A., DENTI, L., RUHRBERG, C. & ZACHARY, I. 2014. Neuropilin 1 (NRP1) hypomorphism combined with defective VEGF-A binding reveals novel roles for NRP1 in developmental and pathological angiogenesis. *Development,* 141**,** 556-62.

FANTIN, A., MADEN, C. H. & RUHRBERG, C. 2009. Neuropilin ligands in vascular and neuronal patterning. *Biochem Soc Trans,* 37**,** 1228-32.

FANTIN, A., SCHWARZ, Q., DAVIDSON, K., NORMANDO, E. M., DENTI, L. & RUHRBERG, C. 2011. The cytoplasmic domain of neuropilin 1 is dispensable for angiogenesis, but promotes the spatial separation of retinal arteries and veins. *Development,* 138**,** 4185-91.

FANTIN, A., VIEIRA, J. M., GESTRI, G., DENTI, L., SCHWARZ, Q., PRYKHOZHIJ, S., PERI, F., WILSON, S. W. & RUHRBERG, C. 2010. Tissue macrophages act as cellular chaperones for vascular anastomosis downstream of VEGF-mediated endothelial tip cell induction. *Blood,* 116**,** 829-40.

FANTIN, A., VIEIRA, J. M., PLEIN, A., DENTI, L., FRUTTIGER, M., POLLARD, J. W. & RUHRBERG, C. 2013a. NRP1 acts cell autonomously in endothelium to promote tip cell function during sprouting angiogenesis. *Blood*.

FANTIN, A., VIEIRA, J. M., PLEIN, A., DENTI, L., FRUTTIGER, M., POLLARD, J. W. & RUHRBERG, C. 2013b. NRP1 acts cell autonomously in endothelium to promote tip cell function during sprouting angiogenesis. *Blood,* 121**,** 2352-62.

FANTIN, A., VIEIRA, J. M., PLEIN, A., MADEN, C. H. & RUHRBERG, C. 2013c. The embryonic mouse hindbrain as a qualitative and quantitative model for studying the molecular and cellular mechanisms of angiogenesis. *Nat Protoc,* 8**,** 418-29.

FEINER, L., WEBBER, A. L., BROWN, C. B., LU, M. M., JIA, L., FEINSTEIN, P., MOMBAERTS, P., EPSTEIN, J. A. & RAPER, J. A. 2001. Targeted disruption of semaphorin 3C leads to persistent truncus arteriosus and aortic arch interruption. *Development,* 128**,** 3061-70.

FENG, Y. Q., LORINCZ, M. C., FIERING, S., GREALLY, J. M. & BOUHASSIRA, E. E. 2001. Position effects are influenced by the orientation of a transgene with respect to flanking chromatin. *Mol Cell Biol,* 21**,** 298-309.

FERKOWICZ, M. J., STARR, M., XIE, X., LI, W., JOHNSON, S. A., SHELLEY, W. C., MORRISON, P. R. & YODER, M. C. 2003. CD41 expression defines the onset of primitive and definitive hematopoiesis in the murine embryo. *Development,* 130**,** 4393-403.

FERKOWICZ, M. J. & YODER, M. C. 2005. Blood island formation: longstanding observations and modern interpretations. *Exp Hematol,* 33**,** 1041-7.

FLAMME, I., BREIER, G. & RISAU, W. 1995. Vascular endothelial growth factor (VEGF) and VEGF receptor 2 (flk-1) are expressed during vasculogenesis and vascular differentiation in the quail embryo. *Dev Biol,* 169**,** 699-712.

FONG, G. H., ROSSANT, J., GERTSENSTEIN, M. & BREITMAN, M. L. 1995. Role of the Flt-1 receptor tyrosine kinase in regulating the assembly of vascular endothelium. *Nature,* 376**,** 66-70.

FONG, G. H., ZHANG, L., BRYCE, D. M. & PENG, J. 1999. Increased hemangioblast commitment, not vascular disorganization, is the primary defect in flt-1 knock-out mice. *Development,* 126**,** 3015-25.

FRANK, D. U., FOTHERINGHAM, L. K., BREWER, J. A., MUGLIA, L. J., TRISTANI-FIROUZI, M., CAPECCHI, M. R. & MOON, A. M. 2002. An Fgf8 mouse mutant phenocopies human 22q11 deletion syndrome. *Development,* 129**,** 4591-603.

FRIEDRICH, E. B., WALENTA, K., SCHARLAU, J., NICKENIG, G. & WERNER, N. 2006. CD34-/CD133+/VEGFR-2+ endothelial progenitor cell subpopulation with potent vasoregenerative capacities. *Circ Res,* 98**,** e20-5.

FRUTTIGER, M. 2002. Development of the mouse retinal vasculature: angiogenesis versus vasculogenesis. *Invest Ophthalmol Vis Sci,* 43**,** 522-7.

FRUTTIGER, M. 2007. Development of the retinal vasculature. *Angiogenesis,* 10**,** 77-88.

FRUTTIGER, M., CALVER, A. R., KRUGER, W. H., MUDHAR, H. S., MICHALOVICH, D., TAKAKURA, N., NISHIKAWA, S. & RICHARDSON, W. D. 1996. PDGF mediates a neuron-astrocyte interaction in the developing retina. *Neuron,* 17**,** 1117-31.

FUJISAWA, H. 2002. From the discovery of neuropilin to the determination of its adhesion sites. *Adv Exp Med Biol,* 515**,** 1-12.

FUJISAWA, H., TAKAGI, S. & HIRATA, T. 1995. Growth-associated expression of a membrane protein, neuropilin, in Xenopus optic nerve fibers. *Dev Neurosci,* 17**,** 343-9.

FUKASAWA, M., MATSUSHITA, A. & KORC, M. 2007. Neuropilin-1 interacts with integrin beta1 and modulates pancreatic cancer cell growth, survival and invasion. *Cancer Biol Ther,* 6**,** 1173-80.

GAGNON, M. L., BIELENBERG, D. R., GECHTMAN, Z., MIAO, H. Q., TAKASHIMA, S., SOKER, S. & KLAGSBRUN, M. 2000. Identification of a natural soluble neuropilin-1 that binds vascular endothelial growth factor: In vivo expression and antitumor activity. *Proc Natl Acad Sci U S A,* 97**,** 2573-8.

GAO, Y., LI, M., CHEN, W. & SIMONS, M. 2000. Synectin, syndecan-4 cytoplasmic domain binding PDZ protein, inhibits cell migration. *J Cell Physiol,* 184**,** 373-9.

GARIANO, R. F. & GARDNER, T. W. 2005. Retinal angiogenesis in development and disease. *Nature,* 438**,** 960-6.

GAVALAS, A., RUHRBERG, C., LIVET, J., HENDERSON, C. E. & KRUMLAUF, R. 2003. Neuronal defects in the hindbrain of Hoxa1, Hoxb1 and Hoxb2 mutants reflect regulatory interactions among these Hox genes. *Development,* 130**,** 5663-79.

GAVARD, J. & GUTKIND, J. S. 2006. VEGF controls endothelial-cell permeability by promoting the beta-arrestin-dependent endocytosis of VE-cadherin. *Nat Cell Biol,* 8**,** 1223-34.

GEHLING, U. M., ERGUN, S., SCHUMACHER, U., WAGENER, C., PANTEL, K., OTTE, M., SCHUCH, G., SCHAFHAUSEN, P., MENDE, T., KILIC, N., KLUGE, K., SCHAFER, B., HOSSFELD, D. K. & FIEDLER, W. 2000. In vitro differentiation of endothelial cells from AC133-positive progenitor cells. *Blood,* 95**,** 3106-12.

GEISSMANN, F., JUNG, S. & LITTMAN, D. R. 2003. Blood monocytes consist of two principal subsets with distinct migratory properties. *Immunity,* 19**,** 71-82.

GEKAS, C., DIETERLEN-LIEVRE, F., ORKIN, S. H. & MIKKOLA, H. K. 2005. The placenta is a niche for hematopoietic stem cells. *Dev Cell,* 8**,** 365-75.

GERBER, H. P., HILLAN, K. J., RYAN, A. M., KOWALSKI, J., KELLER, G. A., RANGELL, L., WRIGHT, B. D., RADTKE, F., AGUET, M. & FERRARA, N. 1999. VEGF is required for growth and survival in neonatal mice. *Development,* 126**,** 1149-59.

GERETTI, E., SHIMIZU, A. & KLAGSBRUN, M. 2008. Neuropilin structure governs VEGF and semaphorin binding and regulates angiogenesis. *Angiogenesis,* 11**,** 31-9.

GERETY, S. S., WANG, H. U., CHEN, Z. F. & ANDERSON, D. J. 1999. Symmetrical mutant phenotypes of the receptor EphB4 and its specific transmembrane ligand ephrin-B2 in cardiovascular development. *Mol Cell,* 4**,** 403-14.

GERHARDT, H., GOLDING, M., FRUTTIGER, M., RUHRBERG, C., LUNDKVIST, A., ABRAMSSON, A., JELTSCH, M., MITCHELL, C., ALITALO, K., SHIMA, D. & BETSHOLTZ, C. 2003. VEGF guides angiogenic sprouting utilizing endothelial tip cell filopodia. *J Cell Biol,* 161**,** 1163-77.

GERHARDT, H., RUHRBERG, C., ABRAMSSON, A., FUJISAWA, H., SHIMA, D. & BETSHOLTZ, C. 2004. Neuropilin-1 is required for endothelial tip cell guidance in the developing central nervous system. *Dev Dyn,* 231**,** 503-9.

GEUTSKENS, S. B., OTONKOSKI, T., PULKKINEN, M. A., DREXHAGE, H. A. & LEENEN, P. J. 2005. Macrophages in the murine pancreas and their involvement in fetal endocrine development in vitro. *J Leukoc Biol,* 78**,** 845-52.

GIGER, R. J., CLOUTIER, J. F., SAHAY, A., PRINJHA, R. K., LEVENGOOD, D. V., MOORE, S. E., PICKERING, S., SIMMONS, D., RASTAN, S., WALSH, F. S., KOLODKIN, A. L., GINTY, D. D. & GEPPERT, M. 2000. Neuropilin-2 is required in vivo for selective axon guidance responses to secreted semaphorins. *Neuron,* 25**,** 29-41.

GILL, M., DIAS, S., HATTORI, K., RIVERA, M. L., HICKLIN, D., WITTE, L., GIRARDI, L., YURT, R., HIMEL, H. & RAFII, S. 2001. Vascular trauma induces rapid but transient mobilization of VEGFR2(+)AC133(+) endothelial precursor cells. *Circ Res,* 88**,** 167-74.

GILLE, H., KOWALSKI, J., LI, B., LECOUTER, J., MOFFAT, B., ZIONCHECK, T. F., PELLETIER, N. & FERRARA, N. 2001. Analysis of biological effects and signaling properties of Flt-1 (VEGFR-1) and KDR (VEGFR-2). A reassessment using novel receptor-specific vascular endothelial growth factor mutants. *J Biol Chem,* 276**,** 3222-30.

GINHOUX, F., GRETER, M., LEBOEUF, M., NANDI, S., SEE, P., GOKHAN, S., MEHLER, M. F., CONWAY, S. J., NG, L. G., STANLEY, E. R., SAMOKHVALOV, I. M. & MERAD, M. 2010. Fate mapping analysis

reveals that adult microglia derive from primitive macrophages. *Science,* 330**,** 841-5.

GINHOUX, F. & JUNG, S. 2014. Monocytes and macrophages: developmental pathways and tissue homeostasis. *Nat Rev Immunol,* 14**,** 392-404.

GIRAUDO, E., INOUE, M. & HANAHAN, D. 2004. An amino-bisphosphonate targets MMP-9-expressing macrophages and angiogenesis to impair cervical carcinogenesis. *J Clin Invest,* 114**,** 623-33.

GITAY-GOREN, H., COHEN, T., TESSLER, S., SOKER, S., GENGRINOVITCH, S., ROCKWELL, P., KLAGSBRUN, M., LEVI, B. Z. & NEUFELD, G. 1996. Selective binding of VEGF121 to one of the three vascular endothelial growth factor receptors of vascular endothelial cells. *J Biol Chem,* 271**,** 5519-23.

GITLER, A. D., LU, M. M. & EPSTEIN, J. A. 2004. PlexinD1 and semaphorin signaling are required in endothelial cells for cardiovascular development. *Dev Cell,* 7**,** 107-16.

GLINKA, Y., STOILOVA, S., MOHAMMED, N. & PRUD'HOMME, G. J. 2011. Neuropilin-1 exerts co-receptor function for TGF-beta-1 on the membrane of cancer cells and enhances responses to both latent and active TGF-beta. *Carcinogenesis,* 32**,** 613-21.

GLUZMAN-POLTORAK, Z., COHEN, T., HERZOG, Y. & NEUFELD, G. 2000. Neuropilin-2 is a receptor for the vascular endothelial growth factor (VEGF) forms VEGF-145 and VEGF-165 [correction]. *J Biol Chem,* 275**,** 29922.

GLUZMAN-POLTORAK, Z., COHEN, T., SHIBUYA, M. & NEUFELD, G. 2001. Vascular endothelial growth factor receptor-1 and neuropilin-2 form complexes. *J Biol Chem,* 276**,** 18688-94.

GOLDIE, L. C., LUCITTI, J. L., DICKINSON, M. E. & HIRSCHI, K. K. 2008. Cell signaling directing the formation and function of hemogenic endothelium during murine embryogenesis. *Blood,* 112**,** 3194-204.

GOMEZ PERDIGUERO, E. & GEISSMANN, F. 2013. Myb-independent macrophages: a family of cells that develops with their tissue of residence and is involved in its homeostasis. *Cold Spring Harb Symp Quant Biol,* 78**,** 91-100.

GOODELL, M. A., BROSE, K., PARADIS, G., CONNER, A. S. & MULLIGAN, R. C. 1996. Isolation and functional properties of murine hematopoietic stem cells that are replicating in vivo. *J Exp Med,* 183**,** 1797-806.

GORDON, E. J., RAO, S., POLLARD, J. W., NUTT, S. L., LANG, R. A. & HARVEY, N. L. 2010. Macrophages define dermal lymphatic vessel calibre during development by regulating lymphatic endothelial cell proliferation. *Development,* 137**,** 3899-910.

GORDON, S. & TAYLOR, P. R. 2005. Monocyte and macrophage heterogeneity. *Nat Rev Immunol,* 5**,** 953-64.

GOUON-EVANS, V., ROTHENBERG, M. E. & POLLARD, J. W. 2000. Postnatal mammary gland development requires macrophages and eosinophils. *Development,* 127**,** 2269-82.

GRANT, M. B., MAY, W. S., CABALLERO, S., BROWN, G. A., GUTHRIE, S. M., MAMES, R. N., BYRNE, B. J., VAUGHT, T., SPOERRI, P. E., PECK, A. B. & SCOTT, E. W. 2002. Adult hematopoietic stem cells provide functional hemangioblast activity during retinal neovascularization. *Nat Med,* 8**,** 607-12.

GRUBER, P. J. & EPSTEIN, J. A. 2004. Development gone awry: congenital heart disease. *Circ Res,* 94**,** 273-83.

GRUNEWALD, M., AVRAHAM, I., DOR, Y., BACHAR-LUSTIG, E., ITIN, A., JUNG, S., CHIMENTI, S., LANDSMAN, L., ABRAMOVITCH, R. & KESHET, E. 2006. VEGF-induced adult neovascularization: recruitment, retention, and role of accessory cells. *Cell,* 124**,** 175-89.

GU, C., LIMBERG, B. J., WHITAKER, G. B., PERMAN, B., LEAHY, D. J., ROSENBAUM, J. S., GINTY, D. D. & KOLODKIN, A. L. 2002. Characterization of neuropilin-1 structural features that confer binding to semaphorin 3A and vascular endothelial growth factor 165. *J Biol Chem,* 277**,** 18069-76.

GU, C., RODRIGUEZ, E. R., REIMERT, D. V., SHU, T., FRITZSCH, B., RICHARDS, L. J., KOLODKIN, A. L. & GINTY, D. D. 2003. Neuropilin-1 conveys semaphorin and VEGF signaling during neural and cardiovascular development. *Dev Cell,* 5**,** 45-57.

GUILBERT, L. J. & STANLEY, E. R. 1980. Specific interaction of murine colony-stimulating factor with mononuclear phagocytic cells. *J Cell Biol,* 85**,** 153-9.

GUILLIAMS, M., DE KLEER, I., HENRI, S., POST, S., VANHOUTTE, L., DE PRIJCK, S., DESWARTE, K., MALISSEN, B., HAMMAD, H. & LAMBRECHT, B. N. 2013. Alveolar macrophages develop from fetal monocytes that differentiate into long-lived cells in the first week of life via GM-CSF. *J Exp Med,* 210**,** 1977-92.

HAGEDORN, L., SUTER, U. & SOMMER, L. 1999. P0 and PMP22 mark a multipotent neural crest-derived cell type that displays community effects in response to TGF-beta family factors. *Development,* 126**,** 3781-94.

HAGEMAN, G. S., LUTHERT, P. J., VICTOR CHONG, N. H., JOHNSON, L. V., ANDERSON, D. H. & MULLINS, R. F. 2001. An integrated hypothesis that considers drusen as biomarkers of immune-mediated processes at the RPE-Bruch's membrane interface in aging and age-related macular degeneration. *Prog Retin Eye Res,* 20**,** 705-32.

HAIGH, J. J., MORELLI, P. I., GERHARDT, H., HAIGH, K., TSIEN, J., DAMERT, A., MIQUEROL, L., MUHLNER, U., KLEIN, R., FERRARA, N., WAGNER, E. F., BETSHOLTZ, C. & NAGY, A. 2003. Cortical and retinal defects caused by dosage-dependent reductions in VEGF-A paracrine signaling. *Dev Biol,* 262**,** 225-41.

HAMILTON, D. L. & ABREMSKI, K. 1984. Site-specific recombination by the bacteriophage P1 lox-Cre system. Cre-mediated synapsis of two lox sites. *J Mol Biol,* 178**,** 481-6.

HARRISON, D. E., ZHONG, R. K., JORDAN, C. T., LEMISCHKA, I. R. & ASTLE, C. M. 1997. Relative to adult marrow, fetal liver repopulates nearly five times more effectively long-term than short-term. *Exp Hematol,* 25**,** 293-7.

HARVEY, R. P. 2002. Patterning the vertebrate heart. *Nat Rev Genet,* 3**,** 544-56.

HE, H., XU, J., WARREN, C. M., DUAN, D., LI, X., WU, L. & IRUELA-ARISPE, M. L. 2012. Endothelial cells provide an instructive niche for the differentiation and functional polarization of M2-like macrophages. *Blood,* 120**,** 3152-62.

HE, Z. & TESSIER-LAVIGNE, M. 1997. Neuropilin is a receptor for the axonal chemorepellent Semaphorin III. *Cell,* 90**,** 739-51.

HEIKINHEIMO, M., SCANDRETT, J. M. & WILSON, D. B. 1994. Localization of transcription factor GATA-4 to regions of the mouse embryo involved in cardiac development. *Dev Biol,* 164**,** 361-73.

HEISS, C., KEYMEL, S., NIESLER, U., ZIEMANN, J., KELM, M. & KALKA, C. 2005. Impaired progenitor cell activity in age-related endothelial dysfunction. *J Am Coll Cardiol,* 45**,** 1441-8.

HENDZEL, M. J., WEI, Y., MANCINI, M. A., VAN HOOSER, A., RANALLI, T., BRINKLEY, B. R., BAZETT-JONES, D. P. & ALLIS, C. D. 1997. Mitosis-specific phosphorylation of histone H3 initiates primarily within pericentromeric heterochromatin during G2 and spreads in an ordered fashion coincident with mitotic chromosome condensation. *Chromosoma,* 106**,** 348-60.

HERBST, S., SCHAIBLE, U. E. & SCHNEIDER, B. E. 2011. Interferon gamma activated macrophages kill mycobacteria by nitric oxide induced apoptosis. *PLoS One,* 6**,** e19105.

HERMAN, J. G. & MEADOWS, G. G. 2007. Increased class 3 semaphorin expression modulates the invasive and adhesive properties of prostate cancer cells. *Int J Oncol,* 30**,** 1231-8.

HERZOG, B., PELLET-MANY, C., BRITTON, G., HARTZOULAKIS, B. & ZACHARY, I. C. 2011. VEGF binding to NRP1 is essential for VEGF stimulation of endothelial cell migration, complex formation between NRP1 and VEGFR2, and signaling via FAK Tyr407 phosphorylation. *Mol Biol Cell,* 22**,** 2766-76.

HERZOG, Y., KALCHEIM, C., KAHANE, N., RESHEF, R. & NEUFELD, G. 2001. Differential expression of neuropilin-1 and neuropilin-2 in arteries and veins. *Mech Dev,* 109**,** 115-9.

HIGH, F. A., JAIN, R., STOLLER, J. Z., ANTONUCCI, N. B., LU, M. M., LOOMES, K. M., KAESTNER, K. H., PEAR, W. S. & EPSTEIN, J. A. 2009. Murine Jagged1/Notch signaling in the second heart field orchestrates Fgf8 expression and tissue-tissue interactions during outflow tract development. *J Clin Invest,* 119**,** 1986-96.

HILBE, W., DIRNHOFER, S., OBERWASSERLECHNER, F., SCHMID, T., GUNSILIUS, E., HILBE, G., WOLL, E. & KAHLER, C. M. 2004. CD133 positive endothelial progenitor cells contribute to the tumour vasculature in non-small cell lung cancer. *J Clin Pathol,* 57**,** 965-9.

HILL, J. M., ZALOS, G., HALCOX, J. P., SCHENKE, W. H., WACLAWIW, M. A., QUYYUMI, A. A. & FINKEL, T. 2003. Circulating endothelial progenitor cells, vascular function, and cardiovascular risk. *N Engl J Med,* 348**,** 593-600.

HIRATSUKA, S., MARU, Y., OKADA, A., SEIKI, M., NODA, T. & SHIBUYA, M. 2001. Involvement of Flt-1 tyrosine kinase (vascular endothelial growth factor receptor-1) in pathological angiogenesis. *Cancer Res,* 61**,** 1207-13.

HIRATSUKA, S., MINOWA, O., KUNO, J., NODA, T. & SHIBUYA, M. 1998. Flt-1 lacking the tyrosine kinase domain is sufficient for normal development and angiogenesis in mice. *Proc Natl Acad Sci U S A,* 95**,** 9349-54.

HIROI, Y., KUDOH, S., MONZEN, K., IKEDA, Y., YAZAKI, Y., NAGAI, R. & KOMURO, I. 2001. Tbx5 associates with Nkx2-5 and synergistically promotes cardiomyocyte differentiation. *Nat Genet,* 28**,** 276-80.

HIRSCHI, K. K. 2012. Hemogenic endothelium during development and beyond. *Blood,* 119**,** 4823-7.

HIRSCHI, K. K., INGRAM, D. A. & YODER, M. C. 2008. Assessing identity, phenotype, and fate of endothelial progenitor cells. *Arterioscler Thromb Vasc Biol,* 28**,** 1584-95.

HIRUMA, T., NAKAJIMA, Y. & NAKAMURA, H. 2002. Development of pharyngeal arch arteries in early mouse embryo. *J Anat,* 201**,** 15-29.

HOEBEN, A., LANDUYT, B., HIGHLEY, M. S., WILDIERS, H., VAN OOSTEROM, A. T. & DE BRUIJN, E. A. 2004. Vascular endothelial growth factor and angiogenesis. *Pharmacol Rev,* 56**,** 549-80.

HOEFFEL, G., WANG, Y., GRETER, M., SEE, P., TEO, P., MALLERET, B., LEBOEUF, M., LOW, D., OLLER, G., ALMEIDA, F., CHOY, S. H., GRISOTTO, M., RENIA, L., CONWAY, S. J., STANLEY, E. R., CHAN, J. K., NG, L. G., SAMOKHVALOV, I. M., MERAD, M. & GINHOUX, F. 2012. Adult Langerhans cells derive predominantly from embryonic fetal liver monocytes with a minor contribution of yolk sac-derived macrophages. *J Exp Med,* 209**,** 1167-81.

HOFFMAN, J. I. & KAPLAN, S. 2002. The incidence of congenital heart disease. *J Am Coll Cardiol,* 39**,** 1890-900.

HOLTWICK, R., GOTTHARDT, M., SKRYABIN, B., STEINMETZ, M., POTTHAST, R., ZETSCHE, B., HAMMER, R. E., HERZ, J. & KUHN, M. 2002. Smooth muscle-selective deletion of guanylyl cyclase-A prevents the acute but not chronic effects of ANP on blood pressure. *Proc Natl Acad Sci U S A,* 99**,** 7142-7.

HORB, M. E. & THOMSEN, G. H. 1999. Tbx5 is essential for heart development. *Development,* 126**,** 1739-51.

HOUSSAINT, E. 1981. Differentiation of the mouse hepatic primordium. II. Extrinsic origin of the haemopoietic cell line. *Cell Differ,* 10**,** 243-52.

HU, D. & CROSS, J. C. 2010. Development and function of trophoblast giant cells in the rodent placenta. *Int J Dev Biol,* 54**,** 341-54.

HUBER, T. L., KOUSKOFF, V., FEHLING, H. J., PALIS, J. & KELLER, G. 2004. Haemangioblast commitment is initiated in the primitive streak of the mouse embryo. *Nature,* 432**,** 625-30.

IDE, H., SELIGSON, D. B., MEMARZADEH, S., XIN, L., HORVATH, S., DUBEY, P., FLICK, M. B., KACINSKI, B. M., PALOTIE, A. & WITTE, O. N. 2002. Expression of colony-stimulating factor 1 receptor during prostate development and prostate cancer progression. *Proc Natl Acad Sci U S A,* 99**,** 14404-9.

INGRAM, D. A., MEAD, L. E., MOORE, D. B., WOODARD, W., FENOGLIO, A. & YODER, M. C. 2005. Vessel wall-derived endothelial cells rapidly proliferate because they contain a complete hierarchy of endothelial progenitor cells. *Blood,* 105**,** 2783-6.

ITALIANI, P. & BORASCHI, D. 2014. From Monocytes to M1/M2 Macrophages: Phenotypical vs. Functional Differentiation. *Front Immunol,* 5**,** 514.

ITAYA, M., SAKURAI, E., NOZAKI, M., YAMADA, K., YAMASAKI, S., ASAI, K. & OGURA, Y. 2007. Upregulation of VEGF in murine retina via monocyte recruitment after retinal scatter laser photocoagulation. *Invest Ophthalmol Vis Sci,* 48**,** 5677-83.

ITO, M. & YOSHIOKA, M. 1999. Regression of the hyaloid vessels and pupillary membrane of the mouse. *Anat Embryol (Berl),* 200**,** 403-11.

IVANOVA, A., SIGNORE, M., CARO, N., GREENE, N. D., COPP, A. J. & MARTINEZ-BARBERA, J. P. 2005. In vivo genetic ablation by Cre-mediated expression of diphtheria toxin fragment A. *Genesis,* 43**,** 129-35.

JAGANNATHAN-BOGDAN, M. & ZON, L. I. 2013. Hematopoiesis. *Development,* 140**,** 2463-7.

JAGER, R. D., MIELER, W. F. & MILLER, J. W. 2008. Age-related macular degeneration. *N Engl J Med,* 358**,** 2606-17.

JAKOBSSON, L., FRANCO, C. A., BENTLEY, K., COLLINS, R. T., PONSIOEN, B., ASPALTER, I. M., ROSEWELL, I., BUSSE, M., THURSTON, G., MEDVINSKY, A., SCHULTE-MERKER, S. & GERHARDT, H. 2010. Endothelial cells dynamically compete for the tip cell position during angiogenic sprouting. *Nat Cell Biol,* 12**,** 943-53.

JEGO, G., LANNEAU, D., DE THONEL, A., BERTHENET, K., HAZOUME, A., DROIN, N., HAMMAN, A., GIRODON, F., BELLAYE, P. S., WETTSTEIN, G., JACQUEL, A., DUPLOMB, L., LE MOUEL, A., PAPANAYOTOU, C., CHRISTIANS, E., BONNIAUD, P., LALLEMAND-MEZGER, V., SOLARY, E. & GARRIDO, C. 2014. Dual regulation of SPI1/PU.1 transcription factor by heat shock factor 1 (HSF1) during macrophage differentiation of monocytes. *Leukemia,* 28**,** 1676-86.

JI, R. P., PHOON, C. K., ARISTIZABAL, O., MCGRATH, K. E., PALIS, J. & TURNBULL, D. H. 2003. Onset of cardiac function during early mouse embryogenesis coincides with entry of primitive erythroblasts into the embryo proper. *Circ Res,* 92**,** 133-5.

JIA, H., CHENG, L., TICKNER, M., BAGHERZADEH, A., SELWOOD, D. & ZACHARY, I. 2010. Neuropilin-1 antagonism in human carcinoma cells inhibits migration and enhances chemosensitivity. *Br J Cancer,* 102**,** 541-52.

JIANG, X., ROWITCH, D. H., SORIANO, P., MCMAHON, A. P. & SUCOV, H. M. 2000. Fate of the mammalian cardiac neural crest. *Development,* 127**,** 1607-16.

JOKHI, P. P., CHUMBLEY, G., KING, A., GARDNER, L. & LOKE, Y. W. 1993. Expression of the colony stimulating factor-1 receptor (c-fms product) by cells at the human uteroplacental interface. *Lab Invest,* 68**,** 308-20.

JONES, E. A., YUAN, L., BREANT, C., WATTS, R. J. & EICHMANN, A. 2008. Separating genetic and hemodynamic defects in neuropilin 1 knockout embryos. *Development,* 135**,** 2479-88.

JOYAL, J. S., SITARAS, N., BINET, F., RIVERA, J. C., STAHL, A., ZANIOLO, K., SHAO, Z., POLOSA, A., ZHU, T., HAMEL, D., DJAVARI, M., KUNIK, D., HONORE, J. C., PICARD, E., ZABEIDA, A., VARMA, D. R., HICKSON, G., MANCINI, J., KLAGSBRUN, M., COSTANTINO, S., BEAUSEJOUR, C., LACHAPELLE, P., SMITH, L. E., CHEMTOB, S. & SAPIEHA, P. 2011. Ischemic neurons prevent vascular regeneration of neural tissue by secreting semaphorin 3A. *Blood,* 117**,** 6024-35.

KAARTINEN, V., DUDAS, M., NAGY, A., SRIDURONGRIT, S., LU, M. M. & EPSTEIN, J. A. 2004. Cardiac outflow tract defects in mice lacking ALK2 in neural crest cells. *Development,* 131**,** 3481-90.

KANNO, S., ODA, N., ABE, M., TERAI, Y., ITO, M., SHITARA, K., TABAYASHI, K., SHIBUYA, M. & SATO, Y. 2000. Roles of two VEGF receptors, Flt-1 and KDR, in the signal transduction of VEGF effects in human vascular endothelial cells. *Oncogene,* 19**,** 2138-46.

KARKKAINEN, M. J., HAIKO, P., SAINIO, K., PARTANEN, J., TAIPALE, J., PETROVA, T. V., JELTSCH, M., JACKSON, D. G., TALIKKA, M., RAUVALA, H., BETSHOLTZ, C. & ALITALO, K. 2004. Vascular endothelial growth factor C is required for sprouting of the first lymphatic vessels from embryonic veins. *Nat Immunol,* 5**,** 74-80.

KAWASAKI, T., KITSUKAWA, T., BEKKU, Y., MATSUDA, Y., SANBO, M., YAGI, T. & FUJISAWA, H. 1999. A requirement for neuropilin-1 in embryonic vessel formation. *Development,* 126**,** 4895-902.

KELLY, R. G. 2012. The second heart field. *Curr Top Dev Biol,* 100**,** 33-65.

KERJASCHKI, D., HUTTARY, N., RAAB, I., REGELE, H., BOJARSKI-NAGY, K., BARTEL, G., KROBER, S. M., GREINIX, H., ROSENMAIER, A., KARLHOFER, F., WICK, N. & MAZAL, P. R. 2006. Lymphatic endothelial progenitor cells contribute to de novo lymphangiogenesis in human renal transplants. *Nat Med,* 12**,** 230-4.

KEYTE, A. & HUTSON, M. R. 2012. The neural crest in cardiac congenital anomalies. *Differentiation,* 84**,** 25-40.

KINDER, S. J., TSANG, T. E., QUINLAN, G. A., HADJANTONAKIS, A. K., NAGY, A. & TAM, P. P. 1999. The orderly allocation of mesodermal cells to the extraembryonic structures and the anteroposterior axis during gastrulation of the mouse embryo. *Development,* 126**,** 4691-701.

KING, B. F. 1993. Development and structure of the placenta and fetal membranes of nonhuman primates. *J Exp Zool,* 266**,** 528-40.

KIRBY, M. L. 1987. Cardiac morphogenesis--recent research advances. *Pediatr Res,* 21**,** 219-24.

KIRBY, M. L., GALE, T. F. & STEWART, D. E. 1983. Neural crest cells contribute to normal aorticopulmonary septation. *Science,* 220**,** 1059-61.

KIRBY, M. L. & HUTSON, M. R. 2010. Factors controlling cardiac neural crest cell migration. *Cell Adh Migr,* 4**,** 609-21.

KISANUKI, Y. Y., HAMMER, R. E., MIYAZAKI, J., WILLIAMS, S. C., RICHARDSON, J. A. & YANAGISAWA, M. 2001. Tie2-Cre transgenic mice: a new model for endothelial cell-lineage analysis in vivo. *Dev Biol,* 230**,** 230-42.

KITSUKAWA, T., SHIMIZU, M., SANBO, M., HIRATA, T., TANIGUCHI, M., BEKKU, Y., YAGI, T. & FUJISAWA, H. 1997. Neuropilin-semaphorin III/D-mediated chemorepulsive signals play a crucial role in peripheral nerve projection in mice. *Neuron,* 19**,** 995-1005.

KITSUKAWA, T., SHIMONO, A., KAWAKAMI, A., KONDOH, H. & FUJISAWA, H. 1995. Overexpression of a membrane protein, neuropilin, in chimeric mice causes anomalies in the cardiovascular system, nervous system and limbs. *Development,* 121**,** 4309-18.

KLIMP, A. H., HOLLEMA, H., KEMPINGA, C., VAN DER ZEE, A. G., DE VRIES, E. G. & DAEMEN, T. 2001. Expression of cyclooxygenase-2 and inducible nitric oxide synthase in human ovarian tumors and tumor-associated macrophages. *Cancer Res,* 61**,** 7305-9.

KNIESEL, U. & WOLBURG, H. 2000. Tight junctions of the blood-brain barrier. *Cell Mol Neurobiol,* 20**,** 57-76.

KOCH, A. E., POLVERINI, P. J., KUNKEL, S. L., HARLOW, L. A., DIPIETRO, L. A., ELNER, V. M., ELNER, S. G. & STRIETER, R. M. 1992. Interleukin-8 as a macrophage-derived mediator of angiogenesis. *Science,* 258**,** 1798-801.

KOCH, S., TUGUES, S., LI, X., GUALANDI, L. & CLAESSON-WELSH, L. 2011. Signal transduction by vascular endothelial growth factor receptors. *Biochem J,* 437**,** 169-83.

KOCHER, A. A., SCHUSTER, M. D., SZABOLCS, M. J., TAKUMA, S., BURKHOFF, D., WANG, J., HOMMA, S., EDWARDS, N. M. & ITESCU, S. 2001. Neovascularization of ischemic myocardium by human bone-marrow-derived angioblasts prevents cardiomyocyte apoptosis, reduces remodeling and improves cardiac function. *Nat Med,* 7**,** 430-6.

KOLODKIN, A. L., LEVENGOOD, D. V., ROWE, E. G., TAI, Y. T., GIGER, R. J. & GINTY, D. D. 1997. Neuropilin is a semaphorin III receptor. *Cell,* 90**,** 753-62.

KONDO, T., HAYASHI, M., TAKESHITA, K., NUMAGUCHI, Y., KOBAYASHI, K., IINO, S., INDEN, Y. & MUROHARA, T. 2004. Smoking cessation rapidly increases circulating progenitor cells in peripheral blood in chronic smokers. *Arterioscler Thromb Vasc Biol,* 24**,** 1442-7.

KRAUSE, D. S., ITO, T., FACKLER, M. J., SMITH, O. M., COLLECTOR, M. I., SHARKIS, S. J. & MAY, W. S. 1994. Characterization of murine CD34, a marker for hematopoietic progenitor and stem cells. *Blood,* 84**,** 691-701.

KRETZER, F. L., MEHTA, R. S., JOHNSON, A. T., HUNTER, D. G., BROWN, E. S. & HITTNER, H. M. 1984. Vitamin E protects against retinopathy of prematurity through action on spindle cells. *Nature,* 309**,** 793-5.

KRISHNAN, A., SAMTANI, R., DHANANTWARI, P., LEE, E., YAMADA, S., SHIOTA, K., DONOFRIO, M. T., LEATHERBURY, L. & LO, C. W. 2014. A detailed comparison of mouse and human cardiac development. *Pediatr Res,* 76**,** 500-7.

KRYSINSKA, H., HOOGENKAMP, M., INGRAM, R., WILSON, N., TAGOH, H., LASLO, P., SINGH, H. & BONIFER, C. 2007. A two-step, PU.1-dependent mechanism for developmentally regulated chromatin remodeling and transcription of the c-fms gene. *Mol Cell Biol,* 27**,** 878-87.

KUBALAK, S. W., HUTSON, D. R., SCOTT, K. K. & SHANNON, R. A. 2002. Elevated transforming growth factor beta2 enhances apoptosis and contributes to abnormal outflow tract and aortic sac development in retinoic X receptor alpha knockout embryos. *Development,* 129**,** 733-46.

KUBOTA, H., AVARBOCK, M. R. & BRINSTER, R. L. 2003. Spermatogonial stem cells share some, but not all, phenotypic and functional characteristics with other stem cells. *Proc Natl Acad Sci U S A,* 100**,** 6487-92.

KUBOTA, Y., TAKUBO, K., HIRASHIMA, M., NAGOSHI, N., KISHI, K., OKUNO, Y., NAKAMURA-ISHIZU, A., SANO, K., MURAKAMI, M., EMA, M., OMATSU, Y., TAKAHASHI, S., NAGASAWA, T., SHIBUYA, M., OKANO, H. & SUDA, T. 2011. Isolation and function of mouse tissue resident vascular precursors marked by myelin protein zero. *J Exp Med,* 208**,** 949-60.

KUCIA, M., RECA, R., JALA, V. R., DAWN, B., RATAJCZAK, J. & RATAJCZAK, M. Z. 2005. Bone marrow as a home of heterogenous populations of nonhematopoietic stem cells. *Leukemia,* 19**,** 1118-27.

KUHN, A., BRACHTENDORF, G., KURTH, F., SONNTAG, M., SAMULOWITZ, U., METZE, D. & VESTWEBER, D. 2002. Expression of endomucin, a novel endothelial sialomucin, in normal and diseased human skin. *J Invest Dermatol,* 119**,** 1388-93.

KUME, T. 2010. Specification of arterial, venous, and lymphatic endothelial cells during embryonic development. *Histol Histopathol,* 25**,** 637-46.

LAIRD, P. W., ZIJDERVELD, A., LINDERS, K., RUDNICKI, M. A., JAENISCH, R. & BERNS, A. 1991. Simplified mammalian DNA isolation procedure. *Nucleic Acids Res,* 19**,** 4293.

LAMBERT, V., LECOMTE, J., HANSEN, S., BLACHER, S., GONZALEZ, M. L., STRUMAN, I., SOUNNI, N. E., ROZET, E., DE TULLIO, P., FOIDART, J. M., RAKIC, J. M. & NOEL, A. 2013. Laser-induced choroidal neovascularization model to study age-related macular degeneration in mice. *Nat Protoc,* 8**,** 2197-211.

LAMOUILLE, S., XU, J. & DERYNCK, R. 2014. Molecular mechanisms of epithelial-mesenchymal transition. *Nat Rev Mol Cell Biol,* 15**,** 178-96.

LANAHAN, A., ZHANG, X., FANTIN, A., ZHUANG, Z., RIVERA-MOLINA, F., SPEICHINGER, K., PRAHST, C., ZHANG, J., WANG, Y., DAVIS, G., TOOMRE, D., RUHRBERG, C. & SIMONS, M. 2013. The neuropilin 1 cytoplasmic domain is required for VEGF-A-dependent arteriogenesis. *Dev Cell,* 25**,** 156-68.

LANAHAN, A. A., HERMANS, K., CLAES, F., KERLEY-HAMILTON, J. S., ZHUANG, Z. W., GIORDANO, F. J., CARMELIET, P. & SIMONS, M. 2010. VEGF receptor 2 endocytic trafficking regulates arterial morphogenesis. *Dev Cell,* 18**,** 713-24.

LANGE, C., EHLKEN, C., STAHL, A., MARTIN, G., HANSEN, L. & AGOSTINI, H. T. 2009. Kinetics of retinal vaso-obliteration and neovascularisation in the oxygen-induced retinopathy (OIR) mouse model. *Graefes Arch Clin Exp Ophthalmol,* 247**,** 1205-11.

LAWSON, N. D., VOGEL, A. M. & WEINSTEIN, B. M. 2002. sonic hedgehog and vascular endothelial growth factor act upstream of the Notch pathway during arterial endothelial differentiation. *Dev Cell,* 3**,** 127-36.

LE NOBLE, F., MOYON, D., PARDANAUD, L., YUAN, L., DJONOV, V., MATTHIJSEN, R., BREANT, C., FLEURY, V. & EICHMANN, A. 2004. Flow regulates arterial-venous differentiation in the chick embryo yolk sac. *Development,* 131**,** 361-75.

LEAK, L. V. & BURKE, J. F. 1966. Fine structure of the lymphatic capillary and the adjoining connective tissue area. *Am J Anat,* 118**,** 785-809.

LEE, C. C., KREUSCH, A., MCMULLAN, D., NG, K. & SPRAGGON, G. 2003. Crystal structure of the human neuropilin-1 b1 domain. *Structure,* 11**,** 99-108.

LEE, J. Y., PARK, C., CHO, Y. P., LEE, E., KIM, H., KIM, P., YUN, S. H. & YOON, Y. S. 2010. Podoplanin-expressing cells derived from bone marrow play a crucial role in postnatal lymphatic neovascularization. *Circulation,* 122**,** 1413-25.

LEE, P., GOISHI, K., DAVIDSON, A. J., MANNIX, R., ZON, L. & KLAGSBRUN, M. 2002. Neuropilin-1 is required for vascular development and is a mediator of VEGF-dependent angiogenesis in zebrafish. *Proc Natl Acad Sci U S A,* 99**,** 10470-5.

LEEK, R. D., HUNT, N. C., LANDERS, R. J., LEWIS, C. E., ROYDS, J. A. & HARRIS, A. L. 2000. Macrophage infiltration is associated with VEGF and EGFR expression in breast cancer. *J Pathol,* 190**,** 430-6.

LEIBOVICH, S. J., POLVERINI, P. J., SHEPARD, H. M., WISEMAN, D. M., SHIVELY, V. & NUSEIR, N. 1987. Macrophage-induced angiogenesis is mediated by tumour necrosis factor-alpha. *Nature,* 329**,** 630-2.

LEONG, K. G., NIESSEN, K., KULIC, I., RAOUF, A., EAVES, C., POLLET, I. & KARSAN, A. 2007. Jagged1-mediated Notch activation induces epithelial-to-mesenchymal transition through Slug-induced repression of E-cadherin. *J Exp Med,* 204**,** 2935-48.

LEONHARDT, A., GLASER, A., WEGMANN, M., SCHRANZ, D., SEYBERTH, H. & NUSING, R. 2003. Expression of prostanoid receptors in human ductus arteriosus. *Br J Pharmacol,* 138**,** 655-9.

LEPORE, J. J., CHENG, L., MIN LU, M., MERICKO, P. A., MORRISEY, E. E. & PARMACEK, M. S. 2005. High-efficiency somatic mutagenesis in smooth muscle cells and cardiac myocytes in SM22alpha-Cre transgenic mice. *Genesis,* 41**,** 179-84.

LEPORE, J. J., MERICKO, P. A., CHENG, L., LU, M. M., MORRISEY, E. E. & PARMACEK, M. S. 2006. GATA-6 regulates semaphorin 3C and is required in cardiac neural crest for cardiovascular morphogenesis. *J Clin Invest,* 116**,** 929-39.

LEWIS, C. E., LEEK, R., HARRIS, A. & MCGEE, J. O. 1995. Cytokine regulation of angiogenesis in breast cancer: the role of tumor-associated macrophages. *J Leukoc Biol,* 57**,** 747-51.

LEWIS, J. S., LANDERS, R. J., UNDERWOOD, J. C., HARRIS, A. L. & LEWIS, C. E. 2000. Expression of vascular endothelial growth factor by macrophages is up-regulated in poorly vascularized areas of breast carcinomas. *J Pathol,* 192**,** 150-8.

LI, A., CHENG, X. J., MORO, A., SINGH, R. K., HINES, O. J. & EIBL, G. 2011. CXCR2-Dependent Endothelial Progenitor Cell Mobilization in Pancreatic Cancer Growth. *Transl Oncol,* 4**,** 20-8.

LI, Q., GUO, Z. K., CHANG, Y. Q., YU, X., LI, C. X. & LI, H. 2015. Gata4, Tbx5 and Baf60c induce differentiation of adipose tissue-derived mesenchymal stem cells into beating cardiomyocytes. *Int J Biochem Cell Biol,* 66**,** 30-36.

LI, Z., LAN, Y., HE, W., CHEN, D., WANG, J., ZHOU, F., WANG, Y., SUN, H., CHEN, X., XU, C., LI, S., PANG, Y., ZHANG, G., YANG, L., ZHU, L., FAN, M., SHANG, A., JU, Z., LUO, L., DING, Y., GUO, W., YUAN, W., YANG, X. & LIU, B. 2012. Mouse embryonic head as a site for hematopoietic stem cell development. *Cell Stem Cell,* 11**,** 663-75.

LIAO, S. & PADERA, T. P. 2013. Lymphatic function and immune regulation in health and disease. *Lymphat Res Biol,* 11**,** 136-43.

LICHANSKA, A. M., BROWNE, C. M., HENKEL, G. W., MURPHY, K. M., OSTROWSKI, M. C., MCKERCHER, S. R., MAKI, R. A. & HUME, D. A. 1999. Differentiation of the mononuclear phagocyte system during mouse embryogenesis: the role of transcription factor PU.1. *Blood,* 94**,** 127-38.

LIM, L. S., MITCHELL, P., SEDDON, J. M., HOLZ, F. G. & WONG, T. Y. 2012. Age-related macular degeneration. *Lancet,* 379**,** 1728-38.

LIN, E. Y., LI, J. F., GNATOVSKIY, L., DENG, Y., ZHU, L., GRZESIK, D. A., QIAN, H., XUE, X. N. & POLLARD, J. W. 2006. Macrophages regulate the angiogenic switch in a mouse model of breast cancer. *Cancer Res,* 66**,** 11238-46.

LIN, E. Y., NGUYEN, A. V., RUSSELL, R. G. & POLLARD, J. W. 2001. Colony-stimulating factor 1 promotes progression of mammary tumors to malignancy. *J Exp Med,* 193**,** 727-40.

LIN, F. J., CHEN, X., QIN, J., HONG, Y. K., TSAI, M. J. & TSAI, S. Y. 2010. Direct transcriptional regulation of neuropilin-2 by COUP-TFII modulates

multiple steps in murine lymphatic vessel development. *J Clin Invest,* 120**,** 1694-707.

LIN, H., LEE, E., HESTIR, K., LEO, C., HUANG, M., BOSCH, E., HALENBECK, R., WU, G., ZHOU, A., BEHRENS, D., HOLLENBAUGH, D., LINNEMANN, T., QIN, M., WONG, J., CHU, K., DOBERSTEIN, S. K. & WILLIAMS, L. T. 2008. Discovery of a cytokine and its receptor by functional screening of the extracellular proteome. *Science,* 320**,** 807-11.

LINTS, T. J., PARSONS, L. M., HARTLEY, L., LYONS, I. & HARVEY, R. P. 1993. Nkx-2.5: a novel murine homeobox gene expressed in early heart progenitor cells and their myogenic descendants. *Development,* 119**,** 419-31.

LIU, C., SHAO, Z. M., ZHANG, L., BEATTY, P., SARTIPPOUR, M., LANE, T., LIVINGSTON, E. & NGUYEN, M. 2001. Human endomucin is an endothelial marker. *Biochem Biophys Res Commun,* 288**,** 129-36.

LIU, J., COPLAND, D. A., HORIE, S., WU, W. K., CHEN, M., XU, Y., PAUL MORGAN, B., MACK, M., XU, H., NICHOLSON, L. B. & DICK, A. D. 2013. Myeloid cells expressing VEGF and arginase-1 following uptake of damaged retinal pigment epithelium suggests potential mechanism that drives the onset of choroidal angiogenesis in mice. *PLoS One,* 8**,** e72935.

LIU, W., SELEVER, J., WANG, D., LU, M. F., MOSES, K. A., SCHWARTZ, R. J. & MARTIN, J. F. 2004. Bmp4 signaling is required for outflow-tract septation and branchial-arch artery remodeling. *Proc Natl Acad Sci U S A,* 101**,** 4489-94.

LLOYD, J. B., BRENT, R. L. & BECKMAN, D. A. 1996. Sources of amino acids for protein synthesis during early organogenesis in the rat. 3. Methionine incorporation. *Placenta,* 17**,** 629-34.

LUO, J., ELWOOD, F., BRITSCHGI, M., VILLEDA, S., ZHANG, H., DING, Z., ZHU, L., ALABSI, H., GETACHEW, R., NARASIMHAN, R., WABL, R., FAINBERG, N., JAMES, M. L., WONG, G., RELTON, J., GAMBHIR, S. S., POLLARD, J. W. & WYSS-CORAY, T. 2013. Colony-stimulating factor 1 receptor (CSF1R) signaling in injured neurons facilitates protection and survival. *J Exp Med,* 210**,** 157-72.

LUTTUN, A., TJWA, M., MOONS, L., WU, Y., ANGELILLO-SCHERRER, A., LIAO, F., NAGY, J. A., HOOPER, A., PRILLER, J., DE KLERCK, B., COMPERNOLLE, V., DACI, E., BOHLEN, P., DEWERCHIN, M., HERBERT, J. M., FAVA, R., MATTHYS, P., CARMELIET, G., COLLEN, D., DVORAK, H. F., HICKLIN, D. J. & CARMELIET, P. 2002. Revascularization of ischemic tissues by PlGF treatment, and inhibition of tumor angiogenesis, arthritis and atherosclerosis by anti-Flt1. *Nat Med,* 8**,** 831-40.

MA, H. Y., XU, J., ENG, D., GROSS, M. K. & KIOUSSI, C. 2013. Pitx2-mediated cardiac outflow tract remodeling. *Dev Dyn,* 242**,** 456-68.

MACATEE, T. L., HAMMOND, B. P., ARENKIEL, B. R., FRANCIS, L., FRANK, D. U. & MOON, A. M. 2003. Ablation of specific expression domains reveals discrete functions of ectoderm- and endoderm-derived FGF8 during cardiovascular and pharyngeal development. *Development,* 130**,** 6361-74.

MADEN, C. H., GOMES, J., SCHWARZ, Q., DAVIDSON, K., TINKER, A. & RUHRBERG, C. 2012. NRP1 and NRP2 cooperate to regulate gangliogenesis, axon guidance and target innervation in the sympathetic nervous system. *Dev Biol,* 369**,** 277-85.

MADISEN, L., ZWINGMAN, T. A., SUNKIN, S. M., OH, S. W., ZARIWALA, H. A., GU, H., NG, L. L., PALMITER, R. D., HAWRYLYCZ, M. J., JONES, A. R., LEIN, E. S. & ZENG, H. 2010. A robust and high-throughput Cre reporting and characterization system for the whole mouse brain. *Nat Neurosci,* 13**,** 133-40.

MAIONE, F., MOLLA, F., MEDA, C., LATINI, R., ZENTILIN, L., GIACCA, M., SEANO, G., SERINI, G., BUSSOLINO, F. & GIRAUDO, E. 2009. Semaphorin 3A is an endogenous angiogenesis inhibitor that blocks tumor growth and normalizes tumor vasculature in transgenic mouse models. *J Clin Invest,* 119**,** 3356-72.

MAMLUK, R., GECHTMAN, Z., KUTCHER, M. E., GASIUNAS, N., GALLAGHER, J. & KLAGSBRUN, M. 2002. Neuropilin-1 binds vascular endothelial growth factor 165, placenta growth factor-2, and heparin via its b1b2 domain. *J Biol Chem,* 277**,** 24818-25.

MANTOVANI, A., SCHIOPPA, T., PORTA, C., ALLAVENA, P. & SICA, A. 2006. Role of tumor-associated macrophages in tumor progression and invasion. *Cancer Metastasis Rev,* 25**,** 315-22.

MANTOVANI, A., SICA, A., SOZZANI, S., ALLAVENA, P., VECCHI, A. & LOCATI, M. 2004. The chemokine system in diverse forms of macrophage activation and polarization. *Trends Immunol,* 25**,** 677-86.

MARCELO, K. L., SILLS, T. M., COSKUN, S., VASAVADA, H., SANGLIKAR, S., GOLDIE, L. C. & HIRSCHI, K. K. 2013. Hemogenic endothelial cell specification requires c-Kit, Notch signaling, and p27-mediated cell-cycle control. *Dev Cell,* 27**,** 504-15.

MARKS, S. C., JR. & LANE, P. W. 1976. Osteopetrosis, a new recessive skeletal mutation on chromosome 12 of the mouse. *J Hered,* 67**,** 11-18.

MARKWALD, R. R., KROOK, J. M., KITTEN, G. T. & RUNYAN, R. B. 1981. Endocardial cushion tissue development: structural analyses on the attachment of extracellular matrix to migrating mesenchymal cell surfaces. *Scan Electron Microsc***,** 261-74.

MARTINEZ, F. O. & GORDON, S. 2014. The M1 and M2 paradigm of macrophage activation: time for reassessment. *F1000Prime Rep,* 6**,** 13.

MASSA, M., ROSTI, V., FERRARIO, M., CAMPANELLI, R., RAMAJOLI, I., ROSSO, R., DE FERRARI, G. M., FERLINI, M., GOFFREDO, L., BERTOLETTI, A., KLERSY, C., PECCI, A., MORATTI, R. & TAVAZZI, L. 2005. Increased circulating hematopoietic and endothelial progenitor cells in the early phase of acute myocardial infarction. *Blood,* 105**,** 199-206.

MATTHEWS, W., JORDAN, C. T., GAVIN, M., JENKINS, N. A., COPELAND, N. G. & LEMISCHKA, I. R. 1991. A receptor tyrosine kinase cDNA isolated from a population of enriched primitive hematopoietic cells and exhibiting close genetic linkage to c-kit. *Proc Natl Acad Sci U S A,* 88**,** 9026-30.

MATTIONI, T., LOUVION, J. F. & PICARD, D. 1994. Regulation of protein activities by fusion to steroid binding domains. *Methods Cell Biol,* 43 Pt A**,** 335-52.

MCCOLM, J. R., GEISEN, P. & HARTNETT, M. E. 2004. VEGF isoforms and their expression after a single episode of hypoxia or repeated fluctuations between hyperoxia and hypoxia: relevance to clinical ROP. *Mol Vis,* 10**,** 512-20.

MCCULLEY, D. J., KANG, J. O., MARTIN, J. F. & BLACK, B. L. 2008. BMP4 is required in the anterior heart field and its derivatives for endocardial cushion

remodeling, outflow tract septation, and semilunar valve development. *Dev Dyn,* 237**,** 3200-9.

MCKENNEY, J. K., WEISS, S. W. & FOLPE, A. L. 2001. CD31 expression in intratumoral macrophages: a potential diagnostic pitfall. *Am J Surg Pathol,* 25**,** 1167-73.

MCKERCHER, S. R., TORBETT, B. E., ANDERSON, K. L., HENKEL, G. W., VESTAL, D. J., BARIBAULT, H., KLEMSZ, M., FEENEY, A. J., WU, G. E., PAIGE, C. J. & MAKI, R. A. 1996. Targeted disruption of the PU.1 gene results in multiple hematopoietic abnormalities. *Embo J,* 15**,** 5647-58.

MCLAREN, J., PRENTICE, A., CHARNOCK-JONES, D. S., MILLICAN, S. A., MULLER, K. H., SHARKEY, A. M. & SMITH, S. K. 1996. Vascular endothelial growth factor is produced by peritoneal fluid macrophages in endometriosis and is regulated by ovarian steroids. *J Clin Invest,* 98**,** 482-9.

MCLENNAN, R., TEDDY, J. M., KASEMEIER-KULESA, J. C., ROMINE, M. H. & KULESA, P. M. 2010. Vascular endothelial growth factor (VEGF) regulates cranial neural crest migration in vivo. *Dev Biol,* 339**,** 114-25.

MEDVINSKY, A. & DZIERZAK, E. 1996. Definitive hematopoiesis is autonomously initiated by the AGM region. *Cell,* 86**,** 897-906.

MEILHAC, S. M., ESNER, M., KELLY, R. G., NICOLAS, J. F. & BUCKINGHAM, M. E. 2004. The clonal origin of myocardial cells in different regions of the embryonic mouse heart. *Dev Cell,* 6**,** 685-98.

MELLICK, A. S., PLUMMER, P. N., NOLAN, D. J., GAO, D., BAMBINO, K., HAHN, M., CATENA, R., TURNER, V., MCDONNELL, K., BENEZRA, R., BRINK, R., SWARBRICK, A. & MITTAL, V. 2010. Using the transcription factor inhibitor of DNA binding 1 to selectively target endothelial progenitor cells offers novel strategies to inhibit tumor angiogenesis and growth. *Cancer Res,* 70**,** 7273-82.

MIAO, H. Q., SOKER, S., FEINER, L., ALONSO, J. L., RAPER, J. A. & KLAGSBRUN, M. 1999. Neuropilin-1 mediates collapsin-1/semaphorin III inhibition of endothelial cell motility: functional competition of collapsin-1 and vascular endothelial growth factor-165. *J Cell Biol,* 146**,** 233-42.

MILDE, F., LAUW, S., KOUMOUTSAKOS, P. & IRUELA-ARISPE, M. L. 2013. The mouse retina in 3D: quantification of vascular growth and remodeling. *Integr Biol (Camb),* 5**,** 1426-38.

MILLAUER, B., WIZIGMANN-VOOS, S., SCHNURCH, H., MARTINEZ, R., MOLLER, N. P., RISAU, W. & ULLRICH, A. 1993. High affinity VEGF binding and developmental expression suggest Flk-1 as a major regulator of vasculogenesis and angiogenesis. *Cell,* 72**,** 835-46.

MIQUEROL, L., GERTSENSTEIN, M., HARPAL, K., ROSSANT, J. & NAGY, A. 1999. Multiple developmental roles of VEGF suggested by a LacZ-tagged allele. *Dev Biol,* 212**,** 307-22.

MITCHELL, C. A., RISAU, W. & DREXLER, H. C. 1998. Regression of vessels in the tunica vasculosa lentis is initiated by coordinated endothelial apoptosis: a role for vascular endothelial growth factor as a survival factor for endothelium. *Dev Dyn,* 213**,** 322-33.

MITTAL, A., PULINA, M., HOU, S. Y. & ASTROF, S. 2013. Fibronectin and integrin alpha 5 play requisite roles in cardiac morphogenesis. *Dev Biol,* 381**,** 73-82.

MORRISON, S. J., HEMMATI, H. D., WANDYCZ, A. M. & WEISSMAN, I. L. 1995. The purification and characterization of fetal liver hematopoietic stem cells. *Proc Natl Acad Sci U S A,* 92**,** 10302-6.

MUKOUYAMA, Y. S., GERBER, H. P., FERRARA, N., GU, C. & ANDERSON, D. J. 2005. Peripheral nerve-derived VEGF promotes arterial differentiation via neuropilin 1-mediated positive feedback. *Development,* 132**,** 941-52.

MULLER, A. M., MEDVINSKY, A., STROUBOULIS, J., GROSVELD, F. & DZIERZAK, E. 1994. Development of hematopoietic stem cell activity in the mouse embryo. *Immunity,* 1**,** 291-301.

MULLER, Y. A., CHRISTINGER, H. W., KEYT, B. A. & DE VOS, A. M. 1997. The crystal structure of vascular endothelial growth factor (VEGF) refined to 1.93 A resolution: multiple copy flexibility and receptor binding. *Structure,* 5**,** 1325-38.

MURGA, M., FERNANDEZ-CAPETILLO, O. & TOSATO, G. 2005. Neuropilin-1 regulates attachment in human endothelial cells independently of vascular endothelial growth factor receptor-2. *Blood,* 105**,** 1992-9.

NADIN, B. M., GOODELL, M. A. & HIRSCHI, K. K. 2003. Phenotype and hematopoietic potential of side population cells throughout embryonic development. *Blood,* 102**,** 2436-43.

NAGASAWA, T., HIROTA, S., TACHIBANA, K., TAKAKURA, N., NISHIKAWA, S., KITAMURA, Y., YOSHIDA, N., KIKUTANI, H. & KISHIMOTO, T. 1996. Defects of B-cell lymphopoiesis and bone-marrow myelopoiesis in mice lacking the CXC chemokine PBSF/SDF-1. *Nature,* 382**,** 635-8.

NAGY, A. 2000. Cre recombinase: the universal reagent for genome tailoring. *Genesis,* 26**,** 99-109.

NAKAMURA, F., TANAKA, M., TAKAHASHI, T., KALB, R. G. & STRITTMATTER, S. M. 1998. Neuropilin-1 extracellular domains mediate semaphorin D/III-induced growth cone collapse. *Neuron,* 21**,** 1093-100.

NAKANO, A., HARADA, T., MORIKAWA, S. & KATO, Y. 1990. Expression of leukocyte common antigen (CD45) on various human leukemia/lymphoma cell lines. *Acta Pathol Jpn,* 40**,** 107-15.

NAKANO, H., LIU, X., ARSHI, A., NAKASHIMA, Y., VAN HANDEL, B., SASIDHARAN, R., HARMON, A. W., SHIN, J. H., SCHWARTZ, R. J., CONWAY, S. J., HARVEY, R. P., PASHMFOROUSH, M., MIKKOLA, H. K. & NAKANO, A. 2013. Haemogenic endocardium contributes to transient definitive haematopoiesis. *Nat Commun,* 4**,** 1564.

NAKAO, S., KUWANO, T., TSUTSUMI-MIYAHARA, C., UEDA, S., KIMURA, Y. N., HAMANO, S., SONODA, K. H., SAIJO, Y., NUKIWA, T., STRIETER, R. M., ISHIBASHI, T., KUWANO, M. & ONO, M. 2005. Infiltration of COX-2-expressing macrophages is a prerequisite for IL-1 beta-induced neovascularization and tumor growth. *J Clin Invest,* 115**,** 2979-91.

NAUG, H. L., BROWNING, J., GOLE, G. A. & GOBE, G. 2000. Vitreal macrophages express vascular endothelial growth factor in oxygen-induced retinopathy. *Clin Experiment Ophthalmol,* 28**,** 48-52.

NIESSEN, K., FU, Y., CHANG, L., HOODLESS, P. A., MCFADDEN, D. & KARSAN, A. 2008. Slug is a direct Notch target required for initiation of cardiac cushion cellularization. *J Cell Biol,* 182**,** 315-25.

NISHIKAWA, S. I., NISHIKAWA, S., HIRASHIMA, M., MATSUYOSHI, N. & KODAMA, H. 1998. Progressive lineage analysis by cell sorting and culture

identifies FLK1+VE-cadherin+ cells at a diverging point of endothelial and hemopoietic lineages. *Development,* 125**,** 1747-57.

NISHIMURA, R., KAWASAKI, T., SEKINE, A., SUDA, R., URUSHIBARA, T., SUZUKI, T., TAKAYANAGI, S., TERADA, J., SAKAO, S. & TATSUMI, K. 2014. Hypoxia-induced proliferation of tissue-resident endothelial progenitor cells in the lung. *Am J Physiol Lung Cell Mol Physiol***,** ajplung 00243 2014.

NOGUCHI, S., MIYAUCHI, K., IMAOKA, S. & KOYAMA, H. 1988. Inability of tamoxifen to penetrate into cerebrospinal fluid. *Breast Cancer Res Treat,* 12**,** 317-8.

NOLAN, D. J., CIARROCCHI, A., MELLICK, A. S., JAGGI, J. S., BAMBINO, K., GUPTA, S., HEIKAMP, E., MCDEVITT, M. R., SCHEINBERG, D. A., BENEZRA, R. & MITTAL, V. 2007. Bone marrow-derived endothelial progenitor cells are a major determinant of nascent tumor neovascularization. *Genes Dev,* 21**,** 1546-58.

NOMURA-KITABAYASHI, A., PHOON, C. K., KISHIGAMI, S., ROSENTHAL, J., YAMAUCHI, Y., ABE, K., YAMAMURA, K., SAMTANI, R., LO, C. W. & MISHINA, Y. 2009. Outflow tract cushions perform a critical valve-like function in the early embryonic heart requiring BMPRIA-mediated signaling in cardiac neural crest. *Am J Physiol Heart Circ Physiol,* 297**,** H1617-28.

NOORT, A. R., VAN ZOEST, K. P., WEIJERS, E. M., KOOLWIJK, P., MARACLE, C. X., NOVACK, D. V., SIEMERINK, M. J., SCHLINGEMANN, R. O., TAK, P. P. & TAS, S. W. 2014. NF-kappaB-inducing kinase is a key regulator of inflammation-induced and tumour-associated angiogenesis. *J Pathol,* 234**,** 375-85.

NOVAK, A., GUO, C., YANG, W., NAGY, A. & LOBE, C. G. 2000. Z/EG, a double reporter mouse line that expresses enhanced green fluorescent protein upon Cre-mediated excision. *Genesis,* 28**,** 147-55.

OKABE, K., KOBAYASHI, S., YAMADA, T., KURIHARA, T., TAI-NAGARA, I., MIYAMOTO, T., MUKOUYAMA, Y. S., SATO, T. N., SUDA, T., EMA, M. & KUBOTA, Y. 2014. Neurons limit angiogenesis by titrating VEGF in retina. *Cell,* 159**,** 584-96.

OKAZAKI, T., EBIHARA, S., TAKAHASHI, H., ASADA, M., KANDA, A. & SASAKI, H. 2005. Macrophage colony-stimulating factor induces vascular endothelial growth factor production in skeletal muscle and promotes tumor angiogenesis. *J Immunol,* 174**,** 7531-8.

OKUNO, Y., NAKAMURA-ISHIZU, A., KISHI, K., SUDA, T. & KUBOTA, Y. 2011. Bone marrow-derived cells serve as proangiogenic macrophages but not endothelial cells in wound healing. *Blood,* 117**,** 5264-72.

OKUNO, Y., NAKAMURA-ISHIZU, A., OTSU, K., SUDA, T. & KUBOTA, Y. 2012. Pathological neoangiogenesis depends on oxidative stress regulation by ATM. *Nat Med,* 18**,** 1208-16.

OLSON, M. C., SCOTT, E. W., HACK, A. A., SU, G. H., TENEN, D. G., SINGH, H. & SIMON, M. C. 1995. PU. 1 is not essential for early myeloid gene expression but is required for terminal myeloid differentiation. *Immunity,* 3**,** 703-14.

OLSSON, A. K., DIMBERG, A., KREUGER, J. & CLAESSON-WELSH, L. 2006. VEGF receptor signalling - in control of vascular function. *Nat Rev Mol Cell Biol,* 7**,** 359-71.

OVCHINNIKOV, D. A., DEBATS, C. E., SESTER, D. P., SWEET, M. J. & HUME, D. A. 2010. A conserved distal segment of the mouse CSF-1 receptor promoter is required for maximal expression of a reporter gene in macrophages and osteoclasts of transgenic mice. *J Leukoc Biol,* 87**,** 815-22.

OZAKI, H., YU, A. Y., DELLA, N., OZAKI, K., LUNA, J. D., YAMADA, H., HACKETT, S. F., OKAMOTO, N., ZACK, D. J., SEMENZA, G. L. & CAMPOCHIARO, P. A. 1999. Hypoxia inducible factor-1alpha is increased in ischemic retina: temporal and spatial correlation with VEGF expression. *Invest Ophthalmol Vis Sci,* 40**,** 182-9.

OZERDEM, U., GRAKO, K. A., DAHLIN-HUPPE, K., MONOSOV, E. & STALLCUP, W. B. 2001. NG2 proteoglycan is expressed exclusively by mural cells during vascular morphogenesis. *Dev Dyn,* 222**,** 218-27.

PALIS, J., ROBERTSON, S., KENNEDY, M., WALL, C. & KELLER, G. 1999. Development of erythroid and myeloid progenitors in the yolk sac and embryo proper of the mouse. *Development,* 126**,** 5073-84.

PARK, E. J., OGDEN, L. A., TALBOT, A., EVANS, S., CAI, C. L., BLACK, B. L., FRANK, D. U. & MOON, A. M. 2006. Required, tissue-specific roles for Fgf8 in outflow tract formation and remodeling. *Development,* 133**,** 2419-33.

PARK, J. E., KELLER, G. A. & FERRARA, N. 1993. The vascular endothelial growth factor (VEGF) isoforms: differential deposition into the subepithelial extracellular matrix and bioactivity of extracellular matrix-bound VEGF. *Mol Biol Cell,* 4**,** 1317-26.

PARK, K. J., PARK, E., LIU, E. & BAKER, A. J. 2014. Bone marrow-derived endothelial progenitor cells protect postischemic axons after traumatic brain injury. *J Cereb Blood Flow Metab,* 34**,** 357-66.

PASTERKAMP, R. J. 2012. Getting neural circuits into shape with semaphorins. *Nat Rev Neurosci,* 13**,** 605-18.

PATEL, A. S., SMITH, A., NUCERA, S., BIZIATO, D., SAHA, P., ATTIA, R. Q., HUMPHRIES, J., MATTOCK, K., GROVER, S. P., LYONS, O. T., GUIDOTTI, L. G., SIOW, R., IVETIC, A., EGGINTON, S., WALTHAM, M., NALDINI, L., DE PALMA, M. & MODARAI, B. 2013. TIE2-expressing monocytes/macrophages regulate revascularization of the ischemic limb. *EMBO Mol Med,* 5**,** 858-69.

PAU, H. 2008. Retinopathy of prematurity: clinic and pathogenesis. Disproportion between apoptosis of vitreal and proliferation of retinal vascularization. *Ophthalmologica,* 222**,** 220-4.

PAYE, J. M., PHNG, L. K., LANAHAN, A. A., GERHARD, H. & SIMONS, M. 2009. Synectin-dependent regulation of arterial maturation. *Dev Dyn,* 238**,** 604-10.

PEICHEV, M., NAIYER, A. J., PEREIRA, D., ZHU, Z., LANE, W. J., WILLIAMS, M., OZ, M. C., HICKLIN, D. J., WITTE, L., MOORE, M. A. & RAFII, S. 2000. Expression of VEGFR-2 and AC133 by circulating human CD34(+) cells identifies a population of functional endothelial precursors. *Blood,* 95**,** 952-8.

PEIRSON, S. N., BUTLER, J. N. & FOSTER, R. G. 2003. Experimental validation of novel and conventional approaches to quantitative real-time PCR data analysis. *Nucleic Acids Res,* 31**,** e73.

PENG, Y., LIU, Y. M., LI, L. C., WANG, L. L. & WU, X. L. 2014. MicroRNA-338 inhibits growth, invasion and metastasis of gastric cancer by targeting NRP1 expression. *PLoS One,* 9**,** e94422.

PETERSEN, P. H., ZOU, K., HWANG, J. K., JAN, Y. N. & ZHONG, W. 2002. Progenitor cell maintenance requires numb and numblike during mouse neurogenesis. *Nature,* 419**,** 929-34.

PHELPS, D. L. 1995. Retinopathy of prematurity. *Pediatr Rev,* 16**,** 50-6.

PICARD, D. 1994. Regulation of protein function through expression of chimaeric proteins. *Curr Opin Biotechnol,* 5**,** 511-5.

PIEDRAFITA, D., PARSONS, J. C., SANDEMAN, R. M., WOOD, P. R., ESTUNINGSIH, S. E., PARTOUTOMO, S. & SPITHILL, T. W. 2001. Antibody-dependent cell-mediated cytotoxicity to newly excysted juvenile Fasciola hepatica in vitro is mediated by reactive nitrogen intermediates. *Parasite Immunol,* 23**,** 473-82.

PIERCE, E. A., AVERY, R. L., FOLEY, E. D., AIELLO, L. P. & SMITH, L. E. 1995. Vascular endothelial growth factor/vascular permeability factor expression in a mouse model of retinal neovascularization. *Proc Natl Acad Sci U S A,* 92**,** 905-9.

PIETRAS, E. M., WARR, M. R. & PASSEGUE, E. 2011. Cell cycle regulation in hematopoietic stem cells. *J Cell Biol,* 195**,** 709-20.

PITULESCU, M. E., SCHMIDT, I., BENEDITO, R. & ADAMS, R. H. 2010. Inducible gene targeting in the neonatal vasculature and analysis of retinal angiogenesis in mice. *Nat Protoc,* 5**,** 1518-34.

PLEIN, A., FANTIN, A. & RUHRBERG, C. 2014. Neuropilin regulation of angiogenesis, arteriogenesis, and vascular permeability. *Microcirculation,* 21**,** 315-23.

PLEIN, A., FANTIN, A. & RUHRBERG, C. 2015a. Neural crest cells in cardiovascular development. *Curr Top Dev Biol,* 111**,** 183-200.

PLEIN, A., RUHRBERG, C. & FANTIN, A. 2015b. The mouse hindbrain: an in vivo model to analyze developmental angiogenesis. *Methods Mol Biol,* 1214**,** 29-40.

PLUMMER, P. N., FREEMAN, R., TAFT, R. J., VIDER, J., SAX, M., UMER, B. A., GAO, D., JOHNS, C., MATTICK, J. S., WILTON, S. D., FERRO, V., MCMILLAN, N. A., SWARBRICK, A., MITTAL, V. & MELLICK, A. S. 2013. MicroRNAs regulate tumor angiogenesis modulated by endothelial progenitor cells. *Cancer Res,* 73**,** 341-52.

POLLARD, J. W. 2009. Trophic macrophages in development and disease. *Nat Rev Immunol,* 9**,** 259-70.

POLTORAK, Z., COHEN, T., SIVAN, R., KANDELIS, Y., SPIRA, G., VLODAVSKY, I., KESHET, E. & NEUFELD, G. 1997. VEGF145, a secreted vascular endothelial growth factor isoform that binds to extracellular matrix. *J Biol Chem,* 272**,** 7151-8.

PORRAS, D. & BROWN, C. B. 2008. Temporal-spatial ablation of neural crest in the mouse results in cardiovascular defects. *Dev Dyn,* 237**,** 153-62.

PORTER, A. G. & JANICKE, R. U. 1999. Emerging roles of caspase-3 in apoptosis. *Cell Death Differ,* 6**,** 99-104.

POWNER, M. B., VEVIS, K., MCKENZIE, J. A., GANDHI, P., JADEJA, S. & FRUTTIGER, M. 2012. Visualization of gene expression in whole mouse retina by in situ hybridization. *Nat Protoc,* 7**,** 1086-96.

PRAHST, C., HEROULT, M., LANAHAN, A. A., UZIEL, N., KESSLER, O., SHRAGA-HELED, N., SIMONS, M., NEUFELD, G. & AUGUSTIN, H. G. 2008. Neuropilin-1-VEGFR-2 complexing requires the PDZ-binding domain of neuropilin-1. *J Biol Chem,* 283**,** 25110-4.

PROKOPI, M., PULA, G., MAYR, U., DEVUE, C., GALLAGHER, J., XIAO, Q., BOULANGER, C. M., WESTWOOD, N., URBICH, C., WILLEIT, J., STEINER, M., BREUSS, J., XU, Q., KIECHL, S. & MAYR, M. 2009. Proteomic analysis reveals presence of platelet microparticles in endothelial progenitor cell cultures. *Blood,* 114**,** 723-32.

QIAN, B. Z., LI, J., ZHANG, H., KITAMURA, T., ZHANG, J., CAMPION, L. R., KAISER, E. A., SNYDER, L. A. & POLLARD, J. W. 2011. CCL2 recruits inflammatory monocytes to facilitate breast-tumour metastasis. *Nature,* 475**,** 222-5.

QUIRICI, N., SOLIGO, D., CANEVA, L., SERVIDA, F., BOSSOLASCO, P. & DELILIERS, G. L. 2001. Differentiation and expansion of endothelial cells from human bone marrow CD133(+) cells. *Br J Haematol,* 115**,** 186-94.

RAAB, S., BECK, H., GAUMANN, A., YUCE, A., GERBER, H. P., PLATE, K., HAMMES, H. P., FERRARA, N. & BREIER, G. 2004. Impaired brain angiogenesis and neuronal apoptosis induced by conditional homozygous inactivation of vascular endothelial growth factor. *Thromb Haemost,* 91**,** 595-605.

RAFII, S., MOHLE, R., SHAPIRO, F., FREY, B. M. & MOORE, M. A. 1997. Regulation of hematopoiesis by microvascular endothelium. *Leuk Lymphoma,* 27**,** 375-86.

RAFII, S., SHAPIRO, F., PETTENGELL, R., FERRIS, B., NACHMAN, R. L., MOORE, M. A. & ASCH, A. S. 1995. Human bone marrow microvascular endothelial cells support long-term proliferation and differentiation of myeloid and megakaryocytic progenitors. *Blood,* 86**,** 3353-63.

RAIMONDI, C., FANTIN, A., LAMPROPOULOU, A., DENTI, L., CHIKH, A. & RUHRBERG, C. 2014. Imatinib inhibits VEGF-independent angiogenesis by targeting neuropilin 1-dependent ABL1 activation in endothelial cells. *J Exp Med,* 211**,** 1167-83.

REBEL, V. I., MILLER, C. L., EAVES, C. J. & LANSDORP, P. M. 1996. The repopulation potential of fetal liver hematopoietic stem cells in mice exceeds that of their liver adult bone marrow counterparts. *Blood,* 87**,** 3500-7.

REHMAN, J., LI, J., ORSCHELL, C. M. & MARCH, K. L. 2003. Peripheral blood "endothelial progenitor cells" are derived from monocyte/macrophages and secrete angiogenic growth factors. *Circulation,* 107**,** 1164-9.

REIFERS, F., WALSH, E. C., LEGER, S., STAINIER, D. Y. & BRAND, M. 2000. Induction and differentiation of the zebrafish heart requires fibroblast growth factor 8 (fgf8/acerebellar). *Development,* 127**,** 225-35.

RELIGA, P., CAO, R., BJORNDAHL, M., ZHOU, Z., ZHU, Z. & CAO, Y. 2005. Presence of bone marrow-derived circulating progenitor endothelial cells in the newly formed lymphatic vessels. *Blood,* 106**,** 4184-90.

REYES, M., DUDEK, A., JAHAGIRDAR, B., KOODIE, L., MARKER, P. H. & VERFAILLIE, C. M. 2002. Origin of endothelial progenitors in human postnatal bone marrow. *J Clin Invest,* 109**,** 337-46.

RIA, R., PICCOLI, C., CIRULLI, T., FALZETTI, F., MANGIALARDI, G., GUIDOLIN, D., TABILIO, A., DI RENZO, N., GUARINI, A., RIBATTI, D., DAMMACCO, F. & VACCA, A. 2008. Endothelial differentiation of hematopoietic stem and progenitor cells from patients with multiple myeloma. *Clin Cancer Res,* 14**,** 1678-85.

RISAU, W. & FLAMME, I. 1995. Vasculogenesis. *Annu Rev Cell Dev Biol,* 11**,** 73-91.

RITTER, M. R., BANIN, E., MORENO, S. K., AGUILAR, E., DORRELL, M. I. & FRIEDLANDER, M. 2006. Myeloid progenitors differentiate into microglia and promote vascular repair in a model of ischemic retinopathy. *J Clin Invest,* 116**,** 3266-76.

ROBIN, C., BOLLEROT, K., MENDES, S., HAAK, E., CRISAN, M., CERISOLI, F., LAUW, I., KAIMAKIS, P., JORNA, R., VERMEULEN, M., KAYSER, M., VAN DER LINDEN, R., IMANIRAD, P., VERSTEGEN, M., NAWAZ-YOUSAF, H., PAPAZIAN, N., STEEGERS, E., CUPEDO, T. & DZIERZAK, E. 2009. Human placenta is a potent hematopoietic niche containing hematopoietic stem and progenitor cells throughout development. *Cell Stem Cell,* 5**,** 385-95.

ROCHA, S. F., SCHILLER, M., JING, D., LI, H., BUTZ, S., VESTWEBER, D., BILJES, D., DREXLER, H. C., NIEMINEN-KELHA, M., VAJKOCZY, P., ADAMS, S., BENEDITO, R. & ADAMS, R. H. 2014. Esm1 modulates endothelial tip cell behavior and vascular permeability by enhancing VEGF bioavailability. *Circ Res,* 115**,** 581-90.

ROGOVE, A. D., LU, W. & TSIRKA, S. E. 2002. Microglial activation and recruitment, but not proliferation, suffice to mediate neurodegeneration. *Cell Death Differ,* 9**,** 801-6.

ROHDE, E., BARTMANN, C., SCHALLMOSER, K., REINISCH, A., LANZER, G., LINKESCH, W., GUELLY, C. & STRUNK, D. 2007. Immune cells mimic the morphology of endothelial progenitor colonies in vitro. *Stem Cells,* 25**,** 1746-52.

ROHDE, E., MALISCHNIK, C., THALER, D., MAIERHOFER, T., LINKESCH, W., LANZER, G., GUELLY, C. & STRUNK, D. 2006. Blood monocytes mimic endothelial progenitor cells. *Stem Cells,* 24**,** 357-67.

ROHM, B., OTTEMEYER, A., LOHRUM, M. & PUSCHEL, A. W. 2000. Plexin/neuropilin complexes mediate repulsion by the axonal guidance signal semaphorin 3A. *Mech Dev,* 93**,** 95-104.

ROSSANT, J. 1996. Mouse mutants and cardiac development: new molecular insights into cardiogenesis. *Circ Res,* 78**,** 349-53.

ROSSIGNOL, M., GAGNON, M. L. & KLAGSBRUN, M. 2000. Genomic organization of human neuropilin-1 and neuropilin-2 genes: identification and distribution of splice variants and soluble isoforms. *Genomics,* 70**,** 211-22.

RUEDIGER, T., ZIMMER, G., BARCHMANN, S., CASTELLANI, V., BAGNARD, D. & BOLZ, J. 2013. Integration of opposing semaphorin guidance cues in cortical axons. *Cereb Cortex,* 23**,** 604-14.

RUHRBERG, C. 2003. Growing and shaping the vascular tree: multiple roles for VEGF. *Bioessays,* 25**,** 1052-60.

RUHRBERG, C. & BAUTCH, V. L. 2013. Neurovascular development and links to disease. *Cell Mol Life Sci,* 70**,** 1675-84.

RUHRBERG, C., GERHARDT, H., GOLDING, M., WATSON, R., IOANNIDOU, S., FUJISAWA, H., BETSHOLTZ, C. & SHIMA, D. T. 2002. Spatially restricted patterning cues provided by heparin-binding VEGF-A control blood vessel branching morphogenesis. *Genes Dev,* 16**,** 2684-98.

RUSSELL, J. S. & BROWN, J. M. 2014. Circulating mouse Flk1+/c-Kit+/CD45- cells function as endothelial progenitors cells (EPCs) and stimulate the growth of human tumor xenografts. *Mol Cancer,* 13**,** 177.

SABINE, V. S., FARATIAN, D., KIRKEGAARD-CLAUSEN, T. & BARTLETT, J. M. 2012. Validation of activated caspase-3 antibody staining as a marker of apoptosis in breast cancer. *Histopathology,* 60**,** 369-71.

SAGA, Y., KITAJIMA, S. & MIYAGAWA-TOMITA, S. 2000. Mesp1 expression is the earliest sign of cardiovascular development. *Trends Cardiovasc Med,* 10**,** 345-52.

SAKABE, M., IKEDA, K., NAKATANI, K., KAWADA, N., IMANAKA-YOSHIDA, K., YOSHIDA, T., YAMAGISHI, T. & NAKAJIMA, Y. 2006. Rho kinases regulate endothelial invasion and migration during valvuloseptal endocardial cushion tissue formation. *Dev Dyn,* 235**,** 94-104.

SAKURAI, E., ANAND, A., AMBATI, B. K., VAN ROOIJEN, N. & AMBATI, J. 2003. Macrophage depletion inhibits experimental choroidal neovascularization. *Invest Ophthalmol Vis Sci,* 44**,** 3578-85.

SALVEN, P., MUSTJOKI, S., ALITALO, R., ALITALO, K. & RAFII, S. 2003. VEGFR-3 and CD133 identify a population of CD34+ lymphatic/vascular endothelial precursor cells. *Blood,* 101**,** 168-72.

SALVESEN, H. B. & AKSLEN, L. A. 1999. Significance of tumour-associated macrophages, vascular endothelial growth factor and thrombospondin-1 expression for tumour angiogenesis and prognosis in endometrial carcinomas. *Int J Cancer,* 84**,** 538-43.

SANDSTEDT, J., JONSSON, M., DELLGREN, G., LINDAHL, A., JEPPSSON, A. & ASP, J. 2014. Human C-kit+CD45- cardiac stem cells are heterogeneous and display both cardiac and endothelial commitment by single-cell qPCR analysis. *Biochem Biophys Res Commun,* 443**,** 234-8.

SANFORD, L. P., ORMSBY, I., GITTENBERGER-DE GROOT, A. C., SARIOLA, H., FRIEDMAN, R., BOIVIN, G. P., CARDELL, E. L. & DOETSCHMAN, T. 1997. TGFbeta2 knockout mice have multiple developmental defects that are non-overlapping with other TGFbeta knockout phenotypes. *Development,* 124**,** 2659-70.

SASMONO, R. T., OCEANDY, D., POLLARD, J. W., TONG, W., PAVLI, P., WAINWRIGHT, B. J., OSTROWSKI, M. C., HIMES, S. R. & HUME, D. A. 2003. A macrophage colony-stimulating factor receptor-green fluorescent protein transgene is expressed throughout the mononuclear phagocyte system of the mouse. *Blood,* 101**,** 1155-63.

SATO, A., SCHOLL, A. M., KUHN, E. N., STADT, H. A., DECKER, J. R., PEGRAM, K., HUTSON, M. R. & KIRBY, M. L. 2011. FGF8 signaling is chemotactic for cardiac neural crest cells. *Dev Biol,* 354**,** 18-30.

SAWADA, M., ITOH, Y., SUZUMURA, A. & MARUNOUCHI, T. 1993. Expression of cytokine receptors in cultured neuronal and glial cells. *Neurosci Lett,* 160**,** 131-4.

SAWAMIPHAK, S., RITTER, M. & ACKER-PALMER, A. 2010. Preparation of retinal explant cultures to study ex vivo tip endothelial cell responses. *Nat Protoc,* 5**,** 1659-65.

SCAVELLI, C., NICO, B., CIRULLI, T., RIA, R., DI PIETRO, G., MANGIERI, D., BACIGALUPO, A., MANGIALARDI, G., COLUCCIA, A. M., CARAVITA, T., MOLICA, S., RIBATTI, D., DAMMACCO, F. & VACCA, A. 2008. Vasculogenic mimicry by bone marrow macrophages in patients with multiple myeloma. *Oncogene,* 27**,** 663-74.

SCHMEISSER, A., GARLICHS, C. D., ZHANG, H., ESKAFI, S., GRAFFY, C., LUDWIG, J., STRASSER, R. H. & DANIEL, W. G. 2001. Monocytes

coexpress endothelial and macrophagocytic lineage markers and form cord-like structures in Matrigel under angiogenic conditions. *Cardiovasc Res,* 49**,** 671-80.

SCHNEIDER, D. J. & MOORE, J. W. 2006. Patent ductus arteriosus. *Circulation,* 114**,** 1873-82.

SCHNIEDERMANN, J., RENNECKE, M., BUTTLER, K., RICHTER, G., STADTLER, A. M., NORGALL, S., BADAR, M., BARLEON, B., MAY, T., WILTING, J. & WEICH, H. A. 2010. Mouse lung contains endothelial progenitors with high capacity to form blood and lymphatic vessels. *BMC Cell Biol,* 11**,** 50.

SCHULTE-MERKER, S., SABINE, A. & PETROVA, T. V. 2011. Lymphatic vascular morphogenesis in development, physiology, and disease. *J Cell Biol,* 193**,** 607-18.

SCHULTHEISS, T. M., BURCH, J. B. & LASSAR, A. B. 1997. A role for bone morphogenetic proteins in the induction of cardiac myogenesis. *Genes Dev,* 11**,** 451-62.

SCHULZ, C., GOMEZ PERDIGUERO, E., CHORRO, L., SZABO-ROGERS, H., CAGNARD, N., KIERDORF, K., PRINZ, M., WU, B., JACOBSEN, S. E., POLLARD, J. W., FRAMPTON, J., LIU, K. J. & GEISSMANN, F. 2012. A lineage of myeloid cells independent of Myb and hematopoietic stem cells. *Science,* 336**,** 86-90.

SCHWARTZ, S. M. & BENDITT, E. P. 1976. Clustering of replicating cells in aortic endothelium. *Proc Natl Acad Sci U S A,* 73**,** 651-3.

SCHWARTZ, S. M. & BENDITT, E. P. 1977. Aortic endothelial cell replication. I. Effects of age and hypertension in the rat. *Circ Res,* 41**,** 248-55.

SCHWARZ, Q., GU, C., FUJISAWA, H., SABELKO, K., GERTSENSTEIN, M., NAGY, A., TANIGUCHI, M., KOLODKIN, A. L., GINTY, D. D., SHIMA, D. T. & RUHRBERG, C. 2004. Vascular endothelial growth factor controls neuronal migration and cooperates with Sema3A to pattern distinct compartments of the facial nerve. *Genes Dev,* 18**,** 2822-34.

SCHWARZ, Q. & RUHRBERG, C. 2010. Neuropilin, you gotta let me know: should I stay or should I go? *Cell Adh Migr,* 4**,** 61-6.

SCOTT, A., POWNER, M. B., GANDHI, P., CLARKIN, C., GUTMANN, D. H., JOHNSON, R. S., FERRARA, N. & FRUTTIGER, M. 2010. Astrocyte-derived vascular endothelial growth factor stabilizes vessels in the developing retinal vasculature. *PLoS One,* 5**,** e11863.

SCOTT, E. W., SIMON, M. C., ANASTASI, J. & SINGH, H. 1994. Requirement of transcription factor PU.1 in the development of multiple hematopoietic lineages. *Science,* 265**,** 1573-7.

SERINI, G., VALDEMBRI, D., ZANIVAN, S., MORTERRA, G., BURKHARDT, C., CACCAVARI, F., ZAMMATARO, L., PRIMO, L., TAMAGNONE, L., LOGAN, M., TESSIER-LAVIGNE, M., TANIGUCHI, M., PUSCHEL, A. W. & BUSSOLINO, F. 2003. Class 3 semaphorins control vascular morphogenesis by inhibiting integrin function. *Nature,* 424**,** 391-7.

SHALABY, F., ROSSANT, J., YAMAGUCHI, T. P., GERTSENSTEIN, M., WU, X. F., BREITMAN, M. L. & SCHUH, A. C. 1995. Failure of blood-island formation and vasculogenesis in Flk-1-deficient mice. *Nature,* 376**,** 62-6.

SHARMA, P. R., ANDERSON, R. H., COPP, A. J. & HENDERSON, D. J. 2004. Spatiotemporal analysis of programmed cell death during mouse cardiac septation. *Anat Rec A Discov Mol Cell Evol Biol,* 277**,** 355-69.

SHEN, J., XIE, B., DONG, A., SWAIM, M., HACKETT, S. F. & CAMPOCHIARO, P. A. 2007. In vivo immunostaining demonstrates macrophages associate with growing and regressing vessels. *Invest Ophthalmol Vis Sci,* 48**,** 4335-41.

SHIMIZU, M., MURAKAMI, Y., SUTO, F. & FUJISAWA, H. 2000. Determination of cell adhesion sites of neuropilin-1. *J Cell Biol,* 148**,** 1283-93.

SHIN, J. Y., HU, W., NARAMURA, M. & PARK, C. Y. 2014. High c-Kit expression identifies hematopoietic stem cells with impaired self-renewal and megakaryocytic bias. *J Exp Med,* 211**,** 217-31.

SHOJI, W., ISOGAI, S., SATO-MAEDA, M., OBINATA, M. & KUWADA, J. Y. 2003. Semaphorin3a1 regulates angioblast migration and vascular development in zebrafish embryos. *Development,* 130**,** 3227-36.

SHORTT, A. J., HOWELL, K., O'BRIEN, C. & MCLOUGHLIN, P. 2004. Chronic systemic hypoxia causes intra-retinal angiogenesis. *J Anat,* 205**,** 349-56.

SILVER, L. & PALIS, J. 1997. Initiation of murine embryonic erythropoiesis: a spatial analysis. *Blood,* 89**,** 1154-64.

SMITH, L. E., WESOLOWSKI, E., MCLELLAN, A., KOSTYK, S. K., D'AMATO, R., SULLIVAN, R. & D'AMORE, P. A. 1994. Oxygen-induced retinopathy in the mouse. *Invest Ophthalmol Vis Sci,* 35**,** 101-11.

SOKER, S., FIDDER, H., NEUFELD, G. & KLAGSBRUN, M. 1996. Characterization of novel vascular endothelial growth factor (VEGF) receptors on tumor cells that bind VEGF165 via its exon 7-encoded domain. *J Biol Chem,* 271**,** 5761-7.

SOKER, S., MIAO, H. Q., NOMI, M., TAKASHIMA, S. & KLAGSBRUN, M. 2002. VEGF165 mediates formation of complexes containing VEGFR-2 and neuropilin-1 that enhance VEGF165-receptor binding. *J Cell Biochem,* 85**,** 357-68.

SOKER, S., TAKASHIMA, S., MIAO, H. Q., NEUFELD, G. & KLAGSBRUN, M. 1998. Neuropilin-1 is expressed by endothelial and tumor cells as an isoform-specific receptor for vascular endothelial growth factor. *Cell,* 92**,** 735-45.

SOLWAY, J., SELTZER, J., SAMAHA, F. F., KIM, S., ALGER, L. E., NIU, Q., MORRISEY, E. E., IP, H. S. & PARMACEK, M. S. 1995. Structure and expression of a smooth muscle cell-specific gene, SM22 alpha. *J Biol Chem,* 270**,** 13460-9.

SORENSEN, I., ADAMS, R. H. & GOSSLER, A. 2009. DLL1-mediated Notch activation regulates endothelial identity in mouse fetal arteries. *Blood,* 113**,** 5680-8.

SORIANO, P. 1999. Generalized lacZ expression with the ROSA26 Cre reporter strain. *Nat Genet,* 21**,** 70-1.

SOROKIN, S. P. & HOYT, R. F., JR. 1992. Macrophage development: I. Rationale for using Griffonia simplicifolia isolectin B4 as a marker for the line. *Anat Rec,* 232**,** 520-6.

SOUFAN, A. T., VAN DEN BERG, G., RUIJTER, J. M., DE BOER, P. A., VAN DEN HOFF, M. J. & MOORMAN, A. F. 2006. Regionalized sequence of myocardial cell growth and proliferation characterizes early chamber formation. *Circ Res,* 99**,** 545-52.

SPOONER, C. J., CHENG, J. X., PUJADAS, E., LASLO, P. & SINGH, H. 2009. A recurrent network involving the transcription factors PU.1 and Gfi1 orchestrates innate and adaptive immune cell fates. *Immunity,* 31**,** 576-86.

SRINIVAS, S., WATANABE, T., LIN, C. S., WILLIAM, C. M., TANABE, Y., JESSELL, T. M. & COSTANTINI, F. 2001. Cre reporter strains produced by

targeted insertion of EYFP and ECFP into the ROSA26 locus. *BMC Dev Biol,* 1**,** 4.

SRINIVASAN, R. S., DILLARD, M. E., LAGUTIN, O. V., LIN, F. J., TSAI, S., TSAI, M. J., SAMOKHVALOV, I. M. & OLIVER, G. 2007. Lineage tracing demonstrates the venous origin of the mammalian lymphatic vasculature. *Genes Dev,* 21**,** 2422-32.

STAHL, A., CONNOR, K. M., SAPIEHA, P., CHEN, J., DENNISON, R. J., KRAH, N. M., SEAWARD, M. R., WILLETT, K. L., ADERMAN, C. M., GUERIN, K. I., HUA, J., LOFQVIST, C., HELLSTROM, A. & SMITH, L. E. 2010. The mouse retina as an angiogenesis model. *Invest Ophthalmol Vis Sci,* 51**,** 2813-26.

STALMANS, I. 2005. Role of the vascular endothelial growth factor isoforms in retinal angiogenesis and DiGeorge syndrome. *Verh K Acad Geneeskd Belg,* 67**,** 229-76.

STALMANS, I., LAMBRECHTS, D., DE SMET, F., JANSEN, S., WANG, J., MAITY, S., KNEER, P., VON DER OHE, M., SWILLEN, A., MAES, C., GEWILLIG, M., MOLIN, D. G., HELLINGS, P., BOETEL, T., HAARDT, M., COMPERNOLLE, V., DEWERCHIN, M., PLAISANCE, S., VLIETINCK, R., EMANUEL, B., GITTENBERGER-DE GROOT, A. C., SCAMBLER, P., MORROW, B., DRISCOL, D. A., MOONS, L., ESGUERRA, C. V., CARMELIET, G., BEHN-KRAPPA, A., DEVRIENDT, K., COLLEN, D., CONWAY, S. J. & CARMELIET, P. 2003. VEGF: a modifier of the del22q11 (DiGeorge) syndrome? *Nat Med,* 9**,** 173-82.

STALMANS, I., NG, Y. S., ROHAN, R., FRUTTIGER, M., BOUCHE, A., YUCE, A., FUJISAWA, H., HERMANS, B., SHANI, M., JANSEN, S., HICKLIN, D., ANDERSON, D. J., GARDINER, T., HAMMES, H. P., MOONS, L., DEWERCHIN, M., COLLEN, D., CARMELIET, P. & D'AMORE, P. A. 2002. Arteriolar and venular patterning in retinas of mice selectively expressing VEGF isoforms. *J Clin Invest,* 109**,** 327-36.

STANCZUK, L., MARTINEZ-CORRAL, I., ULVMAR, M. H., ZHANG, Y., LAVINA, B., FRUTTIGER, M., ADAMS, R. H., SAUR, D., BETSHOLTZ, C., ORTEGA, S., ALITALO, K., GRAUPERA, M. & MAKINEN, T. 2015. cKit Lineage Hemogenic Endothelium-Derived Cells Contribute to Mesenteric Lymphatic Vessels. *Cell Rep*.

STEFATER, J. A., 3RD, LEWKOWICH, I., RAO, S., MARIGGI, G., CARPENTER, A. C., BURR, A. R., FAN, J., AJIMA, R., MOLKENTIN, J. D., WILLIAMS, B. O., WILLS-KARP, M., POLLARD, J. W., YAMAGUCHI, T., FERRARA, N., GERHARDT, H. & LANG, R. A. 2011. Regulation of angiogenesis by a non-canonical Wnt-Flt1 pathway in myeloid cells. *Nature,* 474**,** 511-5.

STENZEL, D., LUNDKVIST, A., SAUVAGET, D., BUSSE, M., GRAUPERA, M., VAN DER FLIER, A., WIJELATH, E. S., MURRAY, J., SOBEL, M., COSTELL, M., TAKAHASHI, S., FASSLER, R., YAMAGUCHI, Y., GUTMANN, D. H., HYNES, R. O. & GERHARDT, H. 2011. Integrin-dependent and -independent functions of astrocytic fibronectin in retinal angiogenesis. *Development,* 138**,** 4451-63.

STOTTMANN, R. W., CHOI, M., MISHINA, Y., MEYERS, E. N. & KLINGENSMITH, J. 2004. BMP receptor IA is required in mammalian neural crest cells for development of the cardiac outflow tract and ventricular myocardium. *Development,* 131**,** 2205-18.

STRAUER, B. E., BREHM, M., ZEUS, T., KOSTERING, M., HERNANDEZ, A., SORG, R. V., KOGLER, G. & WERNET, P. 2002. Repair of infarcted myocardium by autologous intracoronary mononuclear bone marrow cell transplantation in humans. *Circulation,* 106**,** 1913-8.

SUCHTING, S., FREITAS, C., LE NOBLE, F., BENEDITO, R., BREANT, C., DUARTE, A. & EICHMANN, A. 2007. The Notch ligand Delta-like 4 negatively regulates endothelial tip cell formation and vessel branching. *Proc Natl Acad Sci U S A,* 104**,** 3225-30.

SUGISHITA, Y., WATANABE, M. & FISHER, S. A. 2004. The development of the embryonic outflow tract provides novel insights into cardiac differentiation and remodeling. *Trends Cardiovasc Med,* 14**,** 235-41.

SULLIVAN, A. R. & PIXLEY, F. J. 2014. CSF-1R signaling in health and disease: a focus on the mammary gland. *J Mammary Gland Biol Neoplasia,* 19**,** 149-59.

SUN, X., MEYERS, E. N., LEWANDOSKI, M. & MARTIN, G. R. 1999. Targeted disruption of Fgf8 causes failure of cell migration in the gastrulating mouse embryo. *Genes Dev,* 13**,** 1834-46.

SUZUKI, T., SUZUKI, S., FUJINO, N., OTA, C., YAMADA, M., SUZUKI, T., YAMAYA, M., KONDO, T. & KUBO, H. 2014. c-Kit immunoexpression delineates a putative endothelial progenitor cell population in developing human lungs. *Am J Physiol Lung Cell Mol Physiol,* 306**,** L855-65.

SWIRSKI, F. K., NAHRENDORF, M., ETZRODT, M., WILDGRUBER, M., CORTEZ-RETAMOZO, V., PANIZZI, P., FIGUEIREDO, J. L., KOHLER, R. H., CHUDNOVSKIY, A., WATERMAN, P., AIKAWA, E., MEMPEL, T. R., LIBBY, P., WEISSLEDER, R. & PITTET, M. J. 2009. Identification of splenic reservoir monocytes and their deployment to inflammatory sites. *Science,* 325**,** 612-6.

TACHIBANA, K., HIROTA, S., IIZASA, H., YOSHIDA, H., KAWABATA, K., KATAOKA, Y., KITAMURA, Y., MATSUSHIMA, K., YOSHIDA, N., NISHIKAWA, S., KISHIMOTO, T. & NAGASAWA, T. 1998. The chemokine receptor CXCR4 is essential for vascularization of the gastrointestinal tract. *Nature,* 393**,** 591-4.

TAKAGI, S., KASUYA, Y., SHIMIZU, M., MATSUURA, T., TSUBOI, M., KAWAKAMI, A. & FUJISAWA, H. 1995. Expression of a cell adhesion molecule, neuropilin, in the developing chick nervous system. *Dev Biol,* 170**,** 207-22.

TAKAHASHI, T., KALKA, C., MASUDA, H., CHEN, D., SILVER, M., KEARNEY, M., MAGNER, M., ISNER, J. M. & ASAHARA, T. 1999. Ischemia- and cytokine-induced mobilization of bone marrow-derived endothelial progenitor cells for neovascularization. *Nat Med,* 5**,** 434-8.

TAKAHASHI, T., NAKAMURA, F., JIN, Z., KALB, R. G. & STRITTMATTER, S. M. 1998. Semaphorins A and E act as antagonists of neuropilin-1 and agonists of neuropilin-2 receptors. *Nat Neurosci,* 1**,** 487-93.

TAKASHIMA, S., KITAKAZE, M., ASAKURA, M., ASANUMA, H., SANADA, S., TASHIRO, F., NIWA, H., MIYAZAKI JI, J., HIROTA, S., KITAMURA, Y., KITSUKAWA, T., FUJISAWA, H., KLAGSBRUN, M. & HORI, M. 2002. Targeting of both mouse neuropilin-1 and neuropilin-2 genes severely impairs developmental yolk sac and embryonic angiogenesis. *Proc Natl Acad Sci U S A,* 99**,** 3657-62.

TAMMELA, T., ENHOLM, B., ALITALO, K. & PAAVONEN, K. 2005. The biology of vascular endothelial growth factors. *Cardiovasc Res,* 65**,** 550-63.

TAMMELA, T., ZARKADA, G., NURMI, H., JAKOBSSON, L., HEINOLAINEN, K., TVOROGOV, D., ZHENG, W., FRANCO, C. A., MURTOMAKI, A., ARANDA, E., MIURA, N., YLA-HERTTUALA, S., FRUTTIGER, M., MAKINEN, T., EICHMANN, A., POLLARD, J. W., GERHARDT, H. & ALITALO, K. 2011. VEGFR-3 controls tip to stalk conversion at vessel fusion sites by reinforcing Notch signalling. *Nat Cell Biol,* 13**,** 1202-13.

TANAKA, M., KISHI, K., MCCARRON, R. M. & MIYATAKE, T. 1993. The generation of macrophages from precursor cells incubated with brain endothelial cells--a release of CSF-1 like factor from endothelial cells. *Tohoku J Exp Med,* 171**,** 211-20.

TAPIA, C., KUTZNER, H., MENTZEL, T., SAVIC, S., BAUMHOER, D. & GLATZ, K. 2006. Two mitosis-specific antibodies, MPM-2 and phospho-histone H3 (Ser28), allow rapid and precise determination of mitotic activity. *Am J Surg Pathol,* 30**,** 83-9.

THOMAS, G. R., MCCROSSAN, M. & SELKIRK, M. E. 1997. Cytostatic and cytotoxic effects of activated macrophages and nitric oxide donors on Brugia malayi. *Infect Immun,* 65**,** 2732-9.

TIAN, F., ZHOU, A. X., SMITS, A. M., LARSSON, E., GOUMANS, M. J., HELDIN, C. H., BOREN, J. & AKYUREK, L. M. 2010. Endothelial cells are activated during hypoxia via endoglin/ALK-1/SMAD1/5 signaling in vivo and in vitro. *Biochem Biophys Res Commun,* 392**,** 283-8.

TILLO, M., ERSKINE, L., CARIBONI, A., FANTIN, A., JOYCE, A., DENTI, L. & RUHRBERG, C. 2015. VEGF189 binds NRP1 and is sufficient for VEGF/NRP1-dependent neuronal patterning in the developing brain. *Development,* 142**,** 314-9.

TIMMERMAN, L. A., GREGO-BESSA, J., RAYA, A., BERTRAN, E., PEREZ-POMARES, J. M., DIEZ, J., ARANDA, S., PALOMO, S., MCCORMICK, F., IZPISUA-BELMONTE, J. C. & DE LA POMPA, J. L. 2004. Notch promotes epithelial-mesenchymal transition during cardiac development and oncogenic transformation. *Genes Dev,* 18**,** 99-115.

TIMMERMANS, F., PLUM, J., YODER, M. C., INGRAM, D. A., VANDEKERCKHOVE, B. & CASE, J. 2009. Endothelial progenitor cells: identity defined? *J Cell Mol Med,* 13**,** 87-102.

TIN, W. & GUPTA, S. 2007. Optimum oxygen therapy in preterm babies. *Arch Dis Child Fetal Neonatal Ed,* 92**,** F143-7.

TOMANEK, R. J. 1996. Formation of the coronary vasculature: a brief review. *Cardiovasc Res,* 31 Spec No**,** E46-51.

TORRES-VAZQUEZ, J., GITLER, A. D., FRASER, S. D., BERK, J. D., VAN, N. P., FISHMAN, M. C., CHILDS, S., EPSTEIN, J. A. & WEINSTEIN, B. M. 2004. Semaphorin-plexin signaling guides patterning of the developing vasculature. *Dev Cell,* 7**,** 117-23.

TOYOFUKU, T., YOSHIDA, J., SUGIMOTO, T., YAMAMOTO, M., MAKINO, N., TAKAMATSU, H., TAKEGAHARA, N., SUTO, F., HORI, M., FUJISAWA, H., KUMANOGOH, A. & KIKUTANI, H. 2008. Repulsive and attractive semaphorins cooperate to direct the navigation of cardiac neural crest cells. *Dev Biol,* 321**,** 251-62.

TUNG, J. W., HEYDARI, K., TIROUVANZIAM, R., SAHAF, B., PARKS, D. R., HERZENBERG, L. A. & HERZENBERG, L. A. 2007. Modern flow cytometry: a practical approach. *Clin Lab Med,* 27**,** 453-68, v.

UENO, H. & WEISSMAN, I. L. 2006. Clonal analysis of mouse development reveals a polyclonal origin for yolk sac blood islands. *Dev Cell,* 11**,** 519-33.

UENO, T., TOI, M., SAJI, H., MUTA, M., BANDO, H., KUROI, K., KOIKE, M., INADERA, H. & MATSUSHIMA, K. 2000. Significance of macrophage chemoattractant protein-1 in macrophage recruitment, angiogenesis, and survival in human breast cancer. *Clin Cancer Res,* 6**,** 3282-9.

VADIVEL, A., ALPHONSE, R. S., COLLINS, J. J., VAN HAAFTEN, T., O'REILLY, M., EATON, F. & THEBAUD, B. 2013. The axonal guidance cue semaphorin 3C contributes to alveolar growth and repair. *PLoS One,* 8**,** e67225.

VALDEMBRI, D., CASWELL, P. T., ANDERSON, K. I., SCHWARZ, J. P., KONIG, I., ASTANINA, E., CACCAVARI, F., NORMAN, J. C., HUMPHRIES, M. J., BUSSOLINO, F. & SERINI, G. 2009. Neuropilin-1/GIPC1 signaling regulates alpha5beta1 integrin traffic and function in endothelial cells. *PLoS Biol,* 7**,** e25.

VALLEJO-ILLARRAMENDI, A., ZANG, K. & REICHARDT, L. F. 2009. Focal adhesion kinase is required for neural crest cell morphogenesis during mouse cardiovascular development. *J Clin Invest,* 119**,** 2218-30.

VAN CRAENENBROECK, E. M., VAN CRAENENBROECK, A. H., VAN IERSSEL, S., BRUYNDONCKX, L., HOYMANS, V. Y., VRINTS, C. J. & CONRAADS, V. M. 2013. Quantification of circulating CD34+/KDR+/CD45dim endothelial progenitor cells: analytical considerations. *Int J Cardiol,* 167**,** 1688-95.

VAN DEN BERG, G., ABU-ISSA, R., DE BOER, B. A., HUTSON, M. R., DE BOER, P. A., SOUFAN, A. T., RUIJTER, J. M., KIRBY, M. L., VAN DEN HOFF, M. J. & MOORMAN, A. F. 2009. A caudal proliferating growth center contributes to both poles of the forming heart tube. *Circ Res,* 104**,** 179-88.

VAN DEN HOFF, M. J., MOORMAN, A. F., RUIJTER, J. M., LAMERS, W. H., BENNINGTON, R. W., MARKWALD, R. R. & WESSELS, A. 1999. Myocardialization of the cardiac outflow tract. *Dev Biol,* 212**,** 477-90.

VAN FURTH, R. & SLUITER, W. 1986. Distribution of blood monocytes between a marginating and a circulating pool. *J Exp Med,* 163**,** 474-9.

VARIN, A., MUKHOPADHYAY, S., HERBEIN, G. & GORDON, S. 2010. Alternative activation of macrophages by IL-4 impairs phagocytosis of pathogens but potentiates microbial-induced signalling and cytokine secretion. *Blood,* 115**,** 353-62.

VAROL, C., LANDSMAN, L., FOGG, D. K., GREENSHTEIN, L., GILDOR, B., MARGALIT, R., KALCHENKO, V., GEISSMANN, F. & JUNG, S. 2007. Monocytes give rise to mucosal, but not splenic, conventional dendritic cells. *J Exp Med,* 204**,** 171-80.

VASA, M., FICHTLSCHERER, S., AICHER, A., ADLER, K., URBICH, C., MARTIN, H., ZEIHER, A. M. & DIMMELER, S. 2001. Number and migratory activity of circulating endothelial progenitor cells inversely correlate with risk factors for coronary artery disease. *Circ Res,* 89**,** E1-7.

VIEIRA, J. M., SCHWARZ, Q. & RUHRBERG, C. 2007. Selective requirements for NRP1 ligands during neurovascular patterning. *Development,* 134**,** 1833-43.

VINCENT, S. D. & BUCKINGHAM, M. E. 2010. How to make a heart: the origin and regulation of cardiac progenitor cells. *Curr Top Dev Biol,* 90**,** 1-41.

VIRMANI, R., KOLODGIE, F. D., BURKE, A. P., FINN, A. V., GOLD, H. K., TULENKO, T. N., WRENN, S. P. & NARULA, J. 2005. Atherosclerotic plaque progression and vulnerability to rupture: angiogenesis as a source of intraplaque hemorrhage. *Arterioscler Thromb Vasc Biol,* 25**,** 2054-61.

VOGELI, K. M., JIN, S. W., MARTIN, G. R. & STAINIER, D. Y. 2006. A common progenitor for haematopoietic and endothelial lineages in the zebrafish gastrula. *Nature,* 443**,** 337-9.

WALDO, K. L., KUMISKI, D. & KIRBY, M. L. 1996. Cardiac neural crest is essential for the persistence rather than the formation of an arch artery. *Dev Dyn,* 205**,** 281-92.

WANG, B., WEIDENFELD, J., LU, M. M., MAIKA, S., KUZIEL, W. A., MORRISEY, E. E. & TUCKER, P. W. 2004. Foxp1 regulates cardiac outflow tract, endocardial cushion morphogenesis and myocyte proliferation and maturation. *Development,* 131**,** 4477-87.

WANG, H. U., CHEN, Z. F. & ANDERSON, D. J. 1998. Molecular distinction and angiogenic interaction between embryonic arteries and veins revealed by ephrin-B2 and its receptor Eph-B4. *Cell,* 93**,** 741-53.

WANG, J., NAGY, A., LARSSON, J., DUDAS, M., SUCOV, H. M. & KAARTINEN, V. 2006a. Defective ALK5 signaling in the neural crest leads to increased postmigratory neural crest cell apoptosis and severe outflow tract defects. *BMC Dev Biol,* 6**,** 51.

WANG, L., MUKHOPADHYAY, D. & XU, X. 2006b. C terminus of RGS-GAIP-interacting protein conveys neuropilin-1-mediated signaling during angiogenesis. *Faseb J,* 20**,** 1513-5.

WANG, L., ZENG, H., WANG, P., SOKER, S. & MUKHOPADHYAY, D. 2003. Neuropilin-1-mediated vascular permeability factor/vascular endothelial growth factor-dependent endothelial cell migration. *J Biol Chem,* 278**,** 48848-60.

WANG, Y., DUR, O., PATRICK, M. J., TINNEY, J. P., TOBITA, K., KELLER, B. B. & PEKKAN, K. 2009. Aortic arch morphogenesis and flow modeling in the chick embryo. *Ann Biomed Eng,* 37**,** 1069-81.

WHITAKER, G. B., LIMBERG, B. J. & ROSENBAUM, J. S. 2001. Vascular endothelial growth factor receptor-2 and neuropilin-1 form a receptor complex that is responsible for the differential signaling potency of VEGF(165) and VEGF(121). *J Biol Chem,* 276**,** 25520-31.

WIKTOR-JEDRZEJCZAK, W., BARTOCCI, A., FERRANTE, A. W., JR., AHMED-ANSARI, A., SELL, K. W., POLLARD, J. W. & STANLEY, E. R. 1990. Total absence of colony-stimulating factor 1 in the macrophage-deficient osteopetrotic (op/op) mouse. *Proc Natl Acad Sci U S A,* 87**,** 4828-32.

WILLIAMS, J. M., DE LEEUW, M., BLACK, M. D., FREEDOM, R. M., WILLIAMS, W. G. & MCCRINDLE, B. W. 1999. Factors associated with outcomes of persistent truncus arteriosus. *J Am Coll Cardiol,* 34**,** 545-53.

WORZFELD, T. & OFFERMANNS, S. 2014. Semaphorins and plexins as therapeutic targets. *Nat Rev Drug Discov,* 13**,** 603-21.

WU, A., WEI, J., KONG, L. Y., WANG, Y., PRIEBE, W., QIAO, W., SAWAYA, R. & HEIMBERGER, A. B. 2010. Glioma cancer stem cells induce immunosuppressive macrophages/microglia. *Neuro Oncol,* 12**,** 1113-25.

WU, H., XU, J. B., HE, Y. L., PENG, J. J., ZHANG, X. H., CHEN, C. Q., LI, W. & CAI, S. R. 2012. Tumor-associated macrophages promote angiogenesis and lymphangiogenesis of gastric cancer. *J Surg Oncol,* 106**,** 462-8.

WU, Y., ZHONG, Z., HUBER, J., BASSI, R., FINNERTY, B., CORCORAN, E., LI, H., NAVARRO, E., BALDERES, P., JIMENEZ, X., KOO, H., MANGALAMPALLI, V. R., LUDWIG, D. L., TONRA, J. R. & HICKLIN, D. J. 2006. Anti-vascular endothelial growth factor receptor-1 antagonist antibody as a therapeutic agent for cancer. *Clin Cancer Res,* 12**,** 6573-84.

WURDAK, H., ITTNER, L. M., LANG, K. S., LEVEEN, P., SUTER, U., FISCHER, J. A., KARLSSON, S., BORN, W. & SOMMER, L. 2005. Inactivation of TGFbeta signaling in neural crest stem cells leads to multiple defects reminiscent of DiGeorge syndrome. *Genes Dev,* 19**,** 530-5.

XU, Y., YUAN, L., MAK, J., PARDANAUD, L., CAUNT, M., KASMAN, I., LARRIVEE, B., DEL TORO, R., SUCHTING, S., MEDVINSKY, A., SILVA, J., YANG, J., THOMAS, J. L., KOCH, A. W., ALITALO, K., EICHMANN, A. & BAGRI, A. 2010. Neuropilin-2 mediates VEGF-C-induced lymphatic sprouting together with VEGFR3. *J Cell Biol,* 188**,** 115-30.

YAN, D., WANG, X., LI, D., QU, Z. & RUAN, Q. 2011. Macrophages overexpressing VEGF, transdifferentiate into endothelial-like cells in vitro and in vivo. *Biotechnol Lett,* 33**,** 1751-8.

YANG, J., II, M., KAMEI, N., ALEV, C., KWON, S. M., KAWAMOTO, A., AKIMARU, H., MASUDA, H., SAWA, Y. & ASAHARA, T. 2011. CD34+ cells represent highly functional endothelial progenitor cells in murine bone marrow. *PLoS One,* 6**,** e20219.

YEH, H. J., HE, Y. Y., XU, J., HSU, C. Y. & DEUEL, T. F. 1998. Upregulation of pleiotrophin gene expression in developing microvasculature, macrophages, and astrocytes after acute ischemic brain injury. *J Neurosci,* 18**,** 3699-707.

YODER, M. C. 2010. Is endothelium the origin of endothelial progenitor cells? *Arterioscler Thromb Vasc Biol,* 30**,** 1094-103.

YODER, M. C. 2012. Human endothelial progenitor cells. *Cold Spring Harb Perspect Med,* 2**,** a006692.

YODER, M. C., HIATT, K., DUTT, P., MUKHERJEE, P., BODINE, D. M. & ORLIC, D. 1997a. Characterization of definitive lymphohematopoietic stem cells in the day 9 murine yolk sac. *Immunity,* 7**,** 335-44.

YODER, M. C., HIATT, K. & MUKHERJEE, P. 1997b. In vivo repopulating hematopoietic stem cells are present in the murine yolk sac at day 9.0 postcoitus. *Proc Natl Acad Sci U S A,* 94**,** 6776-80.

YONA, S., KIM, K. W., WOLF, Y., MILDNER, A., VAROL, D., BREKER, M., STRAUSS-AYALI, D., VIUKOV, S., GUILLIAMS, M., MISHARIN, A., HUME, D. A., PERLMAN, H., MALISSEN, B., ZELZER, E. & JUNG, S. 2013. Fate mapping reveals origins and dynamics of monocytes and tissue macrophages under homeostasis. *Immunity,* 38**,** 79-91.

YOSHIDA, H., HAYASHI, S., KUNISADA, T., OGAWA, M., NISHIKAWA, S., OKAMURA, H., SUDO, T., SHULTZ, L. D. & NISHIKAWA, S. 1990. The murine mutation osteopetrosis is in the coding region of the macrophage colony stimulating factor gene. *Nature,* 345**,** 442-4.

YUAN, L., MOYON, D., PARDANAUD, L., BREANT, C., KARKKAINEN, M. J., ALITALO, K. & EICHMANN, A. 2002. Abnormal lymphatic vessel development in neuropilin 2 mutant mice. *Development,* 129**,** 4797-806.

ZHANG, Y., SINGH, M. K., DEGENHARDT, K. R., LU, M. M., BENNETT, J., YOSHIDA, Y. & EPSTEIN, J. A. 2009. Tie2Cre-mediated inactivation of plexinD1 results in congenital heart, vascular and skeletal defects. *Dev Biol,* 325**,** 82-93.

ZHOU, J., PASHMFOROUSH, M. & SUCOV, H. M. 2012. Endothelial neuropilin disruption in mice causes DiGeorge syndrome-like malformations via mechanisms distinct to those caused by loss of Tbx1. *PLoS One,* 7**,** e32429.

ZHOU, W., KE, S. Q., HUANG, Z., FLAVAHAN, W., FANG, X., PAUL, J., WU, L., SLOAN, A. E., MCLENDON, R. E., LI, X., RICH, J. N. & BAO, S. 2015. Periostin secreted by glioblastoma stem cells recruits M2 tumour-associated macrophages and promotes malignant growth. *Nat Cell Biol*.

ZOVEIN, A. C., HOFMANN, J. J., LYNCH, M., FRENCH, W. J., TURLO, K. A., YANG, Y., BECKER, M. S., ZANETTA, L., DEJANA, E., GASSON, J. C., TALLQUIST, M. D. & IRUELA-ARISPE, M. L. 2008. Fate tracing reveals the endothelial origin of hematopoietic stem cells. *Cell Stem Cell,* 3**,** 625-36.

ZUMSTEG, A., BAERISWYL, V., IMAIZUMI, N., SCHWENDENER, R., RUEGG, C. & CHRISTOFORI, G. 2009. Myeloid cells contribute to tumor lymphangiogenesis. *PLoS One,* 4**,** e7067.

APPENDIX

FANTIN, A., VIEIRA, J. M., **PLEIN, A.**, DENTI, L., FRUTTIGER, M., POLLARD, J. W. & RUHRBERG, C. 2013. NRP1 acts cell autonomously in endothelium to promote tip cell function during sprouting angiogenesis. *Blood,* 121**,** 2352-62.

FANTIN, A., VIEIRA, J. M., **PLEIN, A.**, MADEN, C. H. & RUHRBERG, C. 2013. The embryonic mouse hindbrain as a qualitative and quantitative model for studying the molecular and cellular mechanisms of angiogenesis. *Nat Protoc,* 8**,** 418-29.

FANTIN, A., HERZOG, B., MAHMOUD, M., YAMAJI, M., **PLEIN, A.**, DENTI, L., RUHRBERG, C. & ZACHARY, I. 2014. Neuropilin 1 (NRP1) hypomorphism combined with defective VEGF-A binding reveals novel roles for NRP1 in developmental and pathological angiogenesis. *Development,* 141**,** 556-62.

PLEIN, A., FANTIN, A. & RUHRBERG, C. 2014. Neuropilin regulation of angiogenesis, arteriogenesis, and vascular permeability. *Microcirculation,* 21**,** 315-23.

PLEIN, A., FANTIN, A. & RUHRBERG, C. 2015. Neural crest cells in cardiovascular development. *Curr Top Dev Biol,* 111**,** 183-200.